



January 2017

Design And Construction Of A Robotic Vehicle To Assist During Planetary Surface Operations

Christopher Anthony Follette

Follow this and additional works at: <https://commons.und.edu/theses>

Recommended Citation

Follette, Christopher Anthony, "Design And Construction Of A Robotic Vehicle To Assist During Planetary Surface Operations" (2017). *Theses and Dissertations*. 2211.
<https://commons.und.edu/theses/2211>

This Thesis is brought to you for free and open access by the Theses, Dissertations, and Senior Projects at UND Scholarly Commons. It has been accepted for inclusion in Theses and Dissertations by an authorized administrator of UND Scholarly Commons. For more information, please contact zeinebyousif@library.und.edu.

DESIGN AND CONSTRUCTION OF A ROBOTIC VEHICLE TO ASSIST
DURING PLANETARY SURFACE OPERATIONS

by

Christopher Anthony Follette

Bachelor of Science, North Dakota State University, 2013

A Thesis

Submitted to the Graduate Faculty

of the

University of North Dakota

In partial fulfillment of the requirements

for the degree of

Master of Science

Grand Forks, North Dakota

August

2017

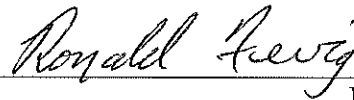
Copyright 2017 Christopher Follette

This thesis, submitted by Christopher Follette in partial fulfillment of the requirements for the Degree of Master of Science from the University of North Dakota, has been read by the Faculty Advisory Committee under whom the work has been done and is hereby approved.



Dr. Pablo de León


Chairperson



Dr. Ronald Fevig

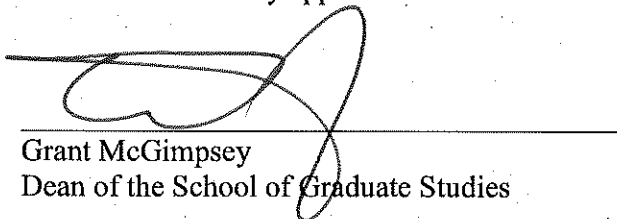


Dr. Reza Fazel-Rezai



Dr. Jeremiah Neubert

This thesis is being submitted by the appointed advisory committee as having met all of the requirements of the School of Graduate Studies at the University of North Dakota and is hereby approved.



Grant McGimpsey
Dean of the School of Graduate Studies

July 24, 2017

Date

PERMISSION

Title Design and Construction of a Robotic Vehicle to Assist During Planetary
Surface Operations

Department Space Studies

Degree Master of Science

In presenting this thesis in partial fulfillment of the requirements for a graduate degree from the University of North Dakota, I agree that the library of this University shall make it freely available for inspection. I further agree that permission for extensive copying for scholarly purposes may be granted by the professor who supervised my thesis work or, in his absence, by the Chairperson of the department or the dean of the School of Graduate Studies. It is understood that any copying or publication or other use of this thesis or part thereof for financial gain shall not be allowed without my written permission. It is also understood that due recognition shall be given to me and to the University of North Dakota in any scholarly use which may be made of any material in my thesis.

Christopher Anthony Follette

July 26th, 2017

TABLE OF CONTENTS

TABLE OF CONTENTS.....	v
LIST OF FIGURES	x
LIST OF TABLES	xvi
ACKNOWLEDGEMENTS	xvii
ABSTRACT.....	xix
CHAPTER I.....	1
INTRODUCTION	1
Complexities of EVA.....	2
Utilizing Robots to Enhance the EVA Experience	4
Astronaut-Rover (ASRO) Field Experiment	4
Thesis Impact	8
EVA Robotic Assistant Project (ERA).....	8
Thesis Impact	15
Electric Tractor	16
Thesis Impact	17
K10.....	17
Thesis Impact	18

Mobile Communication Networks.....	18
Thesis Impact	23
Chapter 1 Conclusion.....	24
CHAPTER II - METHODOLOGY	25
Mechanical Design.....	26
Suspension	26
Rocker-Bogie	26
Dual H-Arm	29
Shocks.....	41
Suspension Stress Analysis.....	42
Drivetrain	45
Motor.....	45
Gearbox.....	56
Driveshaft.....	57
Gearbox-Drive Shaft Coupler	61
Motor-Gearbox Coupler.....	69
Motor and Gearbox Interface Plates	74
Drivetrain Assembly	77

Frame	79
Main Body	79
Antenna and Camera Boom	88
Aluminum Panels	89
Electrical Design	94
Driving System	95
Batteries	95
Motor Controllers	98
Relays	100
Fuses	102
Wires	104
Battery Charger	105
Battery Charger Exhaust Fan	106
Communications System	107
Remote Controller	107
DragonLink Transmitter and Receiver	109
5 Volt BEC	119
12 Volt Camera	120

Boscam 5.8 GHz Video Transmitter and Receiver.....	121
Pan and Tilt Camera Kit	122
Rover Camera Housing.....	123
3-Channel Video Switch.....	125
Videolynx VM-70X Amateur Radio Video Transmitter	126
Video Transmitter Heat Sink	128
MininOSD.....	130
Amateur Radio Cross-band Repeater.....	131
Antennas	132
Chapter 2 Conclusion.....	137
Chapter III: Testing and Conclusions	139
Testing.....	139
Rover Propulsion System.....	140
Rover Remote Control	142
Radio Repeater System	143
Video System	152
Conclusions.....	157
Future Work	158

Appendices.....	161
Appendix A – Manufacturer Engineering Information	162
Appendix B – Engineering Drawings	164
Appendix C – Electrical Drawings	248
References.....	266

LIST OF FIGURES

Figure	Page
Figure 1 - Marsokhod Rover (NASA JPL, 2016).....	5
Figure 2 - Suited Astronaut and Marsokhod (Cabrol N. A., 2000)	7
Figure 3 - ATRV-Jr Robot (NASA JPL, 2017)	10
Figure 4 - ATRV-Jr on the left, ERA (as modified) on right (Burrige R. R., Graham, S&K Electronics, & Titan-Lincom, 2002).....	11
Figure 5 - ERA Performing Test Scenarios – 2000 (Burrige R. R., Graham, S&K Electronics, & Titan-Lincom, 2002).....	12
Figure 6 - ERA and New Mobility Base (Burrige R. R., Graham, Shillcutt, Hirsh, & Kortenkamp, 2003)	13
Figure 7 - ERA Pulling IHOPP (Burrige R. R., Graham, Shillcutt, Hirsh, & Kortenkamp, 2003)	15
Figure 8 - ET hauling the Chariot and Science Trailer (Ross, Kosmo, & Janoiko, 2010)	16
Figure 9 - K10 Rover (NASA, 2009).....	18
Figure 10 - Hybrid Communications Architecture (Alena, Gilbaugh, & Glass, Communication System Architecture for Planetary Exploration, 2001)	20
Figure 11 - Hybrid Repeater (Alena, Gilbaugh, Glass, & Braham, Communication System Architecture for Planetary Exploration, 2001).....	22
Figure 12 - MDRS Communication Architecture (Clancey, et al., 2007)	23

Figure 13 - Mars Science Laboratory (Webster, 2011)	27
Figure 14 - Drive Shaft Dimensions	30
Figure 15 - Inventor Model of Polaris Drive Shaft.....	31
Figure 16 - Double Wishbone Suspension (himalayan, 2012)	32
Figure 17 - Degrees of Freedom and Suspension Motion (Milliken & Milliken, 1995)..	33
Figure 18 - Camber Change due to Front-View IC Length (Milliken & Milliken, 1995)	34
Figure 19 - Instant Center Concept (Milliken & Milliken, 1995).....	35
Figure 20 - Wheel path showing the effects of scrub (Milliken & Milliken, 1995).....	36
Figure 21 - Scrub as a function of IC height (Milliken & Milliken, 1995)	36
Figure 22 - Suspension Members on Knuckle.....	37
Figure 23 - FVSA Top of Travel	38
Figure 24 - FVSA Bottom of Travel.....	39
Figure 25 - Direction of Camber Angles (Auto Dimensions Inc., n.d.)	39
Figure 26 - Rover Suspension Camber	40
Figure 27 - Rover Suspension Scrub	40
Figure 28 - Suspension FEA - Vertical Loading 1-g and 3-g.....	43
Figure 29 - Suspension FEA - Horizontal Loading 1-g & 2-g	44
Figure 30 - Free-Body Diagram of the Rover Wheel	48
Figure 31 - Hill Climb FBD.....	50
Figure 32 - 24 Volt 900 Watt XYD-13 Electric Motor (Currie Technologies, n.d.).....	55
Figure 33 - Anaheim Automation 10:1 Planetary Gearbox (Anaheim Automation, n.d.)	57

Figure 34 – Gearbox/Drive Shaft Coupler V2	62
Figure 35 - Manufactured Gearbox/Drive Shaft Coupler	63
Figure 36 - FEA Setup	64
Figure 37 - FEA Coupler, Max Gearbox Torque, Stress	65
Figure 38 - FEA Coupler, Max Gearbox Torque, Safety Factor	65
Figure 39 - FEA Coupler – Max Gearbox Rated Torque – Stress.....	66
Figure 40 - FEA Coupler, Max Gearbox Rated Torque, Safety Factor	67
Figure 41 - FEA Coupler, Max Gearbox Torque, 4340 Annealed, Safety Factor	68
Figure 42 - FEA Coupler, Max Gearbox Torque, 4340 Annealed, Stress.....	68
Figure 43 - Motor-Gearbox Coupler.....	70
Figure 44 - Motor-Gearbox Coupler Load and Fixed Constraint	71
Figure 45 - Roll-Pin 13.99 Nm Stress and Safety Factor	72
Figure 46 - Motor-Gearbox Coupler 13.99 Nm Stress and Safety Factor	72
Figure 47 - Motor Gearbox Coupler 42 Nm Stress and Safety Factor	73
Figure 48 - Motor Gearbox Coupler Roll Pin - 42 Nm Stress and Safety Factor.....	74
Figure 49 - Motor and Gearbox Mounting Plates	75
Figure 50 - Motor Gearbox Assembly	76
Figure 51 - Motor Gearbox Assembly Torque Location	76
Figure 52 - Motor Gearbox Mounting Assembly Stress and Safety Factor	77
Figure 53 - Inventor Model of Completed Drivetrain	78
Figure 54 - Completed Drivetrain Assembly.....	78

Figure 55 - Side Frame with Suspension Sub-Frame	79
Figure 56 - Manufactured Frame Sides	80
Figure 57 - Frame and Suspension FEA Setup.....	81
Figure 58 – Frame and Suspension FEA – Vertical Load	82
Figure 59 - Frame and Suspension FEA - Horizontal Setup	83
Figure 60 - Frame and Suspension FEA - 2g Horizontal Load	83
Figure 61 - Frame and Suspension FEA - 1g Horizontal Load	84
Figure 62 - Frame FEA - Front Collision Setup	84
Figure 63 - Frame FEA - Front Collision - 3g	85
Figure 64 - Frame FEA - Front Collision - 1g.....	85
Figure 65 - Frame FEA - Front Collision with Plates - 3g	86
Figure 66 - Frame FEA - Front Collision with Plates - 5g	86
Figure 67 - Manufactured Frame and Steel Plates.....	88
Figure 68 - Antenna and Camera Boom	89
Figure 69 – Frame with Aluminum Panels.....	91
Figure 70 - Rover Charging 1	93
Figure 71 - Rover Charging 2	93
Figure 72 - Exide 12 Volt 105 amp-hour battery (Menards, n.d.).....	96
Figure 73 - Batteries Installed in Rover.....	96
Figure 74 - RoboClaw 2x60A (Ion Motion Control, n.d.).....	99
Figure 75 - Cole Hersee 24213 SPST Relay (Amazon, n.d.)	101

Figure 76 - Time-Current chart for ANN Series Fuses (Waytek, 2017)	102
Figure 77 - NOCO Genius Battery Charger (NOCO, n.d.)	105
Figure 78 - Turnigy 9X Radio Controller (Hobbyking, n.d.)	108
Figure 79 - DragonLink V2 Complete System (RobotShop, n.d.)	109
Figure 80 - Isotropic Antenna Radiation Pattern – 3D (19SD348, n.d.)	113
Figure 81 - Dipole Antenna Radiation Pattern (Cisco, 2007).....	113
Figure 82 - Yagi Antenna Radiation Pattern (Cisco, 2007).....	115
Figure 84 - 5 Volt BEC (Hobbywing, n.d.)	120
Figure 85 - 12 Volt Camera (GoolRC, n.d.)	121
Figure 86 - Boscam Video Transmitter and Receiver (Boscam, n.d.).....	122
Figure 87 - Pan and Tilt System (Ready Made RC, n.d.)	123
Figure 88 - Rover Camera Housing Model.....	123
Figure 89 - CNC Milled Camera Housing Pictures	124
Figure 90 - Completed Rover Camera Housing	125
Figure 91 - 3 Channel Video Switch (Hobbyking, n.d.).....	126
Figure 92 - Video Transmitter and Receiver Test	127
Figure 93 - Videolynx VM-70X (Transmit Video, 2017)	127
Figure 94 - Receiving Antenna and Standard Flat Screen Television	128
Figure 95 - VM-70X with Heatsink.....	129
Figure 96 - VM-70X with Heatsink and Stands	129
Figure 97 - MinimOSD Board (3DRobotics, n.d.)	130

Figure 98 - Dual-Band Dipole 446 MHz SWR	135
Figure 99 - Dual-Band Dipole 146 MHz SWR	135
Figure 100 - Dipole Antennas on Rover Boom	136
Figure 101 - Wireless Scale Readout.....	137
Figure 102 - Rover on Wireless Scales.....	137
Figure 103 - TM-D710 During Testing	143
Figure 104 - Line-of-Sight Communications (Seybold, 2005).....	146
Figure 105 - Terrain for the Second Day of Radio Testing	148
Figure 106 - Rover on Dike, Showing Opposite Side	148
Figure 107 - Rover Testing Location. Map data: Google.....	149
Figure 108 - Astronaut Direct Communication Test. Map Data: Google.....	150
Figure 109 - Rover Repeated Audio Test. Map Data: Google	151
Figure 110 - Astronaut Video Test. Map Data: Google.....	154
Figure 112 - Amateur Video Transmitter Test Image 2	155
Figure 111 - Amateur Video Transmitter Test Image 1	155
Figure 113 - Polaris Sportsman 500 Half Shaft Data	162
Figure 114 - Anaheim Automation Gearbox Information	162
Figure 115 - ANN-100 Fuse Specifications (Waytek, 2017)	163

LIST OF TABLES

Table	Page
Table 1 - Weight Estimates for Motor Torque.....	48
Table 2 – Calculated Rover Motor Specifications.....	54
Table 3 - Recommended Current Ratings (Continuous Duty); (Howard W. Sams & Co., 1986).....	104
Table 4 - RC Controller Channel Assignments	109
Table 5 - Radio Repeater Distance	144
Table 6 - Video Transmitter Temperature	156

ACKNOWLEDGEMENTS

I wish to express my sincere appreciation to the members of my advisory committee for their guidance and support during my time in the master's program at the University of North Dakota.

I would like to thank the members of the mechanical engineering machine shop for all of their help and guidance needed to manufacture the components for this rover.

I would like to thank the UND Department of Space Studies for all of their help making this project a reality.

To Julie and Brian,
the most supportive and helpful parents I could ever hope for!

ABSTRACT

In the near future, astronauts will explore new planetary surfaces in the Solar System. To enable peak performance, these astronauts will need to utilize all of the tools at their disposal. It is proposed that one such tool is a planetary surface rover designed specifically to assist the astronauts during their Extra-Vehicular-Activities (EVA's).

This rover is designed and built to operate in concert with existing analog planetary surface infrastructure at the University of North Dakota (UND). This rover will be remotely controlled by an astronaut located on the planetary surface, enabling real-time operation and obstacle avoidance. The rover will act primarily as a relay for audio and video communications between the astronauts in the field and the Inflatable Lunar Habitat (ILH), or another planetary outpost. This rover will be designed to enable storage for tools and samples, freeing the astronauts from the tedious and physically demanding task of carrying items for long distances encumbered by an EVA suit.

This thesis will describe the design of the rover and the rationale for each design decision. Upon completion of the rover, this thesis will report on the real-world performance of the rover, the effectiveness of the subsystems, and the lessons learned as a result of initial testing. Using the rover and the information obtained from this thesis, future astronaut-rover interaction studies will be conducted that will be important to the future of human planetary exploration.

CHAPTER I

INTRODUCTION

As humans advance and continue to explore the solar system they will be faced with new and difficult challenges. Getting to, living on, and exploring new planets all present challenges that need to be solved before any real exploration can take place. These issues are first tackled in on-Earth simulations. The best practices, solutions, and technologies from these simulations are then exported to be used in real space exploration. These simulations are used to test and fine-tune a variety of hypotheses ranging from optimal habitat design to crew psychological and physical fitness. To ensure the first human mission to an extraterrestrial surface since Apollo 17 in 1972 will be a success, proper due-diligence must be first paid on Earth. This thesis will discuss the creation of a rover that will allow greater astronaut efficiency while exploring and working on an analog Martian surface. This rover will enable further testing of technologies and procedures used to make the extra-vehicular activity (EVA) experience safer and more efficient than it has been before. This rover, named the MArs Compliment to Humanity rOver (MACHO), is designed to integrate with the Martian simulation facilities already constructed at the University of North Dakota by the Human Spaceflight Laboratory, primarily the Inflatable Lunar-Martian Habitat (ILMH), Pressurized Electric Rover (PER), and the NDX-2 Spacesuits.

Complexities of EVA

EVA's are incredibly challenging and dangerous. After all, humans aren't made to explore space. We need to bring little pockets of Earth's atmosphere and pressure with us wherever we go. While the astronaut is out of the relative safety of the ship or the habitat, s/he is exposed to a range of dangers. These include, but are not limited to, suit puncture and rapid depressurization, life support system failure, increased exposure to radiation, and micro-meteoroid impacts. There are also risks associated with exploration in general, such as entrapment, falls and physical injury, and overexertion and exhaustion. All of these issues are further amplified while on an extraterrestrial surface where one wrong move can be life-threatening and the hope for rescue slim to none. Given all of these dangers, and considering that most of these dangers will be ever-present while exploring new terrain in space, precautions need to be taken to help make the EVA experience as safe as reasonably possible.

To help keep the astronauts safe, mission planners must reduce the number of unnecessary EVA's and make the astronaut's tasks as simple as possible. As an example, while on location the health and stability of the habitat is a top priority. If the habitat suddenly depressurizes because of an unnoticed leak or puncture, the whole crew inside the habitat will be compromised. Because of this, the habitat needs to be inspected and maintained on a daily schedule. These inspection EVA's, while not complex, comprise a large number of EVA's that expose the astronauts to the dangers outlined above. When catastrophic events can happen from a trivial scrape or pin-prick, unnecessary EVA's need to be reduced. One solution to reduce the number of unnecessary EVA's is to automate the task of habitat inspection and trivial maintenance. This can be accomplished

by a robot, whether human controlled or completely automated makes no difference. If the inspection can be accomplished with the astronauts remaining safely inside the habitat, that is absolutely preferable.

Another way to make EVA's safer is to lessen the burden faced by the astronauts. While astronauts are inside of their space suits they are constantly fighting the atmospheric pressure of their suits. As an example, EVA suits used on the International Space Station are pressurized to 4.3 psi (Newman & Barratt, 1997). There have been many documented cases of astronauts' hands becoming fatigued battling the pressure of the gloves. Imagine squeezing a stress ball whenever grabbing an object or attempting to move your hand. Now imagine this constant elastic stress on every moving part of your body: hands, arms, legs, etc. This exertion will cause astronauts to tire faster and use more energy when compared to performing the same action unencumbered here on Earth. This additional exertion accumulates throughout the course of the EVA and can lead to mental and physical lapses as the sortie continues. Unfortunately, the strain caused by the atmospheric pressure of the suits cannot be avoided, but the activities performed by the astronauts can be modified to make the tasks easier and less physically demanding. Some of these modifications include using robots to transport tools, samples, and extra life-support consumables. If the astronauts do not have to exert themselves carrying these items they will have more energy to perform the required tasks, stay mentally sharp, and hopefully avoid mistakes.

Utilizing Robots to Enhance the EVA Experience

In order to discover what the optimal robot looks like, robots need to be constructed and analog studies performed. These studies will test for the most effective hardware, the best operating practices, and the most effective means of the astronauts in the field interacting with the robots.

Given the need for these studies there have been surprisingly few studies aimed at examining the most effective methods of astronaut-rover interaction. The studies that have been performed will be cataloged and explained in this section.

Astronaut-Rover (ASRO) Field Experiment

The first study, named the “Astronaut-Rover (ASRO) field experiment”, took place February 22-27, 1999 in Silver Lake, Mojave Desert, California. The purpose of this experiment was to study the “interaction between the astronaut and the rover as a complimentary and interactive team” which “is critical to assess but had never been tested before” (Cabrol, et al., 1999). This experiment has six overall goals and objectives. Taken from the paper, these goals are:

1. To identify the operational domains where the EVA astronauts and rovers are complementary and can interact, thus are more likely to collaborate in a safe, productive, and cost effective way for the surface exploration mission.
2. To identify preliminary requirements and recommendations for advanced spacesuits and rovers that facilitate their cooperative and complementary interaction.

3. To develop operational procedures (designated as scenarios) for the astronaut-rover team in the identified domains.
4. To test these procedures during representative mission scenarios [1,2] during field experiments by simulating the exploration of a planetary surface by a human crew interacting with a rover.
5. To train test-subject, simulated Earth-based and/or Lander-based science teams, and automated vehicle operators in mission configuration.
6. To evaluate and understand sociotechnical aspects of the astronaut-rover interaction experiment in order to guide future technology designs.

The astronaut used in this experiment was wearing an I-Suit pressurized at 3.75 PSID and was breathing cryogenic air. The rover used was the NASA Ames Marsokhod



Figure 1 - Marsokhod Rover (NASA JPL, 2016)

Rover that was used during the Rover Field Experiments performed at the same location the two previous weeks. During these previous tests, Marsokhod was operating as a

stand-alone rover traversing the terrain and conducting scientific experiments without the aid of an astronaut. The primary changes to the rover between the two tests were to remove the spectroscopy sensor and add stereo vision tracking from JSC. This stereo vision tracking allowed the rover to autonomously track and follow the EVA astronaut during certain operational modes.

During the test the rover was either controlled remotely from the rover operation center (ROC) located 1.5 km away or operating autonomously. This “local” control allowed for real-time control of the rover without the time delays that result when attempting to manually control a Mars rover from Earth.

In order to achieve the stated goals and objectives outlined above, the study chose four mission operational procedures, or scenarios, to test. The scenarios chosen were:

1. *The rover as a scout.* The rover pre-examines the traverse area and establishes potentially favorable sites for the suited astronaut to work in.
2. *The rover as a video coverage assistant.* During the Apollo missions the second EVA crewmember was responsible for video documenting the first EVA crewmember’s activity in the field. With this task being performed by the rover the second EVA crewmember can do more useful work, making better use of the limited EVA time. This scenario was performed using two different methods: human controlled video tracking via the ROC, and autonomous tracking via the JSC stereo tracking system.
3. *The rover as a field science assistant.* In this scenario the rover would make use of its advanced sensors and scientific instrument payload to perform astronaut directed science. The EVA astronaut would place a colored flag at

an area of interest and the rover would come over and perform the indicated test/experiment. Different colored flags corresponded to different tests. This scenario utilized the greater environmental awareness possessed by the astronaut and the specialized performance of the rover. This scenario also allowed the astronaut to quickly determine which locations were of interest and retreat to the habitat, while the rover performed the time consuming and sometimes tedious tasks of performing the tests.

4. *The rover as a field technical assistant.* The rover was used to carry tools and samples for the suited astronaut. The astronaut also used the capabilities on-board Marsokhod to document sites of interest via the imaging system and communicate remotely with a science team. Two methods were used in this scenario: human control via the ROC and autonomous control via the JSC stereo tracking system (Cabrol, et al., 1999).



Figure 2 - Suited Astronaut and Marsokhod (Cabrol N. A., 2000)

According to the document, all science objectives were achieved while performing the four mission scenarios. Seeing as this was the first rover-astronaut simulation many areas for improvement were discovered. These areas are: “science (including adapted tools for astronauts, instruments for science onboard rovers, relay between rover and astronaut); rover technology; EVA technology; communications; mission operational procedures; gestation of mission duration and data volume; and information technology” (Cabrol, et al., 1999).

Thesis Impact

One of the most applicable lessons learned from the ASRO study was that the robot must be able to keep pace with the human it is assisting. The Marsokhod rover was designed for low energy consumption and was roughly ten times slower than the suited astronaut. This forced the astronaut to take numerous breaks to wait for the robot, wasting time and life support consumables. Another vital lesson was that the science support team, which had access to the video feed from the rover, had great difficulty communicating to the astronaut specific objects/rocks of interest. Future robots will need to have some way of indicating which terrain feature the suited astronaut should examine (Burridge R. R., Graham, S&K Electronics, & Titan-Lincom, 2002).

EVA Robotic Assistant Project (ERA)

Building on the success of, and lessons learned from, ASRO, the EVA Robotic Assistant project (ERA) was started at Johnson Space Center in Houston, Texas in 2000. This project was specifically interested in how to design a robot that can assist someone in a spacesuit while out on an EVA.

Taken from the introduction of the first paper produced from this project, the authors point to three reasons why automation and robotics will be necessary on an exploratory mission:

1. “The scarcity of crewmember time will necessitate the automation of mundane tasks to allow the crew to prioritize objectives and apply their expertise appropriately.”
2. “The volume of assembly, inspection, maintenance, and exploration tasks required for an extended mission will necessitate that some be done without human involvement.”
3. “The need to minimize the inherent risk associated with extra-vehicular activity (EVA) requires that robots perform some of the more hazardous activities (Burridge R. R., Graham, S&K Electronics, & Titan-Lincom, 2002).”

This project worked to produce a usable robot, both in hardware and software. While it needed a functional robot, the program focused more on creating a software package that would best allow the astronaut to interact with the robot and for the robot to interact with other robots. This software was focused on machine learning and automation. As such, much of the paper details the creation of the software tools that allow the rover to function. This thesis will not go into detail about the automation of tasks and how the robot autonomously interacts with the astronaut. This is definitely an area that will need to be explored at a later date, but a rover needs to be built and be operational before any real work can begin on software and automation.

The primary focus for this thesis is the construction of the rover: which parts were used, how effective they were at performing their duties, and what the authors would

change after the completion of their field trials. This information will give practical starting points for the creation of a rover here at UND.

The ERA rover was built off of the ATRV-Jr mobile robot produced by RWI, Inc. A picture of this robot is shown below:

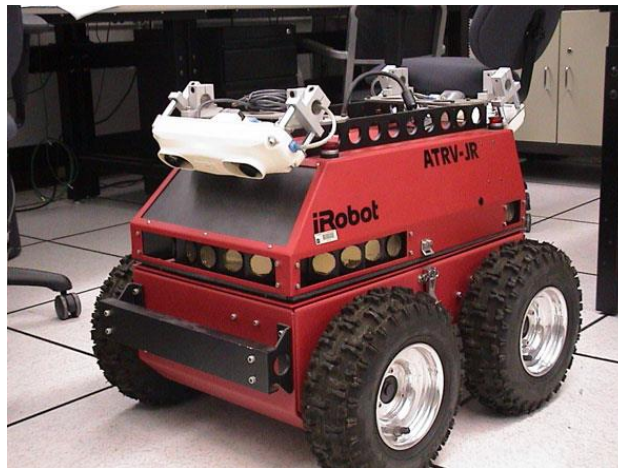


Figure 3 - ATRV-Jr Robot (NASA JPL, 2017)

This rover weighs in at 110 lbs, can support a payload of 55 lbs, and has a run time between 3-6 hours depending on the terrain (Real World Interface, n.d.). To make this robot more compatible to the terrain it would be working, the wheel hubs were moved out and down. This increased the ground clearance from 3 inches to 12 inches. This allowed the robot to maneuver over obstacles that would have previously obstructed the robot. A pan-tilt camera platform was installed to give the controllers a full field of view. A tower was added to mount the camera and antennas near astronaut head height. A trailer hitch was added that allowed the robot to attach to trailers and other objects. Finally, tool palettes were built that fit alongside the robot's tower. These palettes housed frequently used tools and provided a location to store rock samples. A comparison of the robot before and after modification is shown below.

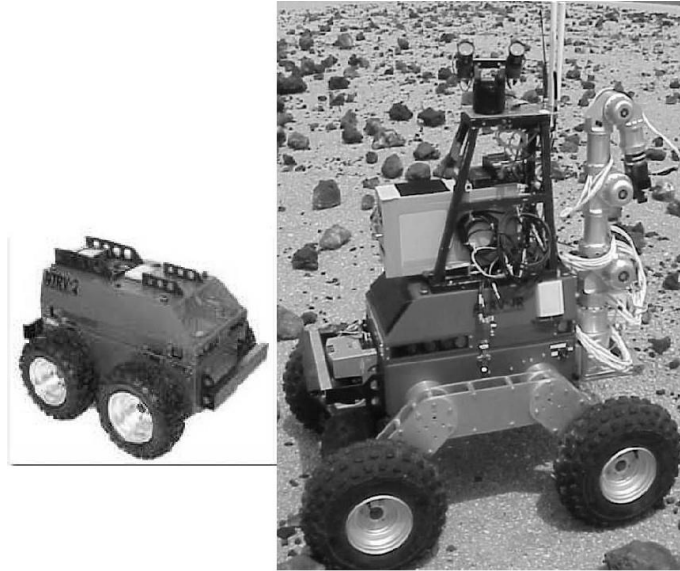


Figure 4 - ATRV-Jr on the left, ERA (as modified) on right (Burrige R. R., Graham, S&K Electronics, & Titan-Lincom, 2002)

The ERA rover was used in three main scenarios during testing near Flagstaff, Arizona in September of 2000. These scenarios were: power cable deployment, solar panel deployment, and a geology traverse. For the power cable and solar panel deployments, ERA autonomously followed the suited EVA astronaut while pulling a trailer that laid out the cable and flexible solar panel. ERA was used for these scenarios because both the cable and the solar panel material were too heavy and cumbersome for the astronaut to deploy. Also, the solar panel was required to be laid out as flat as possible. This was easily accomplished with the rover. During the geology traverse, ERA followed the suited astronaut while carrying tools and providing a space for samples. The astronaut would verbally command ERA to follow or stop, depending if he needed anything from the robot. During all modes ERA attempted to keep a fixed following distance from the astronaut by using its suite of sensors. An image showing the ERA in use can be found below.



Figure 5 - ERA Performing Test Scenarios – 2000 (Burrige R. R., Graham, S&K Electronics, & Titan-Lincom, 2002)

After this initial testing of ERA, the results and lessons learned were tabulated.

Among these lessons were some hardware considerations. While the rover had the battery capacity to assist during a full EVA, the battery capacity was roughly 90-120 minutes (Burrige R. R., Graham, Shillcutt, Hirsh, & Kortenkamp, 2003). This led the team to research ways to increase the “stamina” of the robot. Fuel cells were considered the prime technology for this.

Next, the rigid suspension was deemed inappropriate for the terrain. The suspension transferred the shocks of operation directly to the chassis and onboard instruments, and it also reduced traction when traversing obstacles. New designs would use 4-wheel independent suspension.

Lastly, the robot could only be used while close to an astronaut as it had no way of interacting with the environment. Future plans include a 7-DoF robotic arm that will be able to interact with the environment.

The second iteration of ERA took to the field for the 2002 field tests. This new and improved ERA utilized more robust computing hardware, a 7-DoF manipulator, a new mobility base, and fuel cell integration. The primary upgrades affecting this thesis are the new mobility base and the fuel cell integration.

The new mobility base was completely redesigned following the 2000 field trials. Since the old base was made of rigid links, whenever ERA encountered an obstacle it would lose traction on the other wheels. This would affect its ability to steer and maneuver through the environment. The new mobility base was designed to have 4-wheel independent suspension. This suspension was created using off-the-shelf ATV components.



Figure 6 - ERA and New Mobility Base (Burrige R. R., Graham, Shillcutt, Hirsh, & Kortenkamp, 2003)

In an effort to increase the stamina of ERA, a fuel cell was borrowed from JSC's Power Systems Division. This fuel cell, named IHOPP (ISRU Hydrogen/Oxygen Power Plant), is capable of providing up to 2kW of power for over 11 hours (Burrige R. R., Graham, Shillcutt, Hirsh, & Kortenkamp, 2003). This fuel cell allowed ERA to operate much longer than the lead-acid batteries alone.

The tests performed during this field session were geophone deployment, geology traverse, and operating with the fuel cell.

ERA saw two uses during geophone deployment. The first was to follow the astronaut while pulling a trailer full of geophones. The astronaut would then grab a geophone and

manually place each one. The second use saw ERA following the astronaut and placing the geophone via the 7-DoF manipulator at the astronaut's command. ERA struggled with the automated placement of the geophones. While attempting to place the geophone, the manipulator arm would routinely impact the ground and create a stall condition. This was caused by the software not accurately measuring the distance to the ground.

The geology traverse operated much like it did in the previous mission. Each geology traverse lasted about 20 minutes and ERA followed the astronaut through difficult terrain while performing autonomously approximately 90% of the time. In addition to following the astronaut, ERA also pulled the "Mobile Science Lab", nicknamed the science trailer. This science trailer was filled with geology tools that allowed the astronaut to perform initial analysis of a sample to determine if it was worth keeping or not.

The fuel cell experiment unfortunately hit some snags and didn't go as well as planned. Initially some problems with the new base's software prevented the fuel cell's use in the field. This was remedied by ERA pulling the fuel cell on a trailer. In this way, the fuel cell was proven to power both of the mobility bases. Another problem was

encountered when a crimped hose led to a fatal leak in the system which eliminated any further testing of the IHOPP.



Figure 7 - ERA Pulling IHOPP (Burrige R. R., Graham, Shillcutt, Hirsh, & Kortenkamp, 2003)

Some positive results were gleaned from the 2002 field exercises. First is the proven effectiveness of the new independent suspension mobility base. This mobility base was so successful that it inspired further unpressurized rover development at JSC. This new rover would be an unpressurized crew transport rover, later known as the SCOUT. Another result was the proven use of IHOPP to power the rovers. This would lead to greater fuel cell use in the future. The last positive result was the development of the science trailer. This mobile science lab would be a staple of Desert RATS for years to come.

Thesis Impact

The ERA project was the most directly applicable rover studied during the preparation for this thesis. The rover was designed to directly interface with astronauts and assist in a variety of ways during an EVA. This interaction included pulling a trailer with heavy objects (power cable and solar panels), pulling a trailer full of geophones,

placing geophones with a 7-DoF manipulator, pulling the science trailer, and providing storage for tools and samples. This rover also underwent a significant change between the first and second generation. This change to 4 wheel independent suspension allowed for greater maneuverability and provided rationale to follow this same path with the rover to be built at UND.

The ERA highlighted the necessity of an EVA assistant rover to be flexible, adaptable, and rugged. The rover needs to be powerful enough to pull trailers and objects through rough terrain and allow for the storage of samples and tools.

Electric Tractor

The electric tractor (ET) was a 6-wheel remotely controlled rover used for high-torque applications. The ET was equipped with a power winch, a dozer blade, and a hitch to haul the Chariot (an astronaut transportation device), the science trailer, and other heavy objects. This ET was used during the 2004 and 2005 D-RATS field simulations. An image of the ET pulling the Chariot and science trailer is shown below.



Figure 8 - ET hauling the Chariot and Science Trailer (Ross, Kosmo, & Janoiko, 2010)

The ET proved very effective as a means of transportation and as tractor, performing heavy tasks and pulling objects. In addition to the Chariot and the science trailer, the ET was used to pull an analog Martian power reactor into position. This simulation ultimately failed, as the reactor's sled was inadequately designed. It did highlight the utility of such a high torque vehicle available to the suited astronauts (Ross, Kosmo, & Janoiko, 2010).

Thesis Impact

The ET showed how valuable high-torque rovers are. High-torque motors allow the rovers to do “real work”, such as moving regolith or large pieces of machinery. The rover designed for this thesis should incorporate high-torque motors to further bolster its usefulness to the EVA astronaut.

K10

The K-10 rover is a robotic scout that can operate in both autonomous and tele-operated modes. K-10 was used in the 2006 and 2009 D-RATS simulations. While it was designed for use on the moon, the ideas generated by the rover are valuable and can be applied for the Martian environment. This rover uses a 3D scanning laser (LIDAR) to create 3D terrain models of the area it is inspecting. It is also equipped with a Giga-Pan camera, which allows it to take panoramic images containing more than 1 billion pixels. In addition, the K-10 is equipped with a microscopic imaging camera for taking detailed images of the ground, as well as a variety of surveying instruments. These instruments

include ground penetrating radar, penetrometer, and a neutron spectrometer to search for buried water ice (NASA, 2009).

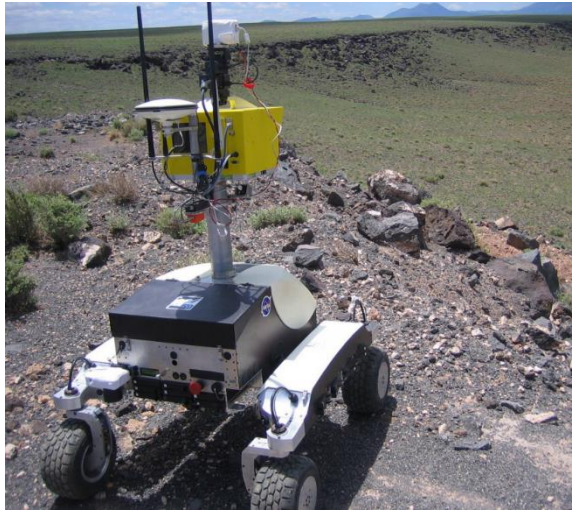


Figure 9 - K10 Rover (NASA, 2009)

This rover was used in the D-RATS simulations to scout an area prior to a planned EVA. This allowed the EVA participants to generate a better plan before encountering an area in person (Ross, Kosmo, & Janoiko, 2010).

Thesis Impact

Since this rover was designed to operate on the moon, it was meant to be operated remotely. Combining this remote control with the advanced scouting abilities of the K10 proved how effective scouting an area prior to an EVA was. Creating a rover that is capable of being used as a pre-EVA scout, as well as an EVA assistant, will be very useful.

Mobile Communication Networks

After the moon landings of the late 1960's and 1970's America set her sights on Mars. Over the years, NASA has developed numerous Mars reference missions. These

missions serve as a blueprint that show how the administration would get to, and survive on, Mars given the current and upcoming technologies at the time. The first Mars reference mission was published in 1997 and the latest addendum was published in 2013. Most Mars analog simulations have taken direction from these documents in one form or another. Technologies have been created that seek to fill an operational void that has been outlined by these reference missions. One such technology is a local wireless communications network.

The first study that looked to create a satellite independent EVA communication network is the 2001 study named “Communication System Architecture for Planetary Exploration.” This study took place at Houghton Crater in the Canadian high arctic. It looked to create an EVA communication architecture that utilized multiple low powered radio repeaters that would allow the EVA astronauts to communicate with the base from multiple kilometers away. The primary rationale for needing this type of ground radio network is because communicating with a satellite is inherently difficult. The ground transceivers need to be more powerful, have higher gain antennas, and be accurately pointed in order to transmit to, and receive from, the orbiting satellite. Providing the necessary equipment at a well-equipped base station usually is not a problem, but these hardware requirements quickly become excessive when trying to make systems small enough to be carried by an astronaut without becoming a burden. This is where the ground based radio repeater network comes into play. The vastly shorter communication distances mean that less powerful transceivers with either omnidirectional or wider-band directional antennas can be used. These local transmitters use between $10^3 - 10^8$ times

less power (30-80 dB) than a comparable satellite link (Alena, Gilbaugh, & Glass, Communication System Architecture for Planetary Exploration, 2001).

This communications architecture is not satellite independent. The base station is still connected to the orbiting satellite (or satellites) via a high power, high gain transceiver. The astronauts are connected to the base station via local radio repeaters. These repeaters can either be permanently placed, or they can be highly mobile. Utilizing both of these communications methods is called a hybrid communications architecture. The figure shown below gives a visual representation of this communication network.

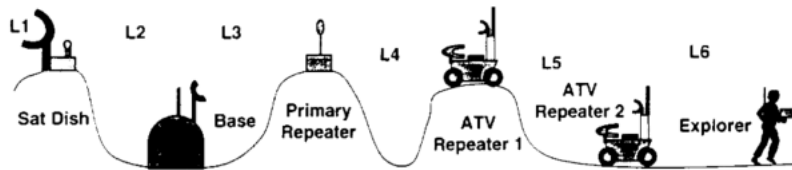


Figure 2. MEX Communications Architecture

Figure 10 - Hybrid Communications Architecture (Alena, Gilbaugh, & Glass, Communication System Architecture for Planetary Exploration, 2001)

One major advantage of the hybrid architecture is its flexibility. Since the repeater links can be moved to wherever they are needed, the astronauts have great flexibility with where they can explore. This allows the same repeaters to be reused in different locations time and again. This will save on launched and landed mass, as well as redundancy on the planet surface.

Another important aspect of this hybrid architecture is that it only needs to cover a 10 km radius from the base. Based on the recommendations from the Mars reference design missions, any EVA over 10 km from base will require the use of a pressurized rover capable of housing the astronauts for multiple days. Such rovers will be required to have their own satellite antennas to communicate with the home base or with Earth. Since the

pressurized rover will be acting as the new base, the same highly mobile repeater networks can be deployed from the rover ensuring the explorers remain in constant contact while on EVA.

These repeaters feature two methods of transmitting data. The first is an in-band, low bandwidth repeater featuring a single omnidirectional antenna. This in-band repeater uses a single radio transceiver. It receives a series of packets from the source, stores them in the radio's memory, and then retransmits them on the same frequency when the source stops transmitting. This allows a single radio to act as a repeater, but with the penalties of a low-gain antenna and a 50% duty cycle. The second type is a multi-band repeater. This system uses two radio transceivers operating on different frequency bands. Each of these radios will use a high gain directional antenna that will allow for the sending for more information. Using two radios in different bands allows for instant retransmission of the incoming data. Whatever is received by one antenna is instantly retransmitted on the other antenna. This allows for essentially lag-free communications. The penalties for this dual-band receiver are that it requires two radios and accurate pointing of the directional antennas. Both types of repeaters are packaged to create a repeater payload. Each repeater has different uses. The in-band, low-bandwidth repeater is primarily used for telemetry,

while the multi-band, high-bandwidth repeater is used for sensor data and video. An image of this hybrid repeater is shown below.

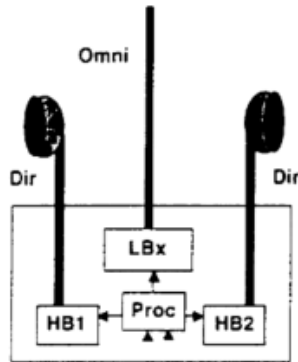


Figure 11 - Hybrid Repeater (Alena, Gilbaugh, Glass, & Braham, Communication System Architecture for Planetary Exploration, 2001)

Since these repeater packages were designed to be mobile they could be easily mounted to a mobile platform. This study utilized repeaters setup on ATV's. During this study, the astronauts would ride their personal ATV's to a location and would perform their EVA. One downside about having the transportation vehicle as the repeater is that in the event the EVA site is down in a valley, the ATV and repeater need to be placed on top of the hill to ensure line of sight with the previous repeater system. This leaves the astronaut to carry all the tools and samples down the hill to the EVA site.

This same relay configuration was used during the 2004 Mars Desert Research Station (MDRS) analog mission in Southwestern Utah. This analog mission lasted for two weeks and had EVA's in two different locations. One notable difference from the 2001 study is that the MDRS mission utilized that ERA rover mentioned in a previous section. In this study, ERA was a part of the repeater network and was used as a repeater node when the astronauts would venture into a crater or a ravine. Using the ERA as a communications repeater hadn't been attempted prior to this study (to my knowledge), so

it was revolutionary in that regard. A figure showing the communications architecture for this MDRS mission is shown below.

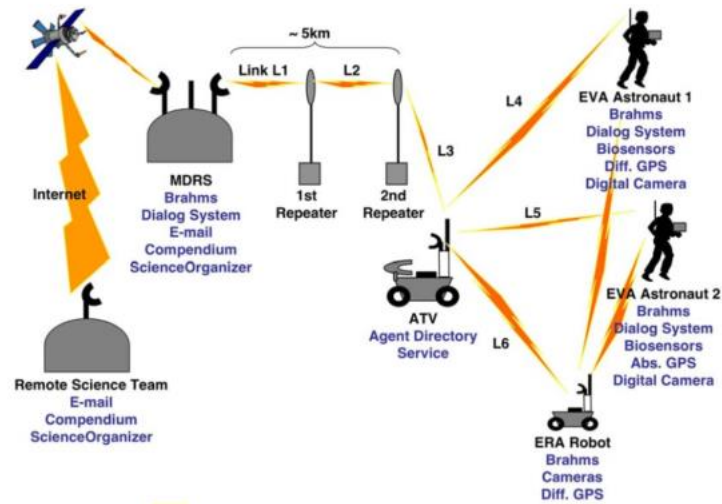


Figure 12 - MDRS Communication Architecture (Clancey, et al., 2007)

Thesis Impact

The communication architecture explained above allows for a highly flexible communications system that enables EVA astronauts to remain in constant communication with the base. This communication is essential because during a true EVA, if the astronaut gets injured or stranded there won't be support personnel around to help him or her. They will be relying on their fellow astronauts to come and save them, but once again, this only happens if the astronauts at base get the message that someone is in danger! This is why a robust communications architecture is so important. While the individual repeater modules used in the simulations were complex, humbler forms of a repeater system can be created to prove the effectiveness of such a system here at UND. In addition, this repeater system will be mounted onto the rover and will be a primary repeater, not just an emergency repeater in the case of ERA at MDRS.

Chapter 1 Conclusion

After analyzing the past studies and literature, the idea to create a new analog rover was fully formed. This rover would incorporate ideas and lessons learned from previous studies and introduce some new features. This new rover would incorporate the following features:

1. Controlled via remote control from the safety of the analog habitat.
2. Able to operate in remote and difficult terrain. Able to traverse hills and rocks.
3. Be of use to the EVA astronauts. Capable of storing tools, samples, and additional objects.
4. Utilize high-torque motors that will allow the rover to do “real work”, such as pulling heavy objects.
5. Be a communications hub for the EVA astronauts. Utilize radio repeaters to “bounce” signals to and from the habitat for an extended communications range without the need for satellites.
6. Have a live-feed camera on the rover to enable remote operation and terrain reconnaissance.
7. Able to be easily modified to accommodate future improvements and mission specific hardware.

Chapter 2 will discuss the design and implementation of the components used to construct the rover.

CHAPTER II - METHODOLOGY

The proposed solution is to create a tele-operated rover that will enhance the EVA experience for the astronauts. To accomplish this goal, the rover needed to be designed to be robust enough to handle the difficult analog Martian terrain and “simple” enough to allow for field repairs should the need arise. This required a design that would integrate elements and components of modern All-Terrain Vehicles (ATVs), robotics, and amateur radios. Getting these different elements and their related subsystems to mesh into a single cohesive package was difficult. The design decisions and associated rationale will be found in the following sections.

It is important to mention that the design was not a completely linear process as it will be laid out in this document. Certain design elements were seriously considered, but when the necessary components could not be found, or could not be found for a reasonable price, the design was forced to change. This caused a lot of iterative design, and required finding new solutions to previously solved problems. This is not a bad thing, on the contrary it shows how the project was able to adapt and change, but it will make the writing and reading process more difficult.

As with most complex systems, one design decision effects many other elements and it is not always obvious which decision influenced the other. Some subsystems develop organically and there was not a single, linear progression. One element was found, but then a constraint changed due to a newly changed element somewhere else, so the previous element was forced to change to accommodate the newly adopted design element, and so on. This recursive, iterative design is accepted and is the way most design needs to be done, but this method makes a comprehensive, linear document such

as this difficult to write. Essentially, keep this fact in mind while reading the following design sections. Just because a section comes before another does not mean that the latter section had zero influence on the design choices in the previous sections. Since every element of the rover was designed and manufactured by me, Chris Follette, the design was highly agile and interconnected. Having intimate knowledge of each component in each subsystem meant that, for the most part, each component was selected to make the entire rover better, not just allow the subsystem to operate.

Mechanical Design

The first problem to be tackled was the mechanical design. This encompassed all of the drivetrain, suspension, and frame components that make up the rover. Essentially, every physical part of the rover that is required to house the electronics and propel the rover.

Suspension

Rocker-Bogie

When the rover was first being conceptualized much effort went into designing a rover that would utilize the Rocker-Bogie suspension. This suspension system has been used by every NASA Mars rover beginning with Sojourner in 1996. This suspension possesses some fantastic qualities. Because of the geometry, no shocks or dampers are required. Also because of the geometry, all six of the wheels remain in contact with the ground at all times. Maintaining this contact allows the rover's weight to be distributed over each wheel. This is important when in soft terrain where excessive force can cause the wheel to sink and become stuck, rendering the rover incapacitated (Harrington &

Voorhees, 2004). This contact is also important during an obstacle traverse as it allows each wheel to help propel the rover over the obstruction.

When using the Rocker-Bogie suspension, each wheel uses its own drive motor and also has a “steering” motor that controls the direction the wheel is pointed. This steering motor allows the rover to perform very tight turns, and could even allow the rover to move horizontally. The drive motors are located inside the wheel and are usually geared down, creating large amounts of torque and slow linear velocities. The steering motors are located above the wheel, allowing for the entire wheel assembly to rotate. On the Mars Science Laboratory, only the front and back wheels have the steering motors. A picture of the Mars Science Laboratory, nicknamed Curiosity, is found below:

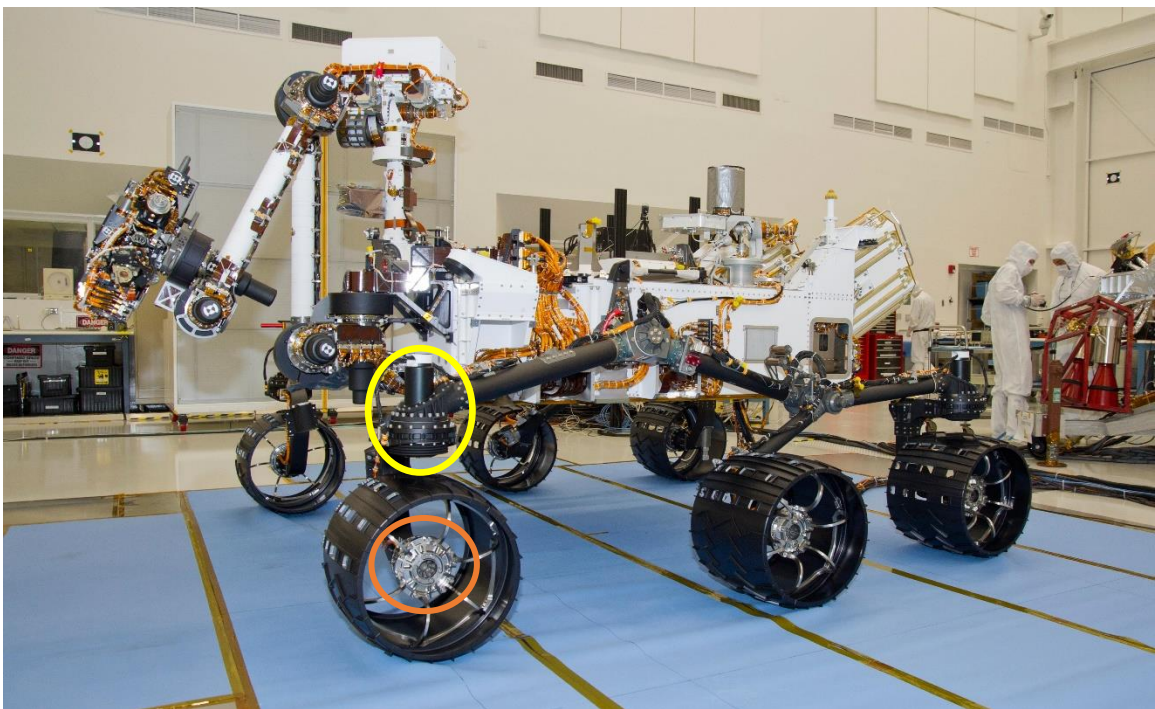


Figure 13 - Mars Science Laboratory (Webster, 2011)

In this picture the steering motor is circled in yellow and the driving motor is circled in orange. The top speed for Curiosity is 4 centimeters (1.5 inches) per second while traveling on hard, flat ground (Jet Propulsion Laboratory, 2016). This suspension

design allows the rover to traverse obstacles as large as, or slightly larger than, a wheel diameter, 50 cm or just over 20 inches in the case of Curiosity. These can be either a hole or a rock/obstruction.

The suspension also includes a differential that helps to even out the force exerted by the wheels. When one side of the suspension goes up, the differential forces the opposite side of the suspension down, thus balancing the weight on each wheel. This differential also causes the rover body to deflect half as much as the wheels, allowing for a smoother ride over uneven terrain when compared to more traditional ATV suspensions.

Unfortunately, after further research it was determined that this suspension is not ideal for an astronaut assistant rover. The rocker-bogie suspension was designed for slow moving, semi-autonomous rovers operating at centimeters per second, not the required 1+ m/s. Also, the independent wheel motors and steering motors proved to be an issue. Trying to find motors that were small enough to fit inside of a wheel while still providing the necessary torque and rpm proved impossible at the budget allocated for this project. It should also be noted that the rocker-bogie suspension does not handle obstacles well while traveling at astronaut speeds. This was analyzed in the paper titled “High-Speed Traversal of Rough Terrain Using a Rocker-Bogie Mobility System” by Miller and Lee. In this paper they say that typically the frame is not strong enough to withstand the forces encountered when hitting an obstacle at walking speeds and that the way rocker-bogies climb obstacles would cause the rover to be damaged or flipped. Miller and Lee developed a method of using image processing to speed up and slow down specific wheels that would allow the rover to “wheelie” over obstacles while at walking speed,

greatly reducing or eliminating the forces on the suspension (Miller & Lee, 2002). This method was too experimental and would require much more time getting the control system tuned in to be operational. The rover needs to be operational with as little “tinkering” as possible.

Dual H-Arm

After researching the Rocker-Bogie suspension and coming to the conclusion that it would not work for this rover, a new suspension had to be chosen. The main criteria for the suspension is that it needed to absorb obstacle impacts at relatively high speeds, allow the drive motors to be inside the body of the rover, and be able to be manufactured in the University of North Dakota machine shop. To meet these requirements, inspiration was taken from the commercial All-Terrain Vehicle market and the author’s previous experience. Commercially produced ATV’s almost all use some variation of a double wishbone suspension for both front and rear wheels. These ATV’s are built to perform off road and are powered using a motor-transmission system and utilize CV joints and shafts that transmit power to the wheels while overcoming obstacles. This system, once adapted to an electric rover, would perform fantastic.

Before designing the suspension, ATV hardware needed to be found. This hardware included the hub the wheel attaches to, knuckle, CV shaft and CV joints. These assemblies were sourced from ATV junkyards as purchasing these components new would have been far too expensive. The drive shaft assembly chosen, a rear 2006 Polaris Sportsman 500 axles and hub, will be discussed in the “Drivetrain – Drive Shaft” section.

Once the drive shaft assembly was chosen, found, and purchased, design on the suspension could begin. Suspension design is primarily dependent on geometry, so it needs to be designed around components that cannot change. For this design the primary dimensions that needed to be obtained from the drive shaft assembly were the distance between the top and bottom suspension mounting holes on the knuckle (D_1), the lengths between sides of the knuckle mounting holes (L_1 and L_2), the maximum degree of bend in the CV joints, and the overall length of the drive shaft assembly (L_0). This information would inform the lengths and angles of the suspension members.

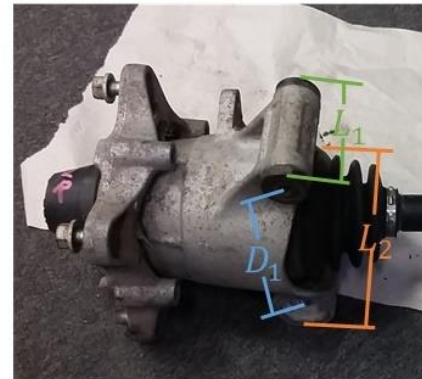


Figure 14 - Drive Shaft Dimensions

The dimensions found on the drive shaft assembly are as follows: $L_0 = 17$ in., $D_1 = 5$ in., $L_1 = 2.925$ in., $L_2 = 4$ in. . . . The maximum bend degree was found to be 30 degrees (Polaris, 2016). Using this information a 3d model of the driveshaft was created in Autodesk Inventor. This model was then used to inform the design of the suspension members.

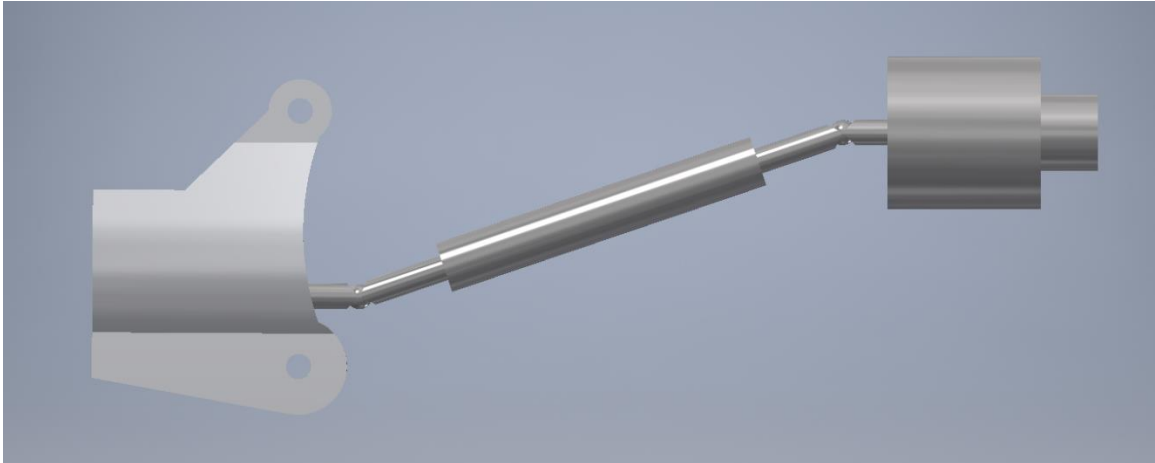


Figure 15 - Inventor Model of Polaris Drive Shaft

The rover will operate using a skid-steer, or tank-drive, method of locomotion. This means that the rover will turn when the wheels on one side of the rover are spinning faster relative to the other side. This relative speed difference will allow the rover to make basic meandering turns, as well as turning in place. This “tank-drive” method was chosen for a few reasons. One was that this method allows for the rover to operate without the need for “steering wheels” as found on a vehicle. This allows for all suspension, motor, and gearbox setups to be exactly the same. It also allows for a simpler remote control setup. Many off-the-shelf motor controllers specialize in this sort of “tank-drive” operation. These motor controllers will be discussed in the “Electronics – Motor Controller” section.

Since the rover will utilize the “tank-drive” method, an even more simple suspension system will be constructed. The double-wishbone suspension, as mentioned above, sees the suspension arms coming to a point, connecting to a ball-joint, and then attaching to the knuckle. These ball joints allow the wheel to rotate about the vertical axis created between top and bottom ball joints on the suspension arms. This rotation is what

allows the wheels to turn and “steer”. The figure below shows a standard double wishbone suspension.



Figure 16 - Double Wishbone Suspension (himalayan, 2012)

Since the rover’s individual wheels will not need to rotate about a vertical axis to steer, a dual H-arm suspension can be created. This H-Arm constrains the knuckle (and effectively the entire drive train) to only deflect vertically, as when going over an obstacle. This is another reason the 2006 Polaris Sportsman 500 rear axle and hub was chosen. This knuckle was originally designed to be used with an H-Arm suspension and only deflect vertically.

The suspension was designed in Autodesk Inventor and was influenced by the suspension design chapter in Milliken and Milliken’s *Race Car Vehicle Dynamics* (RCVD). In the subsection about H-Arm suspensions, the book notes that “the side view swing arm instant center must be at infinity” and that H-Arm suspensions require “only two chassis reaction points instead of three to perform its controlling functions” (Milliken & Milliken, 1995). This means that the top and bottom suspension arm attachment locations on the knuckle must be parallel and the suspension arm chassis attachment locations must be parallel to prevent binding while the suspension travels.

There are six degrees of freedom that will need to be accounted for when designing a suspension system: 3 rotations and 3 translations. Each DoF is along or about the primary X, Y, or Z axes. The 3 rotations are named Caster (X-Axis), Camber (Y-Axis), and Toe (Z-Axis) and the 3 translations are named Scrub (X-Axis, Lateral), Longitudinal (Y-Axis), and Bump/Jounce (Positive Z-Axis) or Rebound/Droop (Negative Z-Axis). A picture showing this geometry is found below.

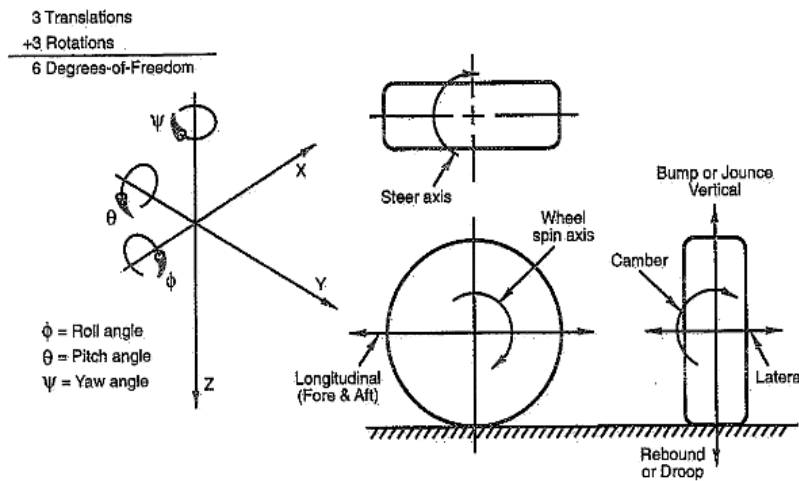


Figure 17.1 Degrees of freedom and suspension motion definitions (Ref. 1).
Figure 17 - Degrees of Freedom and Suspension Motion (Milliken & Milliken, 1995)

Because the rover will utilize an H-Arm suspension, many of these DoF's are already accounted for. The Toe (Yaw angle) will be 0 degrees while using the H-Arm suspension due to the parallel axes formed between the knuckle-suspension attachment and the suspension-chassis attachment and because the individual wheels will not be required to rotate to steer. The Caster (Roll angle) of the suspension will also be 0 degrees since the suspension will be designed and built to have a vertical motion path. The Longitudinal translation will be 0 inches because the Caster angle is 0 (vertical motion). The Camber angle and Scrub will be determined by the Instant Center length and suspension geometry, and the Vertical translation will be determined by the shock

characteristics and allowable CV shaft angles. To show how the Camber angle is determined by the IC length, see the figure below.

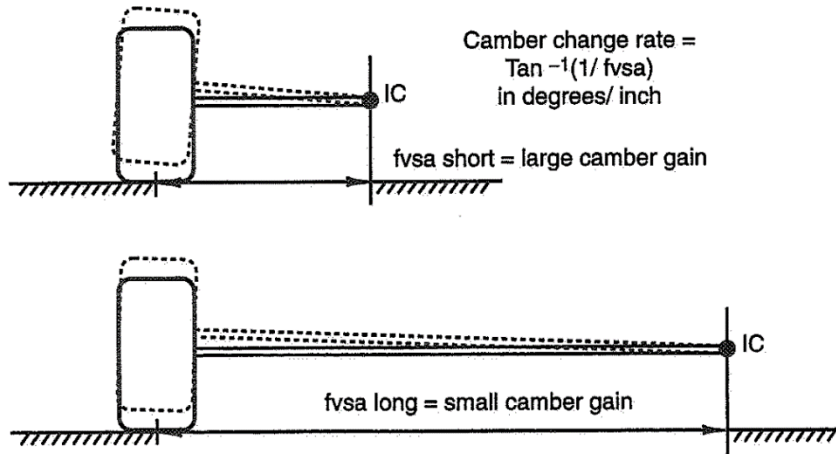


Figure 17.9 Camber change.

Figure 18 - Camber Change due to Front-View IC Length (Milliken & Milliken, 1995)

As seen in the above image, camber change rate is directly correlated to the Front View Swing Arm (FVSA) length. This FVSA is the theoretical member connecting the tire knuckle to the Instant Center. The instant center (IC) is a term used in suspension design and can be created in both the side view and the front view. It is an imaginary point that the wheel will pivot around during suspension travel. This point is found by projecting the suspension arms until they cross paths. The suspension can then be modeled by a single bar linkage originating from the IC. The wheel will essentially follow this imaginary circle created around the IC during its travel up and down the suspension's path of motion. An important clarification is that the IC only models the suspension at the point it was created, plus and minus a small amount of suspension travel. The IC can be thought of as a local, visual predictor of the suspension motion. In order to model the entire suspension path this way, many IC's will need to be created at different points along the suspension path. For instance, creating IC's at different points

is a simple way of testing a suspension for rates of camber change. This concept is explained in the following image taken from RCVD.

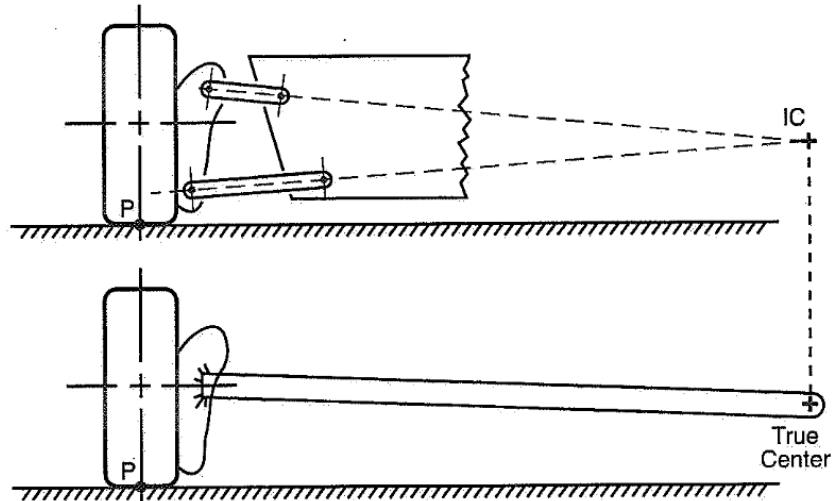


Figure 17.5 Instant center concept.

Figure 19 - Instant Center Concept (Milliken & Milliken, 1995)

The camber change rate is calculated using the equation in Figure 18 and is given the units of degrees per inch of vertical travel. As mentioned earlier, a larger distance between the IC and the wheel will result in less wheel camber throughout the suspension's path of motion. This equation can be found below:

Equation 1

$$\text{Camber Change Rate} \left(\frac{\text{degrees}}{\text{inch}} \right) = \tan^{-1} \frac{1}{FVSA}$$

Next is wheel scrub. Every suspension system will have some amount of scrub. This amount is determined by the length of the control arms and the location of the front view instant center. For scrub to be minimized, the IC needs to be large and located on the ground. When the IC is located above ground level, the wheel will move outward as it rises. When the IC is located below ground level, the wheel will move inward as it rises. The two following figures will further explain wheel scrub. The first will show wheel

scrub in relation to IC location. The second will show a top view of a wheel driving in a straight line while hitting obstacles, forcing the wheel to jounce and rebound resulting in scrub.

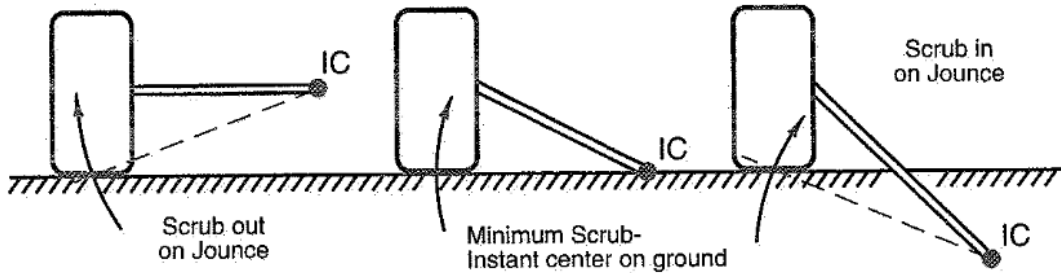


Figure 17.10 Scrub is a function of IC height.

Figure 21 - Scrub as a function of IC height (Milliken & Milliken, 1995)

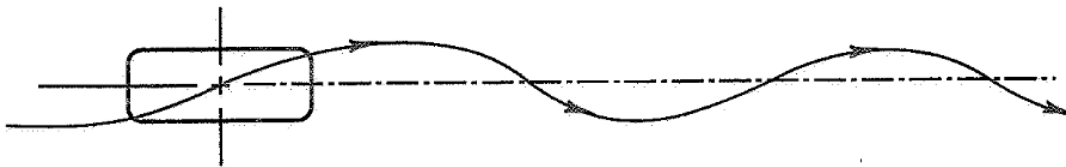


Figure 17.11 Wheel path on rough road with a large amount of scrub.

Figure 20 - Wheel path showing the effects of scrub (Milliken & Milliken, 1995)

When designing the H-Arm suspension of the rover, a large FVSA was chosen. This is because a large FVSA would result in a low rate of camber change and would also reduce the amount of scrub seen by the tire. In order to create a large FVSA, the suspension arms need to have a slightly larger vertical separation on the knuckle than on the chassis. This was accomplished by modeling and tweaking the suspension in Autodesk Inventor.

One of the main problems to overcome was the large amount of material on the CV shaft right before the splined section that is meant to fit into the gearbox on the Polaris Sportsman ATV. This material measured 3" in diameter and the suspension mounting holes on the knuckle measured 5" center to center. In order to produce an

adequate FVSA the chassis suspension mounts were required to be less than the 5" center to center distance on the knuckle. Attempting to design suspension mounts and frame members which allowed the chassis suspension center to center distance to be less than 5", while not impacting the 3" diameter spinning mass on the CV shaft, proved to be challenging. To alleviate this problem, the knuckle suspension center to center distance needed to be increased to a value such that a frame could be constructed that allowed for the 3" diameter CV shaft to rotate unimpeded while still having a smaller suspension center to center distance than the knuckle. To do this, a 3.125" member was added to the top suspension member at a 45° angle. This allowed the top suspension member to artificially increase the knuckle center to center distance by 2.21" without needing to actually increase the knuckle's physical size. The figure below shows this top suspension member on the knuckle.

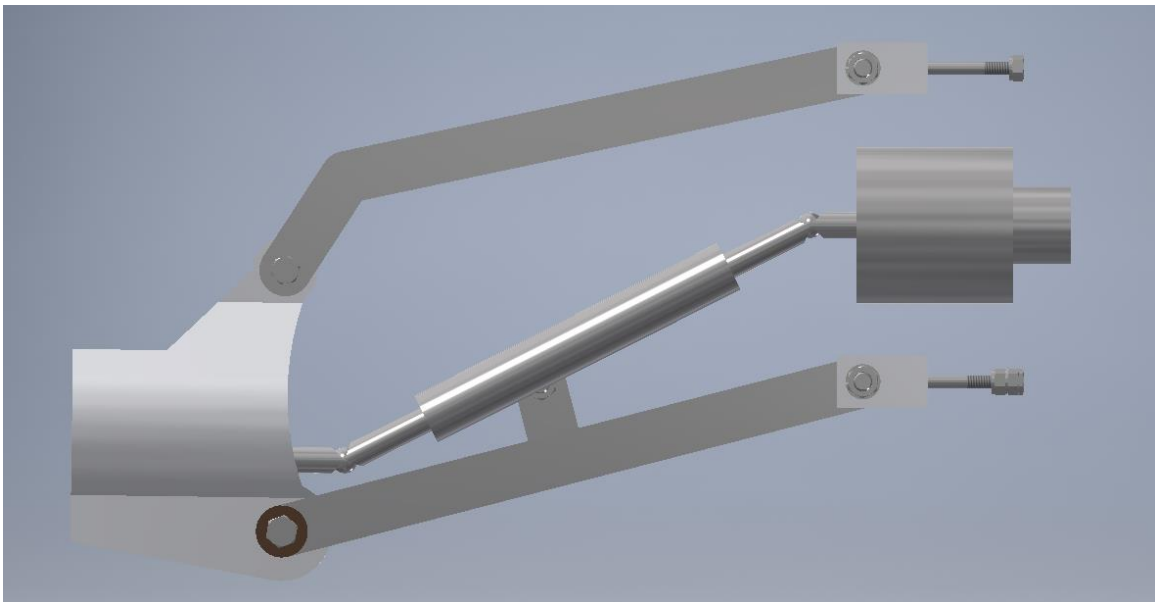


Figure 22 - Suspension Members on Knuckle

This increased knuckle center to center distance allowed for the chassis suspension supports to be placed at 6", allowing for adequate margins around the 3" CV shaft rotating mass. Although the angled piece on the top suspension member allows for the greater center to center distance, it also alters the suspension's camber and scrub characteristics as the point of rotation on the knuckle isn't directly in line with the top suspension member. This was deemed acceptable for two reasons. First, at the relatively slow speeds the rover will be operating the altered camber and scrub experienced by the tire will have negligible effects on overall performance. Second, the rover will be operating at the lower range of the suspension travel since the suspension was designed to operate primarily in this region. At the lower end of suspension travel the camber and scrub values are moderate. The figures below shows the IC for this suspension in maximum and minimum travel location.

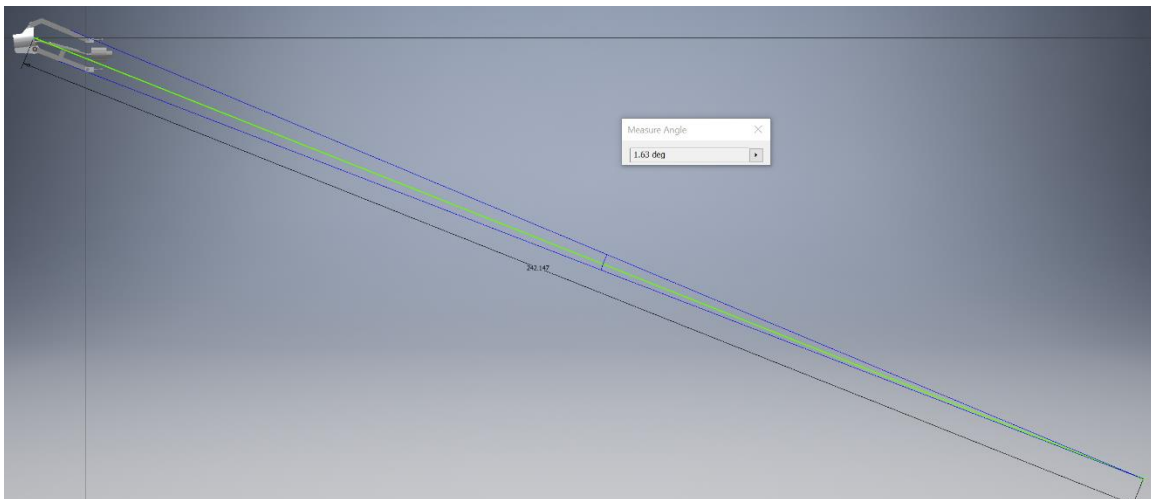


Figure 23 - FVSA Top of Travel

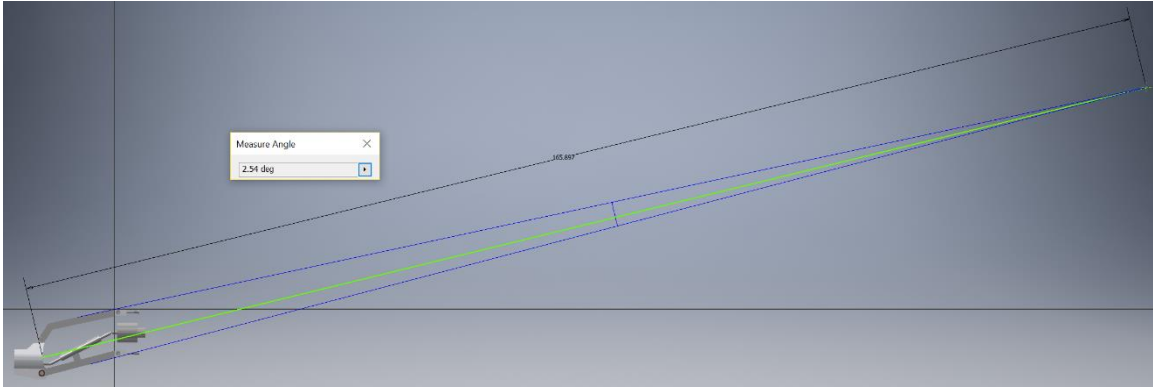


Figure 24 - FVSA Bottom of Travel

The swing arm lengths are 242.147” and 165.897” for the top and bottom, respectively. Based upon these images the expected camber changes would be very slight and the suspension would scrub away from the chassis on jounce while near the bottom of the suspension travel and would scrub towards the chassis on jounce near the top of the suspension travel.

Using the model, incremental measurements of the camber and scrub were taken. To normalize the information, values for the scrub and suspension travel were taken relative to the lowest point of suspension travel. The camber angle was found by measuring the angle formed by the flat face of the knuckle and a vertical plane. The wheel’s axis will be normal to this knuckle face. Directions of the camber angles are seen in the picture below:

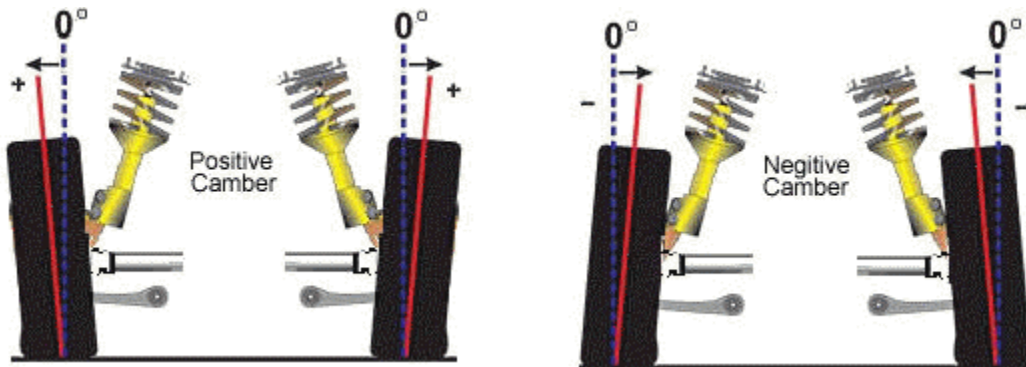


Figure 25 - Direction of Camber Angles (Auto Dimensions Inc., n.d.)

Plots of the camber and scrub characteristics are found below.

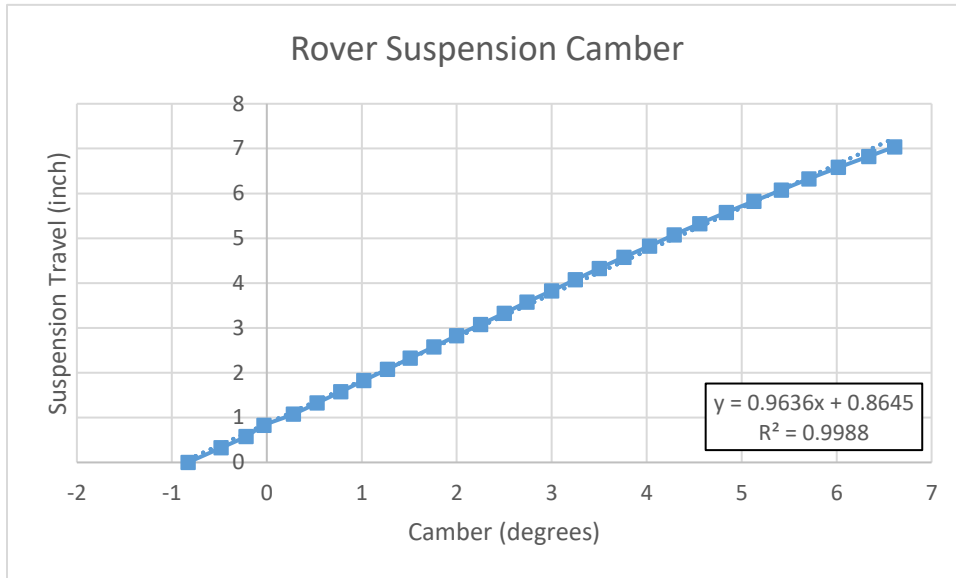


Figure 26 - Rover Suspension Camber

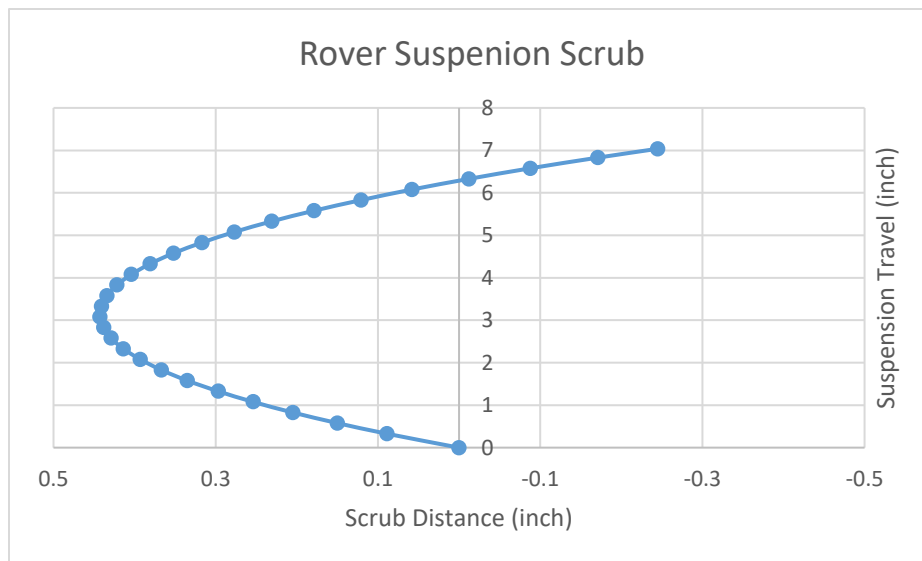


Figure 27 - Rover Suspension Scrub

The camber graph in Figure 15 shows that at the bottom of the suspension path the wheel has a slight negative tilt, changing quickly to a positive tilt. This camber change is nearly a 1:1 linear change with suspension travel with a slope of 0.9636 and a R^2 value of 0.9988. As the suspension reaches the top half of the suspension path, the

camber begins to get a little extreme with angles of 4°-7°. Ideally the suspension will not deflect this high, except under rare circumstance.

The effects of the angled member on the top suspension member are most evident on the camber. Based on Equation 1 and the FVSA lengths found in Figures 23 and 24 the camber change rates at the top and bottom of suspension travel are supposed to be 0.236°/inch at the top and 0.345°/inch at the bottom. Instead of these very small camber rates, the camber change rate that was measured is a consistent rate of change of nearly 1°/inch. This is fairly large, but is acceptable given the use case of the rover.

The scrub graph seen in Figure 27 shows scrub direction as expected by the location of the IC's in Figures 23 and 24. The suspension has a maximum scrub value of 0.443" at just over 3" of suspension travel. These values are within a tolerable range, so the design was finalized. Full engineering drawings can be found in the Appendix. A stress analysis can be found in the Stress Analysis section.

Shocks

The shocks for this rover needed to be ATV quality and capable of the abuse present in an off-road environment. Seeing as the suspension and the frame were custom fabricated, the shocks primary requirements were that they:

1. Could support the weight of the rover and the planned additional payload without excessive droop.
2. Provided adequate travel to allow the suspension through a large range of motion.

These relatively simple requirements allowed for a wide range of shocks to be considered. Also of note is the speed of the rover. Typical ATV's need to perform in off-

road situations while traveling upwards of 15 miles per hour (6.7 m/s). Because this rover would top out at 1.5 m/s the shock load on the rover would be less extreme than that seen by a typical ATV suspension. Once again, price played a big factor in determining which shocks would be chosen. Because of this, aftermarket shocks were purchased from eBay for much less than OEM shocks.

Two pairs of shocks (four total) capable of fitting the 2004 Honda Foreman 450 ATV were selected because of their favorable characteristics. These coil-over shocks have a travel length of 4" and feature 5 different spring pre-load positions for varying loads. The 4" travel will work because the shocks can be mounted at a position on the suspension member that will allow for near full suspension range of motion. The Honda Foreman 450 ATV has a dry weight of 264 kg (ATV.com, 2017). Add in fuel and the weight of a rider and this mass increases to 376 kg. Divide that mass by the 4 wheels, and each wheel is expected to support up to 94 kg while in motion. This is more than the expected rover mass (see Motor section below), and because the rover will be operating slower than the ATV, these shocks are expected to perform adequately. To accommodate these shocks, tabs needed to be welded to the inner suspension member of each suspension system. The location was chosen to protect the shocks from debris encountered while driving the rover in the field. The location of the tabs and the frame member can be found in the Engineering Drawings Appendix.

Suspension Stress Analysis

In order to properly construct the suspension system, a stress analysis needed to be performed. This analysis tested whether the suspension system would fail during the anticipated loading scenarios. The section discussing the motor selection uses a per-wheel

weight of 76.25 kg (167.75 lb.) and an overall rover weight of 305 kg (671 lb.). These forces were used in during the stress analysis to simulate different loadings. The loading scenarios tested were: a single wheel 1-g and 3-g vertical load, and a full rover 1-g and 2-g horizontal load. To test the suspension a simplified model of the suspension was created. This model includes the suspension tube dimensions and materials, but eliminates the extra components such as bushings and bolts. These components are necessary in the real life model, but were shown to make the simulation process very lengthy and complex. The simplified model also uses an inverted “T” member as the driveshaft knuckle. This was to simplify the model and aid in the simulation.

The vertical load cases occur when the rover encounters an obstacle while at speed or when a wheel suddenly clears an obstacle and falls back to the ground. The positive vertical loading occurs in the center of the driveshaft knuckle, with an equal negative loading occurring where the shock attaches to the lower suspension arm. The results are shown below:

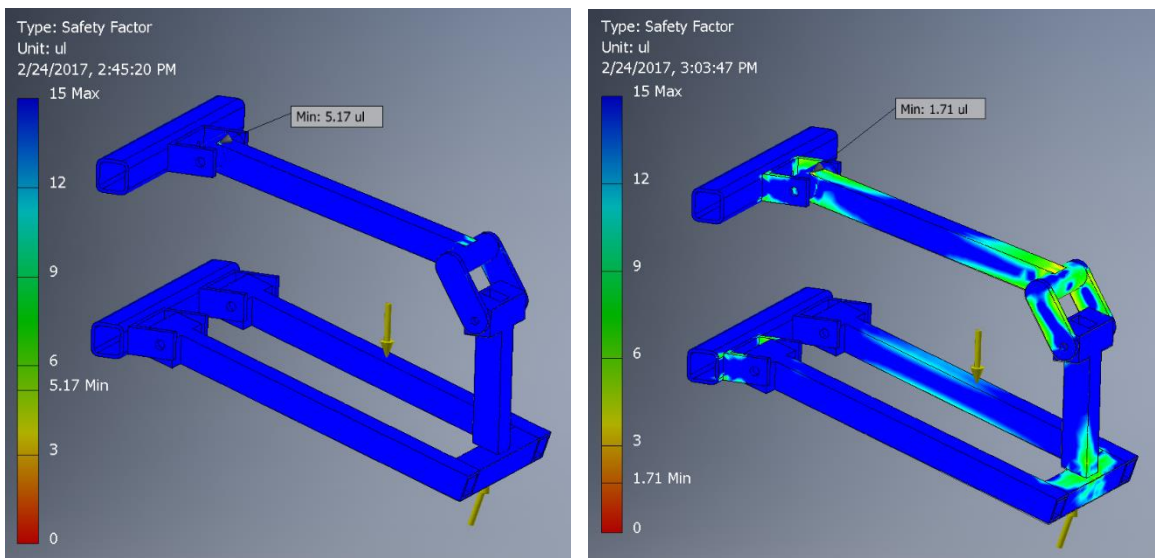


Figure 28 - Suspension FEA - Vertical Loading 1-g and 3-g

As seen in the above images, the suspension system will survive 1 & 3-g vertical loadings. The smallest factor of safety found on the aluminum frame, aluminum brackets, and steel suspension members was 5.17 for the 1-g and 1.71 for the 3-g loading scenarios. This proves that the suspension design is adequate for the vertical loading scenario.

Next the horizontal load cases were tested. The most extreme load cases were tested, because if the suspension could survive these cases all other cases with less extreme loads would not yield the suspension. Because of the design of the rover, the wheels do not project in front of the rover frame. This means that if the rover were to impact a solid object with a wheel, this object would only encounter one wheel and that wheel would have the entire force of the rover behind it. Luckily in real life, the ATV wheel would absorb some of the impact and lessen the impulse seen by the suspension member, but this is difficult to simulate. As was mentioned above, the worst case scenarios were tested. The loads tested were the full mass of the rover impacting a single rover wheel horizontally with accelerations of 1 and 2 times the Earth's gravity. This equated to forces of 3,021 N (671 lb.) and 6,042 N (1242 lb.). The simulations are found below:

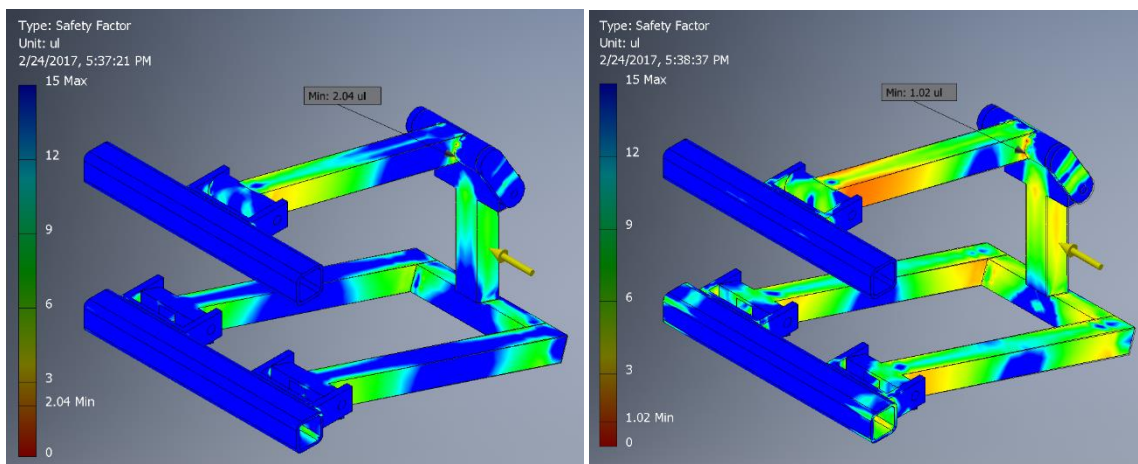


Figure 29 - Suspension FEA - Horizontal Loading 1-g & 2-g

The factors of safety for the horizontal loadings are 2.04 and 1.02 for the 1-g and 2-g loadings, respectively. This shows that the suspension can sustain an impact from a direct horizontal force up to 2-g, or $19.62 \frac{m}{s^2}$. With the rover cruising at the design speed of 1.5 m/s, this 2-g deceleration yields an impact time of 0.0765 seconds. In real life, this impact would be longer because of the yielding of the ATV tire, and the increased impact time decreases the acceleration experienced by the system. As stated above, these simulations aim to test the worst case scenarios experienced by the rover.

If the rover experiences loads that are below the loads tested, the suspension will not yield.

Drivetrain

Motor

For this vehicle DC-electric motors were chosen. The torque-rpm relationship allows these motors to deliver instant power without relying on a “power band” as seen with internal combustion engines. Also, electric motors allowed for a much simpler “remote control” design architecture. This allows the rover to use off-the-shelf motor controllers and essentially turns the rover into a large remote control vehicle. The large difference is that this rover will be hundreds of pounds and will be able to haul substantial amounts of cargo.

The first step in motor selection is to develop an estimate of required power. There are many definitions for power; the definition used during initial motor selection was:

Equation 2

$$P = T * \omega$$

This definition yields power (P) in Watts (W). The inputs include motor rotational velocity, ω (radians per second) and motor torque, T (Newton-meters, N-m). This can be transformed to a more useful equation that uses rotations per minute (RPM).

Equation 3

$$P = \frac{T * RPM}{9.55}$$

For the purposes of this design, the rover needs to keep pace with suited astronauts (RPM) and be able to operate while hauling cargo (Torque). These two requirements have an inverse relationship when applied to electric motors. Theoretically, while an electric motor is initially starting (RPM=0) it will experience a condition of infinite torque. As the RPM's begin to increase, the torque will be proportionally reduced to match the motors specified power rating.

To generate this initial power estimate a few assumptions needed to be made. First was the required RPMs. The average human walks at a pace of 1.42 m/s (Browning, Baker, Herron, & Kram, 2006), so the required motor RPM's and wheel diameter needed to be sized to meet this figure. To simplify the calculations a value of 1.5 m/s was used. Next was the wheel diameter. Since this vehicle will be an off-road vehicle, ATV tires were chosen. These tires have large tread patterns that generate traction in off-road situations where driving conditions are often sand, soil, or loose rocks. A standard ATV tire with a diameter of 22 inches (0.5588 meters) was chosen. Using this information, the required RPM's could be calculated.

The first step was to determine the total distance covered in one minute. This was a simple calculation using the average human walking speed (1.5 m/s) and the chosen length of time, one minute (60 seconds).

Equation 4

$$d = v * t$$

Substituting human walking speed (1.5 m/s) for v , and 60 seconds for t , the total distance covered by the average human walking in one minute, d , is 90 meters.

Next, the circumference of the wheel needed to be calculated to determine how much ground would be covered during a single rotation (assuming no-slip conditions).

Equation 5

$$Circumference = \pi * diameter$$

Substituting 0.5588 meters for the wheel diameter, a circumference of 1.755 meters was calculated. Using the results from Equations 4 & 5, the estimated RPM's can be calculated. This will be accomplished by dividing the length of travel in one minute by the length of travel of a single rotation by the wheel.

Equation 6

$$RPM = \frac{d}{circumference}$$

Substituting values into Equation 6 yields a value of 51.28 wheel rotations per minute. This figure allows for initial motor selection based on RPM.

The next parameter that needed to be calculated was approximate torque. This was a difficult parameter to estimate as it relies on many factors. These include: chassis weight, battery weight, payload weight, hill-climb angle, linear acceleration, and towing

capacity. To begin, a few weight estimates were written down to get started. These can be found in the table below:

Table 1 - Weight Estimates for Motor Torque

Item	Quantity	Mass (kg)	Total (kgs)	Total (N)
Battery	4	25	100	981
Frame	1	35	35	343.35
Suspension Arms	8	5	40	392.4
Shocks	4	5	20	196.2
Shafts, hubs, etc	4	10	40	392.4
Electronics	1	20	20	196.2
Payload	1	50	50	490.5
		Total =	305	2992.05
		Weight per wheel =	76.25	748.0125

According to these estimates, the rover is projected to have a mass of 305 kg with a loading of 76.25 kg at each wheel (assuming an equal load distribution). Many scenarios and torque estimates can be created using this information. First, a free-body diagram (FBD) was created to show the forces at work on each wheel.

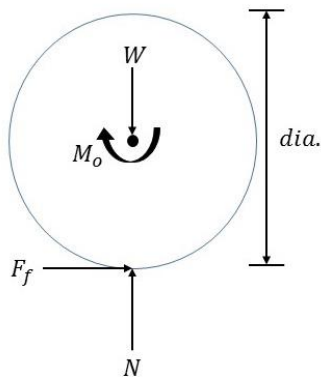


Figure 30 - Free-Body Diagram of the Rover Wheel

In this FBD the variables are:

W = rover weight acting on the wheel

Dia. = Wheel diameter (m)

M_o = Moment created by the motor torque

F_f = Force of friction opposing motion

N = Normal force on the ground due to W

The first simulation will be the rover rolling over loose sand on flat ground. In this simulation the motor torque will need to overcome the force developed by the tire's rolling resistance. This rolling resistance is a function of the normal force on the wheel and the coefficient of rolling friction between the tire and the surface. The coefficient of rolling friction was found to vary from 0.2-0.4 (Engineering Toolbox, 2016). The worst case scenario of 0.4 was used in this simulation. The equation for the rolling resistance is the coefficient of friction multiplied by the weight placed on the wheel.

Equation 7

$$F_f = c * N$$

To solve for the required motor torque, a sum of moments about the tire center was performed.

Equation 8

$$\sum M: M_o - F_f \left(\frac{dia}{2} \right) = 0$$

Which simplifies to:

Equation 9

$$\sum M: M_o = F_f \left(\frac{dia}{2} \right)$$

This means that the motor needs to produce enough torque to overcome the moment created by the rolling resistance friction force. The friction force will produce a moment on the tire with a moment arm equal to the radius of the tire. Plugging values into Equation 9...

Equation 10

$$M_o = (0.4 * 748.0125 N) \left(\frac{0.5588 m}{2} \right)$$

From Equation 9, the maximum motor torque required to overcome the rolling resistance is 83.597 N-m.

Using Equation 3 and the values obtained from Equations 6 and 10, the calculated power required to drive the rover over sandy soil is 448.77 Watts. This value will increase with additional payload on the rover, and will decrease while driving on compacted, smooth terrain. As a note, the rolling resistance value is taken from a table for a car tire driving through loose sand. It can be assumed that ATV tires with the additional knobs and aggressive tread will increase this rolling resistance coefficient. This estimate also does not take drive train efficiency into account, which will require a motor with more power.

The next scenario used to size the motors was the hill climb. During this scenario the rover will be driving up an incline and will need to overcome the rolling resistance of the tires and the gravitational effects of the rover mass trying to pull the rover back down the incline. A FBD for this scenario can be found below:

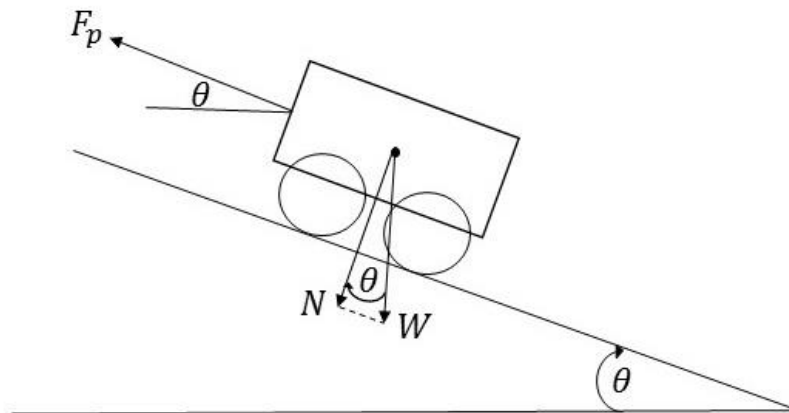


Figure 31 - Hill Climb FBD

The equation for the hill climb is fairly straight forward and can be found below:

Equation 11

$$F_p > F_{rr} + W \sin \theta$$

This states that the pulling force (F_p) must be greater than the rolling resistance and the component of the weight opposing forward progress up the hill. This will be evaluated on a per wheel basis while assuming an equal load on all tires.

For this situation, the normal force (N) transferred to the ground through the tires will be a function of the rover weight (W) and the angle of the incline (θ):

Equation 12

$$N = W \cos \theta$$

For this scenario, the incline angle will be 40 degrees. Using the value of weight per wheel, W, in Table 1, the value found for N was 573.011 N. Using this new normal force the rolling resistance can be calculated for this scenario. The rolling resistance will be calculated as explained above in Equation 7. Using the same coefficient of rolling resistance ($c = 0.4$, loose sand), the rolling resistance force generated was 229.2 N.

The force pulling the rover down the hill was calculated next. This was a simple calculation multiplying the weight of the rover by the sin of the incline angle. Using the values above, this force was found to be 480.81 N. Combining these two opposing forces yields a total of 709.41 N. This means that each motor needs to produce greater than 709.41 N of linear force to propel the rover up the hill. Replacing the friction force in Equation 7 with the total opposing force found above, the moment equation was performed for this scenario. The required torque for an uphill climb in sandy soil is 198.378 N-m.

Using the power equation (Equation 3), the torque found above, and the calculated RPM's for 1.5 m/s travel, the total motor power needed for this maneuver is 1064.98 Watts per wheel.

Also of note in the hill climb scenario is that the static friction force needs to be greater than the force pulling the rover down the hill. If not, the rover will simply slide down the incline. This static friction force is calculated in the same way as the rolling friction force, substituting the coefficient of static friction for the coefficient of rolling resistance.

The final scenario was the tow scenario. For this simulation the rover would be pulling or pushing some object. Once again, the rover would be operating in sandy soil with a coefficient of rolling resistance of 0.4. It was assumed that the object being pulled was a trailer with 4 wheels that are able to fully support and stabilize the weight of the trailer. This assumption allows for a rolling resistance to be calculated for the trailer as opposed to pulling some object over top of the soil where the higher static and dynamic friction coefficients would be used. The rolling resistance forces were calculated the same way as they were for the rover wheels. For this scenario, a trailer mass of 300 kg was used. This created a total rolling resistance force of 1172.2 N. Assuming that the weight was distributed equally over the four wheels, this leaves 294.3 N of rolling resistance for each wheel. This per wheel force will be applied as an opposing force (acting in the same direction as rolling resistance) that each motor will need to compensate for. The trailer rolling resistance force and the rover's rolling resistance force will combine in the moment equation (Equation 9). The resulting torque required to pull a

300 kg, 4 wheeled trailer through sandy soil is 165.8243 N-m, which translates to 890.2 W of motor power.

It should also be noted that a vehicle cannot pull more than the traction force will allow. This traction force is the force created between the wheels and the driving surface. This force is dependent on the vehicle weight fraction acting on that wheel and the traction coefficient between the tire and the driving surface. It is another type of friction force, but instead of opposing motion it allows for the wheels to transfer power to the ground and propel the vehicle forward. This traction force becomes obvious when comparing vehicles trying to accelerate from a stop light in different conditions. During the summer months when the asphalt is dry, accelerating is not an issue, but during the winter months when the intersection becomes covered in ice, the same vehicle may spin its tires without being able to “get a grip” and move forward. This is due to the lower traction coefficient of ice compared to dry asphalt. This becomes an issue while towing because it may be possible to “overload” a vehicle to where the force required to pull an object is more than the vehicle’s traction force on the drive wheels will allow. Different tires and different surface conditions create a vast array of traction coefficients. The knobby design of off-road tires allows them to generate a larger traction coefficient, but this will also increase the rolling resistance coefficient. Like most design considerations, there is a trade-off between different factors and each weighs in for determining what the final selection will be.

After generating the values above, a table was created to centralize the data and more easily display it:

Table 2 – Calculated Rover Motor Specifications

Calculated Rover Motor Specifications			
Scenario	RPM	Torque (N-m)	Power (W)
Flat Driving	51.28	83.597	448.77
Hill Climb (40 degree)	51.28	198.378	1064.98
Flat Tow (300 kg)	51.28	165.8243	890.2

Using this data a motor could be selected. One point to note is that the power needed to be generated by the motor is determined by torque and RPM (Equation 3), so the necessary power could be reduced if a slower speed was deemed acceptable. This slower speed could be used during a hill climb and a tow, depending on how much of a slowdown is acceptable. While generating this data no experimental data was found about minimum rover velocity, so the full-speed velocity was used. In this way the motor and resulting drivetrain components would be able to handle almost anything the analog astronauts threw at them.

Finding a motor that could produce this much torque and the required RPM's was extremely difficult. After much searching, high powered electric scooter motors were found at MonsterScooter.com. These motors are simple high torque brushed electric motors and don't require complex and expensive motor controllers. A picture of the chosen motor is shown below:



*Figure 32 - 24 Volt 900 Watt XYD-13 Electric Motor
(Currie Technologies, n.d.)*

This motor is a 24 Volt, 900 Watt DC-electric scooter motor. It has a maximum RPM of 2600, way over the requirement of 51 RPM. In addition to meeting the power requirement most closely for all analyzed scenarios, another practical consideration used was cost. Throughout the search for motors, three high powered DC-electric motors were found, all scooter motors in this family. The three motors had powers of 450, 750, and 900 Watts. The 450 Watt motor cost \$64.99, the 750 Watt motor cost \$124.99, and the 900 Watt motor cost \$168.99 (Monster Scooter Parts, 2016). Considering that the 900 Watt motor wasn't excessively more than the 750 Watt motor, the 900 Watt motor was chosen. The rationale behind that choice was that since this rover is envisioned to be a valuable piece of research equipment for the Human Spaceflight Laboratory and UND for

the foreseeable future, it would be more cost effective to purchase the highest performing motors during initial construction than it would be to retrofit the rover with more powerful motors at a later date if more power was required. Considering that each wheel is independently powered, four motors are needed. Selecting the most expensive motors is a significant portion of the overall cost for this rover, but it will allow this rover to only be limited by what future researchers envision for the rover instead of the rover's physical capabilities.

Gearbox

Since the selected motors have such a large maximum RPM and the rover only needs 51 RPM, a gearbox was required to reduce the rotational velocity output. Also considering the large amounts of torque required to move the heavy loads in rough terrain, a heavy-duty, industrial quality gearbox was needed. The gearbox chosen was an Anaheim Automation 10:1 planetary gearbox. This particular gearbox, the GBPH-0901-CS-010 boasts a maximum output torque of 419.96 N-m, is rated for an input velocity of 2900 RPM, and has a mass of 3.5 kg (Anaheim Automation, 2016). Both of these values exceed the maximum values found in the previous section (motor rated at 2600 RPM and maximum necessary calculated torque of 198.378 N-m), so the gearbox should operate

during all conditions the rover finds itself in. A picture of the gearbox can be found below:



Figure 33 - Anaheim Automation 10:1 Planetary Gearbox (Anaheim Automation, n.d.)

Engineering drawings taken from the producer’s website can be found in “Appendix A – Manufacturer Engineering Drawings”.

Driveshaft

The driveshaft connects the output of the gearbox to the wheel on the ground. The driveshaft is made up of two constant velocity joints, a splined input, a half-shaft, and the output which is connected to the bearing carrier/knuckle and the associated hardware to attach the wheel. This assembly is of the utmost importance. If a component in this assembly fails, the rotational output from the motor/gearbox will be unable to turn the wheel. Due to the importance and complexity of this assembly, it was decided to purchase a used ATV driveshaft assembly rather than attempting to construct or buy the components piecemeal. As was discussed in the Suspension section, a rear driveshaft was chosen because the knuckle was designed for an H-arm suspension and to only deflect vertically.

Due to the large torque loads the drive shaft will encounter during the conditions outlined in the Motor section above, calculations needed to be performed to ensure the shaft won't fail under load. Due to the suspension design and the design of the drive shaft assembly, the drive shaft will only encounter a torsional load. The drive shaft was designed with plunge-joints on the inboard CV joint which enable operation of the shaft during suspension travel with relatively high amounts of scrub. The drive-shaft assembly chosen, a 2006 Polaris Sportsman 500 rear drive-shaft, has 1.6 inches of total plunge distance. This information was taken from the half-shaft spline data sheet – Plunge/Angle diagram, which can be found in Appendix A – Manufacturer Engineering Information. This +/- 0.8 inches of plunge will accommodate the suspension's +0.5/-0.3 inches of scrub, as found in the Suspension section's Scrub diagram. This excess margins for the plunge/scrub will ensure that the drive shaft will not be loaded in bending during normal operation. This reinforces the claim that the drive shaft will only be loaded in torsion.

When a component fails due to a torque load, it fails due to torsional shear. For this analysis failure is defined when the shaft yields. The Maximum Shear Stress theory predicts torsional yielding when a torsional load exceeds half of the tensile yield strength.

Equation 13

$$S_{sy} = 0.5S_y$$

In this equation S_{sy} denotes yield strength in shear, and S_y denotes tensile yield strength. This formula produces a conservative value for torsional yield strength. This conservative value will help to increase the factor of safety in the assembly.

A torsional load is produced when a torque is applied. This load is maximized at the furthest point from the axis of rotation. For a rod rotating along its long axis, this

furthest point is located on the outer surface of the rod, the radius. This is modeled by the following equation.

Equation 14

$$\tau_{max} = \frac{T * r}{J}$$

Where T is the applied torque (N-m), r is the radius of the shaft (m), and J is the polar second moment of area (m^4). Combining equations for J and the maximum torsional load yields another equation.

Equation 15

$$\tau_{max} = \frac{16 * T}{\pi * d^3}$$

Where T is the applied torque (N-m) and d is the shaft diameter (m). This will produce a value of pressure ($\frac{N}{m^2}$) that can be compared to the shear yield strength.

To find the torque applied to the driveshaft an equation was used that relates motor power and rotational velocity. This is a rework of an equation used in the motor section.

Equation 16

$$T = 9.55 \frac{P}{RPM}$$

Where T is torque (N-m), P is motor power (P), and RPM is rotations per minute. Using the power of the selected motor (900 Watts) and the rotational velocity needed to achieve the target speed of 1.5 m/s (51.28 rotations per minute), the maximum torque is found to be 167.609 N-m. It should be noted that this is the torque at this specific RPM. If the motor/gearbox combination rotates faster the torque load will reduce, and if the motor/gearbox rotates slower the torque load will increase. This torque value, along with

the shaft diameter of 19.05 mm (0.75 inches), was used to find the maximum torsional load. Using Equation 15, the maximum torsion in the rotating drive shaft was calculated to be 123.476 MPa.

To generate a factor of safety for the driveshaft, the material of the drive shafts must be determined. This turned out to be more challenging than expected as no literature could be found on Polaris' website outlining the type of steel and the hardening process used for the drive shafts. As a work around, replacement drive shafts with material information were found on Amazon and eBay. The drive shafts chosen were standard OEM replacement parts, and were not high performance upgrades. This was done because, hopefully, the parts would be produced with the same manufacturing processes and direct comparisons could be made. The drive shafts found on Amazon and eBay were produced with a high strength 4340 Cr-Moly steel shaft. Once found, the material properties were found for this steel using Shigley's Mechanical Engineering Design book. Because the heat treatment used is still unknown, the lowest strength heat treatment found in the book was used. This conservative approach will yield a large "real life" factor of safety. The yield strength used for this evaluation was 855 MPa (for comparison, the largest yield strength produced by a different heat treatment is 1590 MPa). Using the yield strength of 855 MPa, a shear yield strength of 427.5 MPa was calculated.

A factor of safety was then calculated using the shear yield strength and the maximum torsional load. The formula is found below.

Equation 17

$$n = \frac{S_{sy}}{\tau_{max}}$$

Using 427.5 MPa for the shear yield strength and 123.476 MPa for the torsional load, the factor of safety was calculated to be 3.462. This proves that the drive shaft chosen for this build is adequate.

Also, because the drive train is using a gearbox, the maximum allowable torque of the gearbox should be checked against the drive shaft. The maximum torque of the gearbox is 419.96 N-m (found from Anaheim Automation technical documents, Appendix A). This torque will produce a torsional load of 309.381 MPa, which is less than the shear yield strength of 427.5 MPa. As it stands right now, the gearbox will fail before the drive shaft will fail.

Gearbox-Drive Shaft Coupler

The interface between the drive shaft and the gearbox is a critical component in the rover. This coupler will attach the two vastly different shafts, allowing for the torque generated by the motor/gearbox to be transmitted to the drive shaft and wheel. Throughout the course of the design process, this coupler went through three full design iterations before deciding on the design chosen.

One of the major design considerations was the splined input on the drive shaft. The splines allow for torque to be transmitted efficiently, for the drive shaft to be easily removed if maintenance needs to be performed, allows for additional plunge if it is required, and evenly distributes the torque around the entire coupler. The initial design attempted to incorporate these splines into the coupler, but ultimately failed. In order to spline the interior of a cylinder, the cylinder needs to have a through hole which allows

the broach to machine the teeth. This would require a two-part coupler, since the drive shaft input is a larger diameter than the gearbox output shaft. In addition to being a design challenge, this proved difficult because the UND machine shop does not own an interior splining broach and contracting that work with a local machine shop would be prohibitively expensive. Although utilizing the splines would be the ideal solution, this design was scrapped.

The next design was to simply squeeze the input shaft via mechanical force. This was achieved by machining slots in the coupler and tapping and threading bolt holes through the slot, allowing the force of the bolts to squeeze the aluminum coupler around the splined input shaft. The gearbox output has a keyway, so the same bolted slot idea was used for this design as well, except for one slot was machine wider to accept the key. Ultimately this design was manufactured in the UND machine shop out of a billet of 6061 Aluminum. The idea was that with the mechanical force provided by the bolts, the hardened spline teeth on the input shaft would “bite” into the softer aluminum and achieve a similar torque transmitting quality as splining the coupler. This design was manufactured because time was starting to become pressing and decisions needed to be

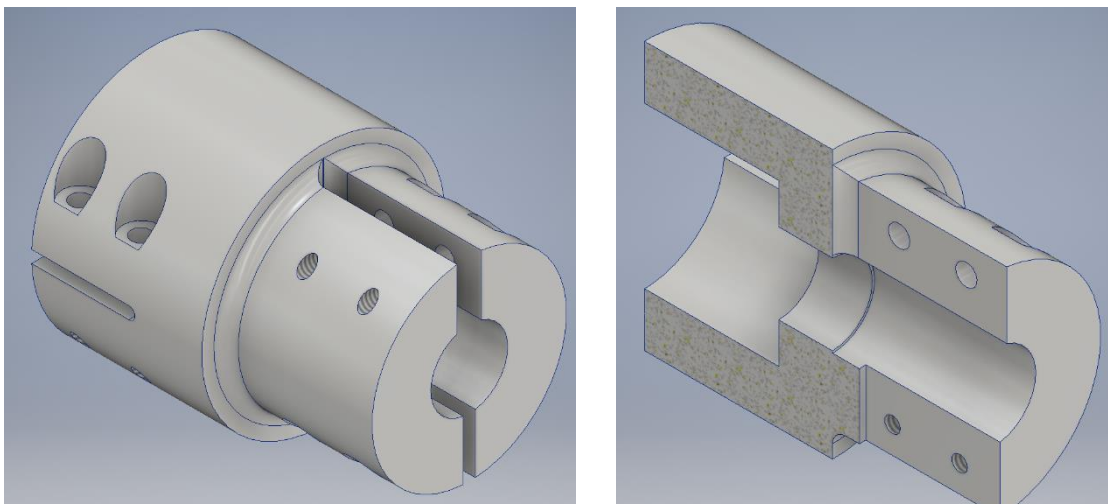


Figure 34 – Gearbox/Drive Shaft Coupler V2

made, even if they weren't completely correct. Pictures of this design can be found below:

This couple was manufactured in the UND mechanical engineering shop. A total of five couplers were machined: four for use in the rover and one as a spare. A picture of a completed coupler is found below:



Figure 35 - Manufactured Gearbox/Drive Shaft Coupler

After construction and integration of the coupler onto the drivetrain, it was found that the clamping force exerted by the bolts was not sufficient. The coupler would spin around the driveshaft when excess torque as created by the gearbox. To remedy this, a through hole was drilled into the driveshaft side of the coupler and the driveshaft input itself. A Grade-8 bolt was then installed to firmly secure the driveshaft to the coupler.

Stress analysis was performed on this couple design in Inventor to test how it would respond to the expected forces exerted by the gearbox. The forces tested were the gearbox maximum torque of 420 N-m (3717 in-lb.) and the gearbox rated torque of

139.98 N-m (1239 in-lb.). The rated torque output of the gearbox closely matches with the expected torque value of the 900 watt motor operating at maximum capacity while propelling the vehicle at the design speed (165.82 N-m).

The stress analysis on the coupler was performed as a static test. To correctly model the forces, a model of the gearbox output shaft was created and all of the corresponding bolts were included. The following pictures show the input force (gearbox output shaft torque) and the fixed constraint (the driveshaft through-bolt).

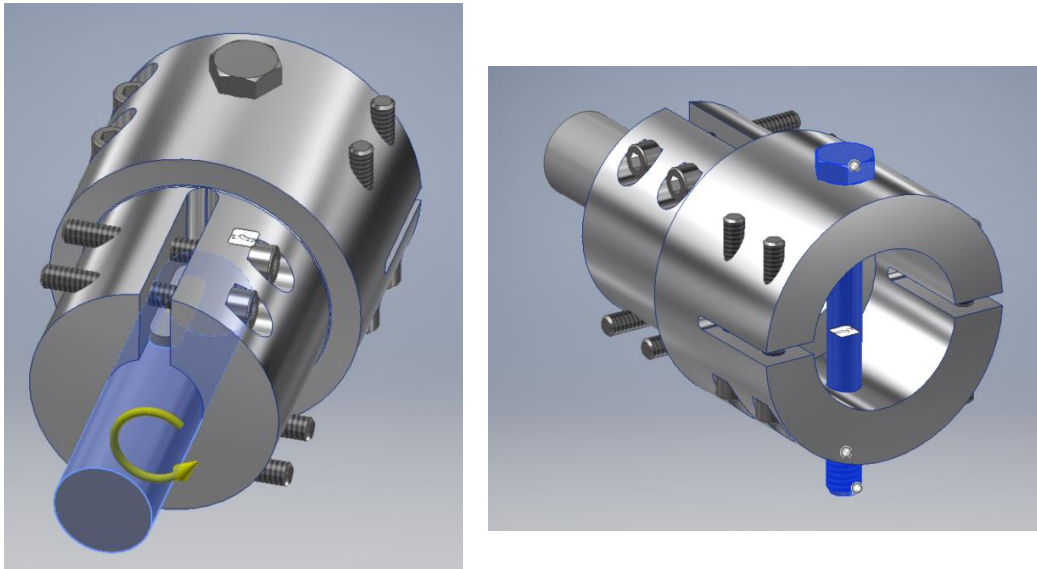


Figure 36 - FEA Setup

The Von Mises stress and the overall safety factor will be shown for each simulation. The safety factor is set to the yield strength of each component. The primary component of concern is the coupler, which is manufactured from Aluminum 6061 with a yield strength of 39,890 psi.

The first simulation shown is the gearbox maximum torque, 420 N-m (3717 in-lb.). The results are as follows:

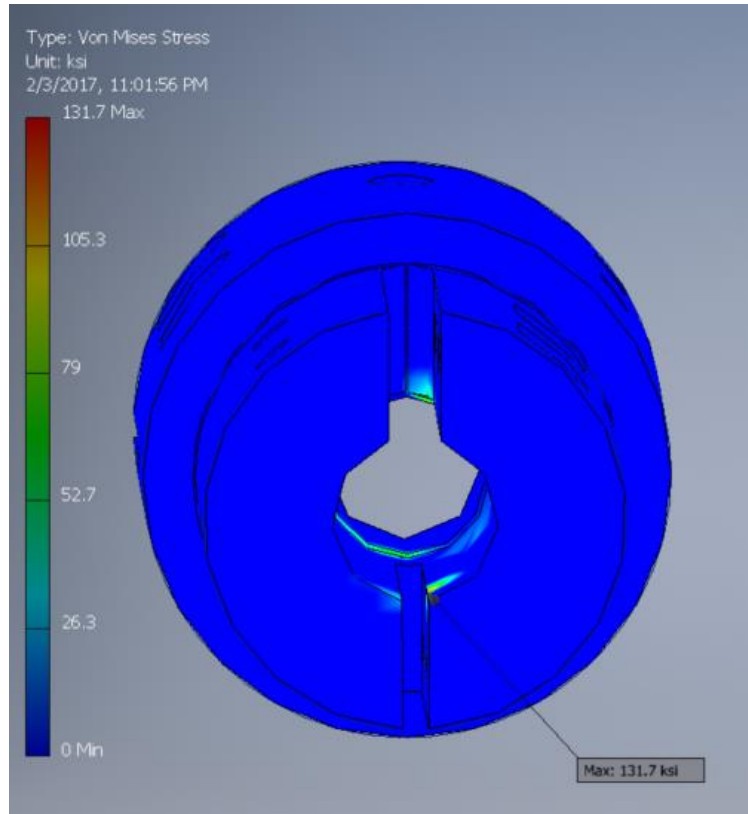


Figure 37 - FEA Coupler, Max Gearbox Torque, Stress

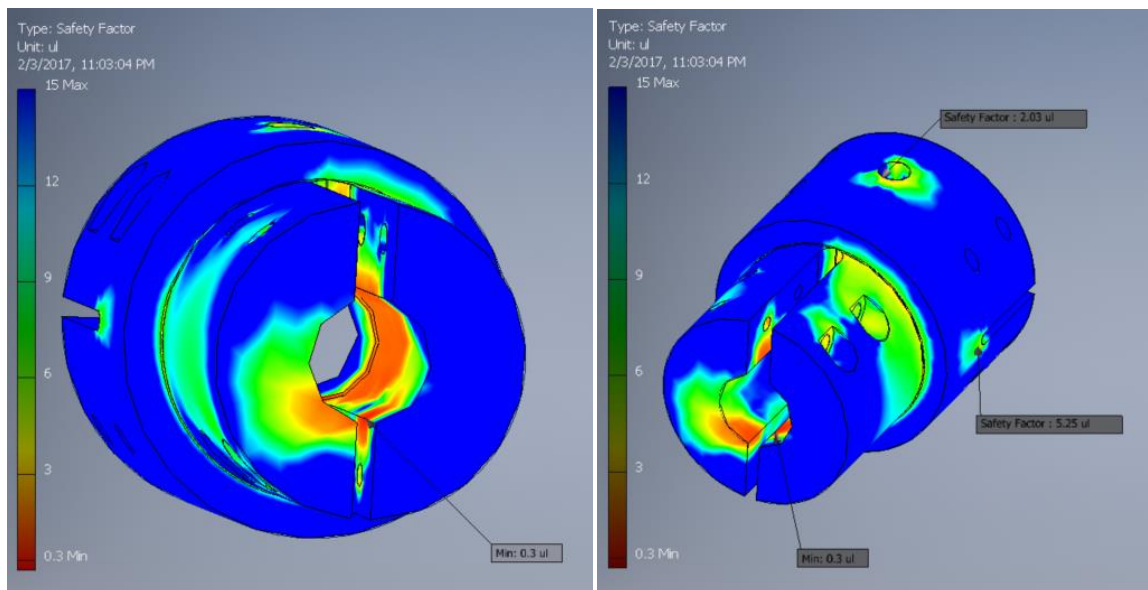


Figure 38 - FEA Coupler, Max Gearbox Torque, Safety Factor

All other components were hidden to obtain these images of the isolated coupler.

As seen in the Stress picture above, the maximum stress found on the coupler while the

gearbox is performing at its maximum is 131.7 ksi. This value is 3.3 times the yield strength of Aluminum 6061, creating a minimum Safety Factor of 0.3. As seen in the “Safety Factor” images above, the orange/red coloration denotes a safety factor of 1 or below. Much of coupler in contact with the gearbox output shaft will yield when the gearbox is at full torque. While not ideal for transmitting full power to the wheels, having the coupler fail before the gearbox will hopefully prevent the expensive gearbox and motor combination from mechanically failing during full torque conditions.

The next simulation analyzed uses the maximum rated gearbox torque of 139.98 N-m (1239 in-lb.). This is the maximum torque the gearbox can sustain indefinitely. This simulation was setup the same as the previous simulation. The results are as follows:

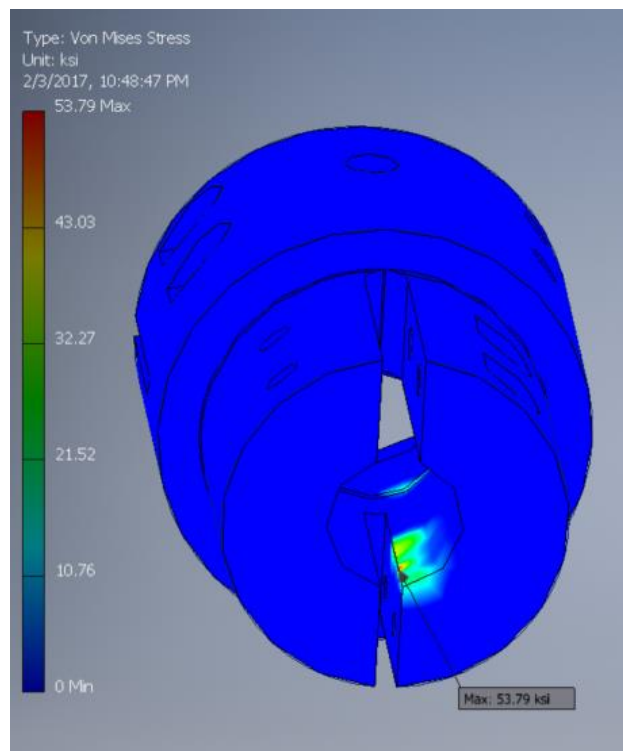


Figure 39 - FEA Coupler – Max Gearbox Rated Torque – Stress

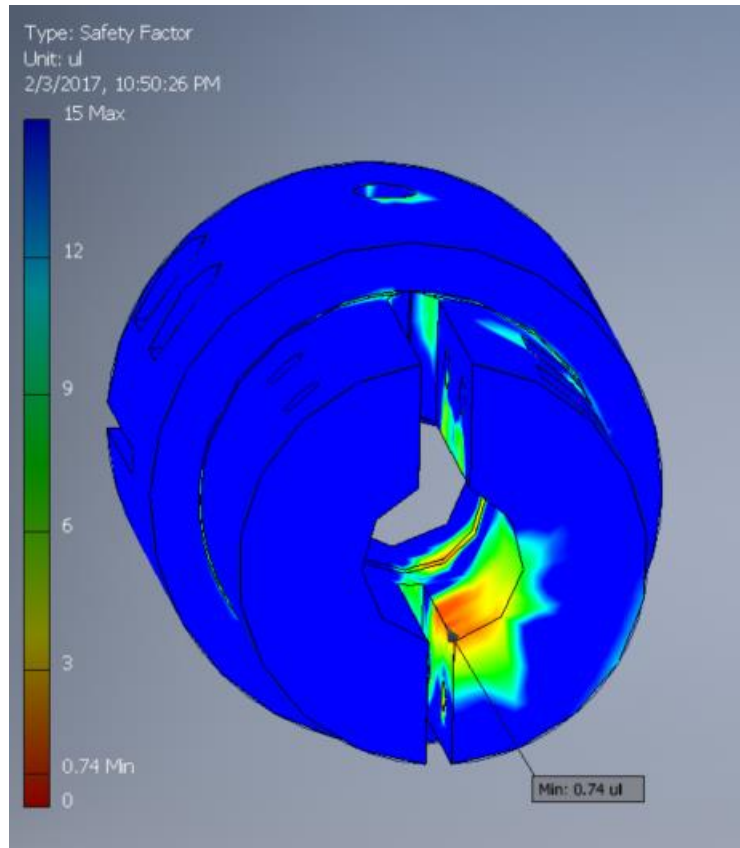


Figure 40 - FEA Coupler, Max Gearbox Rated Torque, Safety Factor

As seen in the image showing the Von Mises stress, the maximum stress seen in this simulation was 53.79 ksi. This value is above the yield strength of Aluminum 6061, thus the safety factor for this torque is below 1. Once again, this coupler will fail when the rated torque value is reached.

As a test, the material of the coupler was changed to annealed 4340 steel. This is the same high strength steel alloy that the drive shaft is made out of. Another simulation was performed using the maximum gearbox torque. The results are as follows:

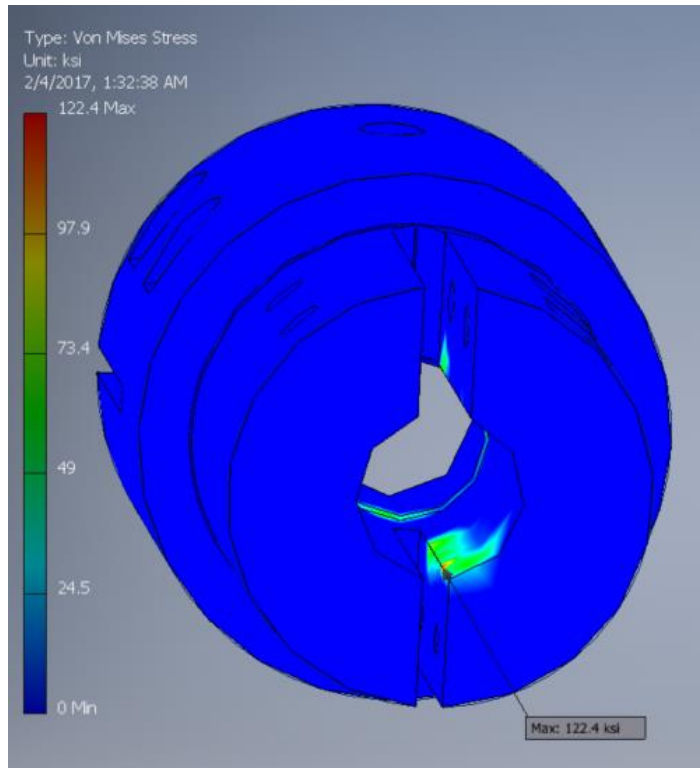


Figure 42 - FEA Coupler, Max Gearbox Torque, 4340 Annealed, Stress

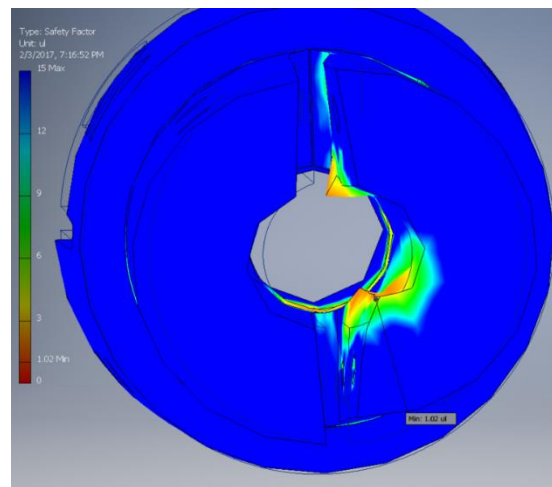
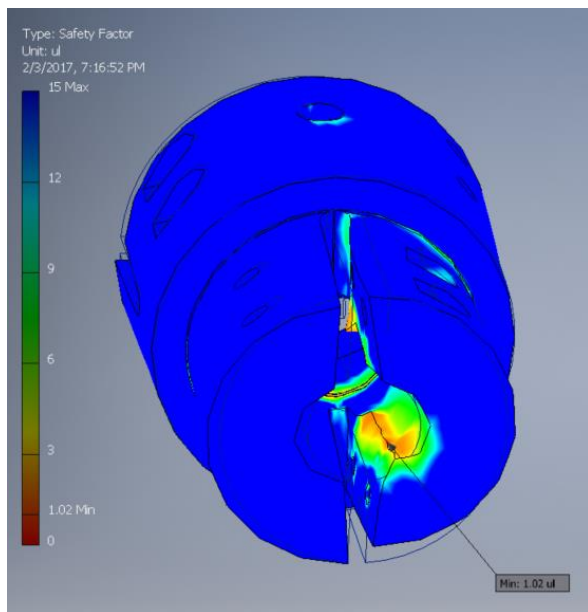


Figure 41 - FEA Coupler, Max Gearbox Torque, 4340 Annealed, Safety Factor

It can be seen that changing the material from Aluminum 6061 to annealed 4340 steel allowed the coupler to withstand the full force of the gearbox. This may be beneficial if the through-bolt attaching the coupler to the driveshaft input was designed to shear at ~90-95% of the maximum torque value. This configuration would allow the drive train system to transmit nearly all of the available power while still protecting the expensive motor and gearbox. In order for this to become a reality, more analysis and design must be performed in order to adequately design such a coupler system.

As seen from the above stress analyses, the aluminum coupler will fail when the drive train experiences very high torques. While not ideal, this coupler will allow for initial testing of the rover and will provide a baseline design for future improvements.

Motor-Gearbox Coupler

In order to transmit the rotational power from the motor to the gearbox, another coupler needed to be constructed. This coupler fits over the existing motor output shaft and attaches to the gearbox input shaft. The motor output shaft came with an 11-tooth sprocket that was attached via a roll-pin and a through hole. This sprocket was removed and was replaced with the coupler. The roll pin and through hole were incorporated in the coupler design.

The coupler was designed to accommodate the motor output shaft, gearbox input, roll pin, and existing motor output through hole. A picture of this coupler is shown below:

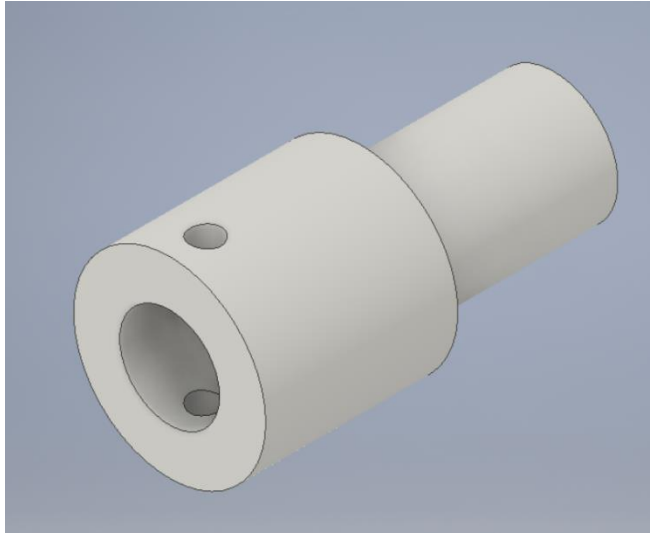


Figure 43 - Motor-Gearbox Coupler

This coupler was manufactured using 1018 Cold-Rolled steel. The engineering drawing can be found in Appendix B. This material was chosen based on availability from the local welding shop and material supplier.

A similar stress analysis was performed on this coupler as was performed on the gearbox-driveshaft coupler. The torsional load was applied to the modeled motor driveshaft and the fixed constraint was applied to the gearbox-side of the coupler. This will simulate the wheels not turning while the motor is in operation. The following images show this experimental setup:

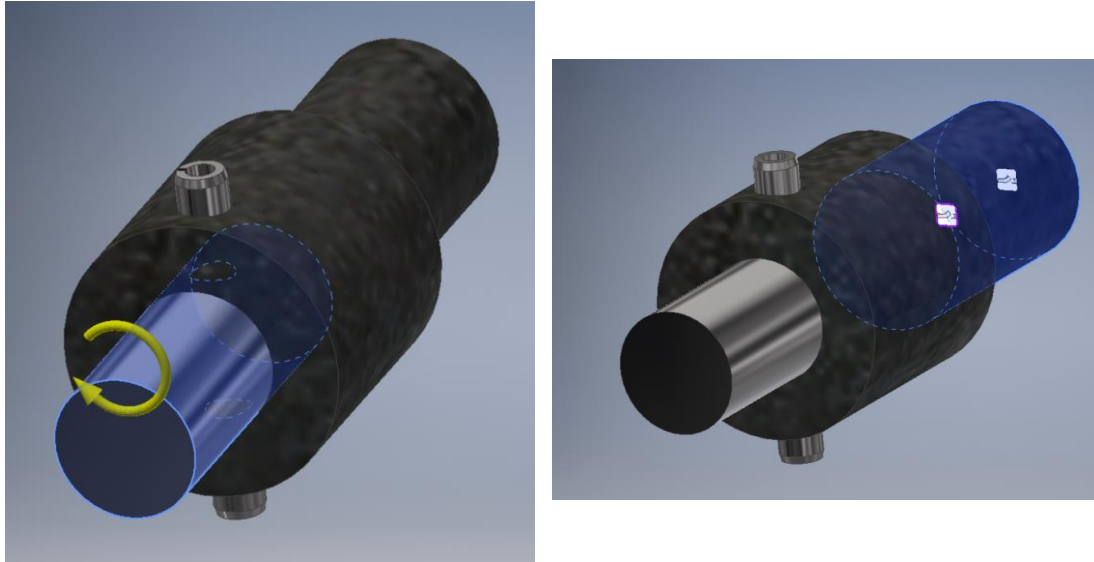


Figure 44 - Motor-Gearbox Coupler Load and Fixed Constraint

The first simulation used a torsional input of 13.99 N-m (123.9 in-lbs). This value was chosen because the gearbox's rated output torque is 139.98 N-m (1239 in-lbs) and the gearbox has a 10:1 ratio. The motor output shaft was not analyzed in this simulation because it is assumed that the motor manufacturer would choose the correct material and design their output shaft to handle the power the motor produces. As such, the components analyzed were the coupler and the roll pin. The stress and safety factor results for the first simulation are as follows:

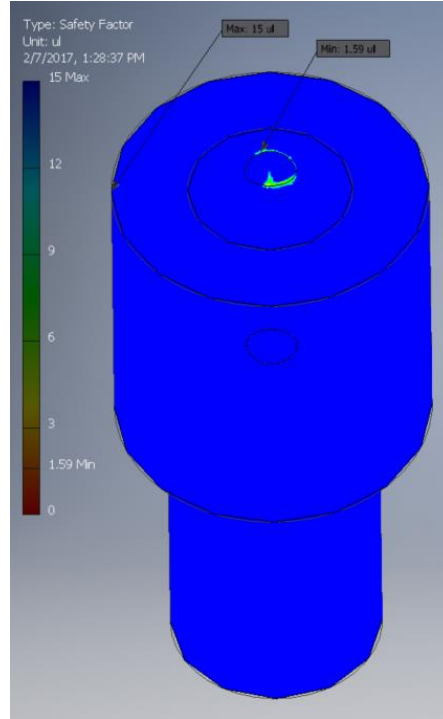
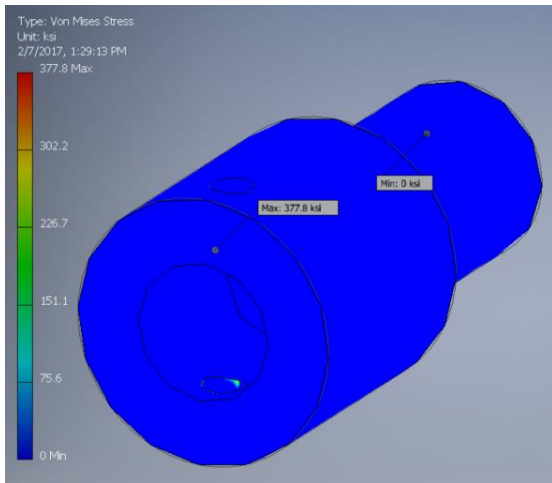


Figure 46 - Motor-Gearbox Coupler 13.99 Nm Stress and Safety Factor

The peak stress is 377.8 ksi and the minimum factor of safety was found to be 1.59. This shows that the coupler will not yield during rated gearbox torque output conditions. Next the roll-pin was analyzed.

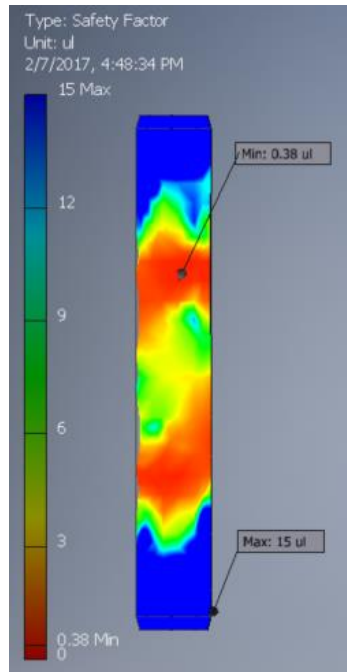
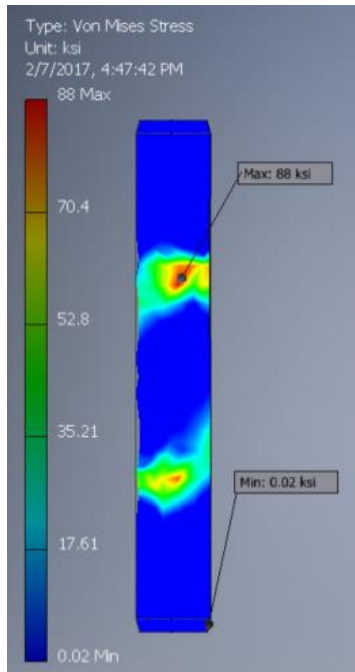


Figure 45 - Roll-Pin 13.99 Nm Stress and Safety Factor

These pictures show that the peak stress was 88 ksi, leading to a minimum factor of safety of 0.38. The pin was the same roll-pin that came assembled with the motor driveshaft and chain sprocket. For analysis purposes it was assumed to be a standard roll-pin made from austenite steel. Even though the analysis shows this pin failing, the pin was used during final construction because it was assumed that the manufacturer would choose an adequate component/material for their motor. If the pin does in fact fail during operation, changing the pin will be trivial. It is also worth noting that allowing the roll-pin to fail before any of the more expensive components is preferable.

The second simulation tested a torsional load of 42 Nm (371.7 in-lbs). This torsional load was chosen from the gearbox's maximum output torque of 420 Nm (3717 in-lbs), then reduced by a factor of 10 via the 10:1 gear reduction. The results for the coupler and pin are found below:

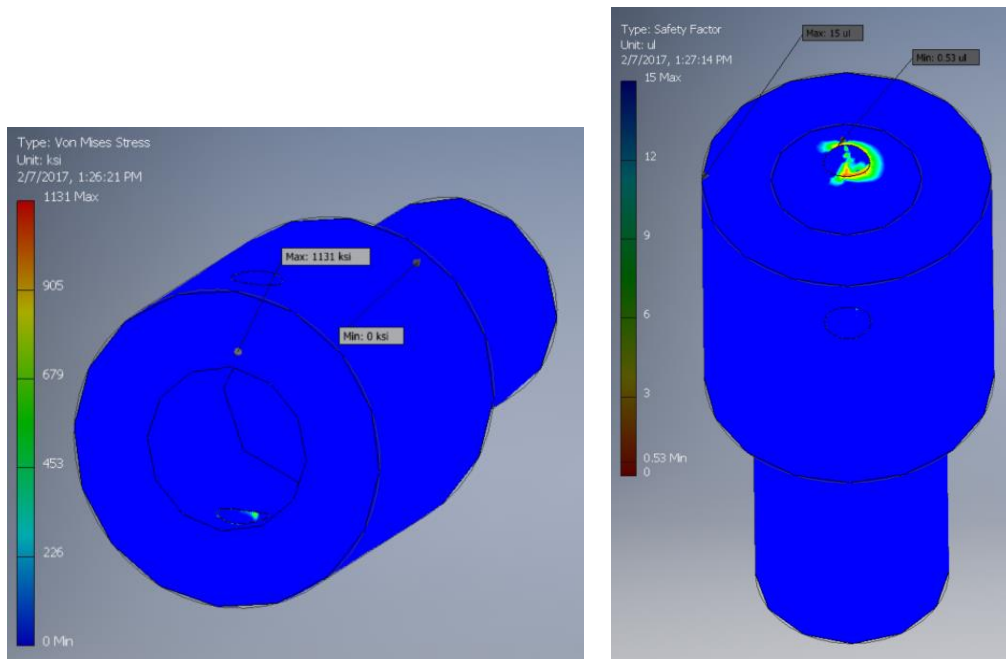


Figure 47 - Motor Gearbox Coupler 42 Nm Stress and Safety Factor

The peak stress was found to be 1131 ksi with a minimum factor of safety of 0.53. Under maximum gearbox load, the coupler will fail. Since the pin failed during the rated

gearbox load which is approximately 1/3 of the peak load, it is guaranteed that the pin will fail under peak gearbox load as well. For completeness, the pin stress and factor of safety images are shown below.

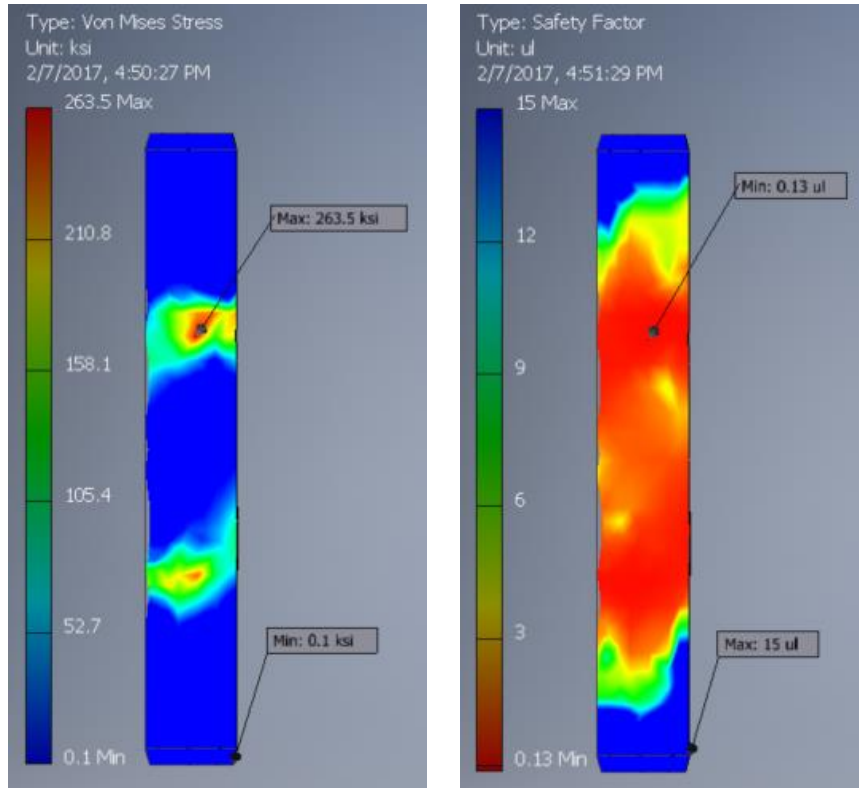


Figure 48 - Motor Gearbox Coupler Roll Pin - 42 Nm Stress and Safety Factor

The maximum stress on the pin is 263.5 ksi and the minimum factor of safety of 0.13. The pin will fail at this load.

Motor and Gearbox Interface Plates

In order to rigidly attach the motor and gearbox and to align their drive axles, interface plates needed to be constructed. These plates are necessary because the motor and the gearbox have different mounting holes; the motor has a 3-hole bolt circle and the gearbox has a 4-hole bolt circle, each of different diameters. To remedy this, the motor

plate was constructed to match up with the motor bolt circle and included three mounting holes which would match up with corresponding holes on the gearbox mounting plate. The gearbox mounting plate was constructed in the same fashion; drilling holes to match with the gearbox bolt circle and then drilling holes to match with the motor mounting plate. These three holes allow the interface plates to align the drive axles and rigidly connect the motor and gearbox. This allows for a purely torsional load to be transferred via the motor output shaft. The gearbox mounting plate has two additional holes near the bottom of the plate that allow for the entire drivetrain to be mounted to a piece of steel angle and then to the bottom steel plate. The mounting plates are made from 1/8" steel plate. Pictures of the mounting plates can be found below:

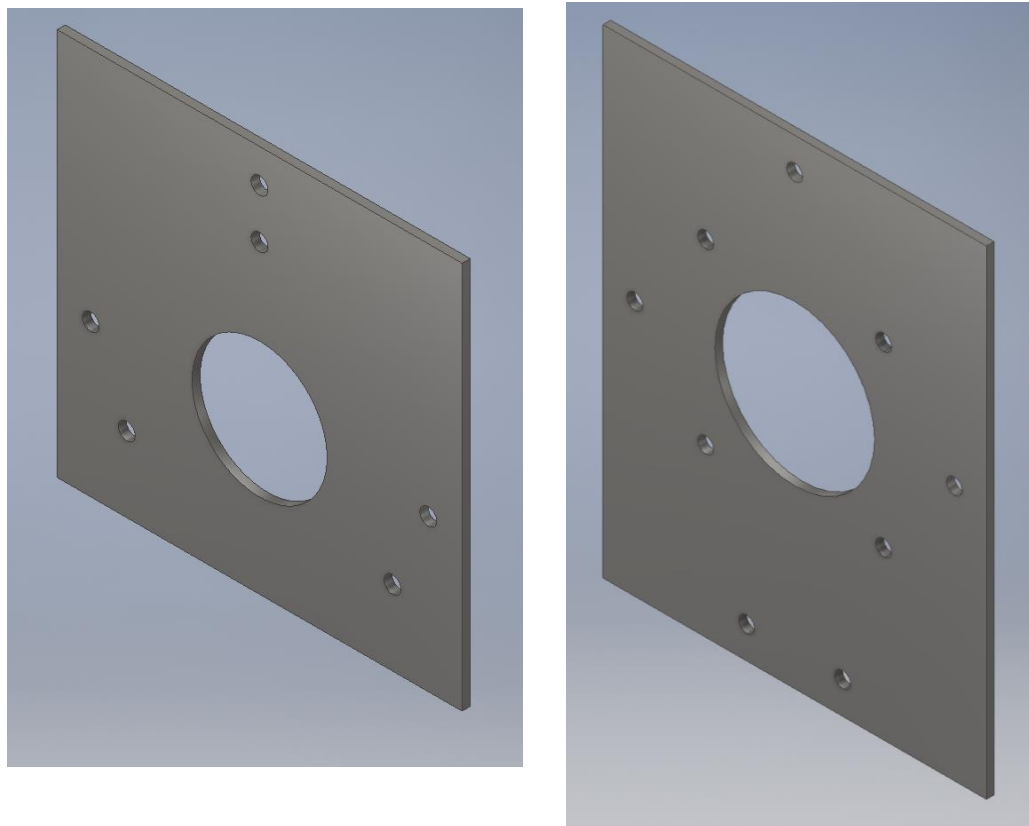


Figure 49 - Motor and Gearbox Mounting Plates

A stress analysis was performed on the whole motor-gearbox assembly. This test was to test the mounting system to ensure it was structurally sound. To test the system, torque was applied to the motor driveshaft and the bolts holding the steel angle to the bottom plate of the rover were held fixed. The assembly is shown below

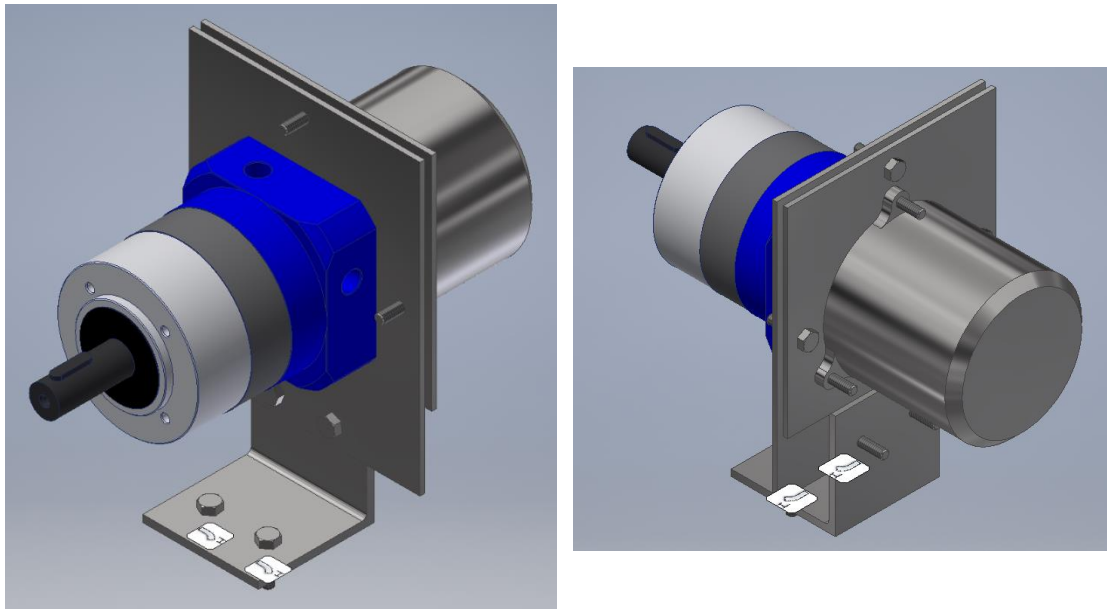


Figure 50 - Motor Gearbox Assembly

As seen in the above image, the bottom bolts are held fixed. The torque load can be seen in the following picture:

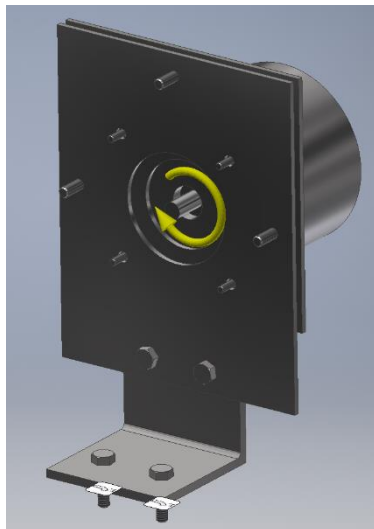


Figure 51 - Motor Gearbox Assembly Torque Location

A torque was 42 Nm (371.7 in-lbs) was applied to the motor driveshaft. The results of the stress analysis are found below:

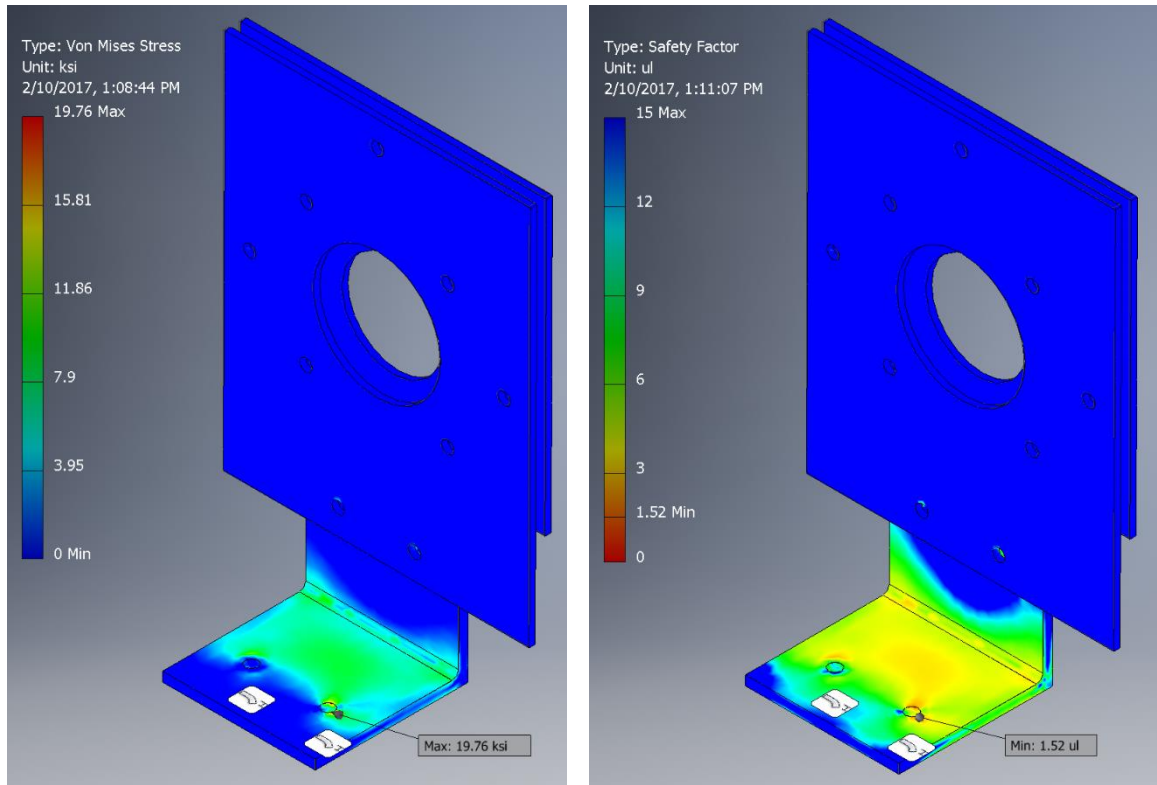


Figure 52 - Motor Gearbox Mounting Assembly Stress and Safety Factor

As seen above, the maximum stress seen was 19.76 ksi at the mounting bolt hole, which translates to a safety factor of 1.52. The mounting system will survive the forces applied from maximum motor torque.

Drivetrain Assembly

Each component of the drivetrain assembly has been chosen and analyzed. Some components were shown to fail at maximum torque load, but it is doubtful that this load will occur under normal operating conditions. If a component does in fact fail, the assembly was designed to be modular and parts can be switched out, or new parts can be

redesigned with the additional knowledge obtained from real world testing. An example of improvements would be to machine the “gearbox output – driveshaft coupler” out of steel, remove the “squeeze channels”, and then perform a hardening heat treatment to obtain the required characteristics. This rover is meant to be a research prototype, so such improvements are expected and encouraged. An images of the completed drivetrain can be found below:

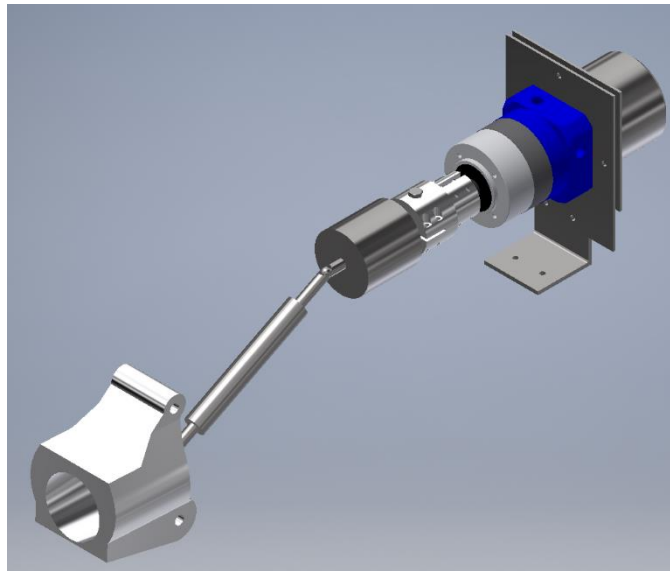


Figure 53 - Inventor Model of Completed Drivetrain



Figure 54 - Completed Drivetrain Assembly

Frame

Main Body

The frame is what gives the rover its shape and houses all of the components. It also contains all of the mounting locations for tools and absorbs impacts incurred throughout its life. The outer dimensions are: 48 inches long, 30 inches wide, and 20 inches tall.

The frame was designed for ease of construction and to give great flexibility for future improvements. It was designed after the drivetrain was completed in order to ensure that all the components would fit properly. The frame was constructed using Aluminum 6061 1.25" square tubing with 1/8" wall thickness. This tubing was chosen for its high strength to weight ratio and for the ease of manufacturability. The aluminum is easy to TIG weld and the flat faces of the square tubing enable items to be mounted to the frame without the need for tabs, as would be required with round tubing.

To reduce material and add strength, the suspension sub-frames were manufactured individually and then welded into the outer frame. The locations of the suspension sub-frame members were chosen based on the suspension arm characteristics

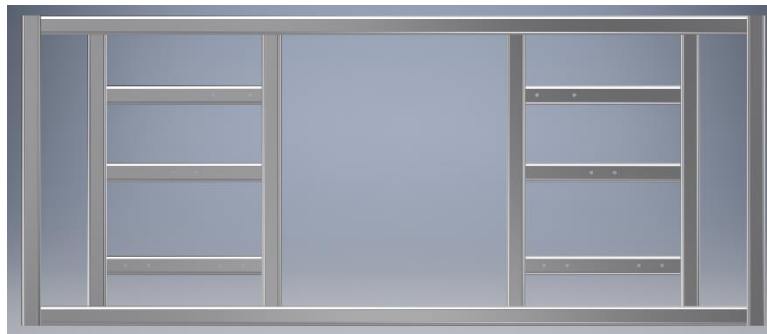


Figure 55 - Side Frame with Suspension Sub-Frame

described in the “Suspension” section. An Inventor image and a manufactured image of the side frame with suspension sub-frame can be found below:



Figure 56 - Manufactured Frame Sides

Some manufacturability design choices were made with regards to the suspension sub-frame. While the rover could have gained an additional 3.25 inches of ground clearance if the bottom suspension member attached to the bottom of the frame instead of the bottom suspension sub-frame member, this was decided against due to structural concerns and worries that if the rover suffered an accident in which the suspension member yielded the frame, the entire side of the frame would need to be rebuilt instead of just a single suspension sub-frame. The bottom suspension sub-frame member was placed where it is relative to the bottom frame member to allow adequate clearance for the TIG welder. If the bottom suspension sub-frame member was placed closer to the bottom frame member additional ground clearance could have been achieved, but welds attaching the suspension sub-frame to the outer frame would have been sacrificed. In this

case, the suspension sub-frame would be attached to the outer frame with only 3 welds per vertical member instead of the preferred 4. If ground clearance proves to be a major issue during testing, the suspension sub-frame can be remanufactured to lower the suspension support members, foregoing the additional weld, and gaining additional ground clearance.

To validate the frame design, stress analyses needed to be performed. The load cases tested were vertical and horizontal suspension loads and a front end collision. The suspension loads were the same loads used to validate the suspension system. The front end collision loads use the full weight of the rover with 1-g, 3-g, and 5-g decelerations acting on the front-bottom frame member. These high accelerations are important because the rover will not have any soft material on the front of the rover to cushion a collision.

The first analysis performed used the suspension loads. To accomplish this the simplified suspension models were placed on the full frame model and the maximum loads were applied to the appropriate locations on the suspension. A solid steel bar was used in place of the shock in order to transfer a worst-case load to the frame. For this

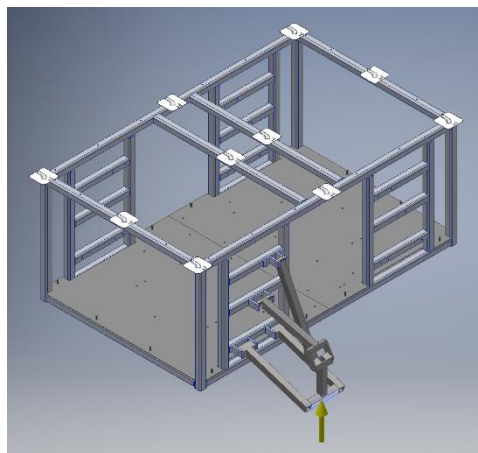


Figure 57 - Frame and Suspension FEA Setup

analysis the top of the frame was held fixed and the load was applied to the bottom of the suspension.

A 3-g, single wheel weight load (503.25 lbs) was applied to the suspension member. Since the suspension analysis was performed in the suspension analysis section, the suspension will be hidden while examining the results. The results are found below.

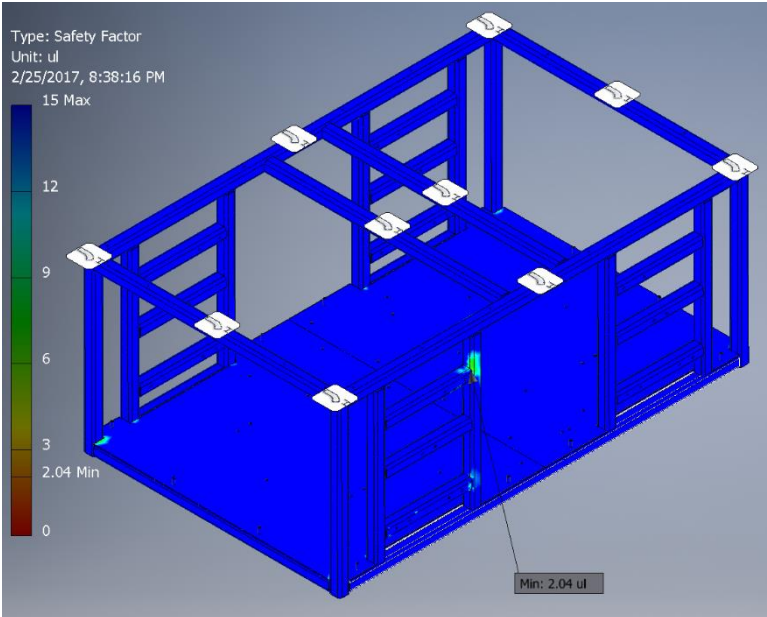


Figure 58 – Frame and Suspension FEA – Vertical Load

The minimum factor of safety on the frame for this analysis is 2.04, located at the frame joint closest to the shock.

The next analysis used the horizontal suspension load. For this, the rear of the frame was held stationary and the 2-g full rover weight load (1342 lbs) was applied to the suspension. The setup is shown below.

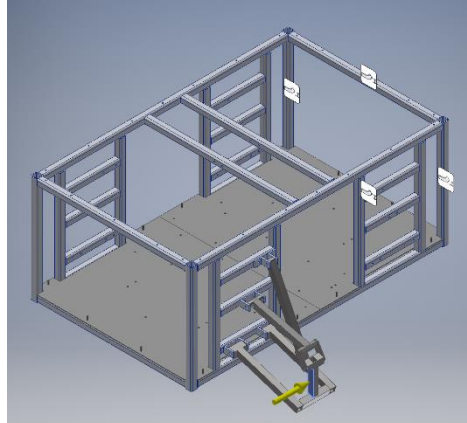


Figure 59 - Frame and Suspension FEA - Horizontal Setup

The results from this simulation were very surprising. Not only did the frame fail at this load, but the frame catastrophically failed. The results are found below.

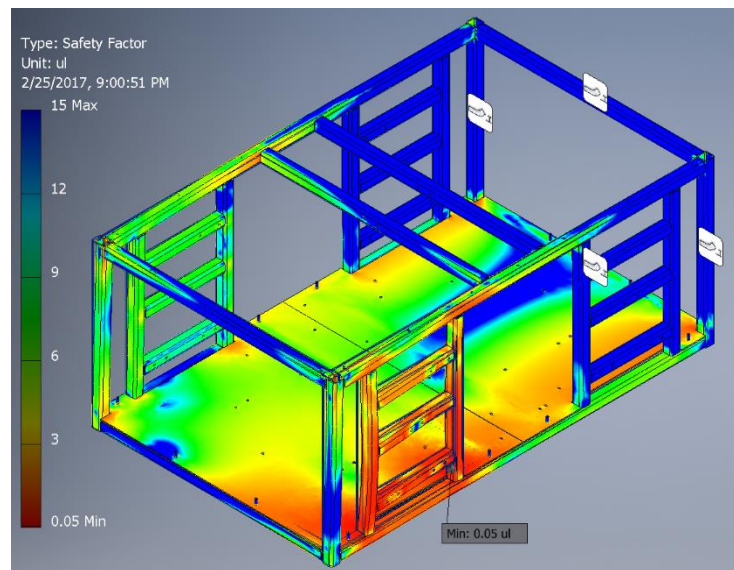


Figure 60 - Frame and Suspension FEA - 2g Horizontal Load

The lowest factor of safety on the frame was shown to be 0.05. This frame is unable to withstand the force of single wheel collision with a deceleration of 2g's. To further test the frame, a simulation with a 1g deceleration force was tested. The results are found below.

The lowest frame factor of safety was found to be 1.1. The frame is able to withstand a single wheel, 1-g deceleration load. This means that the rover operator needs to be careful while traversing environments with objects that may impact a wheel without allowing the wheel to climb over that object.

The next simulation was a front collision on the frame. For this simulation the rear frame members were held stationary and the load was applied to the lower front frame member. The setup is shown below.

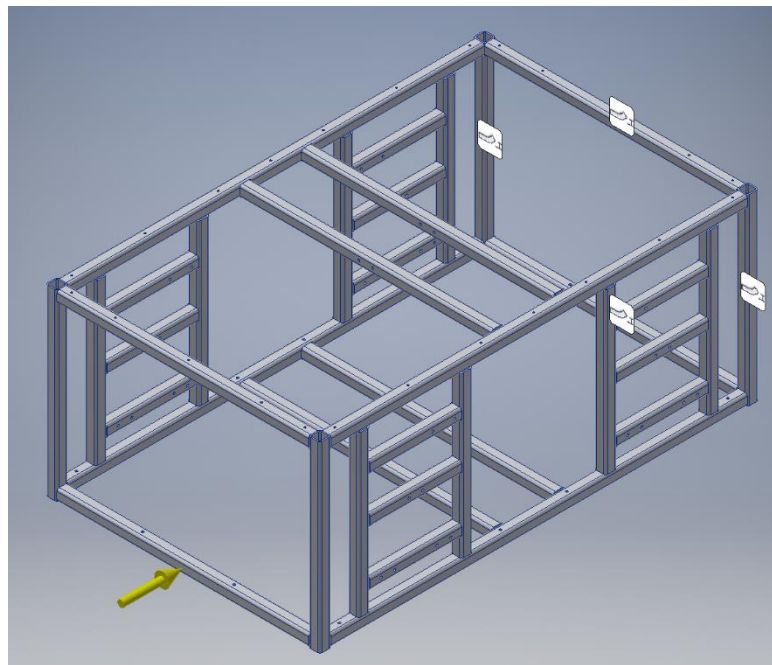


Figure 62 - Frame FEA - Front Collision Setup

The first load applied was a full rover weight, 1-g deceleration. The results are shown below.

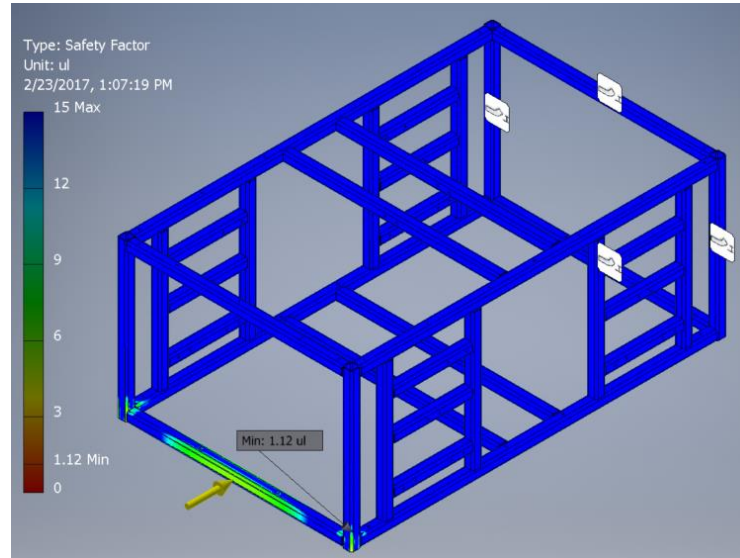


Figure 64 - Frame FEA - Front Collision - 1g

As shown in the above figure, the lowest factor of safety for the frame in a 1-g deceleration is 1.12. This occurs in the bottom front corner of the frame. Next a 3-g deceleration was tested. The results are shown below.

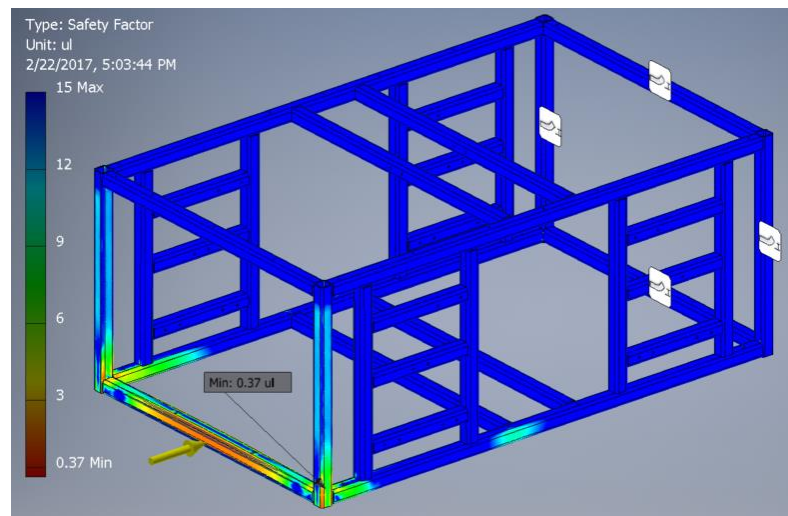


Figure 63 - Frame FEA - Front Collision - 3g

As shown in the figure, the lowest factor of safety is 0.37 in the bottom corner of the frame. The frame needs to be braced in order to withstand the large forces of high decelerations. The next simulation includes the steel plates bolted to the top of the bottom frame members. These steel plates act as the floor inside the rover, but they also act as

braces to support the long sections of the aluminum frame. The first simulation uses the same 3-g deceleration. The results are shown below.

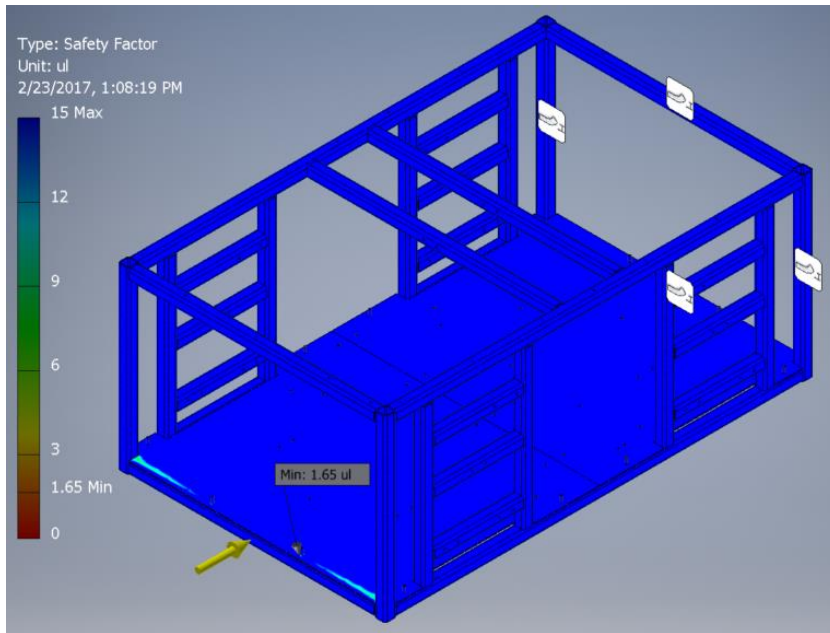


Figure 65 - Frame FEA - Front Collision with Plates - 3g

With the addition of the steel plates, the factor of safety rises to 1.65. The steel plates act as braces and allow the forces to be evenly dissipated throughout the entire structure. The next simulation raises the load to a 5-g deceleration. The results are below.

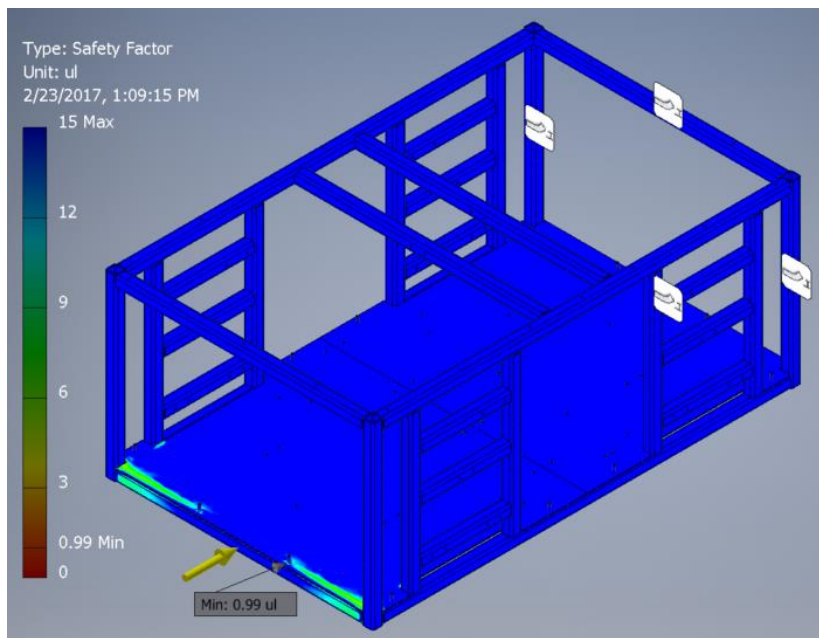


Figure 66 - Frame FEA - Front Collision with Plates - 5g

When the 5-g deceleration was run, the component that had the lowest factor of safety was the bolt attaching the steel plate to the frame. This factor of safety was 0.99. Even though a 5-g deceleration was shown to yield the bolt, this is close enough to pass this simulation. A 5-g deceleration from 1.5 m/s is an impulse time of only 0.0306 seconds. Even though the rover is not designed with crumple zones and to yield when impacted, this impulse time is still very small. If the rover is seen to consistently have high impact front collisions, a heavy duty rubber front bumper can be installed. This bumper was greatly increase the impulse time of the impact, lessening the deceleration, and thus the force seen by the frame.

One point of note is the choice of a steel plate rather than an aluminum plate. The aluminum plate was preferred for its mass and corrosion resistance properties. Unfortunately when comparing prices for a suitably thick aluminum plate vs a suitably thick steel plate, the aluminum plate was too costly. The steel plate adds considerable weight and a corrosive element when placed in contact with the aluminum frame, but these factors were deemed preferable to paying the high cost for the aluminum plate. Countermeasures such as painting the steel plate will be performed to lessen the corrosive potential between the two metals. A picture of the completed frame is shown below.



Figure 67 - Manufactured Frame and Steel Plates

Antenna and Camera Boom

After construction of the frame, the camera and antenna boom needed to be constructed and installed. This boom would allow the rover driving camera to be elevated to around human head height and would give the antennas the clearance they need to not impact the rover during operation.

To install this boom, cross members were installed on the top of the rover. These members are identical to the members on the bottom middle of the frame. These members were included in the Main Body simulations in the previous section. Since this boom is not anticipated to experience any impact loads it was not designed for withstand large forces. This boom is constructed out of a three foot piece of 1.25" aluminum 6061 square tubing. This tubing houses the wires that control the camera servos, the camera feed, the amateur radio repeater antenna, the camera transmitter antenna, and the rover's radio control antenna. The boom has brackets welded onto the bottom that bolt into the cross member support bracket. These brackets rigidly attach the boom to the rover frame.

The boom also supports the antennas for the astronaut helmet camera receivers. An Inventor model of the boom installed on the rover with the antenna booms and camera housing is shown below.



Figure 68 - Antenna and Camera Boom

The antennas will be discussed in their corresponding sections. The camera housing will be discussed in the camera section.

Aluminum Panels

After the frame was constructed and the antenna boom was installed, the outer panels were constructed. These panels shield and enclose the internal components from dust and debris. The panels were manufactured out of aluminum 6061 sheet metal and were bent to shape in the UND machine shop.

Aluminum was chosen for the side panels due to its light weight, corrosion resistance, and durability. Initially a type of plexiglass was envisioned for the panels, but because of the extreme environments the rover would be operated in the material was deemed unsuitable. Risking a panel fracture due to a collision with a rock or an astronaut's tool would compromise the internal components and the integrity of the rover. This was seen as an unacceptable risk, so it was avoided all together. The aluminum sheet metal allowed the panels to be bent to the exact dimensions of the frame and allows for easier mounting of accessories. If the panels were manufactured from plexiglass or plastic, every anchor or hole or mounting location would run the risk of fracturing and compromising the entire panel. Also, sourcing plexiglass or plastic panels large enough to be used for the panels was difficult. When the material was found in the appropriate size, the cost was prohibitively expensive. The aluminum was chosen for the factors mentioned above, as well as the ability to locally source the material for a reasonable price.

Each panel was designed to fit onto the rover in a certain order. The side panels were to be mounted first, then the front and rear panels, then the rear top panel, followed by the front top panel. These panels needed a specified order so each bend could be placed in the correct location and the panels would properly fit over each other. The sheet metal used for the panels is 0.0625 inches thick, so each panel needed to be constructed 0.125 inches longer and taller than the previous panel. This ensured that the panels would nest on top of each other and provide a tight fit. A picture of the panels over the rover frame is shown below.



Figure 69 – Frame with Aluminum Panels

To secure the panels to the rover, the panels were fit onto the rover and adjusted until an optimal fit was achieved. Then holes were drilled through the panels and into the outside wall of the adjacent frame member. This was repeated over the top of the rover. The bottom was attached through the steel plate mounting holes in the frame. After the holes were drilled, the panels were removed and $\frac{1}{4}$ "-20 threads were cut into the top frame members. Threading the frame holes allowed bolts to be fastened to secure the panels without the need for a nut inside the rover, which would have been impossible to tighten.

The side panels were designed to be installed before the suspension mounting brackets. This allows the mounting brackets to be easily changed in the case of a failure, and the side panels to be the “base” panels that the other panels mount on top of. To prepare the panels, suspension mounting holes were marked and drilled. The driveshaft location was then marked and a 3.5 inch diameter hole was cut. This hole is large enough to accommodate the thick end of the Polaris driveshaft with 0.5 inches of deviation. These features are the same on both side panels. Where the panels differ is in the

accessory cutouts. The left panel has a window installed to monitor the battery charging indicator lights and the right panel has an opening for a 120 volt exhaust fan.

The front and rear panels were designed to fit over the side panels. This meant the inside dimension between the folded lips of the panels needed to be 1/8" longer for both the length and height. The front panel is solid, while the rear panel has three cutouts. One for the rover switch box, one for the E-Stop, and one for the 120 volt extension cord input. This switch box houses switches that control the power for the electronics and 2 additional switches that are not yet connected. The Emergency Stop button controls the power to the motor controllers and the motors. The 120 volt extension cord input sends power to the battery charger and exhaust fan.

The top panels were tricky to construct. They needed to be easily removable, yet still provide good coverage against debris while incorporating the antenna boom. The final design chosen was to split the top panel into two sections with an overlap of approximately 3 inches. Both panels have a cutout that snugly fits around the antenna boom. The rear panel is to be laid down first, followed by the front panel. As such, the rear panel is 3/8 inch wider than the frame and the front panel is 1/2 inch wider than the frame. The following pictures show the rover with everything installed, plugged in and charging.

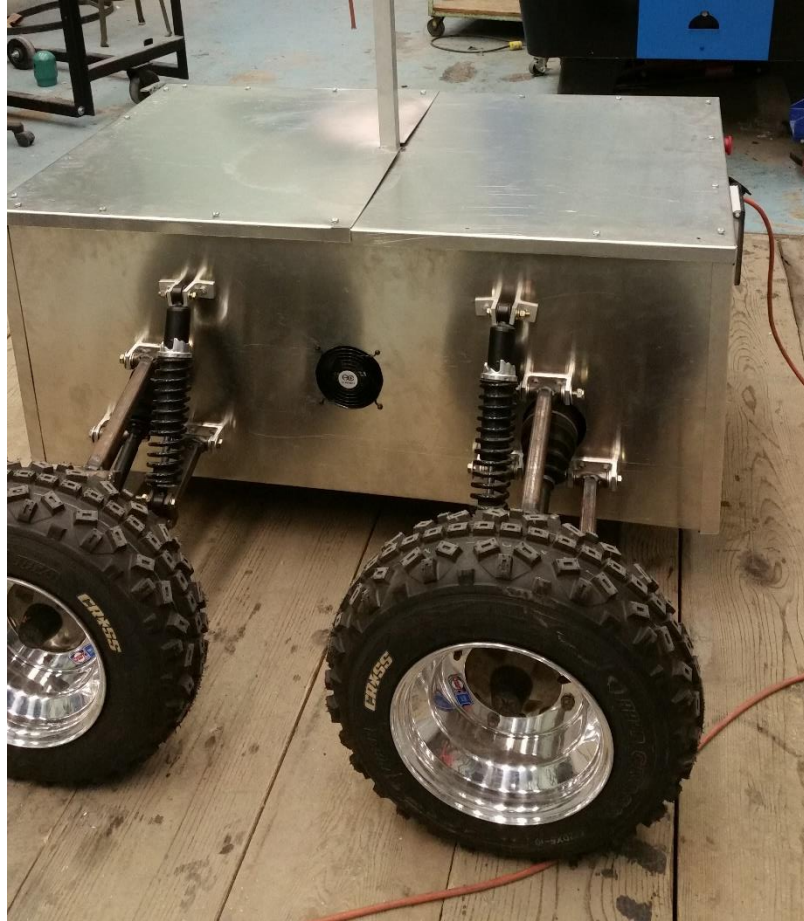


Figure 70 - Rover Charging 1



Figure 71 - Rover Charging 2

Electrical Design

The electrical components give life to the mechanical skeleton of the rover. These components allow the rover to receive commands, operate the drive motors, transmit and receive communications, and move about the environment. There are many systems integrated into this rover and the rationale for each will be explained in the following sections.

Fortunately there was no electrical component design in this rover, meaning every component was chosen “off the shelf” or was easily constructed. The primary rationale determining if a component was selected were:

1. Does the component perform the required function?
2. Is this component able to operate off the supplied voltage?
3. Is this component “rugged” enough to survive the dust and vibration seen during an analog mission?
4. Is this component inexpensive? If not, what makes this component preferable to the less expensive models?

The electrical system was broken up into two distinct sections, each operating on their own circuits. This allowed the rover to have two different power capacities and voltages; one for the driving system and one for the other electrical components. For the remainder of this section these two circuits will be called (1) the driving system, and (2) the communications system. Full electrical system drawings can be found in “Appendix C – Electrical Drawings”.

Driving System

The driving system comprises all of the components on the circuit that runs the four DC motors. This is a relatively bare-bones circuit. The only components are: two 12 volt 105 Amp-hour lead acid batteries, two 12 volt 150 amp-rated relays, four 75 amp diodes, two motor controllers, and eight 50-amp self-resetting fuses. These components will be discussed at length in the following sections.

Batteries

The batteries chosen for this rover need to possess three primary qualities:

1. Operate at the correct voltage for the motors.
2. Store a sufficient amount of charge that will enable rover operation throughout the length of a human EVA.
3. Must not be prohibitively expensive.

The battery type that meets all three criteria are 12 volt, deep cycle marine batteries. These lead-acid batteries are normally found in boats and campers and can be purchased from any big-box store such as Walmart or Menards. A 12 volt, 105 amp-hour battery can be purchased for less than \$100. Since the batteries are lead based, they are cheap, but very heavy. Two of these batteries were purchased for the driving system on the rover. The batteries purchased are “Exide 27MDC 12-Month Nautilus Marine Deep Cycle Battery” from Menards. Each of these batteries weigh 61.2 pounds, so the batteries are large source of weight on the rover. When connected in series, these batteries produce

24 volts with a 105 amp-hour capacity. A third battery was purchased to power the electrical system, which will be discussed later. Pictures of the battery and the batteries installed in the rover can be found below.



Figure 72 - Exide 12 Volt 105 amp-hour battery (Menards, n.d.)



Figure 73 - Batteries Installed in Rover

Referencing the motor specifications, each motor requires 24 volts and has a rated current draw of 34 amps. This equates to a rated current draw of 136 amps when all four motors are running. This is where some design decisions needed to be made with the rover. As mentioned above, the batteries chosen were relatively cheap and will be able to

power the drive system on the rover for a short amount of time. Deep cycle batteries such as these are designed to be discharged to approximately 20% charge remaining, meaning that the battery's capacity in reality is 84 amp-hours, 21 amp-hours less than advertised. Also, when the battery becomes discharged the voltage drops. This means that in order to produce a consistent electrical power (voltage multiplied by current) more current will be drawn as the voltage decreases, further lessening the time the battery can operate. A quick calculation of motor run-time using the batteries can be performed by taking the battery pack capacity divided by the amp load, in this case 84 amp-hours divided by 136 amps. This will yield an approximate run-time of 0.6176 hours, or 37.05 minutes. This run-time only takes into account the time the rover motors are running and using substantial battery power.

To further complicate matters, electric motors draw considerably more current when starting and quickly changing directions. These motors will draw close to the stall current when starting and can draw up to double the stall current when quickly changing directions. The stall current for these motors isn't specified on the data sheets, and unfortunately the department does not have the equipment necessary to experimentally find the stall current for such a motor. Typical values for stall current are in the range of 2-4 times the rated current, which for the motors chosen are between 68-136 amps. Multiply this by the 4 motors, and the stall current load on the batteries is 272-544 amps. This is a huge amp load and steps need to be taken to prevent this load from ruining the batteries and the motor controllers. Hardware was added in an attempt to prevent this load from ruining the batteries and associated drive components.

As mentioned earlier, the batteries chosen are a huge source of weight on the rover and won't power the rover for a significant amount of time. Future improvements for the rover battery system can be lithium-ion batteries or incorporating a hydrogen-oxygen fuel cell. Both of these options could reduce weight and increase run-time, but will be very expensive. As an example, a 24 volt 100 amp-hour lithium ion battery from the online battery retailer lithiumion-batteries.com sells for \$2,600 (Smart Battery, 2017). While this battery provides 100% depth of discharge and is the same weight as a single battery, the cost is over 1/3 of the total cost of the rover. To achieve significantly more run-time, two of these batteries will need to be purchased and connected in parallel. The cost for both of these batteries would be \$5,200, which is almost 75% of the current rover budget. Using a fuel-cell trailer as the ASRO mission did would provide a similar benefit, but with the added cost of the fuel-cell and the challenges of handling and storing hydrogen and oxygen gases. The hope with the batteries chosen is that the rover will be able to showcase its utility and acquire additional grants, allowing for more robust battery packs to be constructed in the future. For the time being, the rover will operate using two 12 volt, 105 amp-hour deep cycle marine batteries wired in series to create the necessary 24 volt system.

Motor Controllers

In order to control the battery power being sent to the motors, the rover needs electronic motor controllers. These motor controllers receive commands from the remote control receiver and send the corresponding amount of power to the motors. Since the motors are capable of using large amounts of current, high-current motor controllers are

required. The motor controllers chosen for this project are RoboClaw 2x60A Motor Controllers, shown below.

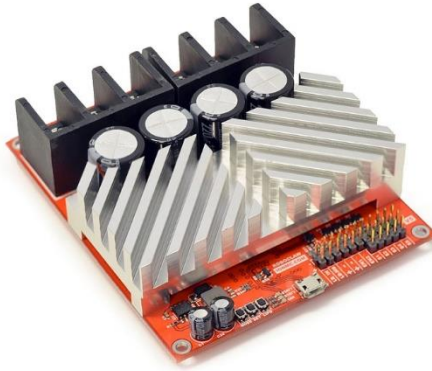


Figure 74 - RoboClaw 2x60A (Ion Motion Control, n.d.)

These motor controllers feature two motor channels with a rated current of 60 amps each, with a peak amp load of 120 amps per channel. These controllers also feature a wide input/output voltage range. The controllers are able to successfully handle voltages up to 34 volts. In addition, the controllers are capable of receiving commands via a remote control receiver. The combination of high current capacity, flexible voltage, and the ability to receive, interpret, and relay remote control commands make these motor controllers the perfect fit for this project.

The rover will feature two of these motor controllers wired in parallel with the remote control receiver. This allows the two controllers to relay commands simultaneously without any transmission lag. Since each motor pulls so many amps, parallel motor controllers were a necessity. Even though both left side and both right side motors will be receiving the same signals, wiring both same-side motors into a single motor controller channel would overpower the controller and fry the internal circuitry. Remember that each motor is rated for 34 amps, and each motor controller channel is rated for 60 amps. With each motor pulling the rated current draw, if they were both wired to the same

motor channel that channel would be seeing a rated current draw of 68 amps. This is already above the rated current draw for the motor controllers and would put heavy stress on the controllers under normal operating conditions. Add in the starting current (stall current) and the motor controller would be unable to survive operating two motors on a single channel. Thus the need for two motor controllers operating in parallel, each channel powering a single motor.

These motor controllers allow the rover to operate in a tank-drive style. While in tank-drive, the rover is able to steer by varying the rotational velocity of the left and right side wheels. This mismatched velocity allows the rover to advance in a curve, or even spin in a circle when the left wheels are spinning forward and the right wheels are spinning backwards (or vice-versa). Finding these motor controllers early in the design process allowed for a suspension design without the need for steering wheels like in a car or an ATV.

Relays

Large amperage, single pole single throw, normally open, continuous duty relays were used to connect the batteries in series to create the 24 volt battery pack. These relays act as a switch which turn the power to the motor controllers and motors on and off. The relays chosen were Cole Hersee 24213 12 Volt, 200A Continuous Duty Solenoid. Two relays are used between the two batteries. Since the maximum amperage a single motor controller can distribute is 240 amps (120 amps maximum per channel, 2 channels per motor controller), a relay was needed that could handle this large load. These relays are rated at 200 amps of continuous use, with a surge rating up to 500 amps. Using one relay

per motor controller ensures adequate load carrying capacity. A picture of the relay is found below.

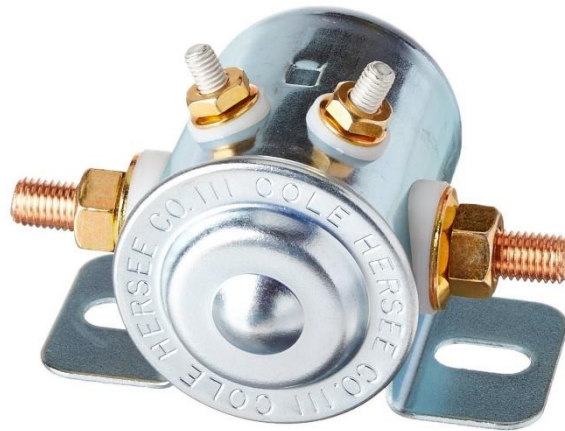


Figure 75 - Cole Hersee 24213 SPST Relay (Amazon, n.d.)

The relays serve two very important functions in the motor electrical system. First, they control the flow of electricity from the batteries to the motor controllers and the motors. The two relay activation coils are wired in a circuit with the Emergency Stop button located on the rear of the rover. Utilizing this E-stop, the driving power can be cut at a moment's notice. When this happens, the relays flip into their "Normally Open" state. While "open", no power can be transmitted through the relay, since the internal circuit has been broken, or "opened". This allows the relays to safely cut power from the motor electrical system.

The second important function these relays serve is to isolate the batteries during battery charging. The rover is equipped with an on-board 3-bank battery charger. This charger is capable of charging all three batteries at a single time. Since the charger is designed to charge 12 volt batteries and not a 24 volt battery pack, the batteries need to be isolated from each other prior to charging. Activating the E-stop "turns off" the relays and isolates the batteries, allowing them to be charged as individual batteries.

Fuses

Fuses are installed on the wires between the battery pack and the motor controllers. Based on conversations with the motor controller manufacturer's support representative, the fuses chosen should not open before a short circuit event as this has a high probability of damaging the motor controller. If a short circuit even occurs the motor controller is already damaged, and the fuse will help prevent damage to the batteries and reduce the chance of a catastrophic failure, such as a battery explosion.

Using the information obtained from the support representative, a fuse needed to be found that would allow the peak current of 240 amps to pass through safely, but would fail quickly at a current much higher than that. A Cooper-Bussmann ANN-100 fuse was

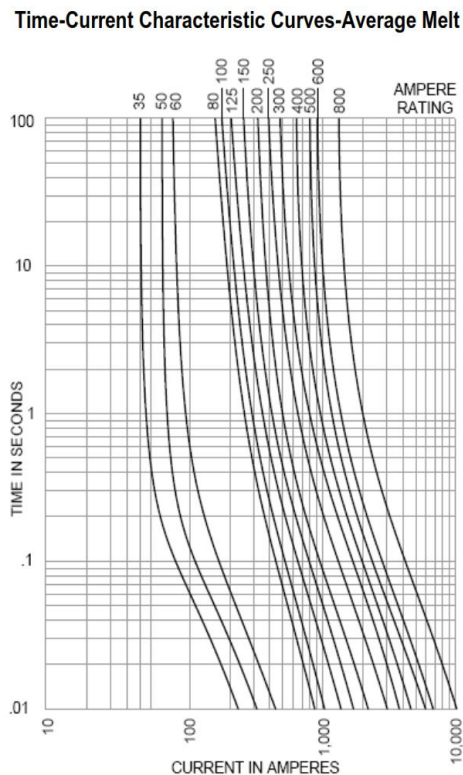


Figure 76 - Time-Current chart for ANN Series Fuses (Waytek, 2017)

chosen. This fuse will handle the nominal load of 120 amps indefinitely and is capable of taking the peak load of 240 amps for over a second. This will allow the fuse to quickly fail if the current exceeds 240 amps. Currents above 240 amps quickly reduce the failure time of the fuse, so if a massive current spike occurs, the fuse will fail and prevent catastrophic failure of the battery pack. The graph shown below is taken from the fuse specification page and shows the average melt time for different amp-rated fuses in the ANN series. The full fuse specification page can be found in Appendix A.

Wires

The wires to run the battery power to the motor controllers and to the motors had to be carefully chosen to accommodate the large amounts of current. To assist in sizing the wire, the following chart from the *Handbook of Electronics Tables and Formulas* was used.

Table 3 - Recommended Current Ratings (Continuous Duty); (Howard W. Sams & Co., 1986)

TABLE 5-1
Recommended Current Ratings (Continuous Duty)

Wire size		Copper conductor (100°C) nominal resistance (Ω/1000 ft)	Maximum current (A)			
AWG	Circular mils		Copper wire		Aluminum wire	
			Wiring in free air	Wiring confined*	Wiring in free air	Wiring confined*
32	63.2	188.0	0.53	0.32		
30	100.5	116.0	0.86	0.52		
28	159.8	72.0	1.4	0.83		
26	254.1	45.2	2.2	1.3		
24	404.0	28.4	3.5	2.1		
22	642.4	22.0	7.0	5.0		
20	1022	13.7	11.0	7.5		
18	1624	6.50	16	10		
16	2583	5.15	22	13		
14	4107	3.20	32	17		
12	6530	2.02	41	23		
10	10,380	1.31	55	33		
8	16,510	0.734	73	46	60	36
6	26,250	0.459	101	60	83	50
4	41,740	0.290	135	80	108	66
2	66,370	0.185	181	100	152	82
1	83,690	0.151	211	125	174	105
0	105,500	0.117	245	150	202	123
00	133,100	0.092	283	175	235	145
000	167,800	0.074	328	200	266	162
0000	211,600	0.059	380	225	303	190

*"Wiring confined" ratings are based on 15 or more wires in a bundle, with the sum of all the actual load currents of the bundled wires not exceeding 20% of the permitted "Wiring confined" sum total carrying capacity of the bundled wires. These ratings approximate 60% of the free-air ratings (with some variations due to rounding). They should be used for wire in harnesses, cable, conduit, and general chassis conditions. Bundles of fewer than 15 wires may have the allowable sum of the load currents increased as the bundle approaches the single-wire condition.

As seen in the chart, the wire gauge that is closest to the maximum current of the motor controllers (120 amps) is the 4 AWG wire with a maximum current in free air of 135 amps. This gauge of wire was used for all connections from the battery pack to the motor controller, and from the motor controller channels to the motors.

During a discussion with the motor controller manufacturer's support representative, he recommended a single 4 AWG wire from the battery to the motor controller. While the motor controller is capable of producing 120 amps per channel, for a total battery draw of 240 amps, the controller has software that will not allow it to continuously output 120 amps per channel. The controller is made to output up to 60 amps continuously, so wire should be sourced for this specification. Based on this recommendation, a single 4 AWG wire capable of transmitting 135 amps continuously will be used.

Battery Charger

The rover is equipped with an on-board battery charger. This allows the rover batteries to be recharged without the lengthy process of removing the batteries. The battery charger chosen is the NOCO Genius Gen 3, 3 Bank 30 Amp charger. An image of this charger can be found below.



Figure 77 - NOCO Genius Battery Charger (NOCO, n.d.)

This charger is designed to be placed permanently onboard marine vessels. Because of this, the charger is waterproof and IP-68 rated to keep out contaminants. This allows the charger to be permanently installed inside the rover.

The three white battery figures on the lower left side of the charger indicate the charging status of each battery. While the batteries are charging, the indicator lights are red for each battery. As each battery completes its charge, the light turns green. When this happens, the charger automatically senses the change of battery state and switches from quick charge mode to battery maintenance mode (NOCO, 2017). This battery maintenance protects from overcharging, overheating, and provides a small charge every 24 hours to ensure the batteries are topped off and fully charged. This charger is powered via an extension cord being plugged in to a 120 volt socket on the rear of the rover. Once again, this allows the battery charger to be permanently installed in the rover.

Battery Charger Exhaust Fan

When lead acid batteries charge, they can create hydrogen gas. In a normal situation, such as charging in a garage or in some other large volume or ventilated area, this hydrogen gas emission will not pose a real threat. Unfortunately, the rover volume is small and charging three batteries simultaneously has the potential to generate a lot of hydrogen. If one of the electronics inside the rover were to spark, it could lead to explosive consequences. To alleviate this risk, an exhaust fan was implemented. This fan shares the 120 volt circuit with the battery charger, so it will turn on when the batteries are being charged. This will help to ensure the safety of the rover and anybody who operates around the rover while it is charging.

This exhaust fan is located on the opposite side of the rover from the battery charger and blows the air from inside of the rover out. Since the batteries are sealed and the charger claims to minimize hydrogen formation, generation of explosive levels of hydrogen are unlikely. Because a hydrogen/battery explosion is a huge safety concern, countermeasures were still put in place. The exhaust fan will further minimize any risk of a hydrogen explosion during charging of the batteries. Figures 70 and 71 at the end of the Aluminum Panels section show the rover plugged in and charging, with the battery charger window displaying the three red lights to indicate charging and the opposite side exhaust fan.

Communications System

The communications system includes every other electronic component that is active when the rover is turned on. Every component is either involved with communicating between the habitat, rover, and astronauts, or is used to power or further facilitate those communications.

Remote Controller

The remote control is what allows the astronaut in the habitat to control the rover over great distances. This is accomplished by the transmitter sending radio signals corresponding to the stick, switch, and knob positions on the controller. These signals are received and demodulated by the receiver, and the corresponding PWM signals are sent to the appropriate control channels. The controller used in this build is a Turnigy 9X

controller with an aftermarket transmitter module and receiver. The transmitter and receiver will be discussed in the following section.



Figure 78 - Turnigy 9X Radio Controller (Hobbyking, n.d.)

The Turnigy 9X controller is an inexpensive 8-channel, 2.4 GHz radio controller. The package says that there are 9 channels, but there are only 8 channels that are controllable via the remote. The four main channels are controlled by the two joysticks. Each axis on each joystick is a separate control channel. The 4 remaining channels are controlled via the various knobs and switches on the remote. Determining which switch/knob controls the associated receiver channel is determined in the onboard remote software. The radio comes with a 100 mW, 2.4 GHz transmitter (RCUniverse.com, 2017). This is 100 mW is equivalent to 20 dBm of transmitting power (Cisco, 2008).

Currently the remote controls 5 output channels on the rover. A table of the remote channel assignments is found below:

Table 4 - RC Controller Channel Assignments

Channel	Control Interface	Action
1	Left Stick - Vertical	Motor Controller - Forward/Reverse
2	Right Stick - Vertical	Rover Camera - Tilt
3	Left Stick - Horizontal	Motor Controller - Left/Right
4	Right Stick - Horizontal	Rover Camera - Pan
5	Left 3-position Switch	Camera Feed Switch
6	(Unassigned)	-
7	(Unassigned)	-
8	(Unassigned)	-

DragonLink Transmitter and Receiver

In order for the rover to communicate at the long distances required for an analog mission, an upgraded radio transmitter and the associated receiver are required. The DragonLink RC system operates on the 433 MHz amateur radio band, which requires the operator to be an FCC licensed amateur radio operator. The transmitter and receiver were



Figure 79 - DragonLink V2 Complete System (RobotShop, n.d.)

upgraded to amateur radio quality equipment to utilize the frequency and power available to communicate over the many miles an analog mission may take place.

The effective distance a radio can operate (clearly transmit and receive a signal) is affected by many factors: operating frequency, environmental conditions (clear, rainy, cloudy, etc.), physical environment (flat land, hilly, urban with buildings, etc.), antenna type (omnidirectional or directional), antenna polarization (horizontal, vertical, right-hand circular, or left-hand circular), transmitting power (higher power travels further than lower power), and the sensitivity of the receiver (a more sensitive receiver needs “less” signal to operate). The study of radio waves, radio hardware, and antennas is very complicated and extremely technical. The explanations and rationale used in this thesis will be comparatively pedestrian.

The primary reason the DragonLink system was chosen is because it enabled longer range communication with the rover. The DragonLink transmitter module is a plug-and-play addition to the Turnigy 9X controller which retrofits the Turnigy to utilize the 433 MHz frequency for radio control. The DragonLink system operates on an amateur radio frequency which is allowed by the FCC to use a much more powerful transmitter than 2.4 GHz radios. As noted in the previous section, the stock Turnigy 9X transmitter emitted a 100 mW signal. The DragonLink transmitter has two power options, a high power and a low power. The low power delivers a 250 mW signal, and the high power delivers a 500 mW signal (Seto, 2012). The high power signal is 5 times as powerful as the stock Turnigy transmitter! A 2.4 GHz transmitter is capped at 125 mW of transmitting power and is restricted to only using omni-directional antennas (Federal Communications Commission, 2017). In contrast, a system operating in the 433 MHz band is capped at

1W of transmitting power and has no restrictions on antennas (Federal Communications Commission, 2017). The higher wattage ceiling and no limits on antennas greatly enhances the capabilities of the DragonLink system.

To show the effectiveness of the DragonLink system, some “radio” calculations need to be made. The radio field uses a term called decibels (dB) to describe some critical performance characteristics. A dB is a unit used to describe a logarithmic change in power/signal with respect to a reference power/signal. Because it is a logarithmic scale, an increase of 3 dB equals a doubling of the transmitter power, a 10dB increase is 10 times stronger, and 30 dB is 1000 times stronger. This unit is applied to transmitting power, antenna performance, and losses throughout the transmission and reception path. Once all of the radio performance parameters have been converted to dB, Link Budgets can be constructed and comparisons between radio systems can be created by simply adding and subtracting the dB values of each system. It is very important to note that the dB is a measure of a ratio, not an absolute value! If all of the dB values use the same reference signal they can be easily compared and manipulated. The formula for calculating a link budget is shown below:

Equation 18

$$Link\ Budget = EIRP - L_{path} + G_{Rx} - TH_{Rx}$$

EIRP = Estimated Isotropic Radiated Power, dBi

L_path = Signal loss through the transmitting medium, dB

G_Rx = Antenna gain of the receiving antenna, dBi

TH_Rx = Lowest signal threshold of the receiving hardware, dB

When the link budget has an excess of signal, it is called a link margin. This link margin is useful when the statistical anomalies occur, such as rain or heavy fog. These

occurrences introduce additional path loss to the system, which reduces the signal available to the receiver.

Estimated Isotropic Radiated Power is a term used to standardize the transmitter using the transmitting power and antenna. The equation for EIRP is shown below:

Equation 19

$$EIRP = P_{Tx} + G_{Tx}$$

Where P_Tx is the power of transmitter in dB, and G_Tx is the antenna gain in dBi. The equation to calculate transmitter power in dB from mW of power is shown below:

Equation 20

$$dB_m = 10 * \log \frac{signal}{reference}$$

For simplicity, the standard reference signal is 1 mW (Seybold, 2005).

Next, antennas need to be quantified. When an antenna produces a stronger signal, it is called “gain”. The comparison of antenna gains have two common reference points. The first is the theoretical isotropic radiator. This antenna radiates in all directions equally. A good way to envision this type of antenna is to picture a singular point of light. This light illuminates everything around it with no locations of focus. The second reference antenna is called a dipole, usually the half-wave dipole. The dipole radiates power in nearly all directions, but has nulls on the ends of the antenna. The point of maximum gain is normal to the center of this antenna. The dipole radiation pattern looks like a donut, and the theoretical isotropic antenna radiation pattern looks like a sphere. Radiation patterns are typically shown using 3 graphs: an X-Z graph (the Elevation plane, side view), an X-Y graph (the Azimuth plane, top down), and a 3D graph showing the

“real” shape of the radiation pattern. Radiation pattern graphs of the two reference antennas are shown below.

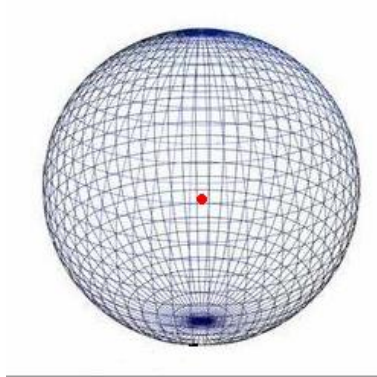


Figure 80 - Isotropic Antenna Radiation Pattern – 3D (19SD348, n.d.)

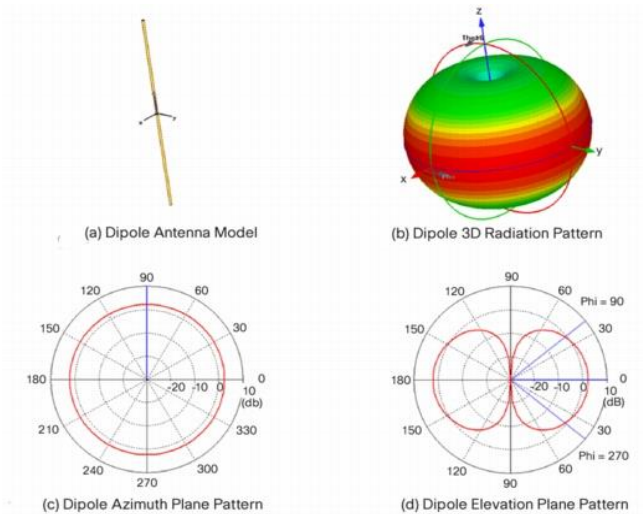


Figure 81 - Dipole Antenna Radiation Pattern (Cisco, 2007)

The decibel scale using the isotropic antenna as a reference is abbreviated dBi, while the decibel scale using the half-wave dipole as the reference is abbreviated dBd. To compare the two scales, the half-wave dipole antenna has a value of 2.14 dBi when compared to the isotropic antenna. This means that the half-wave antenna has a maximum gain of 2.14 dB when compared to the isotropic antenna. This allows for an antenna to be quickly measured in comparison to each type of antenna. If an antenna is

measured in dBi it can be quickly converted to dBd by subtracting 2.14 db, since the dipole antenna is 2.14 dbi.

Directional antennas, such as a Yagi or a dish, are capable of large amounts of gain. This is accomplished at the expense of the effective beam width. Think of directional antennas like a flashlight. The flashlight may have the same bulb and power as the unshielded bulb (isotropic antenna), but the flashlight is able to focus all of the light-energy into a smaller area, greatly illuminating that area and leaving most other locations dark. Typical values of gain are between 5-15 dBi for Yagi antennas and 5-30+ dBi for dish antennas. Directional antennas need to be accurately pointed or their effectiveness is greatly diminished. This pointing adds complexity, especially if the target is constantly moving like a spacecraft or a rover. The use of proper antennas can make or break a radio system. If directional antennas are used on both transmit and receive antennas, huge amounts of gain can be accomplished. A Yagi antenna radiation pattern is shown below:

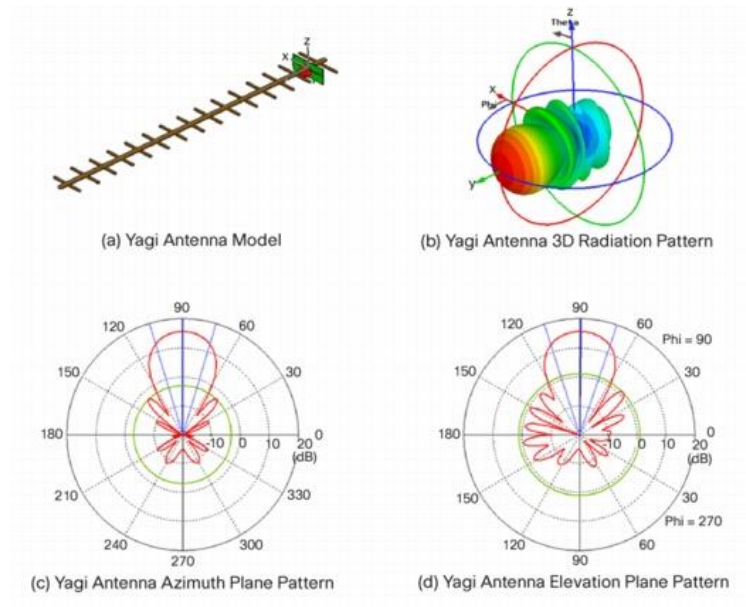


Figure 82 - Yagi Antenna Radiation Pattern (Cisco, 2007)

There are formulas to calculate antenna gain and the lengths of all of the antenna elements. To calculate the link budget, antenna gains are needed for both the transmitting and receiving antenna in dBi. To calculate the EIRP, add the transmitting antenna dBi to the transmitting power in dB.

The next important term is called the Path Loss. Path loss is when the signal degrades while it is being transmitted through the medium to the receive antenna. For instance, path loss in moist air is different than the path loss in dry air. While there are other avenues of signal loss, the path loss is the most significant factor because of its magnitude relative to the other terms (Seybold, 2005). The Path Loss equation is found below:

Equation 21

$$Path Loss (dB) = -20 \log\left(\frac{\lambda}{4\pi d}\right)$$

Where λ = wavelength in meters, and d = distance of the link in meters.

The wavelength is calculated by dividing the speed of light by the frequency of the radio wave being used. The formula is shown below:

Equation 22

$$\lambda = \frac{c}{f}$$

Where c = speed of light, approximately 3×10^8 m/s, and f = frequency of the signal. A 2.4 GHz radio wave has a wavelength of 0.125 meters, and a 433 MHz radio wave has a wavelength of 0.6928 meters. It is important to note that higher frequency radio waves (smaller wavelength) have greater path loss over a fixed distance when compared to lower frequency (larger wavelength) radio waves.

Receiver threshold is a term which describes how sensitive the receiving hardware is. It is the minimum received signal level that will provide reliable operation (Seybold, 2005). This is a hardware specification provided by the hardware manufacturer. As such, the only way to improve this value is to purchase or build more sensitive hardware. The receiver threshold is usually very small, meaning it is a large negative dB value. A typical value is around -80 dB. Since the receiver threshold value is subtracted from the link budget it ends up being an additive term during the calculation.

Now that all the terms for the Link Budget have been described, the analysis of the DragonLink system vs the stock system can commence. During this analysis the receiver sensitivity and receive antenna gain will be held constant. The DragonLink system boasts having a “highly sensitive” receiver, but numerical values could not be found so it was not included in the analysis. The DragonLink receiver uses a half-wave dipole antenna while the stock system uses a whip style antenna. Since values could not be sourced for

the gain of this antenna, it will be easier to hold both antennas constant. Also, the DragonLink transmitter has an SMA jack which allows the use of aftermarket or home-made antennas. Directional antennas can be constructed in the future if additional gain is necessary. The stock system does not allow for home-made or aftermarket antennas. In this analysis the sources for gain and loss will be transmitter power and radio frequency. Keep in mind there are many avenues for the DragonLink to develop additional gain over the stock system. The calculations are shown below:

Link Budget = EIRP - Path Loss + Gain of the Receiver (G_{Rx}) - Threshold of the Receiver (TH_{Rx})

Stock System:

- Frequency = 2.4 GHz (2.4×10^9 Hz)
- λ (wavelength) = $\frac{c}{f} \Rightarrow \frac{3 \times 10^8 \frac{m}{s}}{2.4 \times 10^9 \frac{1}{s}} \Rightarrow \lambda = 0.125 \text{ m}$
- Link distance will be 1 km (1000 meters)
- Transmitter Power = 100 mW
- $G_{Tx} = G_{Rx} = 0$ (held constant)
- $TH_{Rx} = 0$ (no data)

$$EIRP = P_{Tx} + G_{Tx}; P_{Tx} = 10 \log\left(\frac{100mW}{1mW}\right) = 20 \text{ dB}_m; G_{Tx} = 0$$

$$EIRP = 20 \text{ dB}_m + 0 \Rightarrow EIRP = 20 \text{ dB}_m$$

$$Path Loss = -20 \log\left(\frac{\lambda}{4\pi d}\right) \Rightarrow -20 \log\left(\frac{0.125 \text{ m}}{4\pi * 1000m}\right) \Rightarrow Path Loss = 100.046 \text{ dB}$$

$$Link Budget_{Stock System} = (20 - 100.046 + 0 - 0) \text{ dB} \Rightarrow -80.046 \text{ dB}$$

$$Link Budget_{Stock System} = -80.046 \text{ dB}$$

DragonLink System:

- Frequency = 433 MHz (433×10^6 Hz)
- λ (wavelength) = $\frac{c}{f} \Rightarrow \frac{3 \times 10^8 \frac{m}{s}}{433 \times 10^6 \frac{1}{s}} \Rightarrow \lambda = 0.6928 \text{ m}$
- Link distance will be 1 km (1000 meters)
- Transmitter Power = 500 mW
- $G_{Tx} = G_{Rx} = 0$ (held constant)
- $TH_{Rx} = 0$ (held at 0 for comparison with stock receiver)

$$EIRP = P_{Tx} + G_{Tx} ; P_{Tx} = 10 \log \left(\frac{500mW}{1mW} \right) = 26.9897 \text{ dB}_m ; G_{Tx} = 0$$

$$EIRP = 26.9897 \text{ dB}_m + 0 \Rightarrow \text{EIRP} = 26.9897 \text{ dB}_m$$

$$\text{Path Loss} = -20 \log \left(\frac{\lambda}{4\pi d} \right) \Rightarrow -20 \log \left(\frac{0.6928 \text{ m}}{4\pi * 1000 \text{ m}} \right) \Rightarrow \text{Path Loss} = 85.172 \text{ dB}$$

$$\text{Link Budget}_{DragonLink} = (26.9897 - 85.172 + 0 - 0) \text{ dB} \Rightarrow -58.1823 \text{ dB}$$

$$\text{Link Budget}_{DragonLink} = -58.1823 \text{ dB}$$

From the calculations above, it was shown that when holding the antennas and receiver threshold constant, the stock system has a Link Budget of -80.046 dB and the DragonLink system has a Link Budget of -58.1823 dB, a difference of 21.8637 dB! This difference was partly because of the additional transmitter power of the DragonLink system (a 6.9897 dB gain), but it was primarily seen from the radio wave path loss. The 2.4 GHz stock system experiences a 100.046 dB loss, while the 433 MHz DragonLink system experiences an 85.172 dB loss, a difference of 14.874 dB! This difference is independent of the link distance, since each system will be transmitting over the same

distance. The DragonLink system will always experience a gain of 14.874 dB over the stock system just because of the operating frequency!

Since dB is a measure of a ratio, a direct comparison can be made between systems. Rearranging the Power to dB equation will allow for a ratio to be made between systems.

Equation 23

$$Ratio = 10^{\frac{dB}{10}}$$

Substituting 21.8637 for the dB value in the above equation yields a power ratio of 153.592! This value means that the DragonLink system is 153.6 times more powerful than the stock transmitter/receiver system! Add in that the DragonLink transmitter can be retrofitted with a directional transmit antenna and the receiver is “more sensitive” than the stock receiver, and the DragonLink system will continue to improve over the stock system.

5 Volt BEC

To power the DragonLink receiver and all of the other 5V components, a DC-DC 5 volt step down converter was required. This component is called a BEC, which stands for Battery Eliminator Circuit. This plug-and-play circuit takes an input voltage, in this case 12 volts, and steps it down to the required 5 volts needed to power the radio controller receiver, servos, video switch, and video OSD. This BEC is capable of supplying up to 6

amps of current, which is sufficient for this project. A picture of the BEC is shown below.

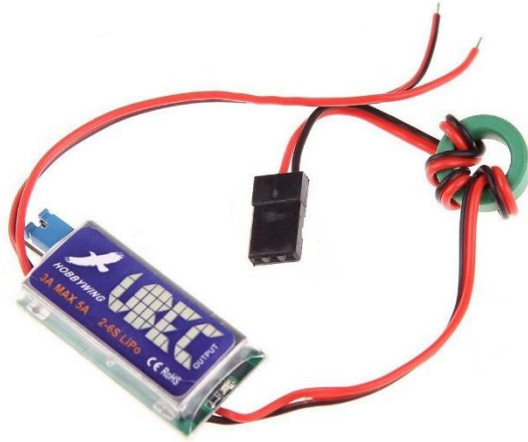


Figure 83 - 5 Volt BEC (Hobbywing, n.d.)

12 Volt Camera

In order for the rover controller to see the terrain the rover is operating in, there needs to be a camera on the rover. In an effort to keep costs low, inexpensive 12 volt cameras were purchased. The cameras selected were \$15 each, and are able to send a compatible video signal to the video switch, on screen display, and rover video transmitter. In addition to the rover, these same cameras were used to create astronaut “helmet cameras”. These “helmet cameras” operate via a battery pack and can be mounted on the EVA suit. The video from these helmet cameras is sent to a video transmitter on the astronaut, which then sends the video stream to a video receiver on-board the rover. The 12 volt camera was selected over a 5 volt camera because the electronics battery on the rover is 12 volts, and also the video transmitter for the helmet camera operates on 12 volts. This allows for a single voltage to be used which simplifies the wiring and reduces

the necessary components. Three camera were purchased: one for the rover's driving camera and two for astronaut helmet cameras.



Figure 84 - 12 Volt Camera (GoolRC, n.d.)

Boscam 5.8 GHz Video Transmitter and Receiver

In order to get the video stream from the astronaut's helmet camera to the rover, small video transmitters and receivers were required. This transmitter and receiver operate on the 5.8 GHz frequency band and have a maximum transmitting power of 200 mW. This video system was chosen because it is inexpensive, light weight, and operates on 12 volts. The transmitter is small and light weight, allowing for unhindered use by the astronaut in the field. The receiver was retrofitted with an antenna extension cable allowing the receiver antennas to be mounted on the rover's antenna boom while the receivers are safely placed within the rover. A receiver and transmitter pair operate on one of eight channels. This channel is selected via mechanical switches on the transmitter and electronically by cycling a button on the receiver. Unfortunately, specifications could not be found about the sensitivity of the receiver so a link budget could not be calculated.

It is important to note that this video system is not a long range system. It is intended to send video to the rover over a relatively short distance. This video is then relayed back to the habitat by the much more powerful rover video transmitter. A picture of the transmitter and receiver is found below.



*Figure 85 - Boscam Video Transmitter and Receiver
(Boscam, n.d.)*

Pan and Tilt Camera Kit

The rover camera allows the operator to see the terrain in front of the rover, but the pan and tilt camera system allows the operator to control exactly where the camera is pointing. This pan and tilt camera system uses a very light weight frame, made from carbon reinforced plastic, to house the servos control the system's movement. The system allows for 360 degree viewing around the rover, greatly increasing the operator's situational awareness and ability to plan a route for the rover. The two servos are controlled via the Turnigy 9X controller and the DragonLink transmitter and receiver. This allows the operator to have full control of the rover's vision and movement. A picture of the pan and tilt system is shown below.

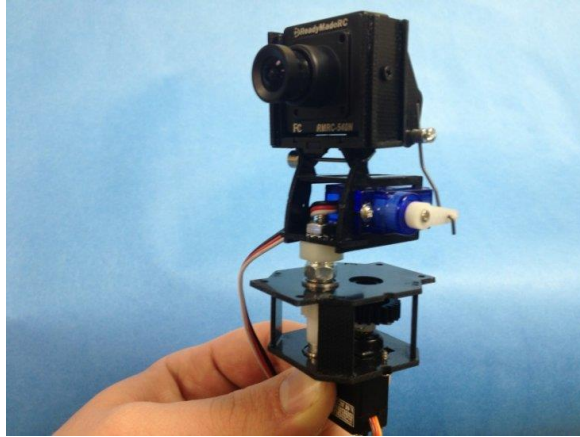


Figure 86 - Pan and Tilt System (Ready Made RC, n.d.)

Rover Camera Housing

A custom housing needed to be designed to accommodate the rover's pan-tilt camera system. This housing needed to provide a mounting location for the pan-tilt system, allow for full range of motion, and securely attach on top of the rover boom. To do this, a custom housing needed to be created. It was modeled using Autodesk Inventor and manufactured using acrylic machined by a CNC mill.

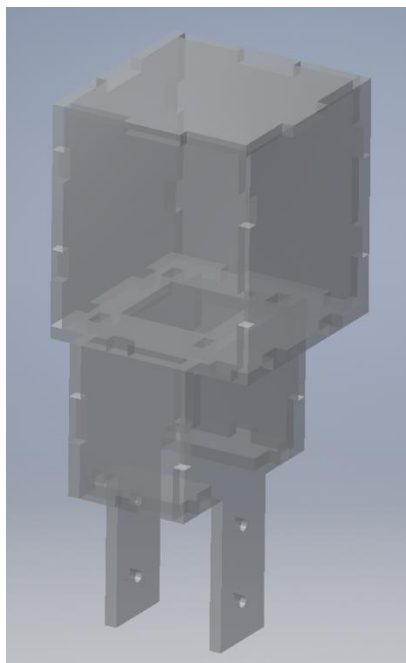


Figure 87 - Rover Camera Housing Model

This housing was designed to be cut from of a single piece of clear acrylic. This necessitated creating interlocking pieces that would form the final housing. A picture showing the results from the CNC process is shown below. The mechanical engineering machine shop's CNC mill was used.



Figure 88 - CNC Milled Camera Housing Pictures

After the pieces were cut out, the corners of the “slots” needed to be filed to make them square. This allowed for an easy assembly.

Once assembled, the pan-tilt camera system was placed into the housing and attached using screws. The wires were ran up the boom and connected to the camera and servos.

The housing was then attached to the rover using machine screws. This final assembly is shown in the figure below.



Figure 89 - Completed Rover Camera Housing

3-Channel Video Switch

To control which video feed is being transmitted by the rover's video transmitter (discussed next section), a remotely controlled video switch was required. This video switch receives a signal from the DragonLink receiver and connects either the rover camera, Suit Camera 1, or Suit Camera 2 to the rover's video transmitter. This switch enables the rover to act as a video repeater. The video switch will receive analog video

signals from the rover camera and both 5.8 GHz video receivers. The switch is powered via the DragonLink receiver and receives the switch signal from a 3-position switch on the Turnigy 9X controller. A picture of the video switch is found below.



Figure 90 - 3 Channel Video Switch (Hobbyking, n.d.)

Videolynx VM-70X Amateur Radio Video Transmitter

The same logic to use the DragonLink transmitter over the stock transmitter was applied to the video transmitting system on the rover. As seen in a previous section, inexpensive 5.8 GHz video transmitters were used to send video from the astronauts to the rover. As proven in the DragonLink section, higher frequency radio waves experience greater path loss than lower frequency waves. Also, amateur radio equipment is capable of transmitting a much more powerful signal and can make use of home-made antennas to generate additional gain. Given the distance the rover is to be operating at, these low power, high frequency video transmitters would not be able to perform adequately. To solve this, the Videolynx VM-70X was chosen. This video transmitter produces a signal in the 433 MHz amateur radio signal band and has a transmit power up to 5 Watts. This will allow the habitat to receive the video feed from the rover or the astronauts and make decisions about a rover path or to help document an EVA.

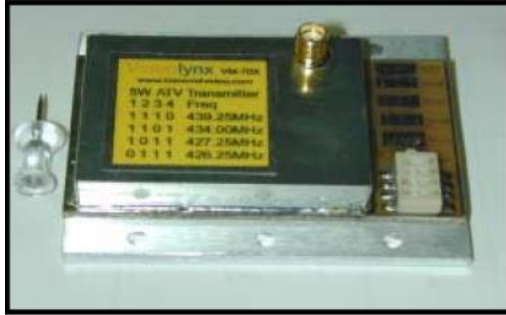


Figure 92 - Videolynx VM-70X (Transmit Video, 2017)

The transmitter will transmit the video on the 439.25 MHz frequency. This frequency corresponds to cable channel 60. This allows most televisions to receive the signal produced from this transmitter using an antenna plugged into the “cable” input. During testing, a simple $\frac{1}{2}$ wavelength dipole antenna was fabricated for both the transmit and receive antennas. These dipole antennas allowed the television to receive the signal transmitted by the rover. These dipole antennas used two $\frac{1}{4}$ wavelength elements, 6.72 inches long each. A successful test of the video system is shown in the below two images. The first image shows the rover boom with antennas and camera and with the receiving television in the background. The ATV antenna is the left-most antenna. The second image is a close up of the television and the receiving antenna.

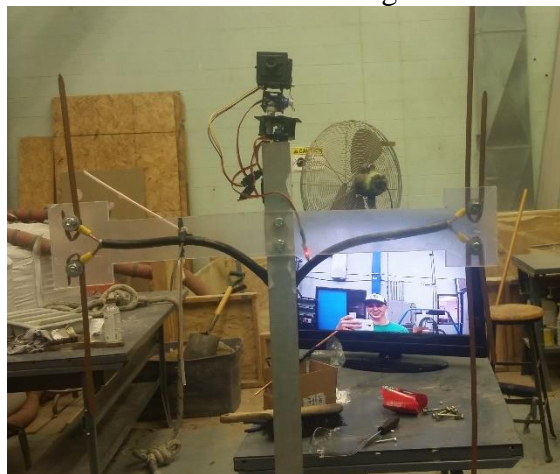


Figure 91 - Video Transmitter and Receiver Test

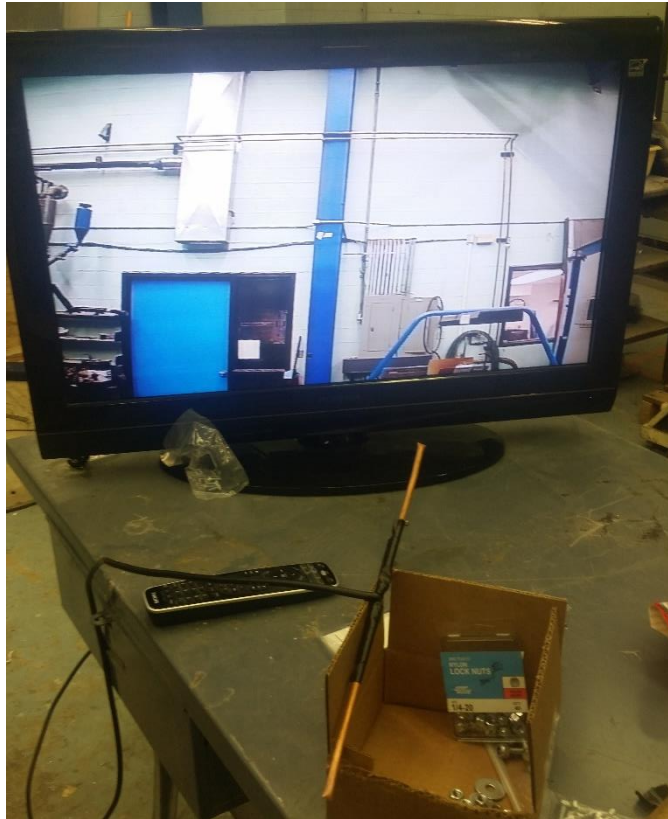


Figure 93 - Receiving Antenna and Standard Flat Screen Television

This transmitter can transmit for extended periods of time, which is what the rover needs. According to the user manual, the transmitter needs to be attached to a heat sink to avoid accumulating heat and burning out the transmitter. The following section discusses the heat sink.

Video Transmitter Heat Sink

The VM-70X needs a heat sink in order to continuously transmit the video feed back to the habitat. A desktop computer CPU heatsink with built-in fan was chosen. This heatsink uses a relatively large mass of aluminum with aluminum fins and a 12 volt fan to force air through the fins to remove the heat via convection. This heatsink will be turned on the entire time the rover is turned on and the video transmitter is operating.

In order to mount the transmitter to the heatsink, mounting holes needed to be drilled and tapped. The VM-70X was placed on top of the heatsink and the hole locations were marked. The holes were then drilled and tapped to accept the machine screws used to mount the VM-70X. Before the transmitter was connected to the heatsink, thermal paste was applied to the heatsink. This would ensure proper heat transfer between the transmitter and the heatsink. The below image shows the heatsink with drilled and tapped holes and the underside of the transmitter.

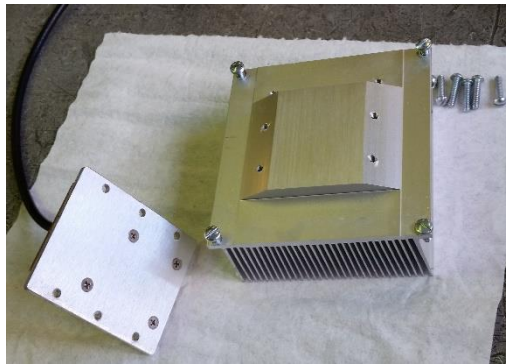


Figure 94 - VM-70X with Heatsink

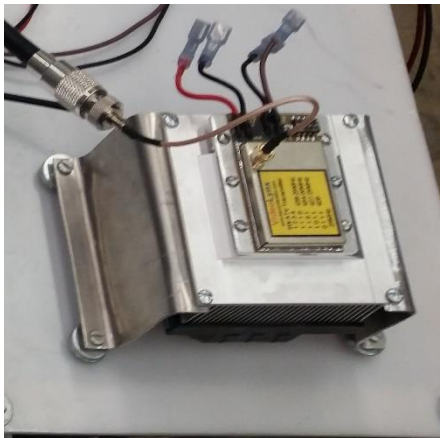


Figure 95 - VM-70X with Heatsink and Stands

After the transmitter was attached to the heatsink, the heatsink needed to be attached to the electronics panel with adequate clearance on the bottom to allow proper air flow. This was accomplished by manufacturing aluminum stands. The stands were created by bending aluminum sheet metal and attaching to the mounting locations on the heatsink. The stands can be seen in the below image.

MinimOSD

Since the VM-70X is a piece of amateur radio hardware, the transmitter is required by law to either show or verbally speak their call sign at the beginning of the transmission, the end of the transmission, and at least once every 10 minutes during the transmission. This was accomplished by utilizing an on-screen display with the appropriate call sign. An on-screen display is more commonly known as a heads-up display. It overlays the incoming video stream with text, and then outputs the resulting video stream. This component was one of the more challenging aspects of this project. A plug-and-play on-screen display (OSD) capable of displaying a user-input call sign could be purchased for a couple hundred dollars, but that was outside the budget for this project. To solve this, an open-source OSD project board was located with an active community. This board is called the MinimOSD and is primarily used in the hobby aircraft community. This board can be purchased for less than \$15. A picture of this board is found below.

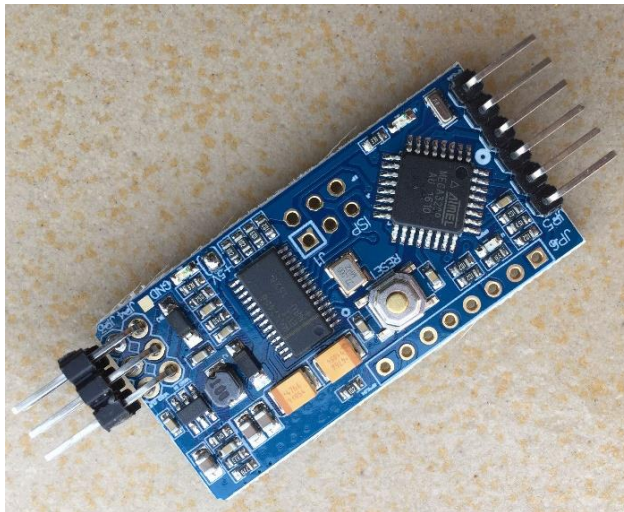


Figure 96 - MinimOSD Board (3DRobotics, n.d.)

This MinimOSD is able to be programmed using an FTDI-USB interface board and a custom GUI and software created this for OSD project. All of this software was sourced from the MinimOSD github project page. Using the GUI the callsign, flash interval, and

callsign location were programmed into the board's memory. All other functions were disabled. Some intriguing functions that could be integrated with future development require a GPS module and include position, velocity, distance from "home", and a compass pointing to "home" to make navigation easier.

The MinimOSD is built to fully integrate with hobby aircraft flight controllers, but this project only needs the OSD to display the operator's callsign. As such, the only connections are +5V and ground to power the unit, the output video feed from the video switcher as the input, and the video output from the MinimOSD. The video output then connects to the VM-70X to be transmitted back to the habitat. In this way the callsign will always be overlaid on the video stream regardless of the video stream being broadcast.

Amateur Radio Cross-band Repeater

The amateur radio cross-band repeater is the backbone of the astronaut communication system on the rover. The radio chosen for this is the Kenwood TM-D710. This radio allows the rover to act as an audio repeater, greatly increasing the communication distance between the astronauts and the habitat. The radio operates on the 2-meter (144 MHz) and the 70-cm (440 MHz) wavelength radio bands simultaneously. This allows the rover to receive a transmission on the 2-meter band and instantly retransmit the signal on the 70-cm band and vice-versa. Hardware that performs this kind of action is known as a repeater.

Once again, amateur radio hardware was chosen due to the lower frequencies, greater transmitting power, and the possibility to use homemade directional antennas. This radio has 3 transmitting powers: high (50 Watts), medium (10 Watts), and low (5 Watts) (Kenwood Corporation). This huge transmitting power allows the radio system to send radio signals very long distances.

During a simulation, the habitat will use a similar dual-band radio. This will ensure that any communications sent from the astronauts and rover on the two active channels will be received at the habitat. While in operation, the habitat will send the audio signals on the 2 meter band because these signals will experience less path loss compared to the 70 cm waves. They will then be repeated by the rover onto the 70 cm band and will be received by the astronaut's "walky-talkies" operating on the 70 cm band. The astronauts will then send their reply to the rover on the 70 cm band, which will be retransmitted to the habitat on the 2 meter band. Using the rover as a repeater in this way will allow communications up to two times the radio horizon (if the rover is placed at the radio horizon for the habitat and the for the astronauts). It should also be noted that the astronauts' personal radios will also be able to communicate directly with the habitat, but hand held "walky-talkies" generally have transmitting powers of less than 5 Watts and lack full size or directional antennas. The astronauts will be able to communicate with each other only using their personal radios.

Antennas

This section will discuss some additional antenna parameters that were not discussed in the DragonLink section. The first parameter is polarity. Antenna polarization is defined

as the orientation of the plane that contains the electric field component of the radiated waveform (Seybold, 2005). Most times, as is the case with the rover, antenna polarization can be determined from simple inspection; vertical dipoles produce radio waves with a vertical polarization, whereas horizontal dipoles produce horizontally polarized radio waves. There are other polarizations, such as right-hand circular, left-hand circular, or any other angle between horizontal and vertical. What is important is that antennas with opposite polarizations than the transmitted wave (horizontal vs. vertical, RHCP vs. LHCP) will theoretically not receive any power from the wave. This is called Cross-Polarization Discrimination (XPD). Unfortunately, this perfect isolation between polarizations is not possible in the real world, but large amounts of power rejection is still seen. If more information was wanted, "Introduction to RF Propagation" by Seybold goes much more in-depth and provides the reader with involved equations to calculate how much power rejection is obtained from differently polarized antennas.

Antenna polarization and XPD is used to help the communications antennas on the rover antenna boom. The rover uses 3 amateur radio devices to communicate with the habitat. In an attempt to help isolate each antenna from the others, special attention needed to be paid to the antennas. The DragonLink antenna is receive only, and the transmitter has a maximum power of 0.5 Watts. The other two antennas on the rover, the video transmitter and the radio repeater, operate with much higher wattages (5 Watts and 10-50 Watts respectively). Thus, the DragonLink antenna needs to be isolated as much as possible. This was achieved by turning the DragonLink antenna horizontal, thus oppositely polarizing it from the vertically polarized, high wattage transmitting antennas of the video transmitter and the radio repeater. This polarization, alongside the maximum

frequency separation possible, allowed the DragonLink antenna to be as isolated as possible. This requires the transmitting antenna to be horizontally polarized as well.

The second parameter is voltage standing wave ratio (VSWR), standing wave ratio (SWR) for short. This ratio is used to measure the energy reflected back to the transmitter from the antenna, caused by an impedance mismatch between the transmitter and the antenna. A simple equation used to measure SWR is found below.

Equation 24

$$SWR = \frac{E_f + E_r}{E_f - E_r}$$

Where E_f is energy transmitted and E_r is energy reflected back to the transmitter. An SWR of 1:1 means that all of the energy has been radiated as RF from the antenna and no energy has been reflected back towards the transmitter. Typical usable values for SWR are between 1:1 and 1.5:1. Since SWR can be measured as a ratio of forward and reflected energy, SWR meters can be placed in-line between the transmitter and antenna to measure SWR real time. In this way, SWR can be used as a way to tune the antenna for a specific frequency or a frequency band and is also a convenient way to measure antenna efficiency. An SWR meter was used in this project to tune the antennas used for the VM-70X video transmitter and for the TM-D710 radio repeater.

Half-wave dipole antennas were created for each of the transmitters. The TM-D710 needed an antenna capable of transmitting on both the 144 MHz (2-meter) band and the 440 MHz (70 cm) band. This required the creation of dual-band dipole antenna. Antenna plans were sourced from amateur radio operator KG0ZZ's website (KG0ZZ, 2011). Using these plans the dual-band dipole antenna was constructed. The SWR was then

measured using an SWR meter and the antenna was tuned to the operating frequencies. Tuning an antenna consists of trimming the ends of the antenna until the antenna is



Figure 98 - Dual-Band Dipole 146 MHz SWR



Figure 97 - Dual-Band Dipole 446 MHz SWR

resonant at the desired frequencies. This is measured by observing an SWR of near 1:1. Pictures are shown below of the dual-band dipole antenna tuned to the frequencies 146 MHz and 446 MHz.

An SWR of 1.2:1 was observed for 146 MHz and an SWR of ~1.35:1 was observed for 446 MHz. This antenna has been shown to be below the 1.5:1 threshold for both operating frequencies.

A single frequency dipole antenna was created for the video transmitter. A half wave dipole was created and was tuned using the SWR meter in the same way as the dual-band dipole above was. No images were taken during the manufacture and testing of that antenna. The two antennas can be found in the image below.



Figure 99 - Dipole Antennas on Rover Boom

Chapter 2 Conclusion

After many months designing and manufacturing the rover, it was fully assembled and ready for testing. With everything mounted, the final weight was, oddly enough,

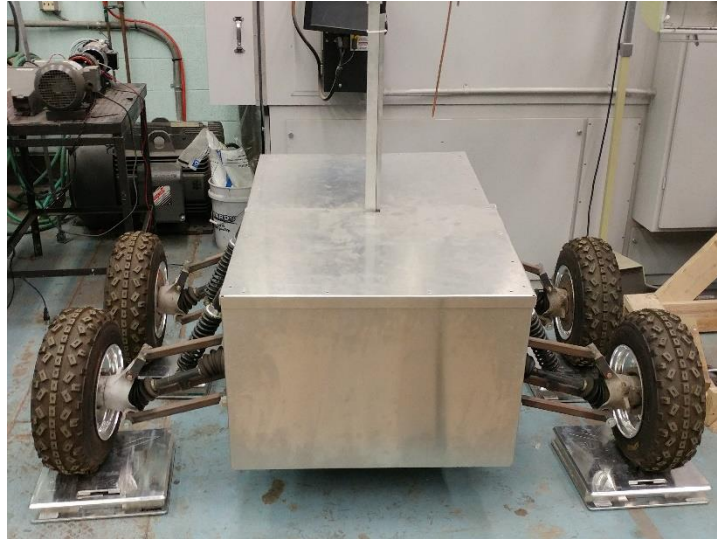


Figure 101 - Rover on Wireless Scales

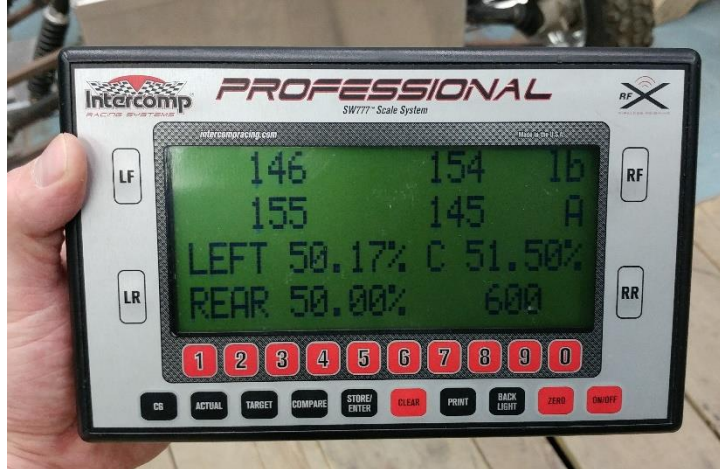


Figure 100 - Wireless Scale Readout

exactly 600 lbs. The weight was measured using four wireless vehicle scales. A picture of the weighing setup and the readout is shown below.

This weight corresponds quite well with the estimated weight of 615 lbs, although the manufactured rover does not include 100 lbs of estimated payload. This accurate estimation allows for the motor torque calculations to be directly applicable.

With the rover completed, it is now ready for testing.

Chapter III: Testing and Conclusions

Testing

The best way to test an EVA assistant rover would be to use the rover during an analog mission. Unfortunately no analog missions are scheduled at UND before the end of the spring 2017 semester, so “real world” testing cannot be accomplished. Instead, individual tests of the subsystems that make up the rover will be performed. The systems that need to be tested are:

- Rover propulsion system – How long will the rover be able to drive? How far can the rover drive? How much can it pull? How steep of a hill can it climb?
- Rover remote control – How far can the rover be away from the transmitter and still receive a signal? How far away from base can the rover operate?
- The radio repeater system – How much distance can be gained by using the repeater? How far can transmissions be made using the omni-directional antennas?
- The video transmission system – How far can the astronaut suit cameras transmit? How far away can the amateur video transmitter be received using an omni-directional antenna? How long can the video transmitter be used before it exceeds the upper limits of the operating temperature?

Rover Propulsion System

Testing the rover propulsion system was the first test to be performed. The rover had been in the works for over 18 months at this point, so the possibility of testing was very enticing. The test took place on a gravel country road in rural North Dakota. This road was completely isolated; no homes, no trees, and no powerlines creating spurious RF emissions. The terrain was completely flat, so this test would serve as a great baseline for future tests, such as how driving time would vary when pulling a load, or driving up a hill.

To begin the test, the rover was to drive straight away from the makeshift base (the vehicle and trailer that hauled the rover out to location) to see how far the rover could drive before signal was lost. The batteries on the rover and in the controller were fully charged prior to this test. The DragonLink module was set to “High Power” and the transmitter was held horizontal to ensure the transmitting antenna matched the horizontal polarity of the receive antenna.

The test began, and the rover drove straight down the road. The rover drove for approximately 100 yards before it stopped. Attempts to move the rover with the controller were unsuccessful. The test was halted to attempt to diagnose the problem. When the rover cover was removed to inspect the electronics, the smell of burnt circuit board rushed out. The rover only made it 100 yards before the motor controllers gave out. This quickly ended the rover propulsion testing. The baseline has been set at 100 yards.

Reasons for the motor controller failure were discussed, and a possible answer was settled on. During the initial testing of the propulsion system, the motor battery bank was wired using the two 12 volt deep cycle batteries in parallel. This created a 12 volt, 210

Amp-hour battery bank. The rationale was that halving the voltage would halve the rotational velocity of the motors (University of Minnesota, 2014), and since the rover only needed to approximately 50 wheel RPM it would be easier to throttle the high RPM scooter motors via the voltage than with a throttling control on the transmitter. It was determined that by halving the voltage, the current was doubled so the motor could produce the required power. This increased current load caused the motor controllers to fail. To remedy this, the battery bank was rewired to create a 24 volt system. The motor controllers were replaced and the test was attempted again. To ensure the motor controller and motors were wired correctly, the rover was placed on jack stands and the motors were run. The motors operated correctly, so the rover was placed on the ground to begin a test on UND campus. As the rover started to move forward and turn to position itself to leave the Mechanical Engineering garage, the motor controllers failed once again. The same burnt circuit board smell emanated from the rover. The cause of this failure was determined to be an over-current situation on the motor controllers while the rover was attempting to turn. Turning the rover causes one side's wheels to spin forward and the other side to spin in reverse. This difference in spinning wheels essentially causes the inside wheels to "spin out." This requires the wheels to overcome the coefficient of static friction between the tires and the surface. While on the wooden garage floor (wood planks for an easily removable cover on the vehicle maintenance pit) the rubber off-road wheels on the rover developed a high coefficient of friction, which required high amounts of torque (and therefore current) to spin the wheels and turn the rover. The motor controllers were again sent back to the manufacturer, along with a motor, for testing. This testing, performed at the motor controller manufacturer's facility in California, verified

that the controllers and motor were compatible. The problem with the motor controllers repeatedly failing has been determined to be an over-current issue during instances of peak current/torque. This is caused by the rover's weight, the off-road tires, and the medium the rover is driving on. The rover is able to successfully turn in place (the highest torque turn) in the grass and in gravel, but a turn in place is not recommended while on asphalt or wood. The motor controllers and motor were returned to UND and reinstalled. Full propulsion testing for the rover was not completed. New, higher capacity motor controllers will be required to continue this project in the future. The current motor controllers will operate the rover, but the motors are pushing the controllers to their limits. An unforeseen obstacle or accidental bump of the control stick has the capability to produce an over-current event and permanently damage the motor controllers again.

Rover Remote Control

The rover remote control was never tested to its limits. This was not a deliberate omission. The remote control distance was planned to be tested at the same time as the rover distance driving test. After the emotion of the rover failing, testing of the remote control distance was forgotten. This was planned to be remedied during the second attempt of the driving distance test which was scheduled to occur after the motor controllers were repaired and the driving system was switched over to the 24 volt system. Unfortunately this test never occurred either, as the rover never made it out of the garage. At the time of this writing, the remote control maximum distance is unknown.

Radio Repeater System

The radio repeater system was tested after the motor controllers failed during the propulsion test. This was accomplished by setting the radio to cross-band repeater mode and setting the frequencies to 146.500 MHz and 446.700 MHz. The transmission power was varied on the radio; 146.500 MHz was set to medium power, while 446.700 MHz was set to high power. These powers were chosen to in order to produce the strongest signals while minimizing the impact on other systems. When the 146.500 band was set to high transmission power, it would cause the pan-tilt camera servos to shake severely. This occurred even with grounded shielding surrounding all exposed wires leading to and from the servos. An image showing the radio interface with frequencies is shown below.



Figure 102 - TM-D710 During Testing

These two frequencies were also set on two Baofeng handheld radios; a UV-5R and a UV-82 HP. The UV-5R is an inexpensive entry level radio and can be had for under \$30. The UV-82 HP is a higher quality Baofeng handheld. It features higher transmitting power and overall better hardware. During this test, the UV-82 HP was the transmitting

radio and the UV-5R was the receiving radio. This was done because the UV-82 HP is capable of higher transmitting power, so it is able to transmit a stronger signal.

This test was performed by keeping the rover stationary and driving away from the rover in a vehicle. Two people would exit the vehicle, take a few steps to either side, and key the radio. The signal would travel from the UV-82 HP to the rover, get repeated on the opposite band, and then received by the UV-5R. In this way, the signal was traveling twice the distance from the rover to the vehicle. A successful transmission was when the person receiving the repeated signal could accurately understand the transmission. During this test, both signals were tested as the primary transmitting signal. This means that both the 146.500 MHz and the 446.700 MHz signal were sent from the UV-82 HP to the UV-5R through the rover at each location. This was performed to determine the best signal to be sent from the handhelds and the best signal to be sent from the rover. The best signal is determined by the most distance covered without affecting other systems on the rover. This transmission test was performed every 0.25 mile as measured by the vehicle odometer. A table of the results can be found below.

Table 5 - Radio Repeater Distance

	Tx	Rx	Tx	Rx
Distance from Rover (mile)	146.5	446.7	446.7	146.5
0.25	Yes			Yes
0.5	Yes			Yes
0.75	Yes			Yes
1	Yes			Yes
1.25	Yes			Yes
1.5	Yes			Yes
1.75	Yes			Yes
2	Yes			No
2.25	Yes			No
2.5	Yes			No
2.75	No			No

As the above table shows, the maximum one way distance of 2.5 miles was achieved by transmitting from the UV-82 HP on 146.500 MHz and receiving on the UV-5R on 446.700 MHz. This combination produced a total radio distance of 5 miles using an

omni-directional half-wave dipole antenna on the rover and small whip antennas (also omni-directional) on the handhelds.

Using the repeater in this configuration (rover receiving on 146.5 and transmitting on 446.7) allows for the transmission power to be set at low for 146.5 (VHF) and high for 446.7 (UHF). Setting VHF to low power will also help to eliminate the servo shake experienced by the camera servos.

It should be stated that these tests represent a fairly conservative maximum distance. The Baofeng radios are not known to be objectively “good” radios, but they are affordable and transmit on the amateur radio bands. This meant that they were available to be tested with, so they were used. More distance is predicted if higher quality handhelds are used (Kenwood, Motorola, Yaesu, etc) featuring more sensitive hardware. Also, during an analog simulation an amateur radio ground station radio (such as the Kenwood TM-D710 used as the cross band repeater) is expected to be used at the habitat. Utilizing a more powerful radio (the TM-D710 can transmit up to 50 Watts while the handhelds could only transmit up to 5 Watts) with either a directional Yagi or a half-wave dipole antenna could yield much greater results.

As for the range that could be expected; the radio horizon for line-of-sight (LOS) radio communication is approximated by

Equation 25

$$d \cong \sqrt{2h} \text{ (Seybold, 2005)}$$

This formula is based on the 4/3 Earth model and will only hold true for radio communications on Earth.

In this formula, “d” is distance in miles, and “h” is height of the transmitting antenna in feet. Using this approximation, the theoretical maximum radio communication distance from a height of 6 feet (approximately head height and rover antenna height) is 3.46 miles one way. If both the rover and the astronaut were transmitting from a height of 6 feet, the maximum distance they could be separated by is (3.46 miles * 2 = 6.92 miles). The following image helps to explain radio LOS communication.

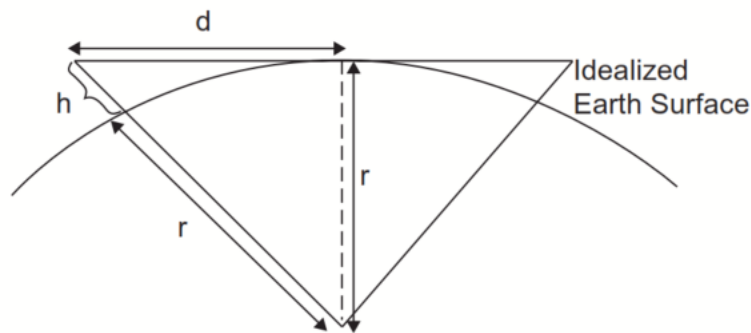


Figure 103 - Line-of-Sight Communications (Seybold, 2005)

It can be seen how increasing antenna height can have drastic changes to transmitting distance. Because of this, it is recommended that the habitat antennas be placed as high as possible to cover as much ground as possible. As an example, if the habitat antennas were placed 20 feet high, they would have a LOS distance of 6.32 miles. The habitat’s LOS value added with the rover’s LOS value of 3.46 yields 9.78 miles. The rover’s LOS is a radial distance from the antenna, so the rover’s LOS also extends in the opposite direction from the habitat, adding an additional 3.46 miles to the link distance. Add in the astronaut’s LOS value of 3.46 miles and the total distance the habitat should theoretically be able to communicate with the astronauts is 16.70 miles. This distance is assuming terrain free land (much like North Dakota or the Martian desert) and ideal radio conditions. The observed radio communication distance will be less than the theoretical, but this goes to show the value of adding the mobile radio repeater. In this theoretical flat

land example, the rover repeater added 6.92 miles of radio communication distance. This additional distance is great, but the real value of the repeater comes from the ability to transmit “behind” objects that block the radio signals from the habitat. Such obstacles could be a hill, the bottom of a dry river bed, or a valley. These tests were undertaken in a second radio testing day. It needs to be stated that the Earth-bound radio tests will have a larger range than the same tests on Mars or the moon. This is due to Mars and the moon’s smaller physical size. The radii of each body is less than the Earth, so the horizon will be closer. Also, Earth is equipped with a magnetic core and an ionized atmosphere that help to propagate radio signals over the horizon.

For this test, the rover was transported to a park in East Grand Forks, Minnesota. This park is near the Red Lake River, so it has a permanent dike. This dike is one of the largest hills in the area and served as the potential obstacle to test the rover repeater system. Each side of the dike has large flat areas that offer relatively long sight lines (for the line-of-sight radio communications). For this test to be successful, the rover needs to successfully facilitate communications between the “astronaut” exploring an area behind the hill and the base camp on the opposite side of the hill. Ideally, the astronaut and base

camp would be unable to communicate before introduction of the rover repeater system.

The following picture shows some of the terrain utilized during the test.



Figure 104 - Terrain for the Second Day of Radio Testing

The opposite side of the dike can be seen in this picture.



Figure 105 - Rover on Dike, Showing Opposite Side

As seen in the photos, the dike provides a solid barrier between the plains behind the dike, and the flood plain next to the river. A satellite image of the area is shown below:



Figure 106 - Rover Testing Location. Map data: Google

The GPS coordinates for the rover at this location are (47° 55.121, -97° 00.528).

The first test was to have test-subjects walk in opposite directions from the rover; one walking South-East into the soccer fields, and the other walking North-West into the flood plain. During this test the rover was turned off and the test subjects were communicating directly via handheld amateur radios on the 2-meter band. The idea was that the dike would provide enough of a natural barrier to inhibit direct communication between the test subjects. Unfortunately, when the test-subjects were at the maximum distances they could walk before crossing major roads or another bridge, they still had clear communication. The dike had no impact on direct communication between the test-

subjects at this short distance. The maximum distance the test-subjects reached is 0.78 miles and their locations are shown below:

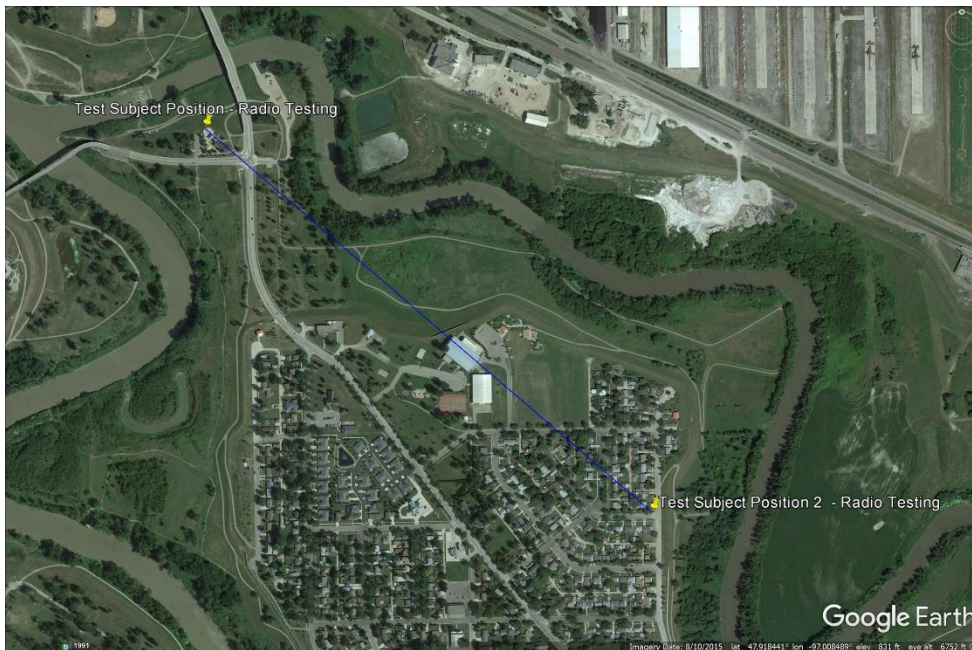


Figure 107 - Astronaut Direct Communication Test. Map Data: Google

Test Subject Position 1: N47° 55.342' W97° 01.000'

Test Subject Position 2: N47° 54.894' W97° 00.240'

When this test concluded, the two test participants were unable to see each other. There were many trees and the dike obstructing the direct line of site between the two, so it was surprising that the communication link was as clear as it was.

Because the dike proved to be an ineffective obstacle, the testing plan for the repeater needed to be adapted. The repeater test would no longer prove the capability to transmit voice “around” an obstacle, but would be a second test of the communication distance gained by utilizing the repeater. This alteration to the testing plan is unfortunate, but is necessary as a potential obstacle large enough to create an effective radio shadow cannot be located near Grand Forks.

This repeater test consisted of the rover and two test subjects. The rover was placed on the dike, test subject 1 (TS1) was close by the rover (within 100 yards), and the test subject 2 (TS2) was in a vehicle driving away from the rover. TS1 would transmit to the rover on 446.700 MHz and the rover would retransmit the signal on 146.500 MHz. TS2 would then receive the transmission while inside the vehicle driving away from the testing location. To accurately find when the signal dropped out, TS1 would speak into the radio every 10 seconds. When TS2 would no longer clearly hear the signal, the location would be marked and the test would be concluded. While driving away from the rover, TS2 was able to clearly hear TS1 retransmitted through the rover for an extended distance. The test was concluded without finding the maximum one way repeated transmission range of the rover. At the test conclusion, TS2 was 4.15 miles away from the rover. An image showing the locations is shown below:

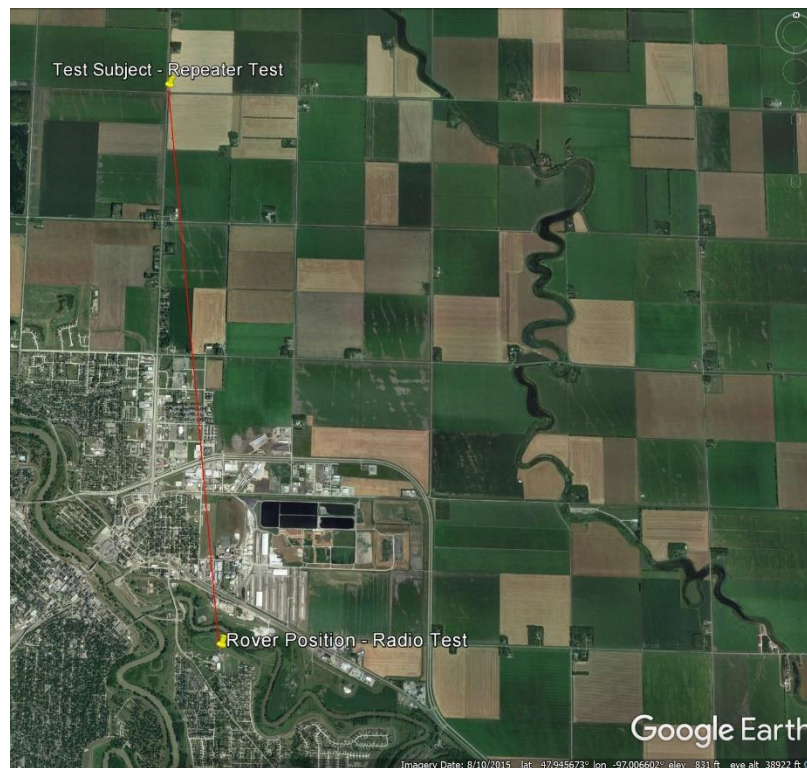


Figure 108 - Rover Repeated Audio Test. Map Data: Google

Rover Position: N47° 55.121' W97° 00.528'

TS2 Position: N47° 58.666' W97° 01.220'

The received audio was being transmitted through the city of East Grand Forks and was being received clearly inside of a vehicle by a handheld radio. The distance and clarity of the transmission was shocking. Even though this was only a one-way test, the transmission distance improved by 166% over the previous repeater test. This test is a good simulation of the base receiving a transmission from the rover, as the base would have a high powered radio capable of transmitting a similarly powered signal back to the rover for retransmission to the astronauts. It is unsure whether the handheld radios, with their less powerful transmitters and less efficient antennas, would be able to clearly transmit to the rover at this distance. Handheld transmission at this distance was not tested.

One reason for this large distance is that the rover was placed on a hill that is higher in elevation than the receiving radio. The rover's ground elevation was 841 feet above sea level and the receiver's elevation was 829 feet. This is a difference of 12 feet (assuming that both antennas were approximately 6 feet off the ground at the time of the test). According to Equation 25 (radio LOS calculation) the theoretical maximum LOS is 4.898 miles. This calculation is in agreement with the tested distance of 4.15 miles.

Video System

The video system needed three primary tests. These tests were:

1. Transmitting distance of the astronaut helmet cameras.
2. Transmitting distance of the amateur radio video transmitter.
3. Maximum temperature reached by the amateur radio video transmitter during extended use.

The first test performed was to find the transmitting distance of the 5.8 GHz astronaut helmet camera system. This was performed after the radio repeater test on the gravel road. To find this distance, the camera and transmitter were turned on, the rover video receiver was turned on and switched to the appropriate channel, and the rover video transmitter was turned on. This would allow the television on location to receive the video feed from the helmet camera.

The test was carried out by holding the transmitter and camera and then walking away from the rover. The person monitoring the television called the test subject with a cell phone when the video became unusable. This spot was then marked on the gravel road and was measured. The maximum distance this video transmitter was able to perform was 0.5 miles.

A second test of the 5.8 GHz system was performed on May 26th. For this test the rover was placed on top of a dike in East Grand Forks (near the same location as the repeater test), a base with a television was established in a park shelter approximately 50 yards from the rover, and the test subject walked Northwest away from the rover in possession of the camera/5.8 GHz transmitter system. This test was to confirm the measurements taken on the gravel road during the initial test of the video system. This distance and locations can be seen in the following image, showing the locations of the rover and the test subject at test conclusion.



Figure 109 - Astronaut Video Test. Map Data: Google

Test Subject: N47° 55.217' W97° 00.942'

Rover: N47° 55.135' W97° 00.487'

The maximum distance recorded during this test was 0.36 miles. As can be seen in the satellite image above, the video stream was being transmitted through trees. These trees played a major role in the reception of the video feed to the rover. While the test subject was walking through, and past, the trees the transmission would sporadically cut in and out. The video feed would go from clear to nonexistent. It is assumed this is due to the trees and their leaves creating interference and disrupting the line-of-sight to the rover. The test was concluded when the test subject reached the crest of another dike for the other river in the image. If the test subject had more room and the path back to the rover was clear of obstructions, more distance could have been obtained. While this test did not duplicate the range of the initial gravel road test (0.36 miles compared to 0.5 miles), it does verify that distances of that magnitude are achievable.

The second test was to find the maximum distance the amateur radio video transmitter could transmit the video feed. This was accomplished by turning on the amateur video transmitter, setting it to transmit the wired rover camera, moving the television and half-wave dipole to the vehicle, and then driving away from the rover. The test was concluded when the video quality was no long usable. The following images show a clear image, and the final image used to measure the transmitting distance.



Figure 111 - Amateur Video Transmitter Test Image 1



Figure 110 - Amateur Video Transmitter Test Image 2

Notice in the second picture that a test subject is standing outside holding the antenna and the television is receiving such a low signal that it is actually displaying “No Signal” on the screen. The second picture was taken at a distance of 1 mile. This range will be increased by utilizing a directional antenna on the habitat.

The final test was to measure how hot the amateur radio video transmitter became during continued use. In the VM-70X user manual it states that the maximum operating temperature is 65 degrees Celsius (149 degrees Fahrenheit) and that if the transmitter is used on high power it should use some kind of heat sink. This test will be deemed successful if the temperature of the video transmitter stays below 149 degrees Fahrenheit under constant use with the aid of the CPU heatsink. This test was performed until the temperature stabilized for multiple readings for multiple minutes. To test the temperature, the video transmitter and heat sink fan were turned on and the temperature of the video transmitter was taken using an infrared thermometer. The temperature was taken once a minute for the first 5 minutes, and then once every 5 minutes until the temperature stabilized. The results are shown in the following table.

Table 6 - Video Transmitter Temperature

Video Transmitter Temperature	
Time (minutes)	Temperature (F)
0	75
1	81
2	85
3	88
4	91
5	91
10	100
15	104
20	101
25	99
30	99

The temperature stabilized right around 100 degrees Fahrenheit after 10 minutes. This means the VM-70X will not exceed the maximum operating temperature. The temperature test for the amateur video transmitter is a success.

Conclusions

This thesis set out to create the most effective EVA assistant rover that has been produced thus far. Design elements and functionality were sourced from all previous analog rovers, and the best features were combined into a single package. This rover features a radio repeater that increases communication distance between the habitat and astronauts on the ground, a video transmitter that sends live-feed video from the rover and astronaut helmet cameras, and the proposed strength to be able to do “real work” during an analog mission, such as pull an astronaut to safety should they get injured or pull a heavy object into a better position on the planetary surface. Unfortunately, due to the motors’ high current requirements and the motor controllers’ inability to safely provide that current, much of the envisioned testing was not able to be accomplished. As such, much of the qualification for this rover to be deemed a revolutionary instrument has yet to be accomplished.

Of the testing that has been performed, the rover has proven viable in its role as a communications hub and as a vital link between the habitat and the astronauts in the field. The testing has verified that all of the communication subsystems are operational and that they provide additional communication coverage. Using omni-directional antennas, the base is able to receive rover video up to 1 mile away and receive a rover-repeated

transmission up to 4.15 miles away. The rover is able to receive a video transmission from an astronaut up to 0.5 miles away and receive an astronaut radio transmission up to 2.5 miles away. All of these distance are terrain dependent and could also be improved by utilizing high gain antennas.

While it was unable to be tested to its limits, the mechanical design of the rover is a success. It was able to house all of the necessary components of the rover: batteries, motors, gearboxes, radios, and various electronics. While driving the rover around UND's campus, the rover was able to successfully drive over a street curb while at speed, demonstrating the performance of the suspension system and the overall efficacy of the chassis. The mechanical design of this rover is the structure and glue that holds the project together. Unfortunately, these components were unable to shine because of shortcomings of other electrical components. While various electrical components will surely be replaced as the future technology improves, the mechanical design and construction of the rover should prove to be solid for years to come.

A very important aspect of this rover is that it lays the groundwork for many studies to come. Once the new higher amperage motor controllers are purchased and installed, this rover will prove to be another asset that makes UND Space Studies one of the best analog facilities in the world.

Future Work

As mentioned above, there is still work that needs to be done on this rover. The first obvious project is purchasing and installing higher amperage motor controllers. These

new motor controllers are rated for 120 amps, with a peak of 160 amps, per channel. The major drawback is these motor controllers cost \$500 each (Ion Motion Control, 2017) and the rover requires two of them. This has proven to be a necessary cost to get the rover fully operational.

Next is the creation of tool and sample storage on the rover. This can take the form of cabinets, drawers, or whatever other design the Human Spaceflight Laboratory team sees fit. Tool and sample storage is a critical element of the rover that the author did not have the time to create. The ability of these storage areas to efficiently integrate with the suited astronauts is crucial, so much thought and design should go into the creation of those components.

Next, directional antennas need to be created for all three of the habitat antennas (rover control, audio radio, video reception), especially for the video reception antenna. For the rover to be truly effective, it will need to have long range operation capability. This long range capability will be a combination of the DragonLink RC amateur radio transmitter and the VM-70X amateur radio video transmitter. If the astronaut controlling the rover inside the habitat is unable to see the surrounding terrain, the rover cannot be successfully piloted. A high gain antenna used to receive the rover's video feed is essential for proper functionality of the rover. Using high gain directional antennas creates additional design considerations. In order for these antennas to be effective, they need to be accurately pointed at the target. This will require antenna pointing control systems, either manual or automatic.

Since the rover is electrically controlled, it should be able to be converted to a partly autonomous system. Utilizing an autopilot to follow astronauts, or to traverse to GPS

waypoints automatically, would serve as a huge benefit to the analog astronauts of the future. This would be a large project, but it would make the rover even more comparable to the rovers used and created in NASA studies.

While the rover is not completely finished, the work accomplished in this thesis will serve as a foundation for many projects, and hopefully many theses, in the years to come.

Appendices

Appendix A – Manufacturer Engineering Information

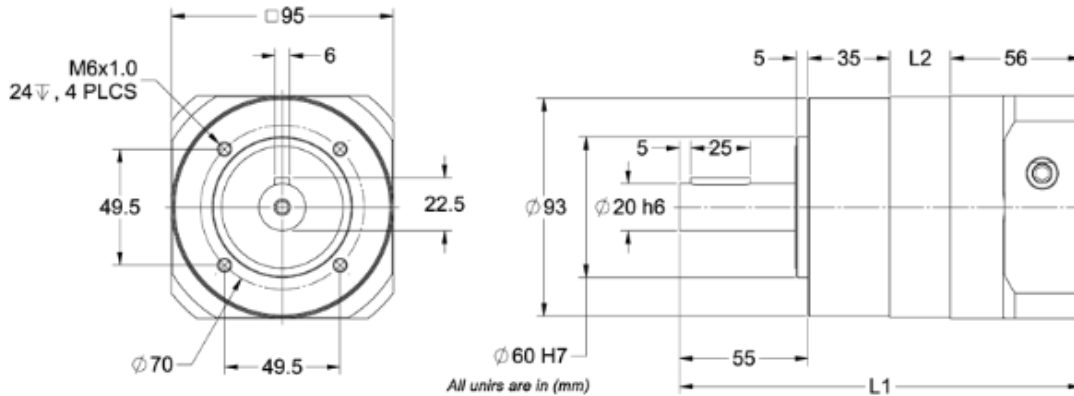


Table 1		Gearbox Specifications									
Prefix	Gear Ratio (X:1)	Rated Output Torque (in-lb)	Max Output Torque (in-lb)	Backlash Maximum (arc-min)	Rated Input Speed (RPM)	Stages	Efficiency (%)	Torsional Rigidity (Nm/arcmin)	L1 Length (mm)	L2 Length (mm)	Weight (lbs)
GBPH-0901-CS-003	3	1239	3717	11	2600	1	97	11	172	36	7.7
GBPH-0901-CS-004	4	1487	4461	11	2600	1	97	11	172	36	7.7
GBPH-0901-CS-005	5	1372	4116	11	2600	1	97	11	172	36	7.7
GBPH-0901-CS-007	7	1469	4408	11	2900	1	97	11	172	36	7.7
GBPH-0901-CS-010	10	1239	3717	11	2900	1	97	11	172	36	7.7

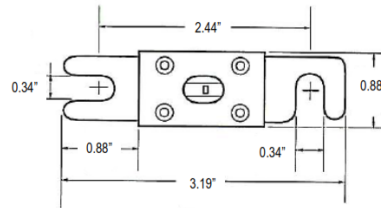
Figure 113 - Anaheim Automation Gearbox Information

SPM Rr.	ASM #	Half Shaft Splines	Outer CV Splines	Inner CV Splines	Plunge/Angle Diagram
	1332935		DIFFERENTIAL INTERFACE ANS B92-1 EXTERNAL INVOLUTE SPLINE FILLET ROOT SIDE FIT (HARDENED) NO. OF TEETH 26 PITCH 24748 PRESSURE ANGLE 45° PITCH DIAMETER 1.0833 REF. BASE DIAMETER 766 REF. FORM DIAMETER 1.0560 MAJOR DIAMETER 1.1250/1.1150 MINOR DIAMETER 1.0320 MIN. CIRC. TOOTH THICKNESS MAX. EFFECTIVE .0738 MIN. ACTUAL .0702 MIN. MEAS. OVER PINS 1.2155 REF. PIN DIAMETER .080	DOJ STEM EXTERNAL SPLINE EXTERNAL INVOLUTE SPLINE (HARDENED) ANS B92-1 FILLET ROOT SIDE FIT NO. OF TEETH 36 PITCH 24748 PRESSURE ANGLE 45° PITCH DIAMETER 1.5000 REF. BASE DIAMETER 1.0807 REF. FORM DIAMETER 1.4710 MAJOR DIAMETER 1.5420/1.5320 MINOR DIAMETER 1.448 MIN. CIRC. TOOTH THICKNESS MAX. EFFECTIVE .0738 MIN. ACTUAL .0690 MIN. MEAS. OVER PINS 1.6312 REF. PIN DIAMETER .080	
	1332881		WHEEL HUB INTERFACE EXTERNAL INVOLUTE SPLINE (HARDENED) FILLET ROOT SIDE FIT NO. OF TEETH 20 PITCH 24748 PRESSURE ANGLE 45° PITCH DIAMETER .6333 REF. BASE DIAMETER .5893 REF. FORM DIAMETER .596 MAJOR DIAMETER .8757/.865 MINOR DIAMETER .782 MIN. CIRC. TOOTH THICKNESS MAX. EFFECTIVE .0738 MIN. ACTUAL .0702 MAX. MEAS. OVER PINS .9657 REF. MIN. MEAS. OVER PINS .9143 PIN DIAMETER .080	DIFFERENTIAL INTERFACE ANS B92-1 EXTERNAL INVOLUTE SPLINE FILLET ROOT SIDE FIT (HARDENED) NO. OF TEETH 22 PITCH 24748 PRESSURE ANGLE 45° PITCH DIAMETER .9167 REF. BASE DIAMETER .6482 REF. FORM DIAMETER .6870 MAJOR DIAMETER .9587/.9480 MINOR DIAMETER .866 MIN. CIRC. TOOTH THICKNESS MAX. EFFECTIVE .0738 MIN. ACTUAL .0701 MAX. MEAS. OVER PINS 1.0494 REF. MIN. MEAS. OVER PINS 1.0477 PIN DIAMETER .080	
	1333008		WHEEL HUB INTERFACE EXTERNAL INVOLUTE SPLINE (HARDENED) FILLET ROOT SIDE FIT NO. OF TEETH 26 PITCH 24748 PRESSURE ANGLE 45° PITCH DIAMETER 1.0833 REF. BASE DIAMETER 766 REF. FORM DIAMETER 1.0560 MAJOR DIAMETER 1.1250/1.1150 MINOR DIAMETER 1.0320 MIN. CIRC. TOOTH THICKNESS MAX. EFFECTIVE .0738 MIN. ACTUAL .0702 MIN. MEAS. OVER PINS 1.2155 REF. PIN DIAMETER .080	DIFFERENTIAL INTERFACE ANS B92-1 EXTERNAL INVOLUTE SPLINE FILLET ROOT SIDE FIT (HARDENED) NO. OF TEETH 28 PITCH 24748 PRESSURE ANGLE 45° PITCH DIAMETER 1.1666 REF. BASE DIAMETER .8250 REF. FORM DIAMETER 1.1375 MAJOR DIAMETER 1.2080/1.1980 MINOR DIAMETER 1.115 MIN. CIRC. TOOTH THICKNESS MAX. EFFECTIVE .0738 MIN. ACTUAL .0700 MIN. MEAS. OVER PINS 1.2975 REF. PIN DIAMETER .080	

Figure 112 - Polaris Sportsman 500 Half Shaft Data

ANN Fuses Very Fast-Acting

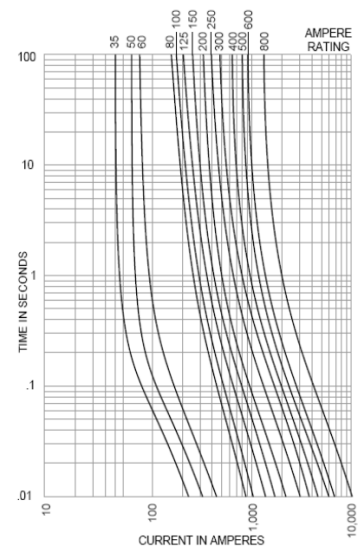
Waytek Stock No.	Amps
46161	10
46162	35
46163	40
46164	50
46167	60
46168	80
46169	90
46180	100
46181	125
46182	150
46187	175
46183	200
46184	250
46185	300
46188	325
46189	350
46186	400
46200	500
46206	600
46208	700
46209	800



Features:

- Voltage: 80V DC (or less), 125 VAC (or less)
- Interrupting Rating: 2,700 amps DC, 2,500 amps AC
- UL Recognized: 35-400A, 500A DC only, Guide JFHR2, File E56412
- Very fast-acting (high speed of responses to short-circuit currents)
- An open link element is visible through a mica window

Time-Current Characteristic Curves-Average Melt

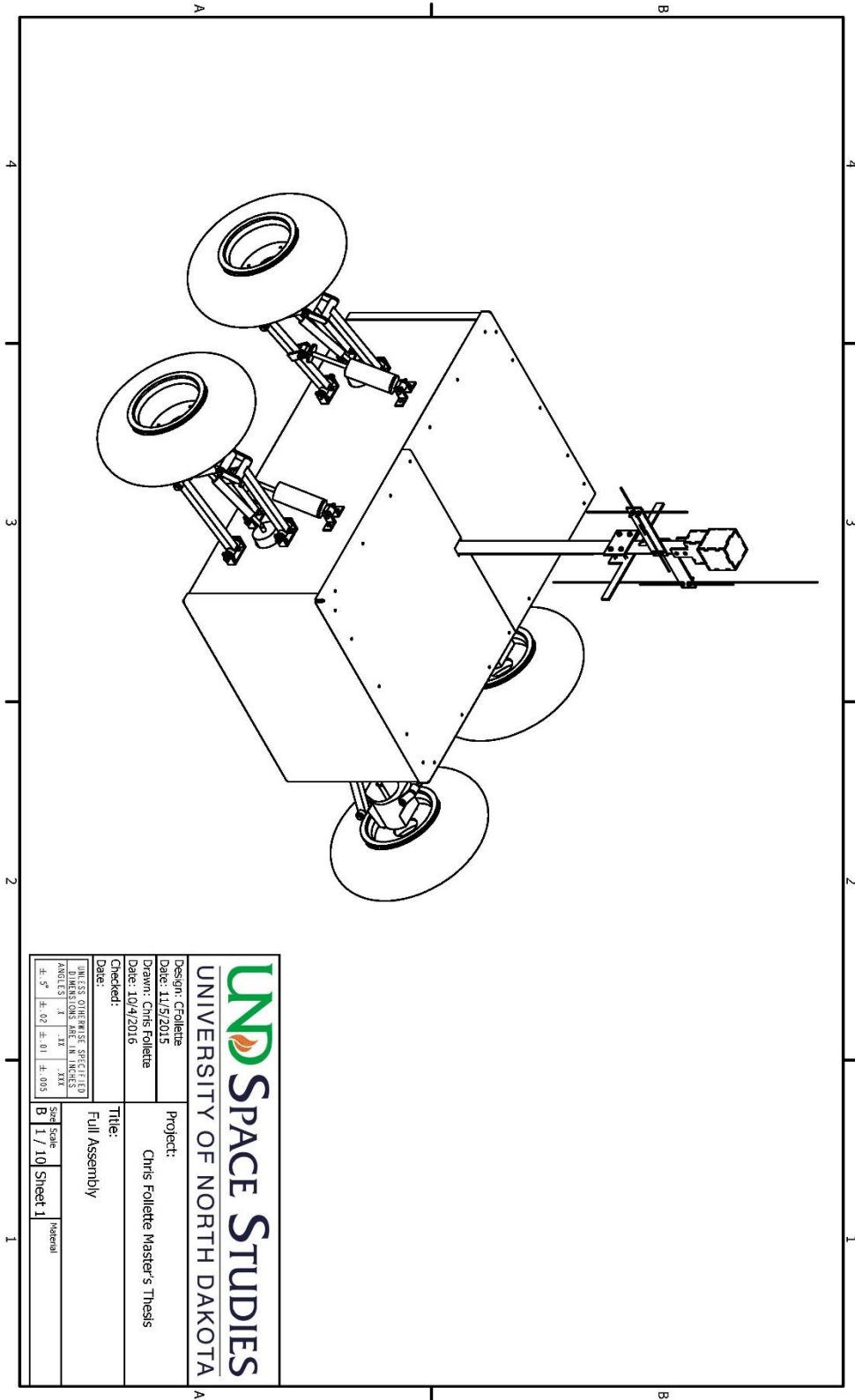


UNCONTROLLED DOCUMENT
 All information provided by manufacturer
 Updated 1/27/2011

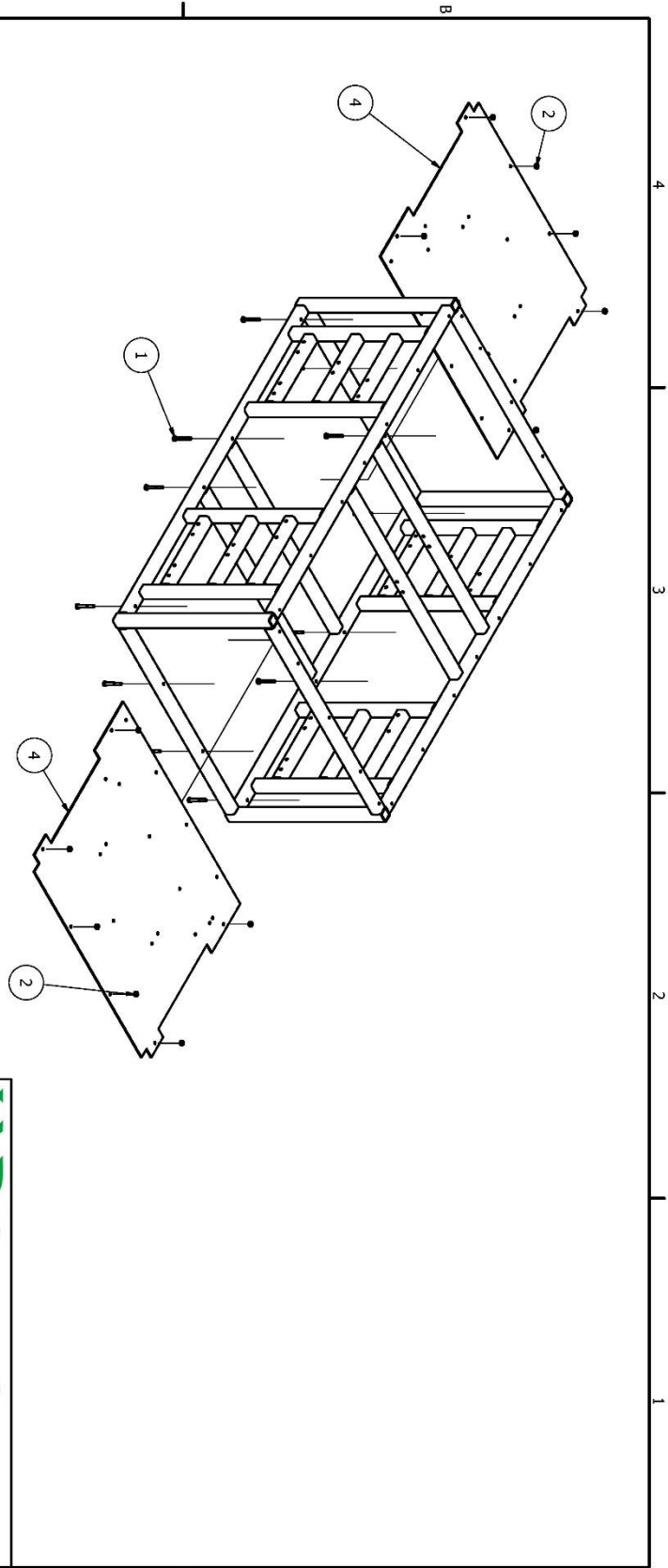
www.waytekwire.com
 Phone | 800.328.2724 | 952.949.0765
 Fax | 800.858.0319 | 952.949.0965

Figure 114 - ANN-100 Fuse Specifications (Waytek, 2017)

Appendix B – Engineering Drawings



UNIVERSITY OF NORTH DAKOTA		SPACE STUDIES	
Design: Cedelete Date: 11/9/2015 Drawn: Chris Follette Date: 10/4/2016 Checked: Date:			
Project:		Chris Follette Master's Thesis	
Title:		Full Assembly	
DIMENSIONS SPECIFIED IN DIMENSIONS ARE IN INCHES ANGLES IN DEGREES		Tolerances: ±.05 ±.02 ±.01 ±.005	Scale: 1 / 10 Sheet 1 of 1 Material:



NOTES:
 1. INSTALL THE STEEL BOTTOM PLATES AND SECURE WITH 6 BOLTS PER PLATE

PARTS LIST	
ITEM	DESCRIPTION
4	Steel Plate Bottom
1	Hex Bolt - UNC (Regular Thread - .125)
2	Hex Nuts (Ftinch Series) Hex Nut

UNIVERSITY OF NORTH DAKOTA
SPACE STUDIES

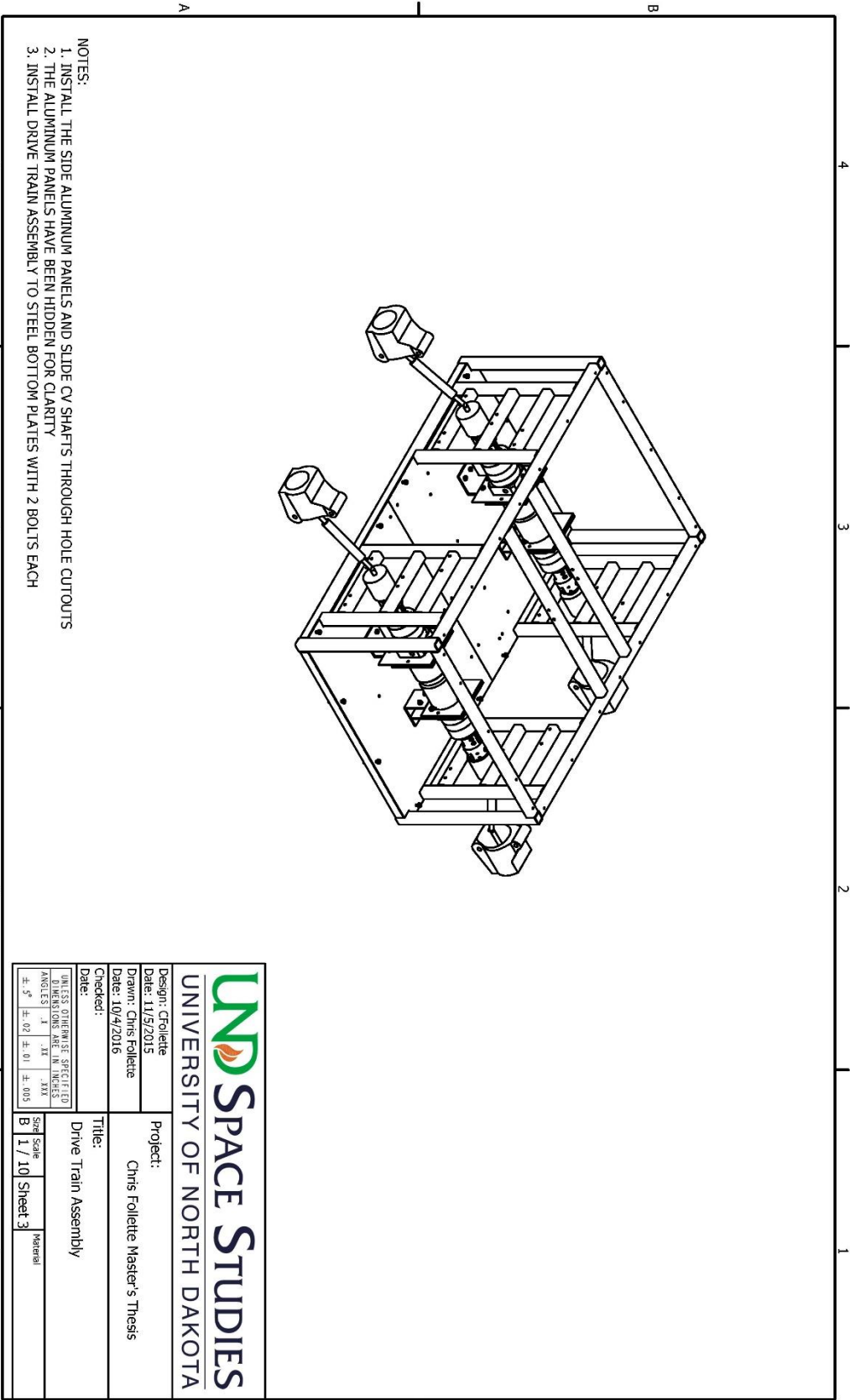
Design: Cfollette
 Date: 11/5/2015
 Drawn: Chris Folllette
 Date: 10/4/2016
 Checked:

Project:
 Chris Folllette Master's Thesis

Title:
 Full Assembly - Steel Bottom Plate

Size Scale: B
 1 / 10
 Sheet 2

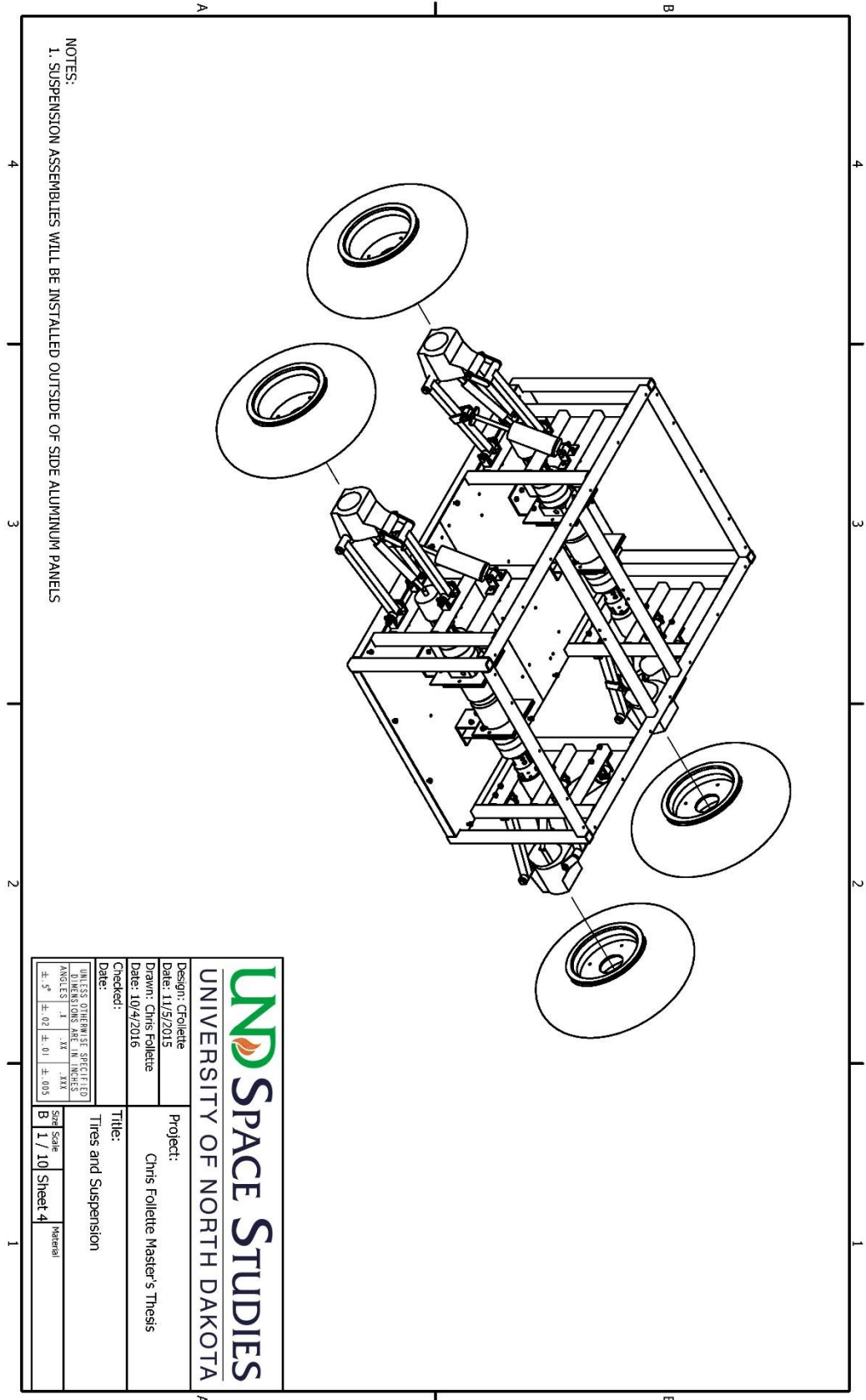
UNLESS OTHERWISE SPECIFIED
 DIMENSIONS ARE IN INCHES
 ANGLES ±.5° ±.01 ±.005



- NOTES:
1. INSTALL THE SIDE ALUMINUM PANELS AND SLIDE CV SHAFTS THROUGH HOLE CUTOUTS
 2. THE ALUMINUM PANELS HAVE BEEN HIDDEN FOR CLARITY
 3. INSTALL DRIVE TRAIN ASSEMBLY TO STEEL BOTTOM PLATES WITH 2 BOLTS EACH

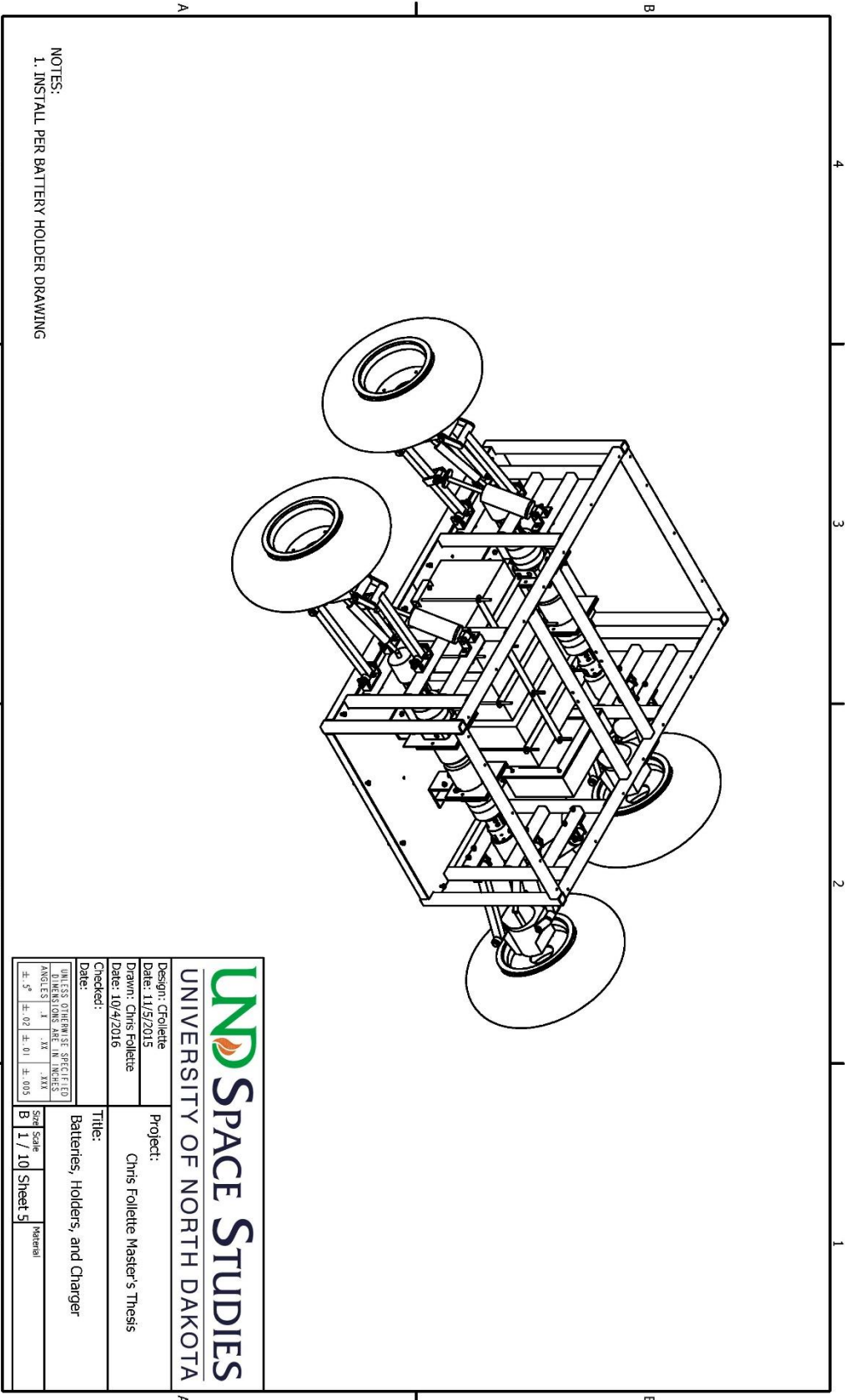
UND SPACE STUDIES
 UNIVERSITY OF NORTH DAKOTA

Design: Cfollette	Project:
Date: 11/9/2015	Chris Folllette Master's Thesis
Drawn: Chris Folllette	
Date: 10/4/2016	
Checked:	Title:
Date:	Drive Train Assembly
UNLESS OTHERWISE SPECIFIED DIMENSIONS ARE IN INCHES	Size Scale
ANGLES 1° 1/4° .001	B 1 / 10 Sheet 3
±.5° ±.02 ±.01 ±.003	Material




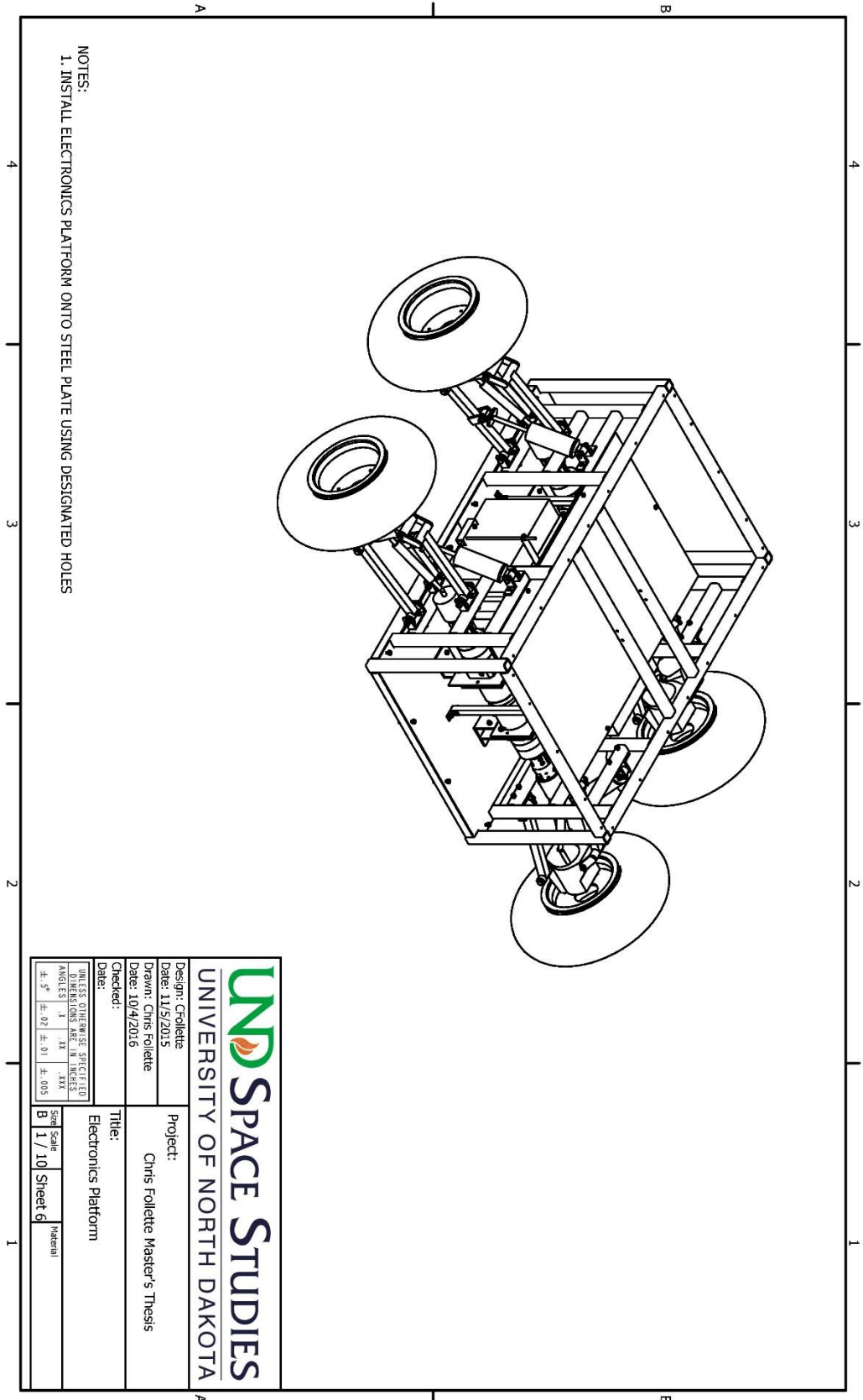
NOTES:
 1. SUSPENSION ASSEMBLIES WILL BE INSTALLED OUTSIDE OF SIDE ALUMINUM PANELS

UNIVERSITY OF NORTH DAKOTA	
Design: Crollette Date: 11/9/2015 Drawn: Chris Follotte Date: 10/4/2016 Checked: Date:	Project: Chris Follotte Master's Thesis Title: Tires and Suspension
UNLESS OTHERWISE SPECIFIED DIMENSIONS ARE IN INCHES ANGLES ° ±.5' ±.01 ±.003	Size Scale B 1 / 10 Sheet 4 Material



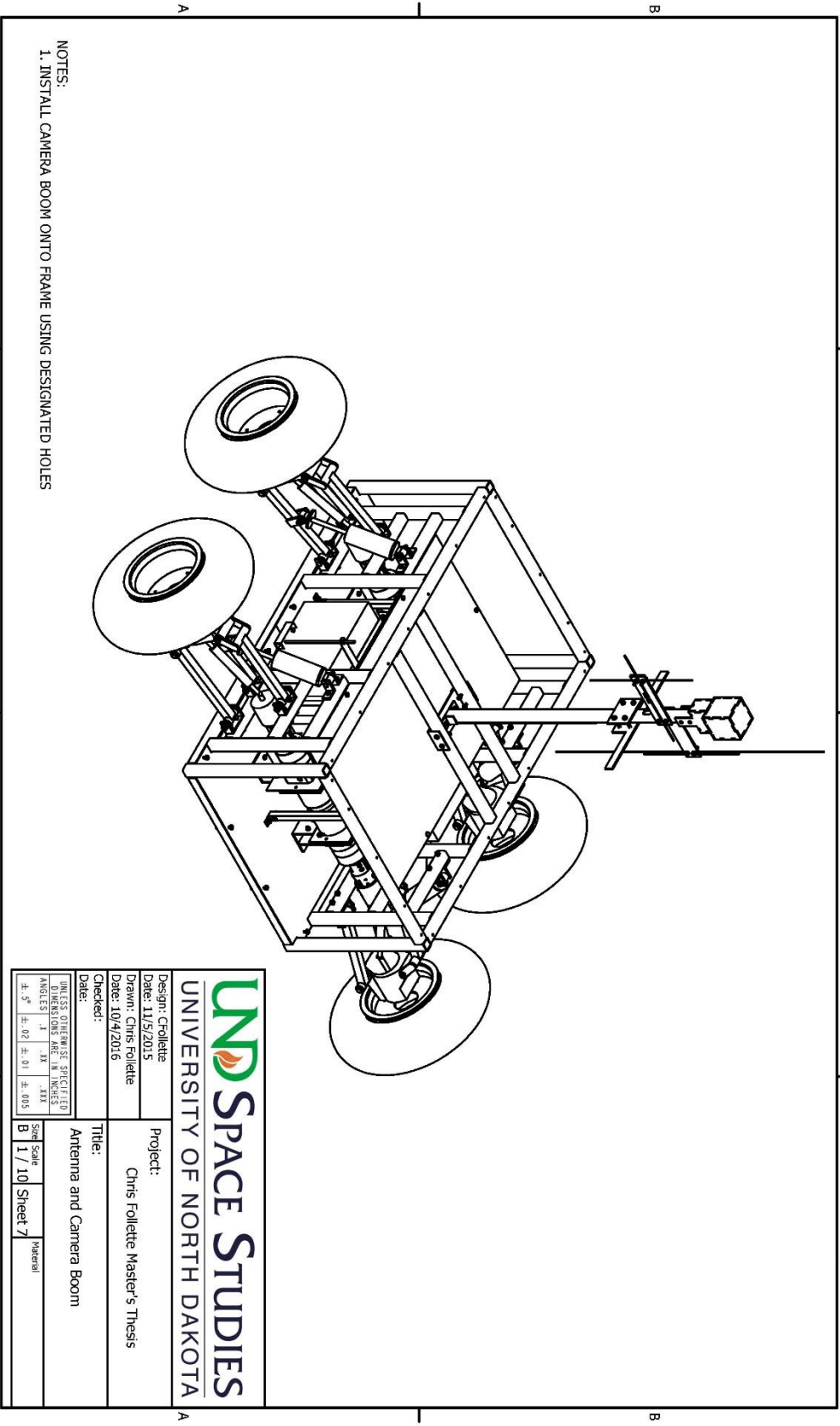
NOTES:
 1. INSTALL PER BATTERY HOLDER DRAWING

	
UNIVERSITY OF NORTH DAKOTA	
Design: Crollette Date: 11/9/2015	Project: Chris Follotte Master's Thesis
Drawn: Chris Follotte Date: 10/4/2016	Title: Batteries, Holders, and Charger
Checked: Date:	Material:
UNLESS OTHERWISE SPECIFIED DIMENSIONS ARE IN INCHES ANGLES IN DEGREES	Size Scale B 1 / 10 Sheet 5
±.5° ±.02 ±.01 ±.003	Material



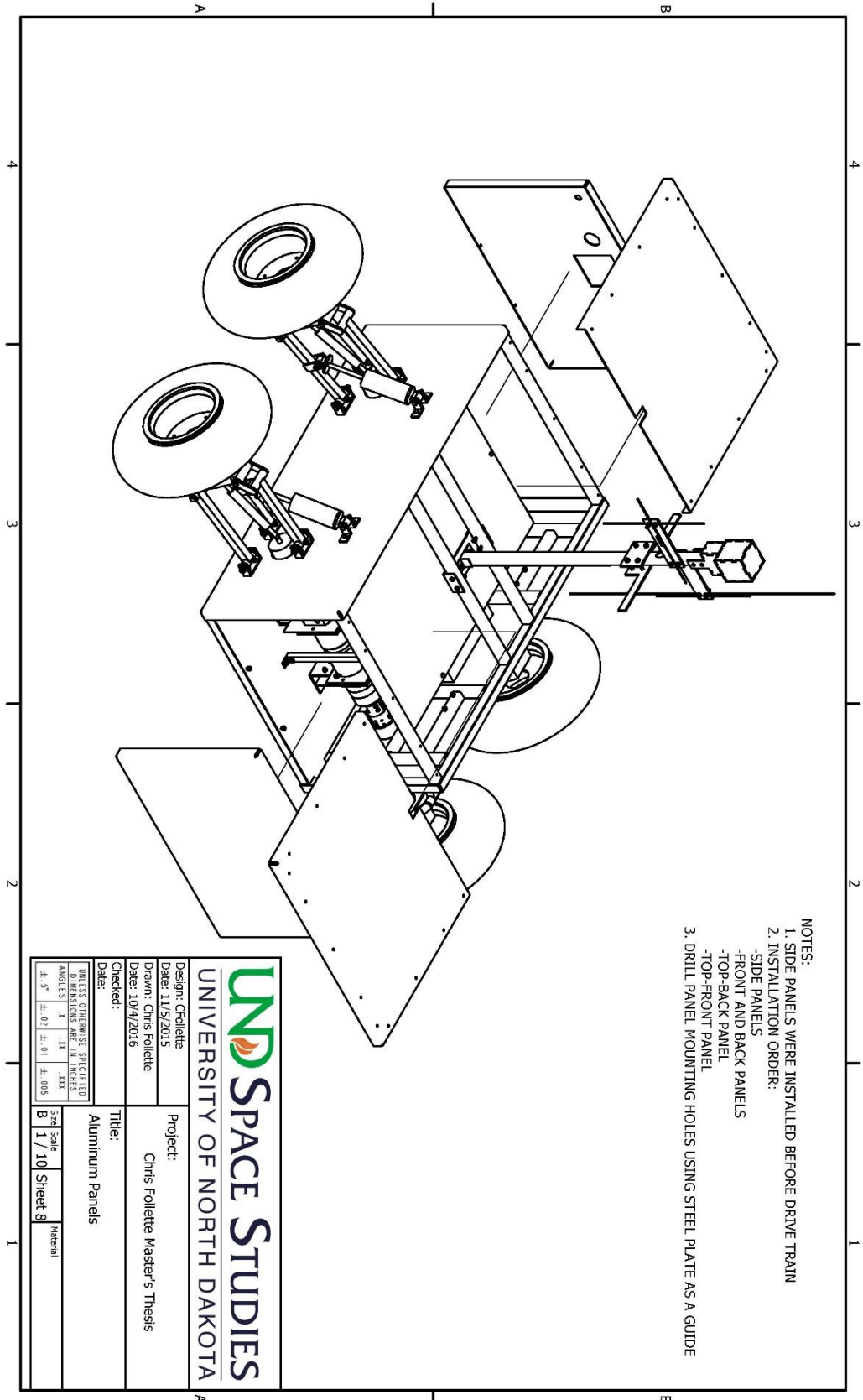
NOTES:
 1. INSTALL ELECTRONICS PLATFORM ONTO STEEL PLATE USING DESIGNATED HOLES

		Project:	
		Chris Folllette Master's Thesis	
Design: Crollette		Title:	
Date: 11/5/2015		Electronics Platform	
Drawn: Chris Folllette		Sheet	Material
Date: 10/4/2016		B	1 / 10 Sheet C
Checked:			
<small>UNLESS OTHERWISE SPECIFIED DIMENSIONS ARE IN INCHES FRACTIONS 1/16 .001 DECIMALS .1 .01 .005 ANGLES 1° .01°</small>			



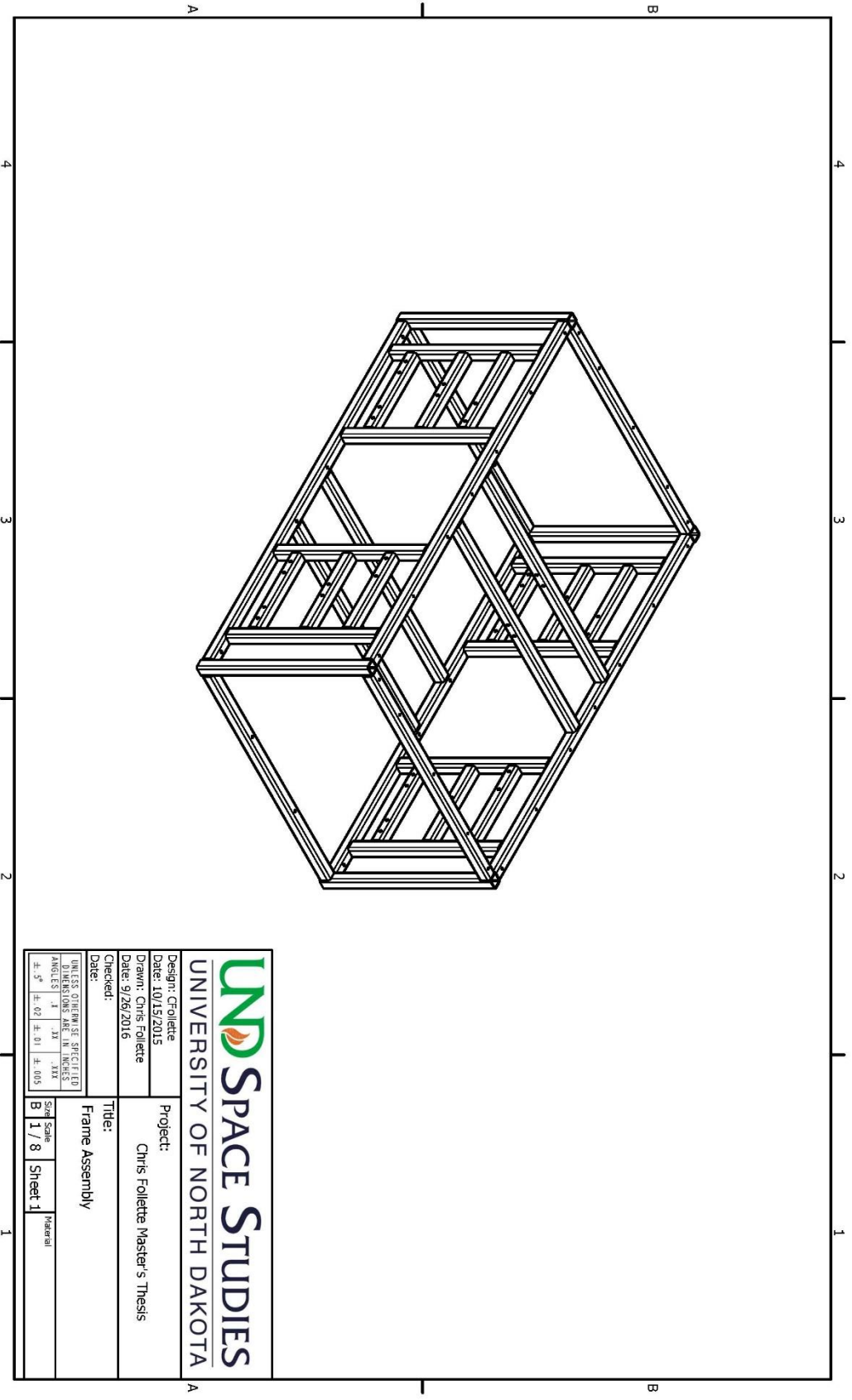
NOTES:
 1. INSTALL CAMERA BOOM ONTO FRAME USING DESIGNATED HOLES

	
UNIVERSITY OF NORTH DAKOTA	
Design: Crollette Date: 11/5/2015	Project: Chris Folllette Master's Thesis
Drawn: Chris Folllette Date: 10/4/2016	Title: Antenna and Camera Boom
Checked: Date:	Size B 1 / 10 Sheet 7
UNLESS OTHERWISE SPECIFIED DIMENSIONS ARE IN INCHES ANGLES ° .1 .25 .5 .75 .875 ± .5 ± .02 ± .01 ± .005	Material

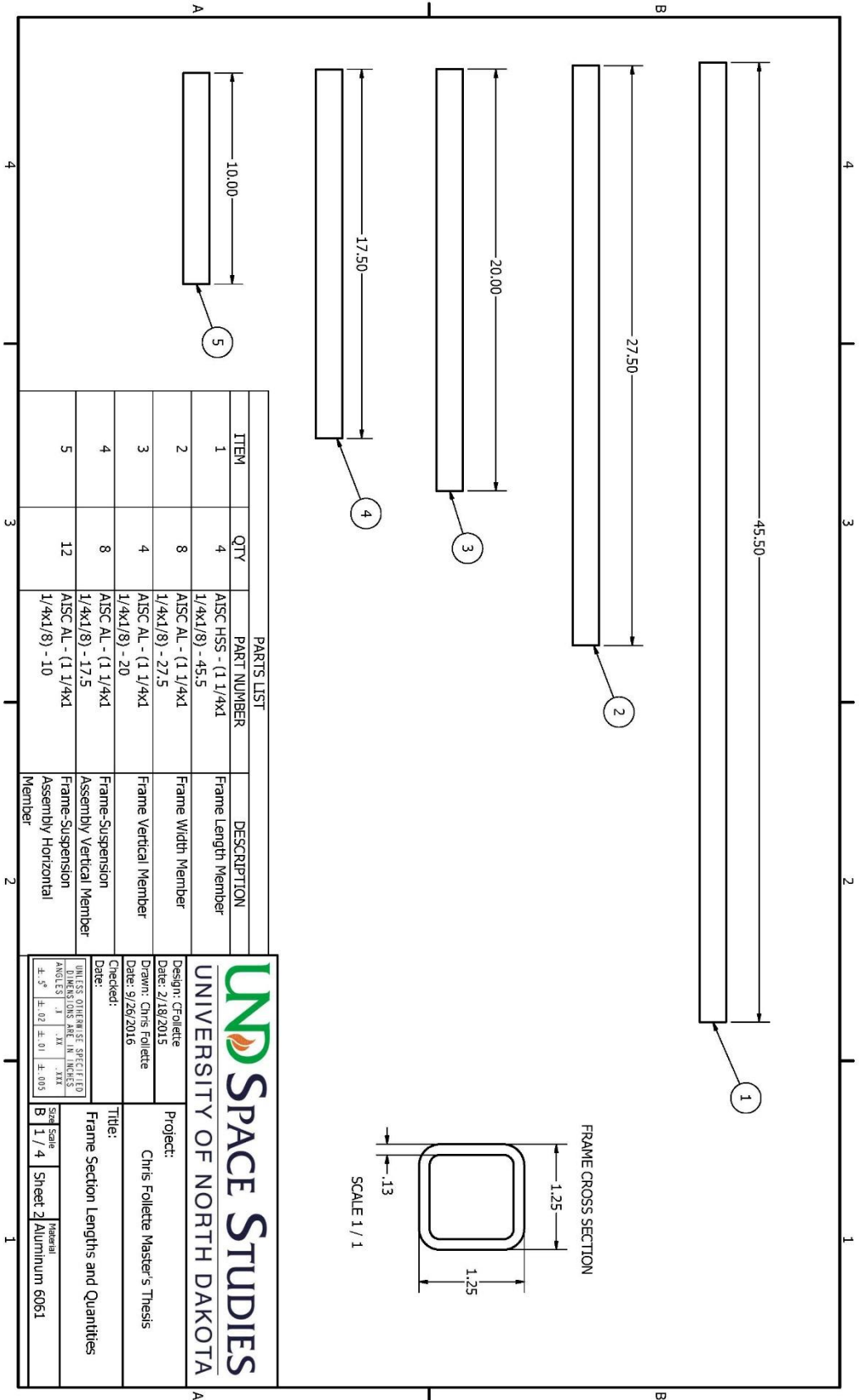


- NOTES:
1. SIDE PANELS WERE INSTALLED BEFORE DRIVE TRAIN
 2. INSTALLATION ORDER:
 - SIDE PANELS
 - FRONT AND BACK PANELS
 - TOP-BACK PANEL
 - TOP-FRONT PANEL
 3. DRILL PANEL MOUNTING HOLES USING STEEL PLATE AS A GUIDE

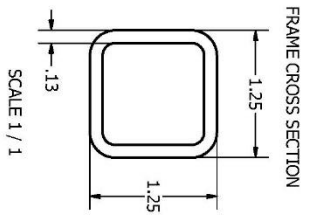
		Project:	
		Chris Follotte Master's Thesis	
Design: Crollette		Date: 11/5/2015	
Drawn: Chris Follotte		Date: 10/4/2016	
Checked:		Date:	
<small>UNLESS OTHERWISE SPECIFIED DIMENSIONS ARE IN INCHES</small>			
±.5"	±.02	±.01	±.005
Sheet Scale	B	1 / 10	Sheet 8
Title:		Material	
Aluminum Panels			



	
UNIVERSITY OF NORTH DAKOTA	
Design: C.Follette	Project:
Date: 10/19/2015	Chris Follette Master's Thesis
Drawn: Chris Follette	
Date: 9/26/2016	
Checked:	Title:
	Frame Assembly
<small>TOLERANCES UNLESS OTHERWISE SPECIFIED</small> <small>DIMENSIONS ARE IN INCHES</small> <small>ANGLES .1 .33 .333</small> <small>± .5° ± .02 ± .01 ± .005</small>	
Std Scale	Sheet 1
B 1 / 8	Material



PARTS LIST			
ITEM	QTY	PART NUMBER	DESCRIPTION
1	4	AISC HSS - (1) 1/4x1	Frame Length Member
2	8	AISC AL - (1) 1/4x1	Frame Width Member
3	4	AISC AL - (1) 1/4x1	Frame Vertical Member
4	8	AISC AL - (1) 1/4x1	Frame-Suspension Assembly Vertical Member
5	12	AISC AL - (1) 1/4x1	Frame-Suspension Assembly Horizontal Member



UNIVERSITY OF NORTH DAKOTA
SPACE STUDIES

Project: Chris Foliotte Master's Thesis

Design: CFoliotte
Date: 2/18/2015

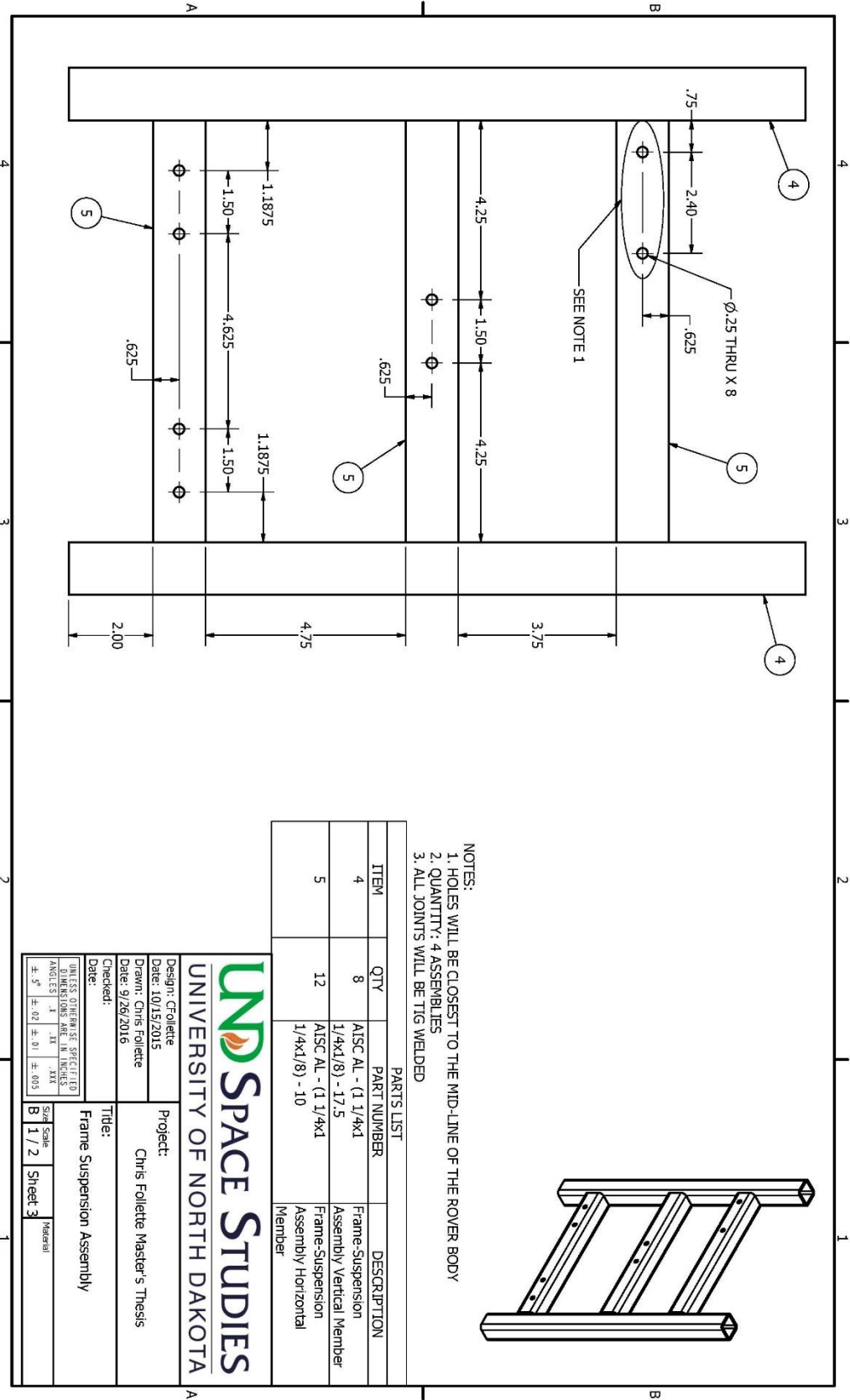
Drawn: Chris Foliotte
Date: 9/28/2016

Checked:

Title: Frame Section Lengths and Quantities

UNLESS OTHERWISE SPECIFIED			
DIMENSIONS	FRACTIONS	DECIMALS	TOLERANCES
ANGLES	°	.01	.005
± .5°	± .02	± .01	± .005

Sheet Scale	Material	Sheet	Material
B 1 / 4	Aluminum 6061	Sheet 2	Aluminum 6061



- NOTES:
1. HOLES WILL BE CLOSEST TO THE MID-LINE OF THE ROVER BODY
 2. QUANTITY: 4 ASSEMBLIES
 3. ALL JOINTS WILL BE TIG WELDED

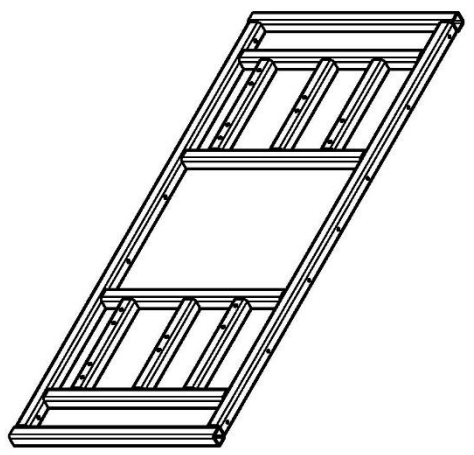
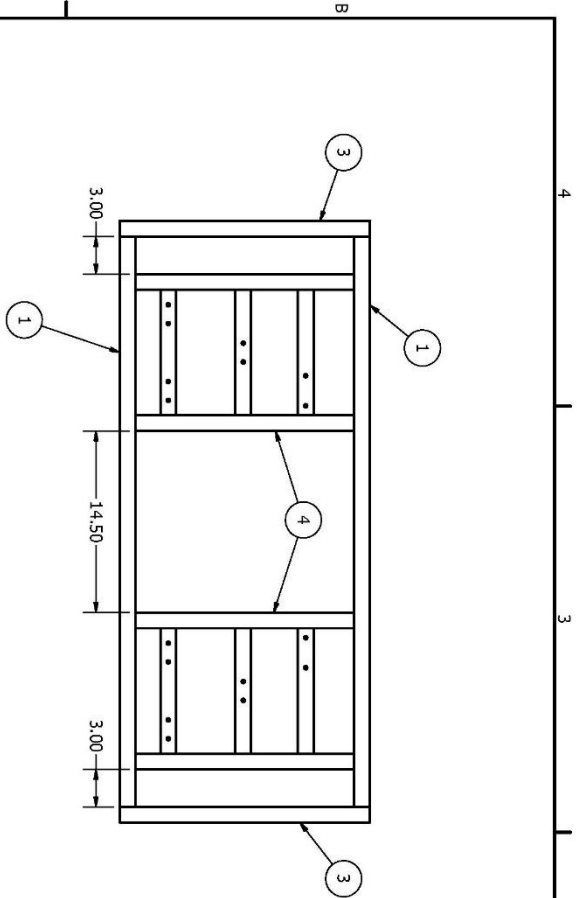
PARTS LIST			
ITEM	QTY	PART NUMBER	DESCRIPTION
4	8	AISC AL - (1 1/4x1)	Frame-Suspension Assembly Vertical Member
5	12	AISC AL - (1 1/4x1)	Frame-Suspension Assembly Horizontal Member

Design: CFollette
 Date: 10/15/2015
 Drawn: Chris Follette
 Date: 9/26/2016
 Checked:
 Date:

Project: Chris Follette Master's Thesis
 Title: Frame Suspension Assembly

UNLESS OTHERWISE SPECIFIED
 DIMENSIONS ARE IN INCHES
 ANGLES .1 .XX .XXX
 ± .5° ± .02 ± .01 ± .005

Std Scale B 1 / 2 Sheet 3 Material



NOTES:
 1. ALL JOINTS ARE TIG WELDED
 2. QUANTITY: 2 ASSEMBLIES

PARTS LIST			
ITEM	QTY	PART NUMBER	DESCRIPTION
3	4	AISC AL - (1) 1/4x1	Frame Vertical Member
1	4	AISC HSS - (1) 1/4x1	Frame Length Member
4	8	AISC AL - (1) 1/4x1 1/4x1(8) - 45.5	Frame-Suspension Assembly Vertical Member

Design: Ffollette
 Date: 10/15/2015
 Drawn: Chris Ffollette
 Date: 9/26/2016
 Checked:
 Date:

Project:
Chris Ffollette Master's Thesis

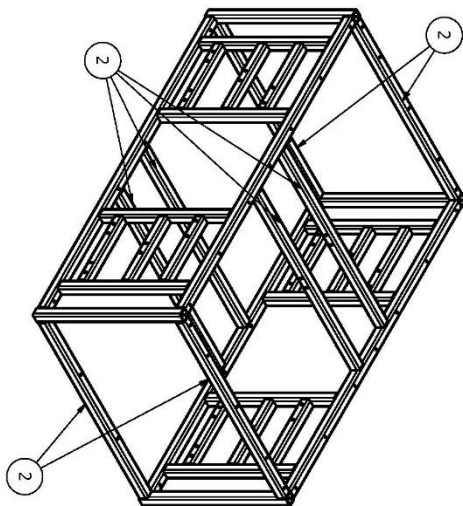
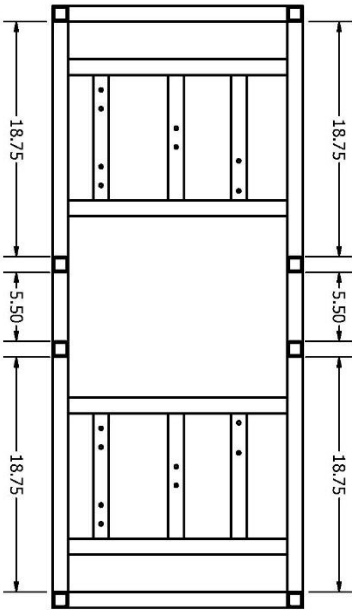
Title:
Frame Side Assembly

<small>UNLESS OTHERWISE SPECIFIED DIMENSIONS ARE IN INCHES</small>	<small>ANGLES</small>	<small>FINISH</small>
±.05	±.02	±.01
±.003	±.01	±.003

Sheet Scale
B 1 / 8

Sheet #
4

Material



ITEM	QTY	PART NUMBER	DESCRIPTION
3	4	AISC AL - (1) 1/4x1 1/4x1(8) - 20	Frame Vertical Member
1	4	AISC HSS - (1) 1/4x1 1/4x1(8) - 45.5	Frame Length Member
2	8	AISC AL - (1) 1/4x1 1/4x1(8) - 27.5	Frame Width Member
4	8	AISC AL - (1) 1/4x1 1/4x1(8) - 17.5	Frame-Suspension Assembly Vertical Member
5	12	AISC AL - (1) 1/4x1 1/4x1(8) - 10	Frame-Suspension Assembly Horizontal Member

NOTES:
1. ALL JOINTS ARE TTIG WELDED

4 3 2 1

UND SPACE STUDIES
UNIVERSITY OF NORTH DAKOTA

Design: C'Follette
Date: 10/15/2015

Drawn: Chris Follette
Date: 9/26/2016

Checked:

Date:

Project: Chris Follette Master's Thesis

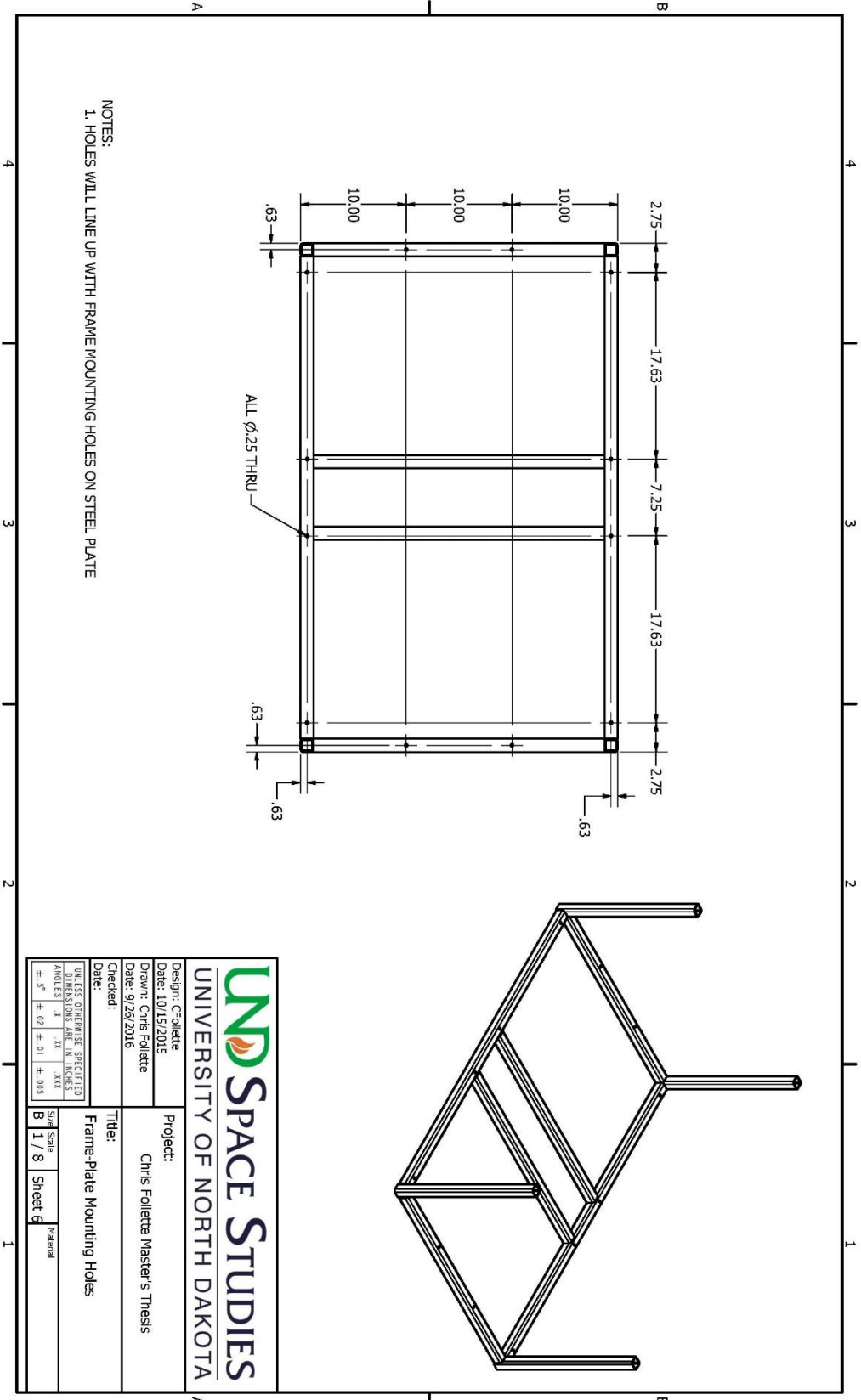
Title: Frame Cross-Members

Scale: 1/8

Sheet: 5

Material:

DIMENSIONS SHOWN UNLESS SPECIFIED	
DIMENSIONS ARE IN INCHES	
ANGLES .1	.XXX
± .5°	± .01
± .02	± .005



NOTES:
 1. HOLES WILL LINE UP WITH FRAME MOUNTING HOLES ON STEEL PLATE

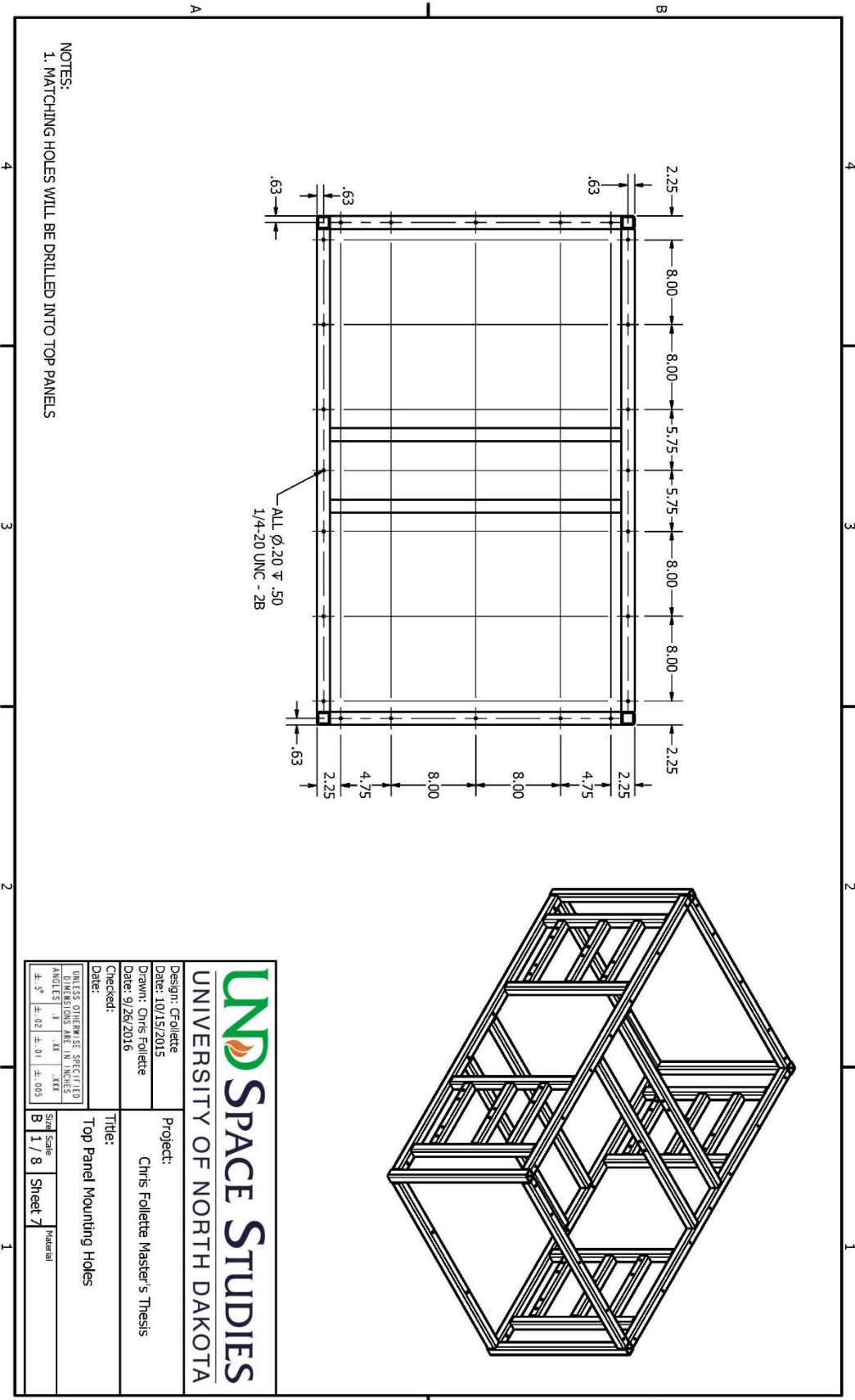
UNIVERSITY OF NORTH DAKOTA
SPACE STUDIES

Design: C.Follette
 Date: 10/15/2015
 Drawn: Chris Follette
 Date: 9/28/2016
 Checked:
 Date:

Project:
 Chris Follette Master's Thesis

Title:
 Frame-Plate Mounting Holes

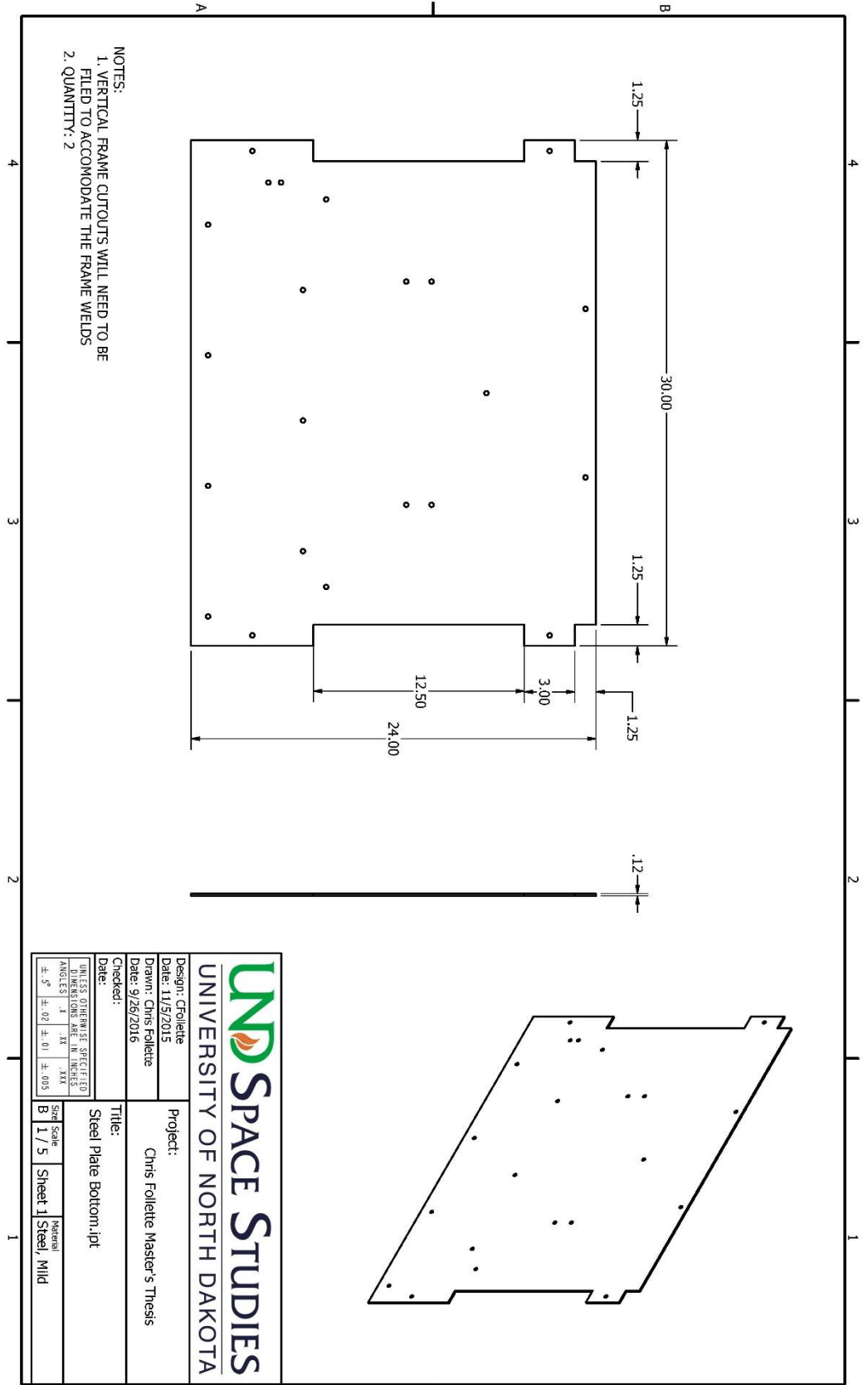
UNLESS OTHERWISE SPECIFIED DIMENSIONS ARE IN INCHES	Scale	Material
ANGLES: I XX XIX	B 1/8	Sheet 6
± .5° ± .02 ± .01 ± .005		



NOTES:
1. MATCHING HOLES WILL BE DRILLED INTO TOP PANELS

UNIVERSITY OF NORTH DAKOTA
SPACE STUDIES

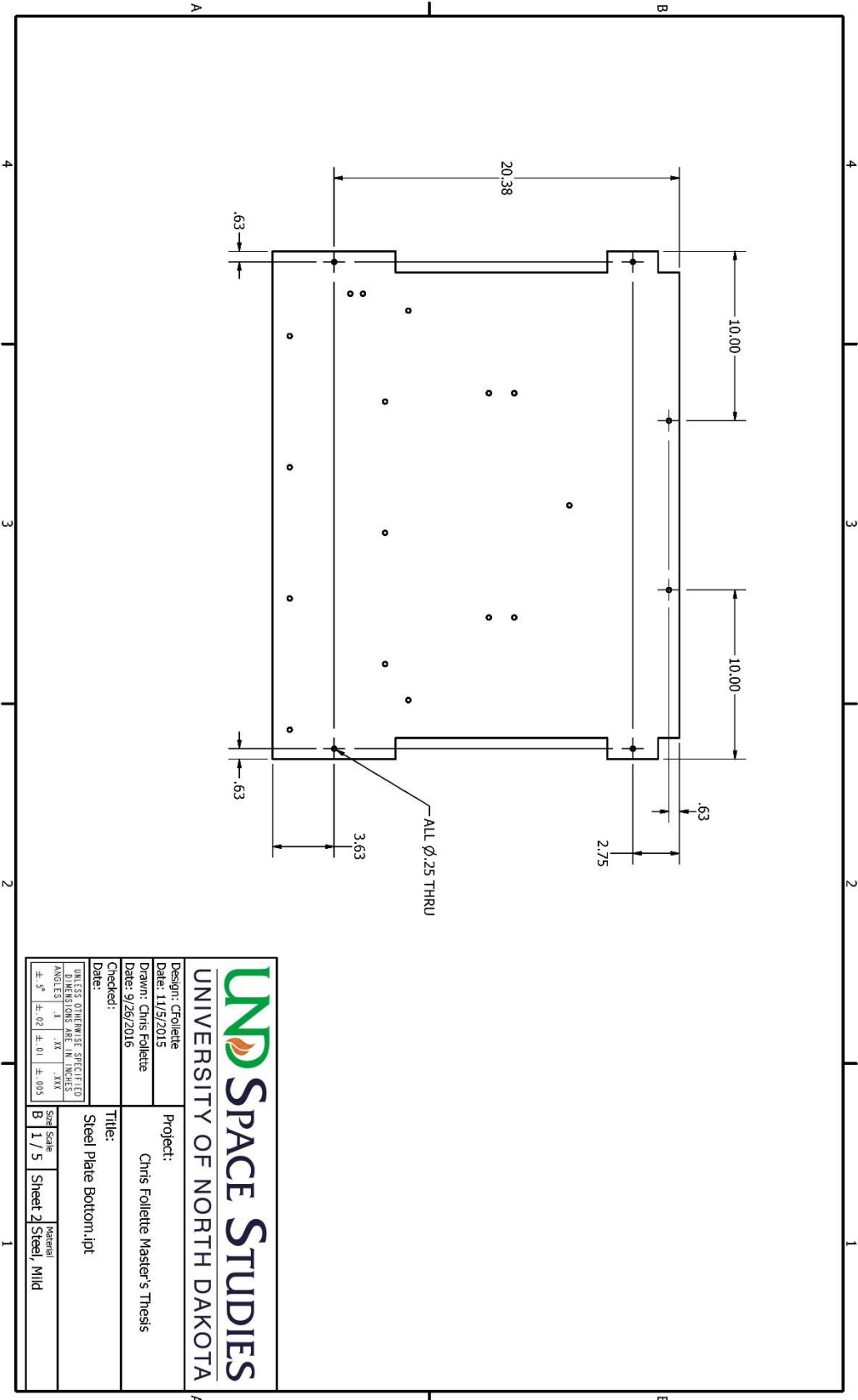
Design: CFollette	Project:		
Date: 10/15/2015	Chris Follette Master's Thesis		
Drawn: Chris Follette			
Date: 9/26/2016			
Checked:	Title:		
Date:	Top Panel Mounting Holes		
UNLESS OTHERWISE SPECIFIED DIMENSIONS ARE IN INCHES			
± .5"	± .02	± .01	± .005
Size Scale	Sheet	Material	
B	1 / 8	Sheet 7	



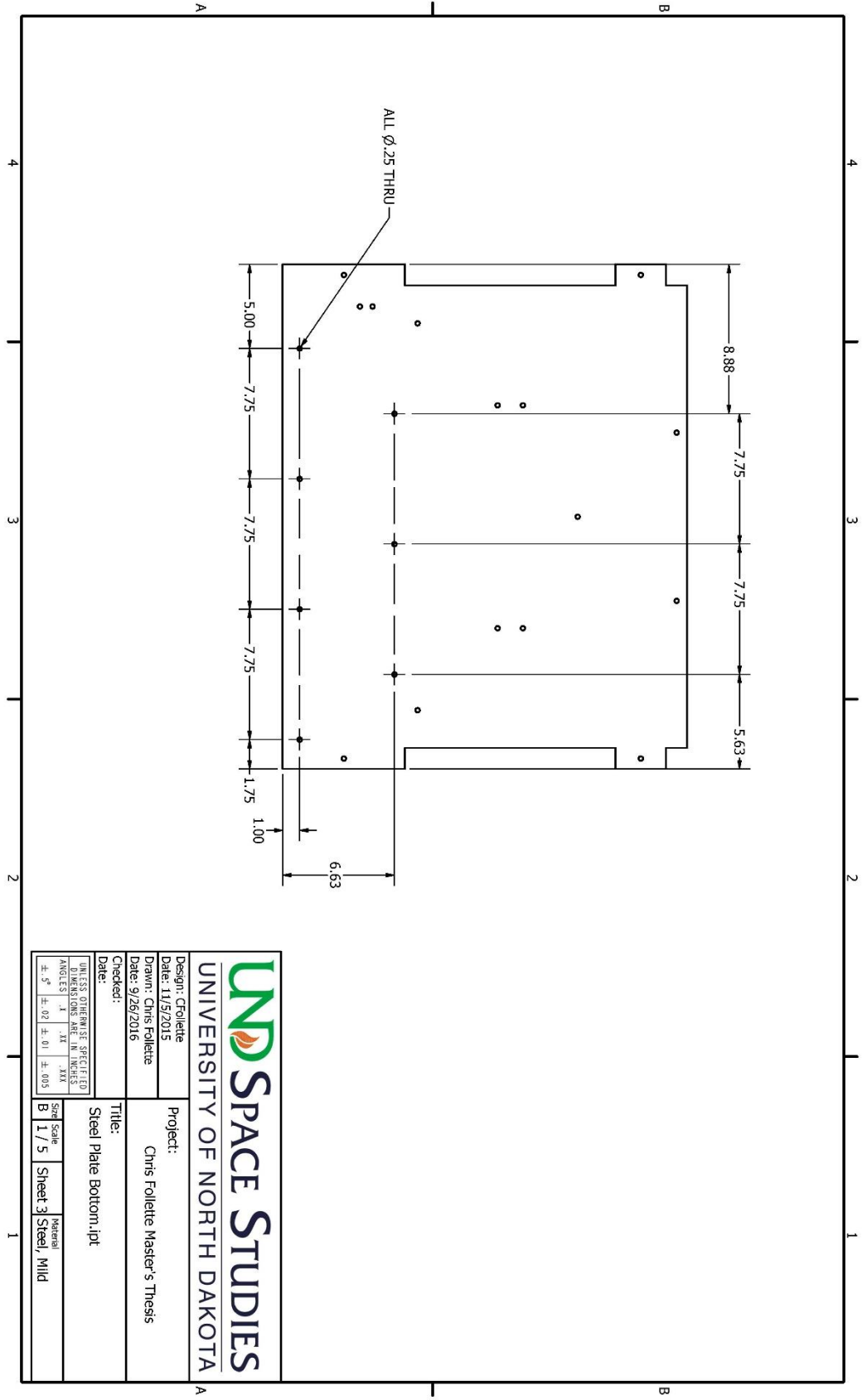
- NOTES:
 1. VERTICAL FRAME CUTOUTS WILL NEED TO BE FILED TO ACCOMMODATE THE FRAME WELDS
 2. QUANTITY: 2

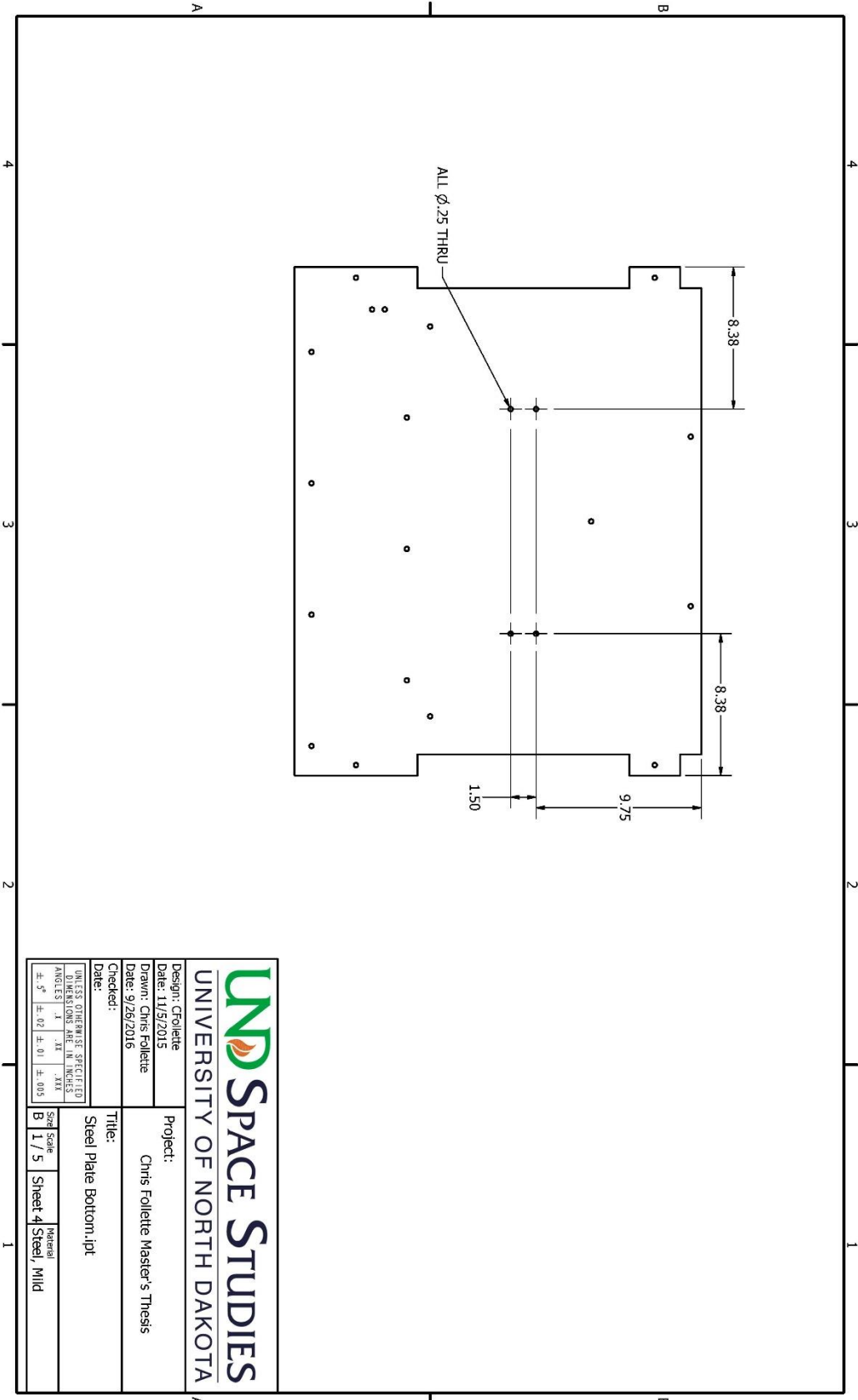
UND SPACE STUDIES
 UNIVERSITY OF NORTH DAKOTA

Design: Chrollette	Project:				
Date: 11/9/2015	Chris Folllette Master's Thesis				
Drawn: Chris Folllette					
Date: 9/26/2016					
Checked:	Title:				
	Steel Plate Bottom.ipt				
UNLESS OTHERWISE SPECIFIED DIMENSIONS ARE IN INCHES					
ANGLES	IN	IN	IN	IN	IN
±.5°	±.02	±.01	±.005		
Size	Scale	Material			
B	1 / 5	Sheet 1	Steel, Mild		



Design: CFollette	Project:												
Date: 11/9/2015	Chris Follette Master's Thesis												
Drawn: Chris Follette													
Date: 9/26/2016													
Checked:	Title:												
Date:	Steel Plate Bottom.ipt												
<small>UNLESS OTHERWISE SPECIFIED DIMENSIONS ARE IN INCHES</small>													
<table border="1"> <tr> <td>±.5°</td> <td>±.02</td> <td>±.01</td> <td>±.003</td> </tr> <tr> <td>±.1</td> <td>±.1A</td> <td>±.1XX</td> <td></td> </tr> </table>	±.5°	±.02	±.01	±.003	±.1	±.1A	±.1XX		<table border="1"> <tr> <td>Size</td> <td>Material</td> </tr> <tr> <td>B</td> <td>Steel, Mild</td> </tr> </table>	Size	Material	B	Steel, Mild
±.5°	±.02	±.01	±.003										
±.1	±.1A	±.1XX											
Size	Material												
B	Steel, Mild												
Scale	Sheet 2												
1 / 5	Steel, Mild												





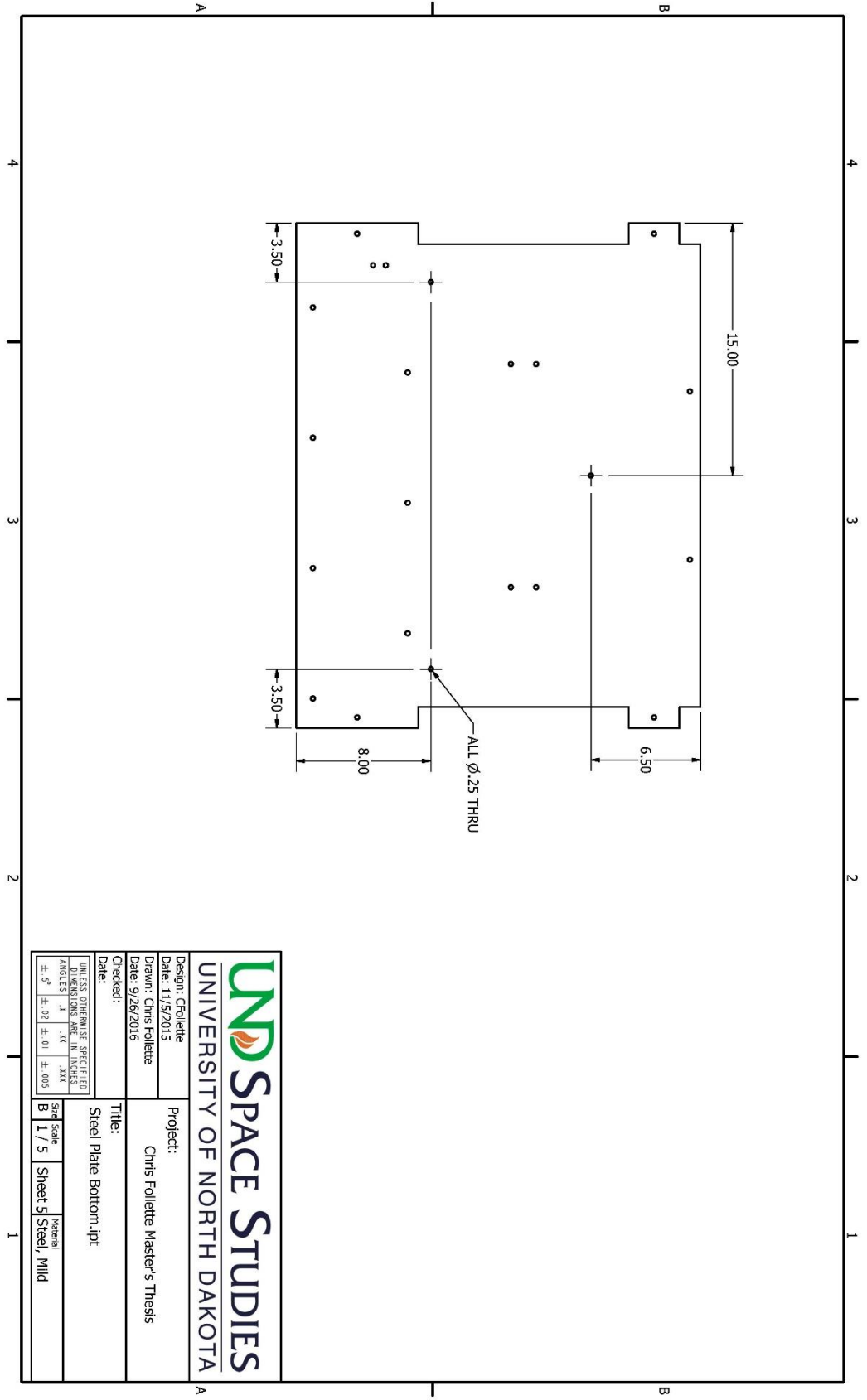
UND SPACE STUDIES
UNIVERSITY OF NORTH DAKOTA

Design: CFollette
Date: 11/5/2015
Drawn: Chris Follette
Date: 9/26/2016
Checked:

Project: Chris Follette Master's Thesis

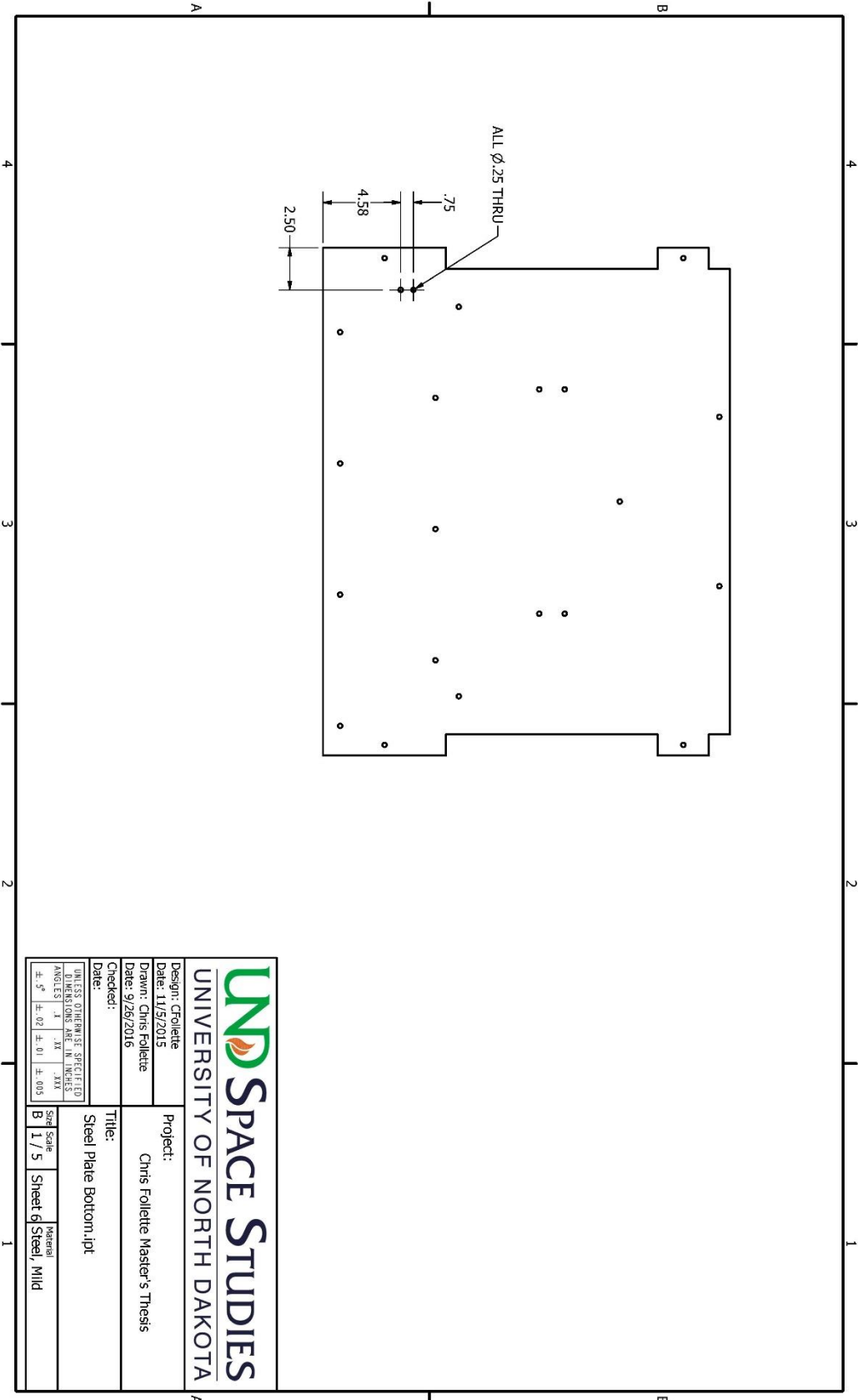
Title: Steel Plate Bottom.ipt

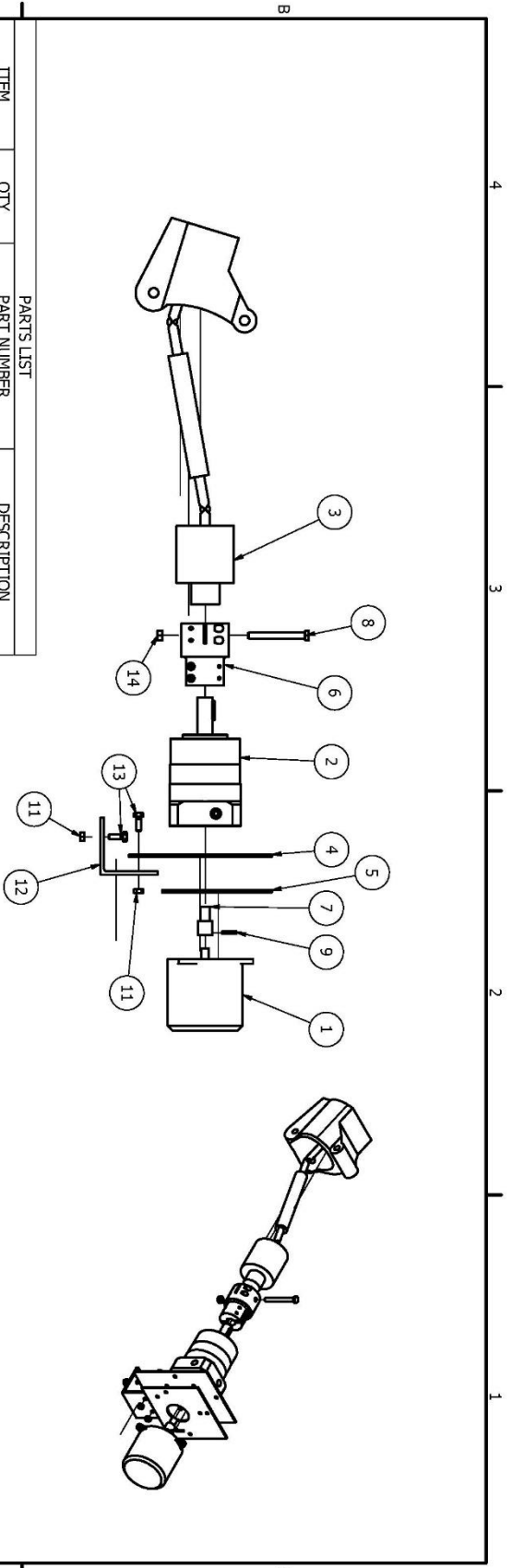
UNLESS OTHERWISE SPECIFIED		Size	Material
ANGLES	1/4" x 1/4" x .015	B	Steel, Mild
TOLERANCES	±.02 ±.01 ±.003	1 / 5	Sheet 4



UNIVERSITY OF NORTH DAKOTA
SPACE STUDIES

Design: Cfollette	Project:
Date: 11/9/2015	Chris Folllette Master's Thesis
Drawn: Chris Folllette	
Date: 9/26/2016	
Checked:	Title:
	Steel Plate Bottom.ipt
UNLESS OTHERWISE SPECIFIED DIMENSIONS ARE IN INCHES	
ANGLES	± .5°
	± .02
	± .01
	± .003
Size	B
Scale	1 / 5
Sheet	5
Material	Steel, Mild



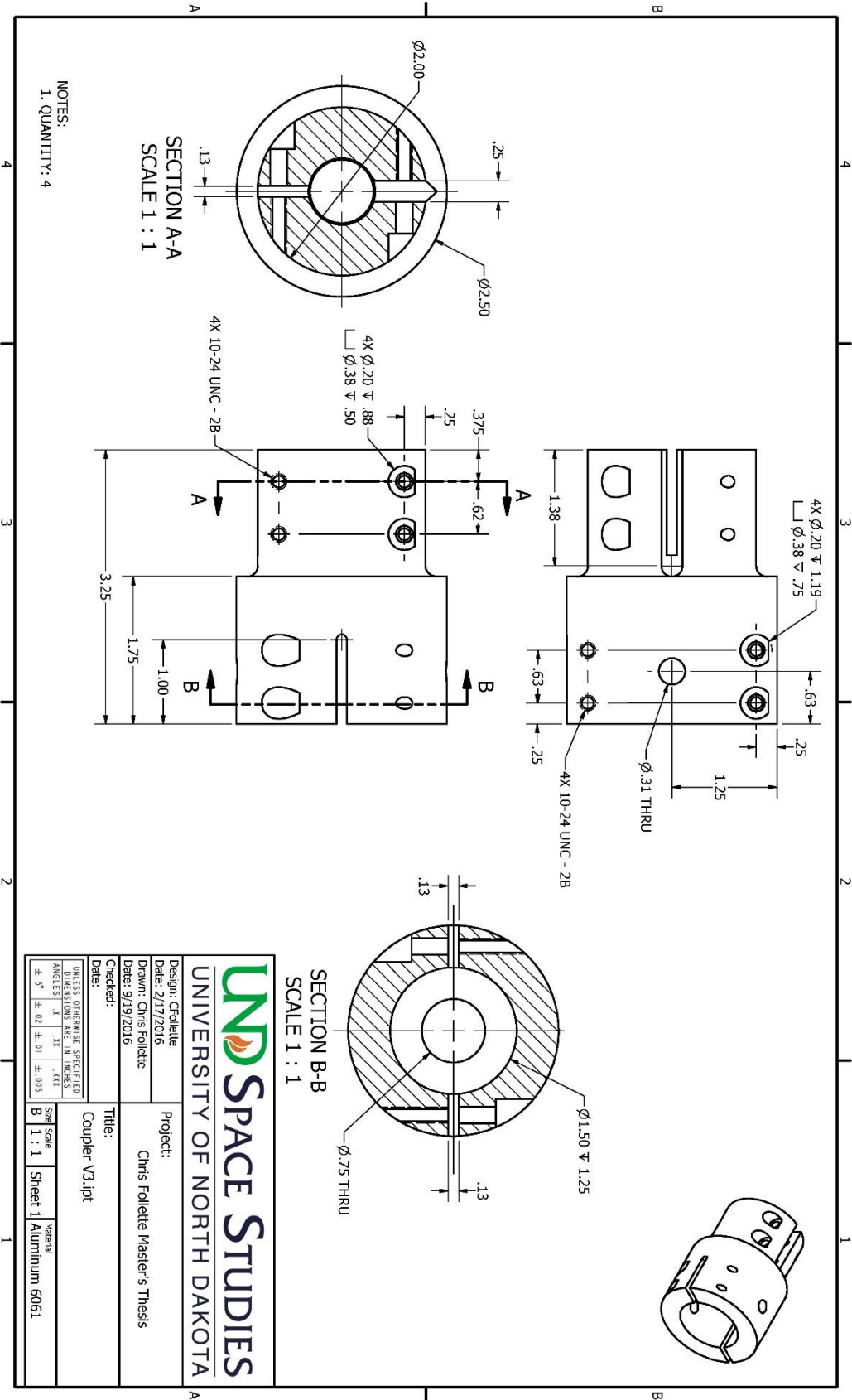


PARTS LIST		
ITEM	QTY	DESCRIPTION
1	1	Monster Scooter 900 Watt Motor
2	1	Anahem Automation GBPH-0901-CS Planetary Gearbox
3	1	CV Shaft
4	1	Gearbox Mounting Plate
5	1	Motor Mounting Plate
6	1	Coupler V3
7	1	Motor-Gearbox coupler pin
8	1	ANSI B18.2.1 - 5/16-18 UNC - 3
9	1	ANSI B18.8.2 - 1/8 x 3/4
11	4	ANSI B18.2.2 - 1/4 - 20 Hex Nuts (Inch Series) Hex Nut
12	1	Steel Angle - 3 inch
13	4	ANSI/ASME B18.2.1 - 1/4-20 UNC - 0.75 Hex Bolt - UNC (Regular Thread - Inch)
14	1	ANSI B18.2.2 - 5/16 - 18 Hex Nuts (Inch Series) Hex Nut

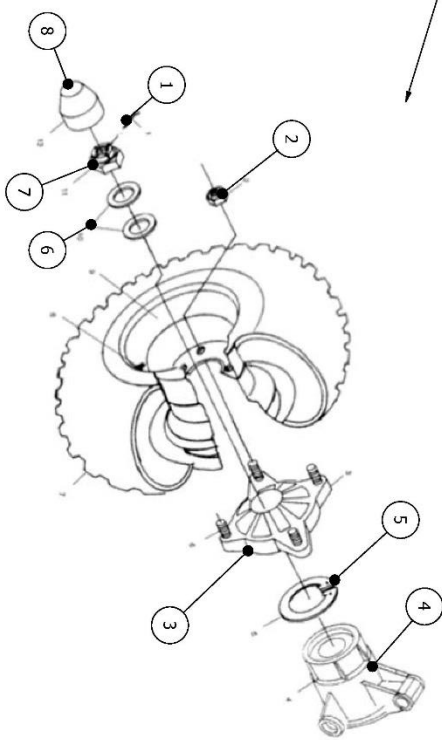
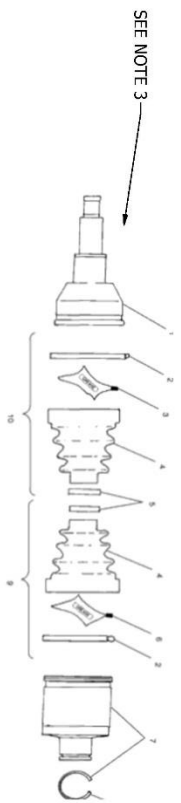
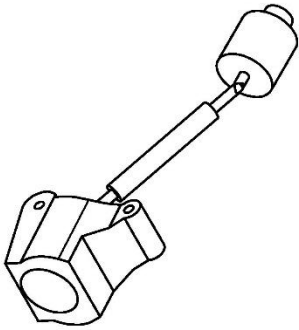
NOTES:
1. QUANTITY: 4

Design: Ffollette
Date: 9/2/2015
Drawn: Chris Ffollette
Date: 9/27/2016

Checked:		Title:	
Date:		Motor-Gearbox Assy.iam	
DESIGN OTHERWISE SPECIFIED DIMENSIONS ARE IN INCHES		Scale	Material
± .05	± .01	B 1 / 5	Sheet 1



NOTES:
1. QUANTITY: 4



NOTES:
 1. REAR AXLE HUB ASSEMBLY FROM 2002-2007 POLARIS SPORTSMAN 500
 2. PART NUMBERS ARE POLARIS PART NUMBERS
 3. REAR DRIVE SHAFT ASSEMBLY FROM 2002-2007 POLARIS SPORTSMAN 500

ITEM	QTY	PART NUMBER	DESCRIPTION
1	1	7661404	Pin, Cotter
2	4	7542459	Nut, Flange Lock
3	1	5131649	Hub, Rear Wheel
4	1	5134206	Wheel Bearing Carrier
5	1	7710440	Ring, Retaining
6	1	7555796	Washer, Cone
7	1	7543005	Nut, Castle
8	1	5413427	Cover, Dust, Hub

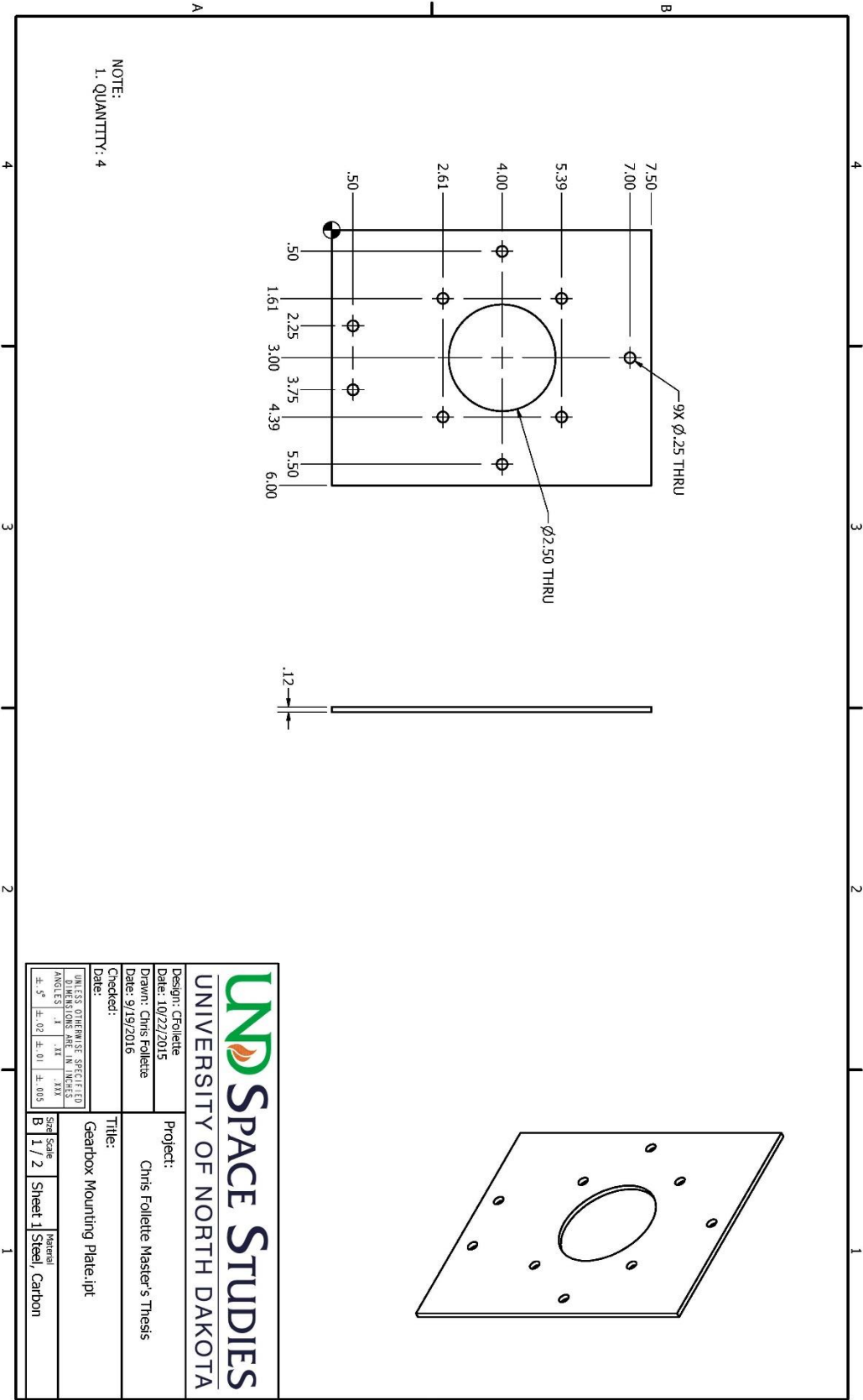
UNIVERSITY OF NORTH DAKOTA
SPACE STUDIES

Design: Crollette
 Date: 8/31/2015
 Drawn: Chris Follette
 Date: 10/4/2016
 Checked:

Project: Chris Follette Master's Thesis
 Title: CV Shaft/lam

UNLESS OTHERWISE SPECIFIED
 DIMENSIONS ARE IN INCHES
 ANGLES IN DEGREES
 ±.5° ±.02 ±.01 ±.003

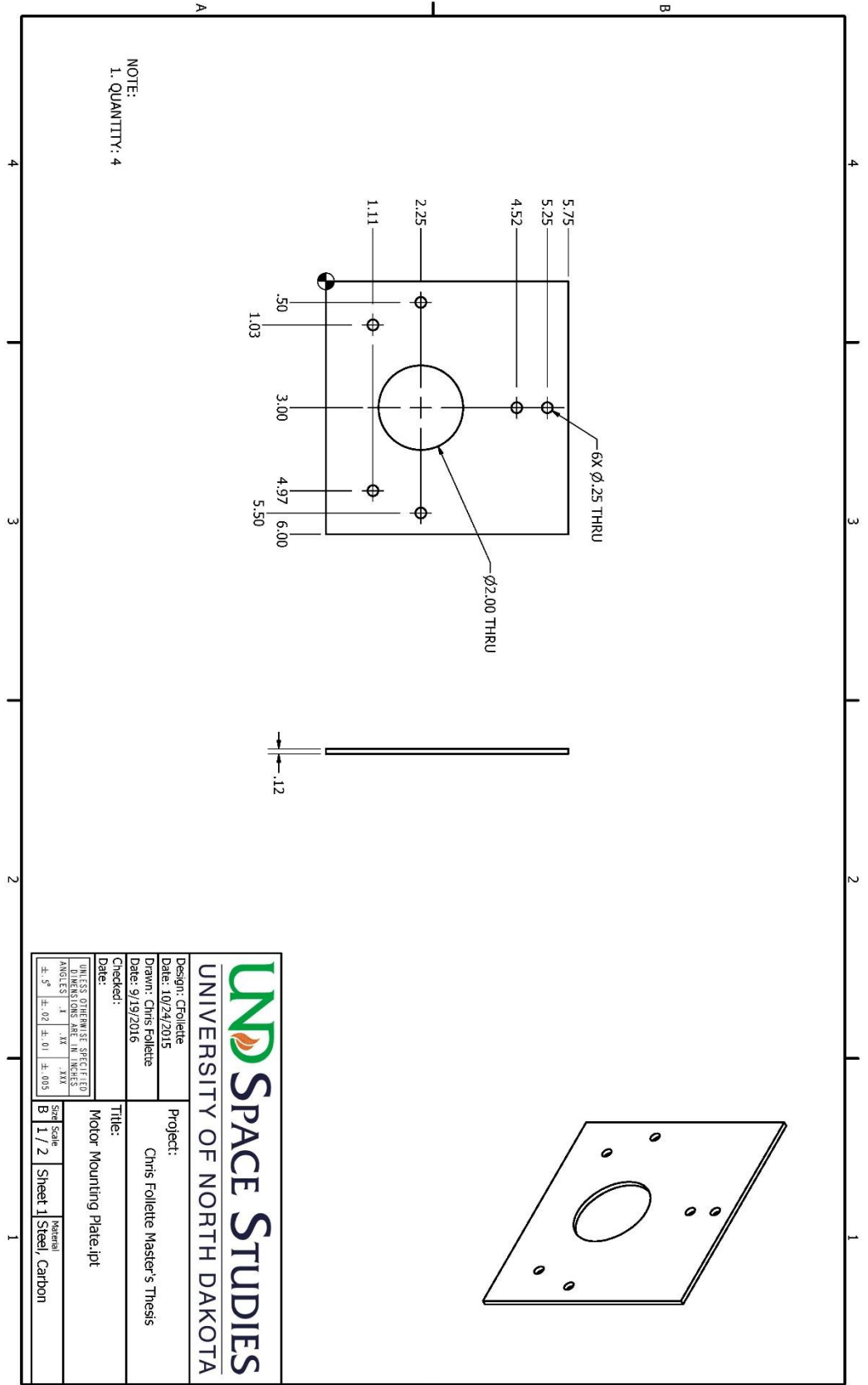
Size Scale: B 1 / 5 Sheet 1
 Material:



NOTE:
1. QUANTITY: 4

UNIVERSITY OF NORTH DAKOTA
UNDSpace STUDIES

Design: Cfollette	Project:
Date: 10/22/2015	Chris Folllette Master's Thesis
Drawn: Chris Folllette	
Date: 9/19/2016	
Checked:	Title:
	Gearbox Mounting Plate.ipt
UNLESS OTHERWISE SPECIFIED DIMENSIONS ARE IN INCHES	
ANGLES	1° .1° .5°
	±.02 ±.01 ±.005
Size	Sheet 1
Scale	1 / 2
Material	Steel, Carbon



NOTE:
1. QUANTITY: 4

UNIVERSITY OF NORTH DAKOTA
SPACE STUDIES

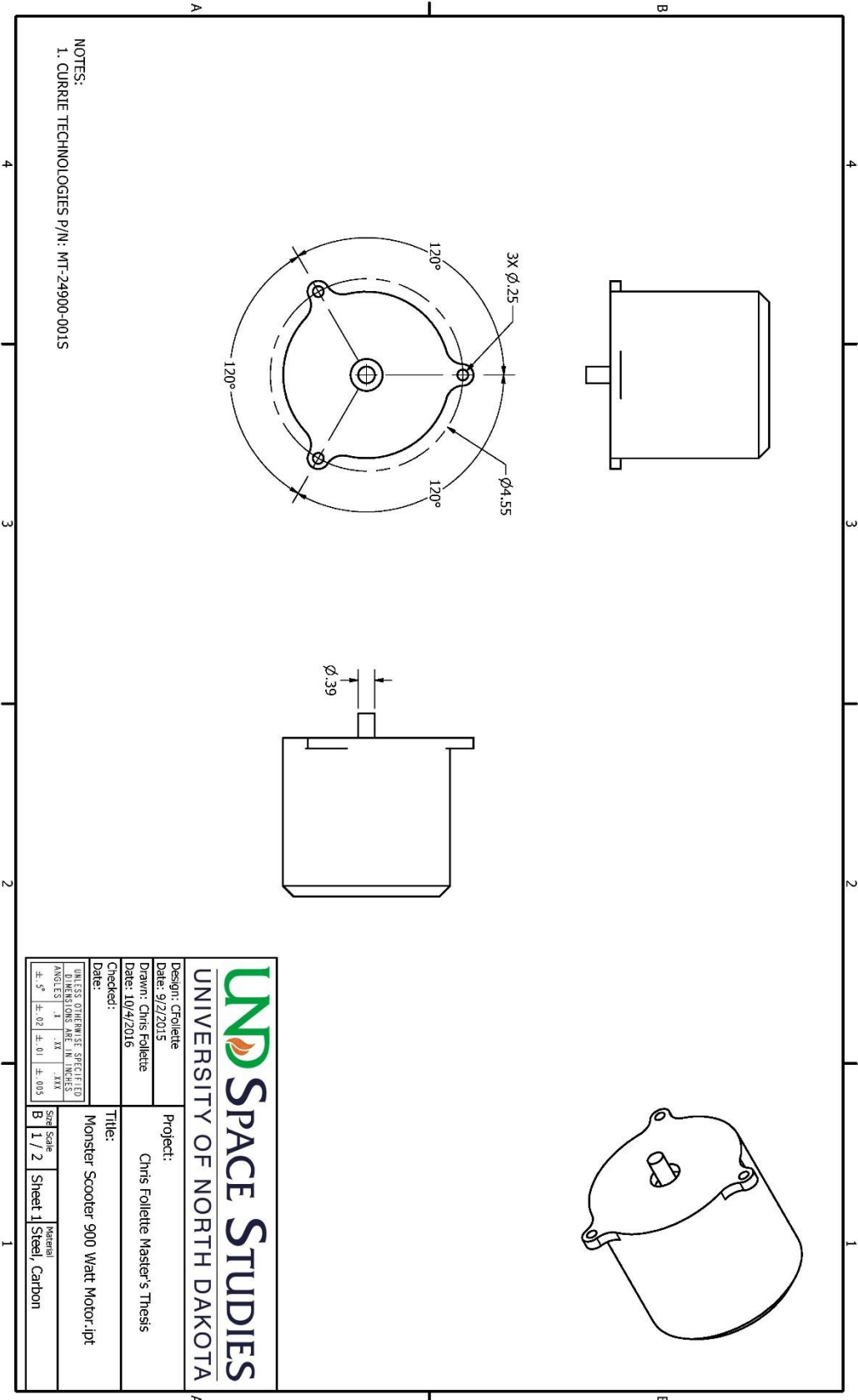
Design: Cfollette
 Date: 10/24/2015
 Drawn: Chris Follette
 Date: 9/19/2016
 Checked:

Project:
 Chris Follette Master's Thesis

Title:
 Motor Mounting Plate.ipt

UNLESS OTHERWISE SPECIFIED
 DIMENSIONS ARE IN INCHES
 ANGLES IN DEGREES
 ±.5° ±.02 ±.01 ±.003

Size Scale: B
 1 / 2
 Sheet 1 of 1
 Material: Steel, Carbon



NOTES:
 1. CURRIE TECHNOLOGIES P/N: MT-24900-001S

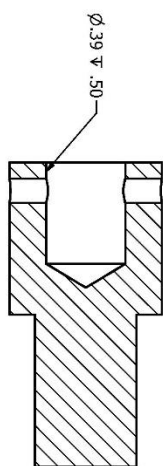
UNIVERSITY OF NORTH DAKOTA
SPACE STUDIES

Design: CFollette
 Date: 9/2/2015
 Drawn: Chris Follette
 Date: 10/4/2016
 Checked:

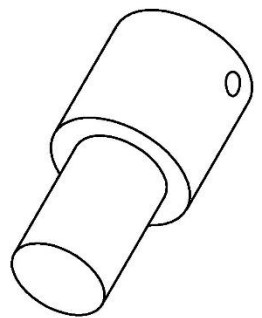
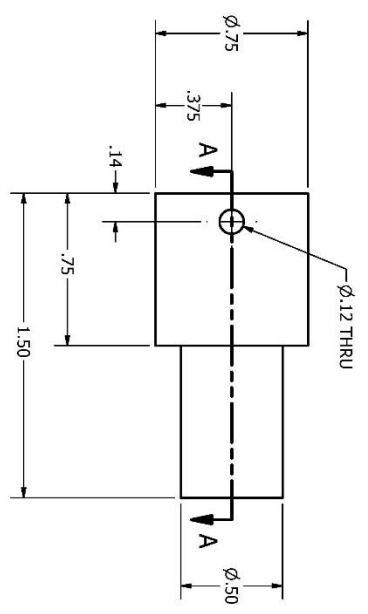
Title: Monster Scooter 900 Watt Motor.ipt

UNLESS OTHERWISE SPECIFIED
 DIMENSIONS ARE IN INCHES
 ANGLES IN DEGREES
 ±.01 ±.01 ±.005

Size Scale: B 1 / 2
 Material: Sheet 1 Steel, Carbon

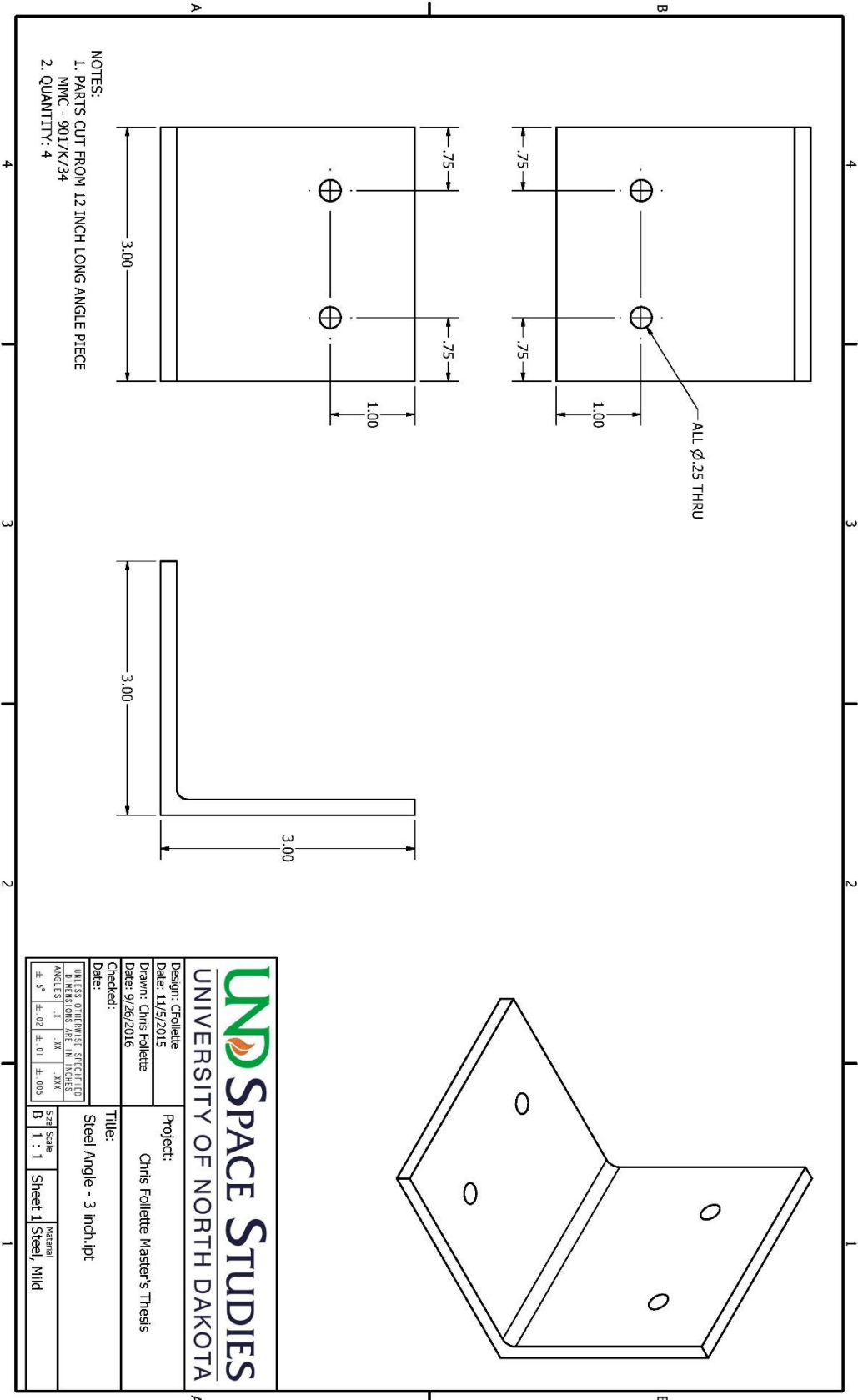


SECTION A-A
SCALE 2 : 1



NOTES:
1. QUANTITY: 4

		UNIVERSITY OF NORTH DAKOTA	
Design: Cfollette	Project:	Chris Folllette Master's Thesis	
Date: 2/18/2016	Drawn: Chris Folllette	Date: 9/27/2016	
Checked:	Title:	Motor-Gearbox coupler pin.ipt	
<small>UNLESS OTHERWISE SPECIFIED DIMENSIONS ARE IN INCHES ANGLES IN DEGREES</small>		Size Scale	Material
±.5°	±.02	±.01	±.003
B	2 : 1	Sheet 1	Steel




- NOTES:
 1. PARTS CUT FROM 12 INCH LONG ANGLE PIECE
 MMC - 9017K734
 2. QUANTITY: 4

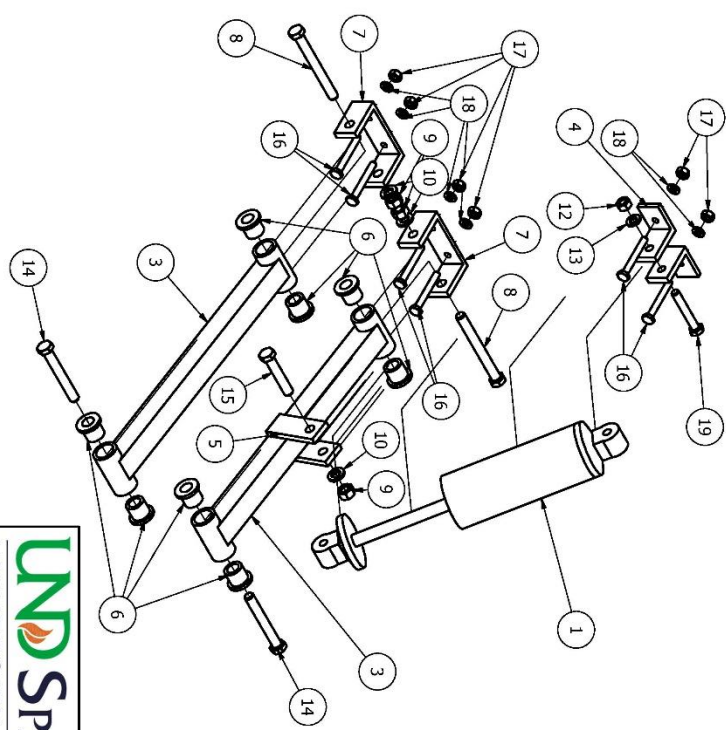
UNIVERSITY OF NORTH DAKOTA	
Design: Cfollette	Project:
Date: 11/9/2015	Chris Folllette Master's Thesis
Drawn: Chris Folllette	
Date: 9/26/2016	
Checked:	Title:
	Steel Angle - 3 inch, 1pt
<small>UNLESS OTHERWISE SPECIFIED DIMENSIONS ARE IN INCHES ANGLES °</small>	<small>Size Scale</small> B 1 : 1
<small>±.5° ±.02 ±.01 ±.003</small>	<small>Material</small> Sheet 1 Steel, Mild

PARTS LIST			
ITEM	QTY	PART NUMBER	DESCRIPTION
1	1	Honda Foreman 450 Shock	
2	1	Top Suspension Arm - Steel	
3	1	Lower H Arm - Steel	
4	2	Aluminum Shock Mount	
5	2	Shock Mount H-Arm Tab	
6	10	0.75 in OD Flanged bearing - 6338K423	STEP AP203
7	3	Aluminum Tab - Suspension	
8	3	ANSI B18.2.1 - 3/8-16 UNC - 3.5	Hex Cap Screw
9	4	ANSI B18.2.2 - 3/8 - 16	Hex Nuts (Inch Series) Hex Nut
10	4	ASME B18.21.1 - 3/8	Regular Helical Spring Lock Washers(Inch Series)
11	1	ANSI B18.2.1 - 5/16-18 UNC - 4	Hex Cap Screw
12	2	ANSI B18.2.2 - 5/16 - 18	Hex Nuts (Inch Series) Hex Nut
13	2	ASME B18.21.1 - 5/16	Regular Helical Spring Lock Washers(Inch Series)
14	2	ANSI B18.2.1 - 3/8-16 UNC - 2.75	Hex Cap Screw
15	1	ANSI B18.2.1 - 3/8-16 UNC - 2	Hex Cap Screw
16	8	ANSI B18.2.1 - 1/4-20 UNC - 2	Hex Cap Screw
17	8	ANSI B18.2.2 - 1/4 - 20	Hex Nuts (Inch Series) Hex Nut
18	8	ASME B18.21.1 - 1/4	Regular Helical Spring Lock Washers(Inch Series)
19	1	ANSI B18.2.1 - 5/16-18 UNC - 2	Hex Cap Screw

NOTES:
1. PARTS LIST IS FOR A SINGLE SUSPENSION ASSEMBLY
2. TOTAL QUANTITY OF PARTS WILL BE "PARTS LIST * 4"

 UNDSpace STUDIES UNIVERSITY OF NORTH DAKOTA		Project: Chris Follotte Master's Thesis	
Design: Cfollette Date: 10/9/2015 Drawn: Chris Follotte Date: 9/28/2016 Checked:		Title: Suspension System	
<small>UNLESS OTHERWISE SPECIFIED DIMENSIONS ARE IN INCHES</small> INCHES: 1/16 1/8 3/16 1/4 3/8 1/2 5/8 3/4 7/8 1 1 1/8 1 1/4 1 1/2 1 3/4 2 2 1/4 2 1/2 3 3 1/2 4 4 1/2 5 5 1/2 6 6 1/2 7 7 1/2 8 9 10 MILLIMETERS: 0.5 1 1.5 2 2.5 3 3.5 4 4.5 5 5.5 6 6.5 7 7.5 8 8.5 9 9.5 10 10.5 11 11.5 12 12.5 13 13.5 14 14.5 15 15.5 16 16.5 17 17.5 18 18.5 19 19.5 20 20.5 21 21.5 22 22.5 23 23.5 24 24.5 25 25.5 26 26.5 27 27.5 28 28.5 29 29.5 30 30.5 31 31.5 32 32.5 33 33.5 34 34.5 35 35.5 36 36.5 37 37.5 38 38.5 39 39.5 40 40.5 41 41.5 42 42.5 43 43.5 44 44.5 45 45.5 46 46.5 47 47.5 48 48.5 49 49.5 50		Size Scale B 1 / 3	Sheet 1 Material

PARTS LIST			
ITEM	QTY	PART NUMBER	DESCRIPTION
1	1	Honda Foreman 450 Shock	
3	1	Lower H Arm - Steel	
4	2	Aluminum Shock Mount	
5	2	Shock Mount H-Arm Tab	
6	10	0.75 in OD Flanged bearing - 6338K423	STEP AP203
7	3	Aluminum Tab - Suspension	
8	3	ANSI B18.2.1 - 3/8-16 UNC - 3.5	Hex Cap Screw
9	4	ANSI B18.2.2 - 3/8 - 16	Hex Nuts (Inch Series) Hex Nut
10	4	ASME B18.21.1 - 3/8	Regular Helical Spring Lock Washers(Inch Series)
12	2	ANSI B18.2.2 - 5/16 - 18	Hex Nuts (Inch Series) Hex Nut
13	2	ASME B18.21.1 - 5/16	Regular Helical Spring Lock Washers(Inch Series)
14	2	ANSI B18.2.1 - 3/8-16 UNC - 2.75	Hex Cap Screw
15	1	ANSI B18.2.1 - 3/8-16 UNC - 2	Hex Cap Screw
16	8	ANSI B18.2.1 - 1/4-20 UNC - 2	Hex Cap Screw
17	8	ANSI B18.2.2 - 1/4 - 20	Hex Nuts (Inch Series) Hex Nut
18	8	ASME B18.21.1 - 1/4	Regular Helical Spring Lock Washers(Inch Series)
19	1	ANSI B18.2.1 - 5/16-18 UNC - 2	Hex Cap Screw



UNDSpace STUDIES
UNIVERSITY OF NORTH DAKOTA

Project: Chris Folllette Master's Thesis

Date: 10/9/2015

Drawn: Chris Folllette

Date: 9/28/2016

Checked:

Title: Lower Suspension Arms and Shock

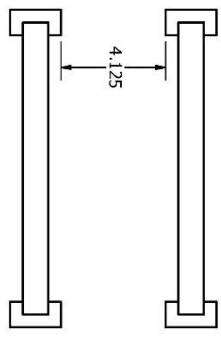
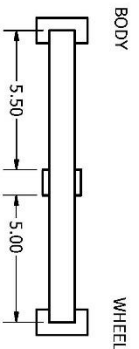
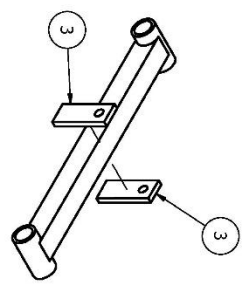
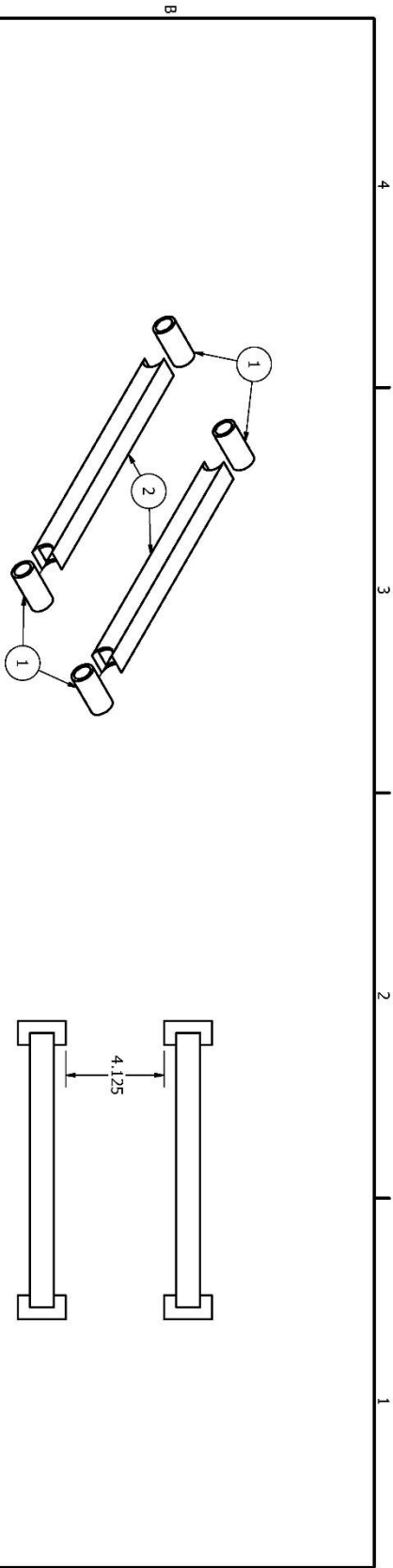
Size: B

Scale: 1 / 4

Sheet: 3

Material:

UNLESS OTHERWISE SPECIFIED	
DIMENSIONS ARE IN INCHES	
ANGLES	° ' " .XXX
±.5°	±.02 ±.01 ±.005

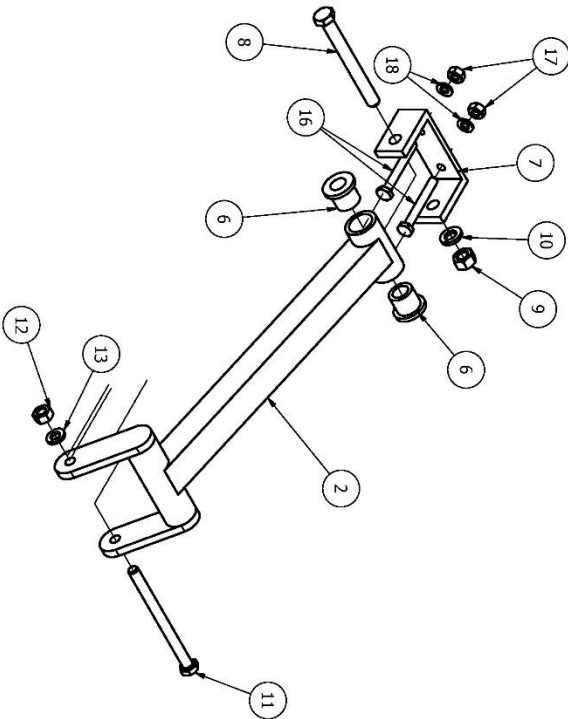


- NOTES:
1. ALL COMPONENTS ARE MIG WELDED
 2. QUANTITY: 4 SETS
 3. SHOCK MOUNT TABS ARE WELDED 5 INCHES FROM THE WHEEL SIDE OF THE H-ARM
 4. SHOCK MOUNT TABS ARE WELDED TO THE "INSIDE" H-ARM MEMBER

ITEM	QTY	PART NUMBER
1	4	Steel Tube - 2 inches
2	2	Square Tube - Steel 11.5
3	2	Shock Mount H-Arm

 UNDSpace STUDIES UNIVERSITY OF NORTH DAKOTA		Design: Cfollette Date: 11/5/2015	Project: Chris Folllette Master's Thesis
		Drawn: Chris Folllette Date: 9/22/2016	
Title: Lower H Arm - Steel Iam		Checked: Date:	Material
UNLESS OTHERWISE SPECIFIED DIMENSIONS ARE IN INCHES. ANGLES IN DEGREES.		Size Scale B 1 / 4	Sheet 1

ITEM	QTY	PART NUMBER	DESCRIPTION
2	1	Top Suspension Arm - Steel	
6	10	0.75 In OD Flanged bearing - 6338K423	STEP AP203
7	3	Aluminum Tab - Suspension	
8	3	ANSI B18.2.1 - 3/8-16 UNC - 3.5	Hex Cap Screw
9	4	ANSI B18.2.2 - 3/8 - 16	Hex Nuts (Inch Series) Hex Nut
10	4	ASME B18.21.1 - 3/8	Regular Helical Spring Lock Washers(Inch Series)
11	1	ANSI B18.2.1 - 5/16-18 UNC - 4	Hex Cap Screw
12	2	ANSI B18.2.2 - 5/16 - 18	Hex Nuts (Inch Series) Hex Nut
13	2	ASME B18.21.1 - 5/16	Regular Helical Spring Lock Washers(Inch Series)
16	8	ANSI B18.2.1 - 1/4-20 UNC - 2	Hex Cap Screw
17	8	ANSI B18.2.2 - 1/4 - 20	Hex Nuts (Inch Series) Hex Nut
18	8	ASME B18.21.1 - 1/4	Regular Helical Spring Lock Washers(Inch Series)



UNIVERSITY OF NORTH DAKOTA
SPACE STUDIES

Design: Crouette
Date: 10/9/2015
Drawn: Chris Follotte
Date: 9/28/2016

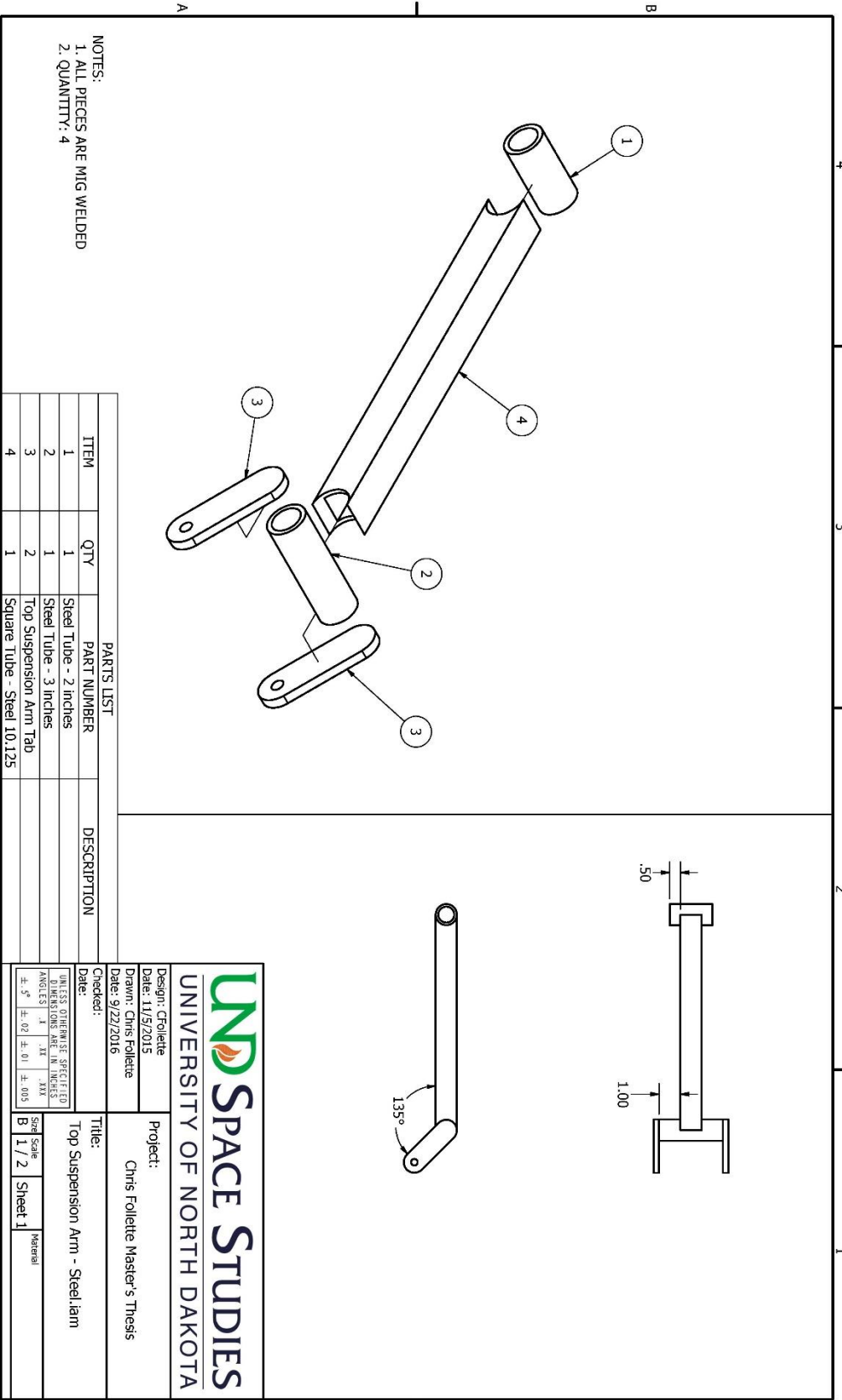
Project:
Chris Follotte Master's Thesis

Title:
Upper Suspension Arm

UNLESS OTHERWISE SPECIFIED
DIMENSIONS ARE IN INCHES
ANGLES IN DEGREES
±.5° ±.02 ±.01 ±.003

Size Scale: B
1 / 3
Sheet 2

Material



NOTES:
 1. ALL PIECES ARE MIG WELDED
 2. QUANTITY: 4

ITEM	QTY	PART NUMBER	DESCRIPTION
1	1		Steel Tube - 2 inches
2	1		Steel Tube - 3 inches
3	2		Top Suspension Arm Tab
4	1		Square Tube - Steel 10.125

UNIVERSITY OF NORTH DAKOTA

SPACE STUDIES

Design: Cfollette
 Date: 11/5/2015
 Drawn: Chris Folllette
 Date: 9/22/2016

Checked:
 Date:

UNLESS OTHERWISE SPECIFIED
 DIMENSIONS ARE IN INCHES
 ANGLES IN DEGREES
 ±.5° ±.01 ±.005

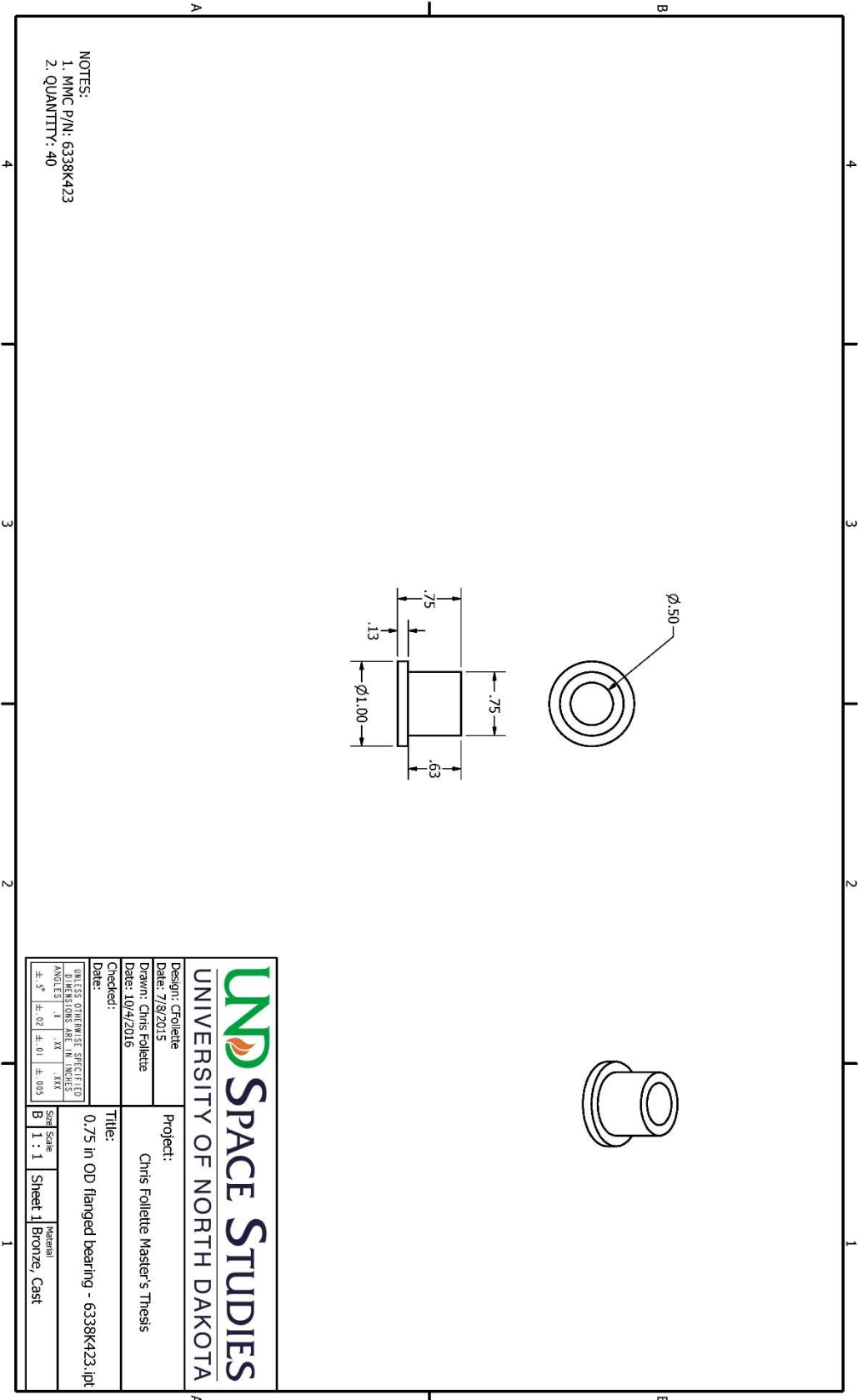
Project:
Chris Folllette Master's Thesis

Title:
Top Suspension Arm - Steel/lam

Size Scale:
1 / 2

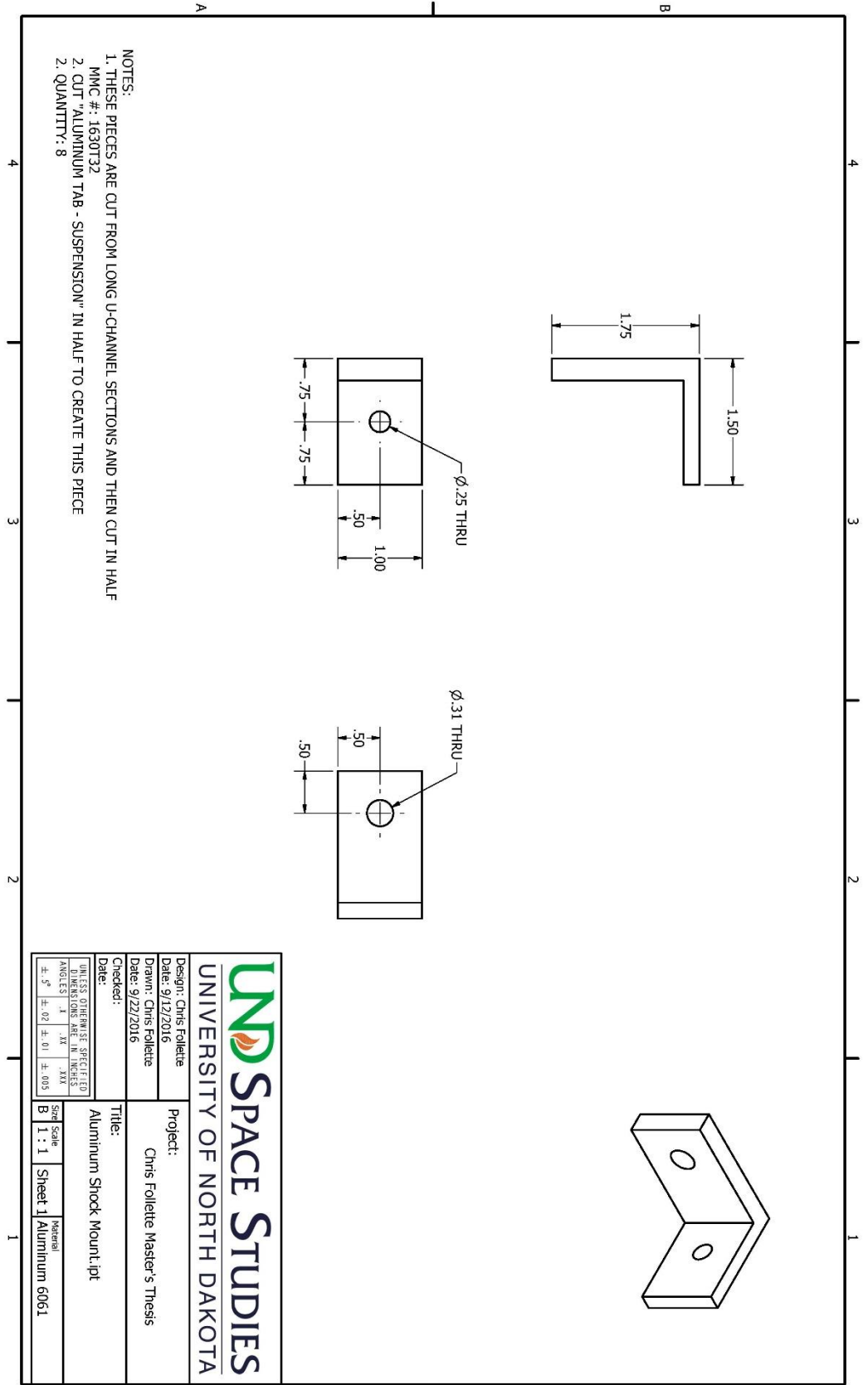
Sheet:
1

Material:



NOTES:
 1. M/MC P/N: 6338K423
 2. QUANTITY: 40

Design: CFollette	Project:											
Date: 7/8/2015	Chris Follette Master's Thesis											
Drawn: Chris Follette												
Date: 10/4/2016												
Checked:	Title:											
Date:	0.75 in OD flanged bearing - 6338K423.ipt											
<small>UNLESS OTHERWISE SPECIFIED DIMENSIONS ARE IN INCHES.</small>												
<table border="1"> <tr> <td>ANGLES</td> <td>± .5°</td> <td>± .02</td> <td>± .01</td> <td>± .003</td> </tr> </table>	ANGLES	± .5°	± .02	± .01	± .003	<table border="1"> <tr> <td>Size</td> <td>Scale</td> <td>Material</td> </tr> <tr> <td>B</td> <td>1 : 1</td> <td>Sheet 1 Bronze, Cast</td> </tr> </table>	Size	Scale	Material	B	1 : 1	Sheet 1 Bronze, Cast
ANGLES	± .5°	± .02	± .01	± .003								
Size	Scale	Material										
B	1 : 1	Sheet 1 Bronze, Cast										



- NOTES:
1. THESE PIECES ARE CUT FROM LONG U-CHANNEL SECTIONS AND THEN CUT IN HALF
 2. CUT "ALUMINUM TAB - SUSPENSION" IN HALF TO CREATE THIS PIECE
- MMC #: 1630T32
 QUANTITY: 8

UNIVERSITY OF NORTH DAKOTA

SPACE STUDIES

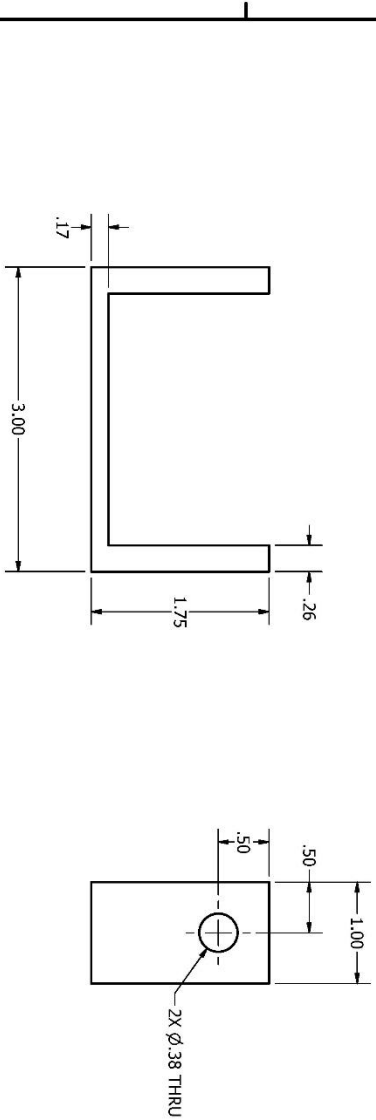
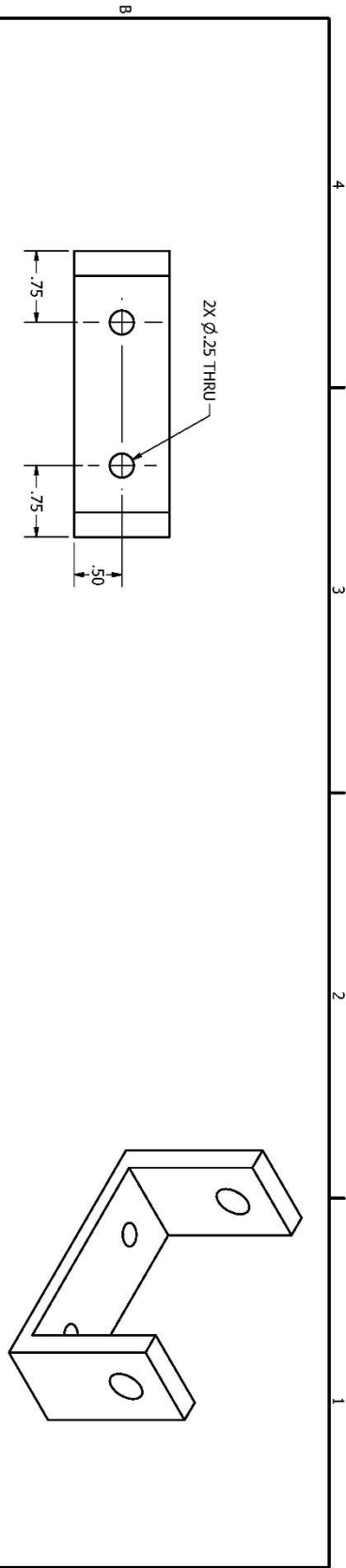
Design: Chris Follette
 Date: 9/12/2016

Drawn: Chris Follette
 Date: 9/22/2016

Checked:

Project:		Chris Follette Master's Thesis	
Title:		Aluminum Shock Mount.lpt	
Size	Scale	Sheet	Material
B	1 : 1	1	Aluminum 6061

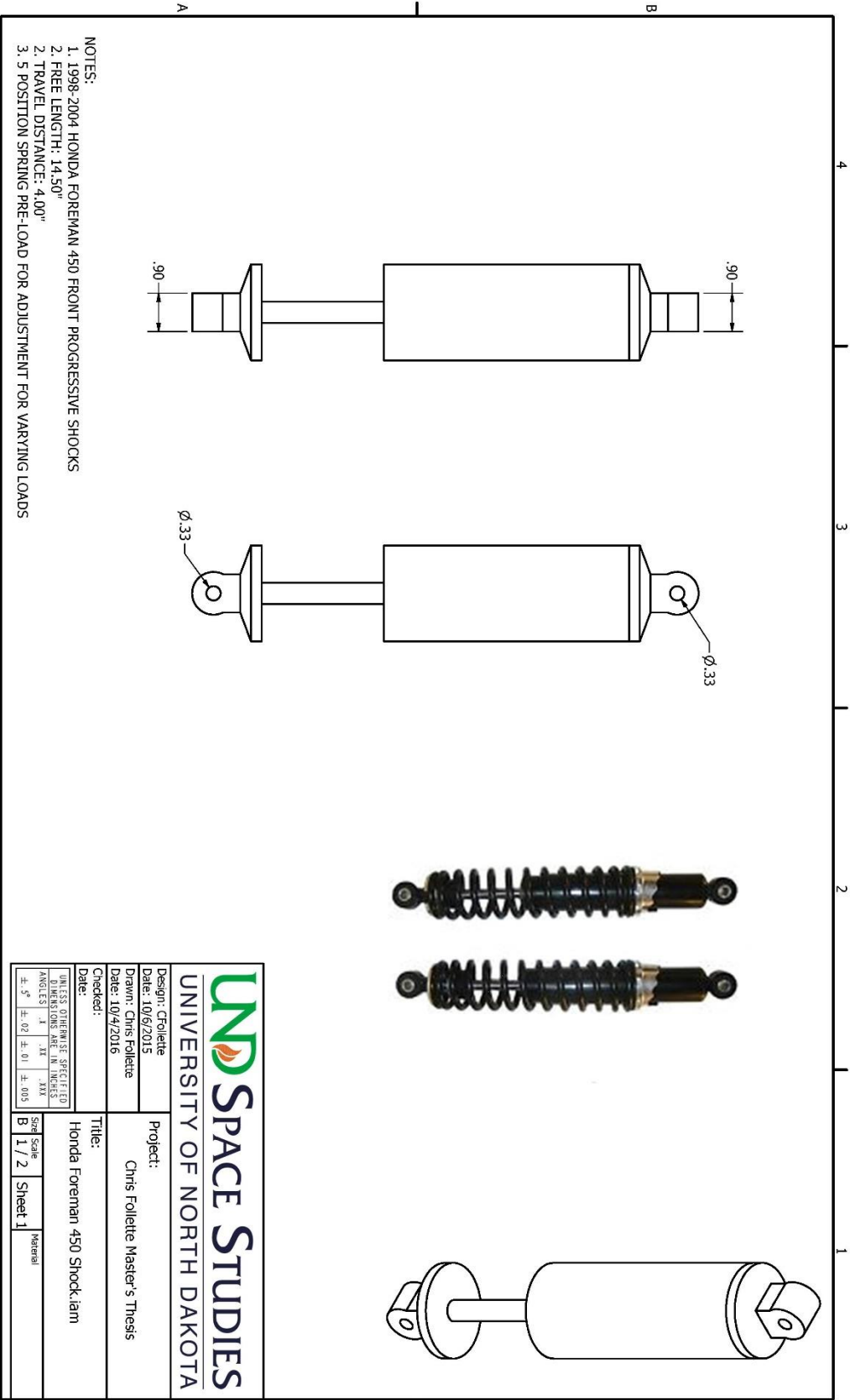
UNLESS OTHERWISE SPECIFIED DIMENSIONS ARE IN INCHES
 ANGLES 1° 1/4° .005
 ±.05 ±.02 ±.01 ±.003



NOTES:
 1. THESE PIECES ARE CUT FROM LONG U-CHANNEL SECTIONS
 2. QUANTITY: 16

4 3 2 1

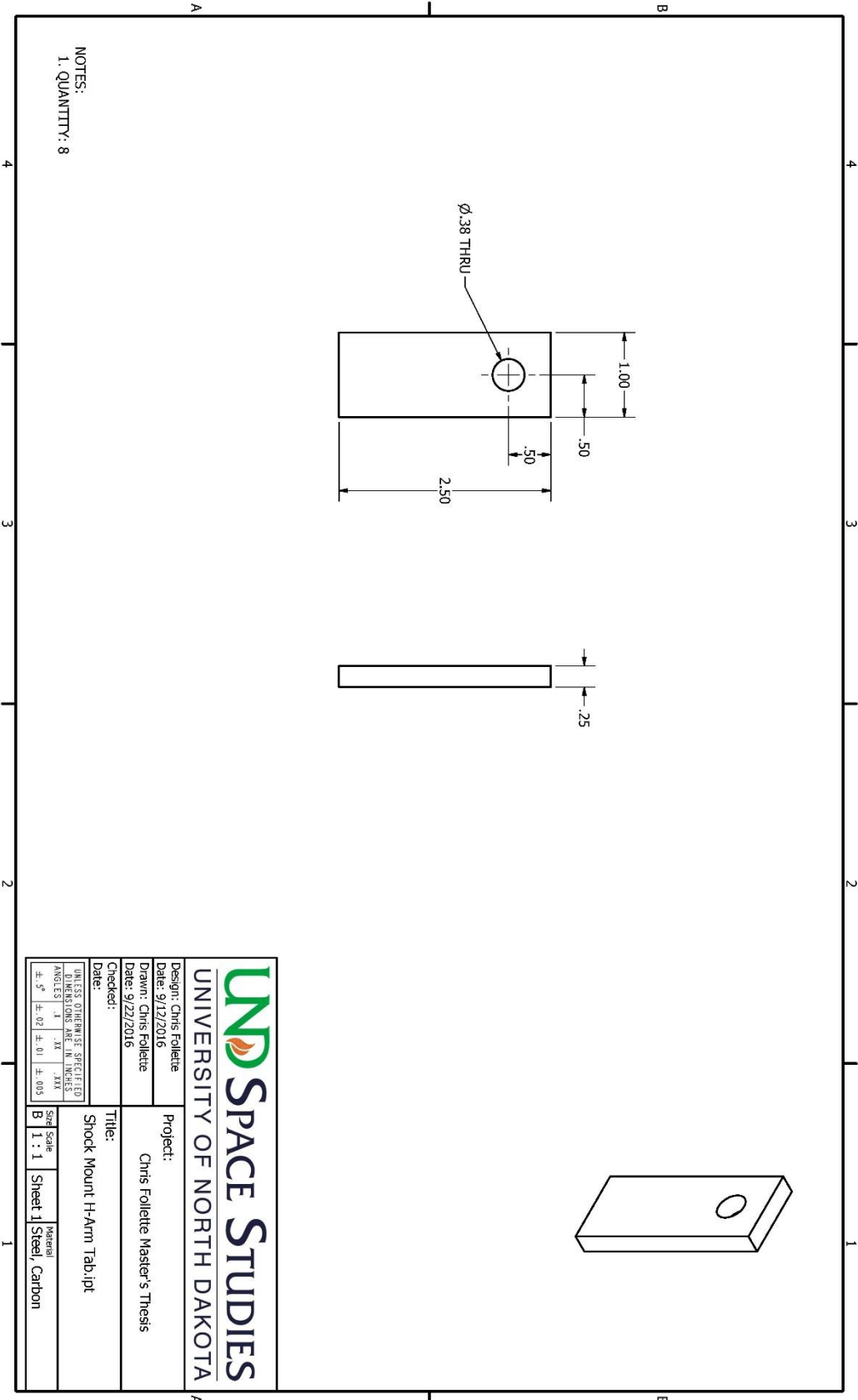
		UNIVERSITY OF NORTH DAKOTA	
		Project: Chris Follotte Master's Thesis	
Design: Chris Follotte Date: 9/12/2016		Drawn: Chris Follotte Date: 9/21/2016	
Checked:		Title: Aluminum Tab - Suspension.ipt	
UNLESS OTHERWISE SPECIFIED DIMENSIONS ARE IN INCHES.		Material: Aluminum 6061	
TOLERANCES:	FRACTIONS	DECIMALS	ANGLES
$\pm .01$	$\pm .01$	$\pm .005$	$\pm .5^\circ$
Size Scale: B		Sheet 1 of 1	



- NOTES:
1. 1998-2004 HONDA FOREMAN 450 FRONT PROGRESSIVE SHOCKS
 2. FREE LENGTH: 14.50"
 3. TRAVEL DISTANCE: 4.00"
 - 5 POSITION SPRING PRE-LOAD FOR ADJUSTMENT FOR VARYING LOADS

UNIVERSITY OF NORTH DAKOTA
SPACE STUDIES

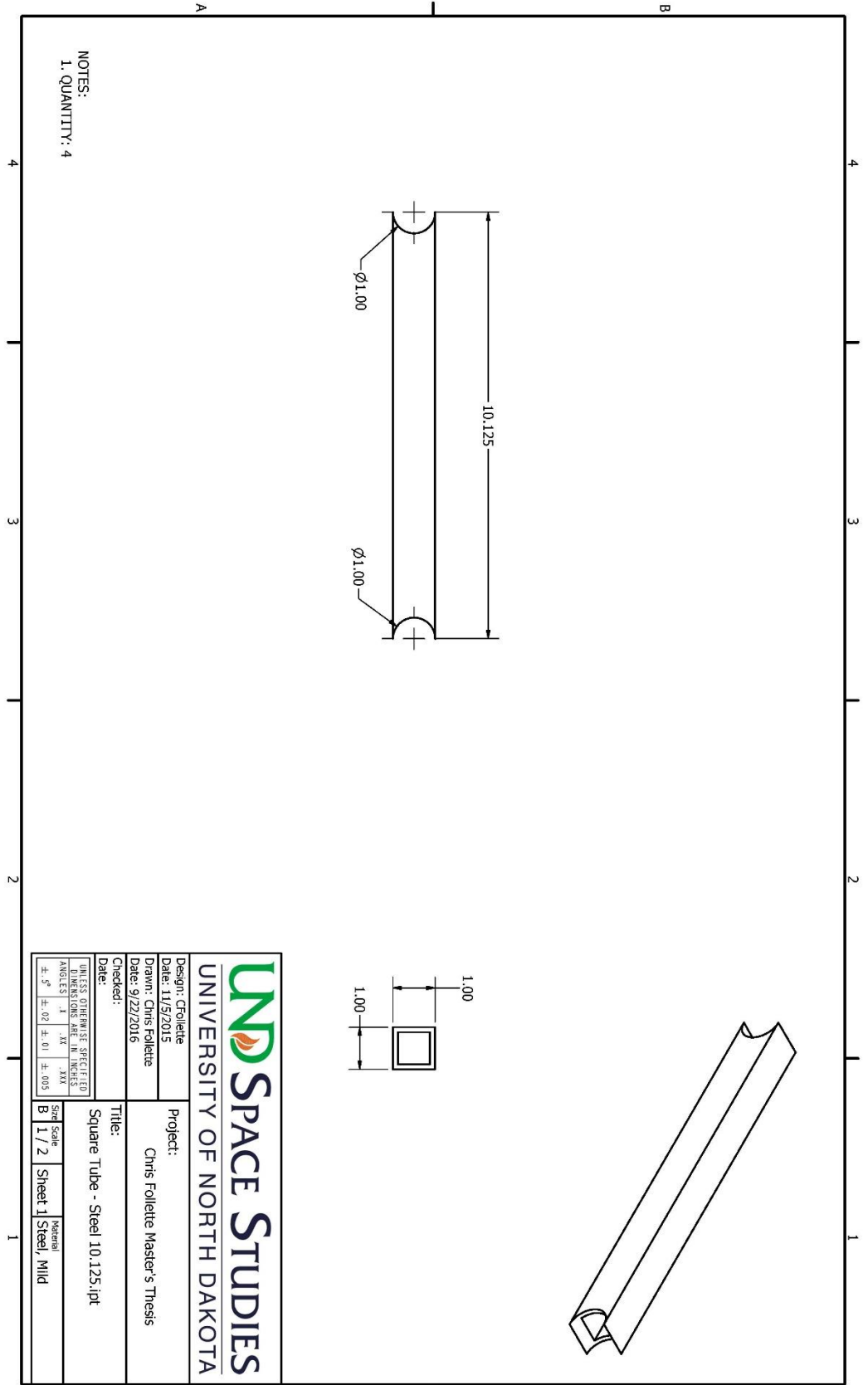
Design: Cfollette Date: 10/6/2015 Drawn: Chris Follette Date: 10/4/2016 Checked: Date:	Project: Chris Follette Master's Thesis Title: Honda Foreman 450 Shock.lam
UNLESS OTHERWISE SPECIFIED DIMENSIONS ARE IN INCHES ANGLES IN DEGREES	
±.5° ±.02 ±.01 ±.003	.125 .125 .125 .125 .125 .125 .125 .125 .125 .125 .125 .125 .125 .125 .125 .125
Size Scale B 1 / 2	Sheet 1 Material



NOTES:
1. QUANTITY: 8

UND SPACE STUDIES
UNIVERSITY OF NORTH DAKOTA

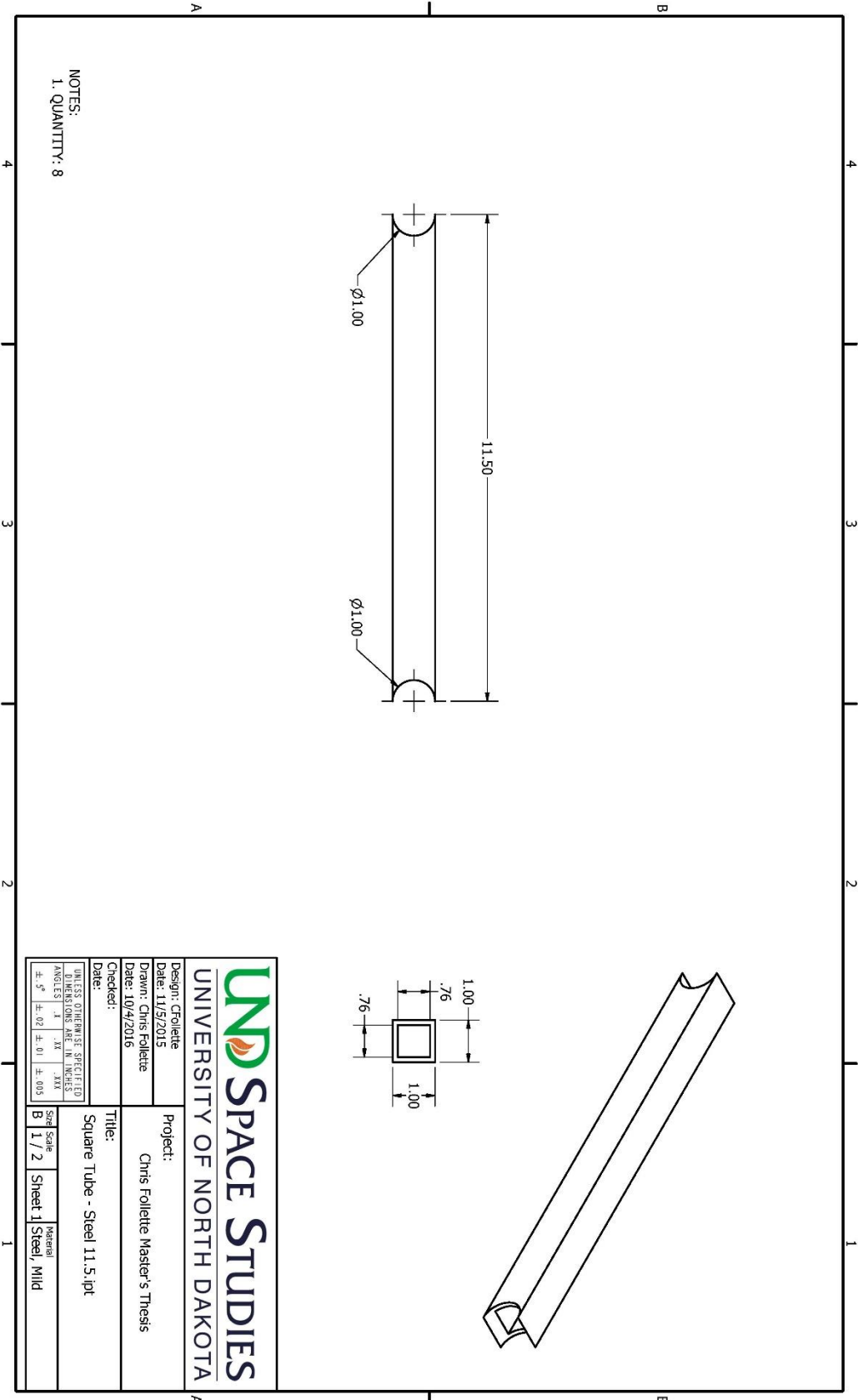
Design: Chris Follette	Project:		
Date: 9/12/2016	Chris Follette Master's Thesis		
Drawn: Chris Follette			
Date: 9/22/2016			
Checked:	Title:		
	Shock Mount H-Arm Tab.ipt		
UNLESS OTHERWISE SPECIFIED DIMENSIONS ARE IN INCHES			
±.5°	±.01	±.01	±.005
Size	Scale	Material	
B	1 : 1	Sheet 1	Steel, Carbon



NOTES:
1. QUANTITY: 4

UND SPACE STUDIES
UNIVERSITY OF NORTH DAKOTA

Design: Cfollette	Project:			
Date: 11/9/2015	Chris Folllette Master's Thesis			
Drawn: Chris Folllette				
Date: 9/22/2016				
Checked:	Title:			
	Square Tube - Steel 10.125.ipt			
UNLESS OTHERWISE SPECIFIED DIMENSIONS ARE IN INCHES				
ANGLES	IN	IN	IN	IN
±.5°	±.02	±.01	±.005	
Size	Scale	Material		
B	1 / 2	Sheet 1 Steel, Mild		



NOTES:
1. QUANTITY: 8

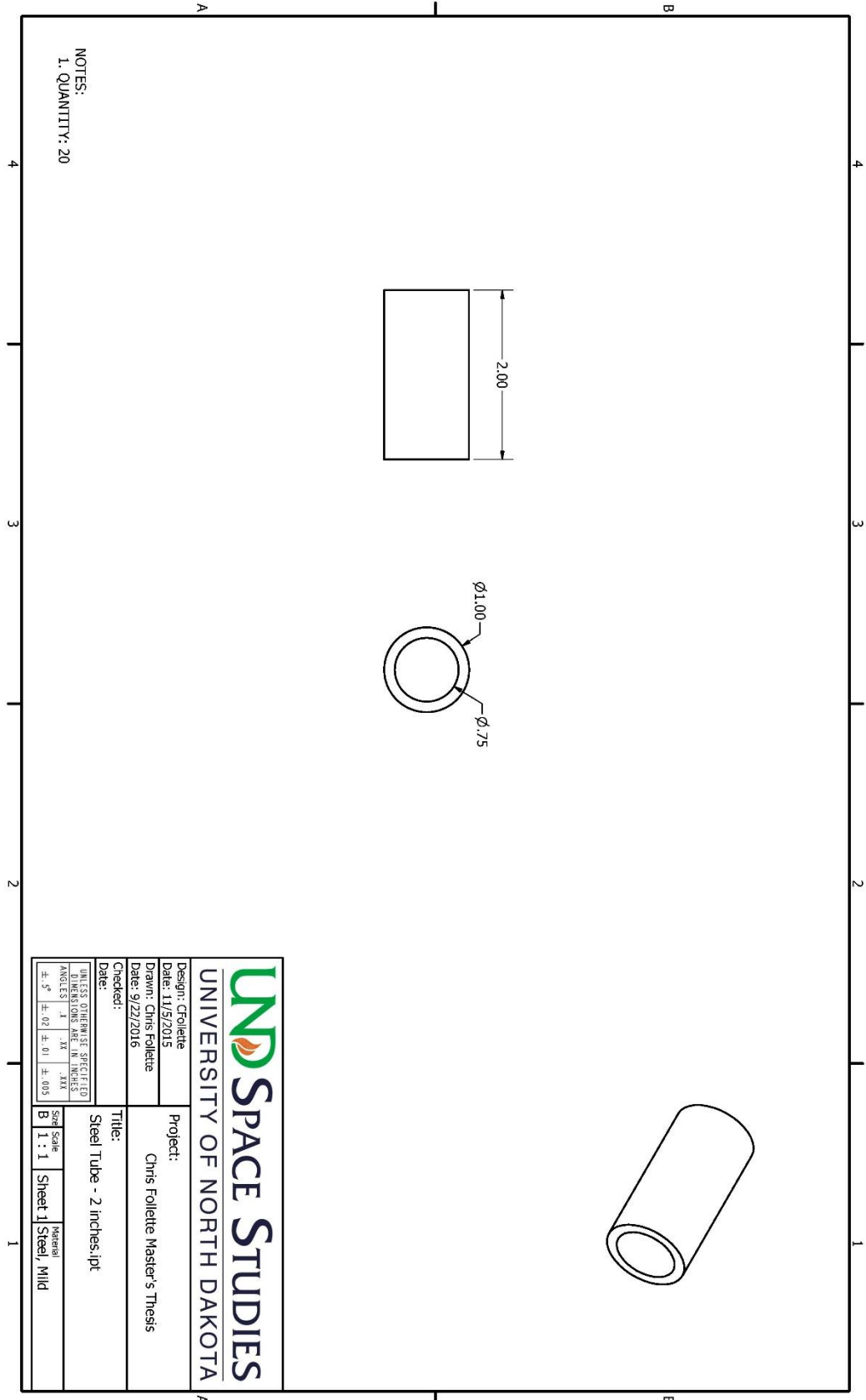
UND SPACE STUDIES
UNIVERSITY OF NORTH DAKOTA

Design: Crollette
Date: 11/5/2015

Project:
Drawn: Chris Follotte
Date: 10/4/2016
Title: Chris Follotte Master's Thesis

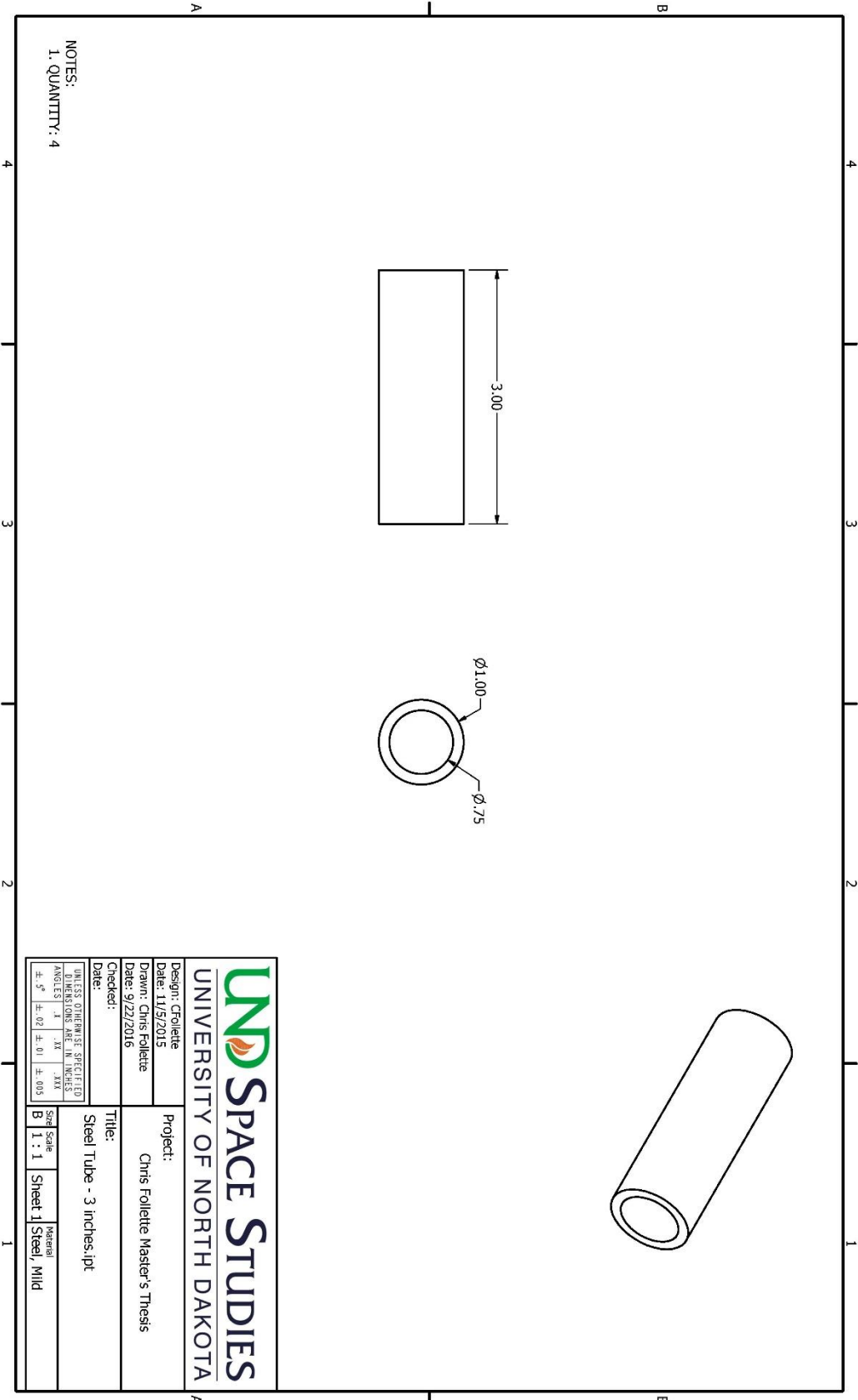
Title: Square Tube - Steel 11.5.ipt

UNLESS OTHERWISE SPECIFIED	Size	Material
DIMENSIONS ARE IN INCHES	B	1 Steel, Mild
ANGLES	1 / 2	Sheet
± .5°	± .01	± .005



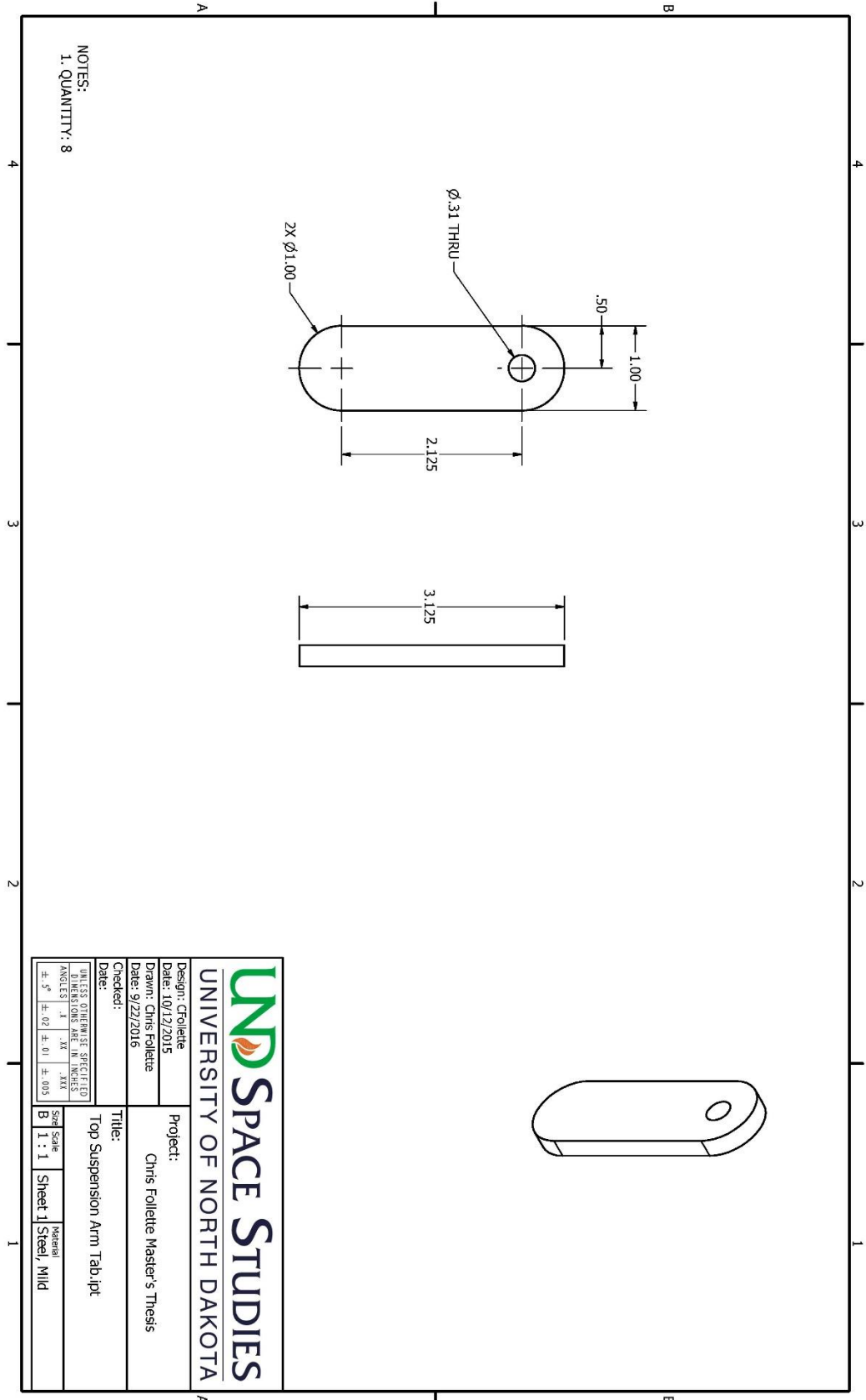
NOTES:
1. QUANTITY: 20

		Design: Cfollette Date: 11/9/2015	
		Drawn: Chris Folllette Date: 9/22/2016	
Checked:		Title: Steel Tube - 2 inches ipt	
<small>UNLESS OTHERWISE SPECIFIED DIMENSIONS ARE IN INCHES.</small>		Size Scale B	Material Steel, Mild
<small>±.5°</small>	<small>±.02</small>	<small>±.01</small>	<small>±.003</small>



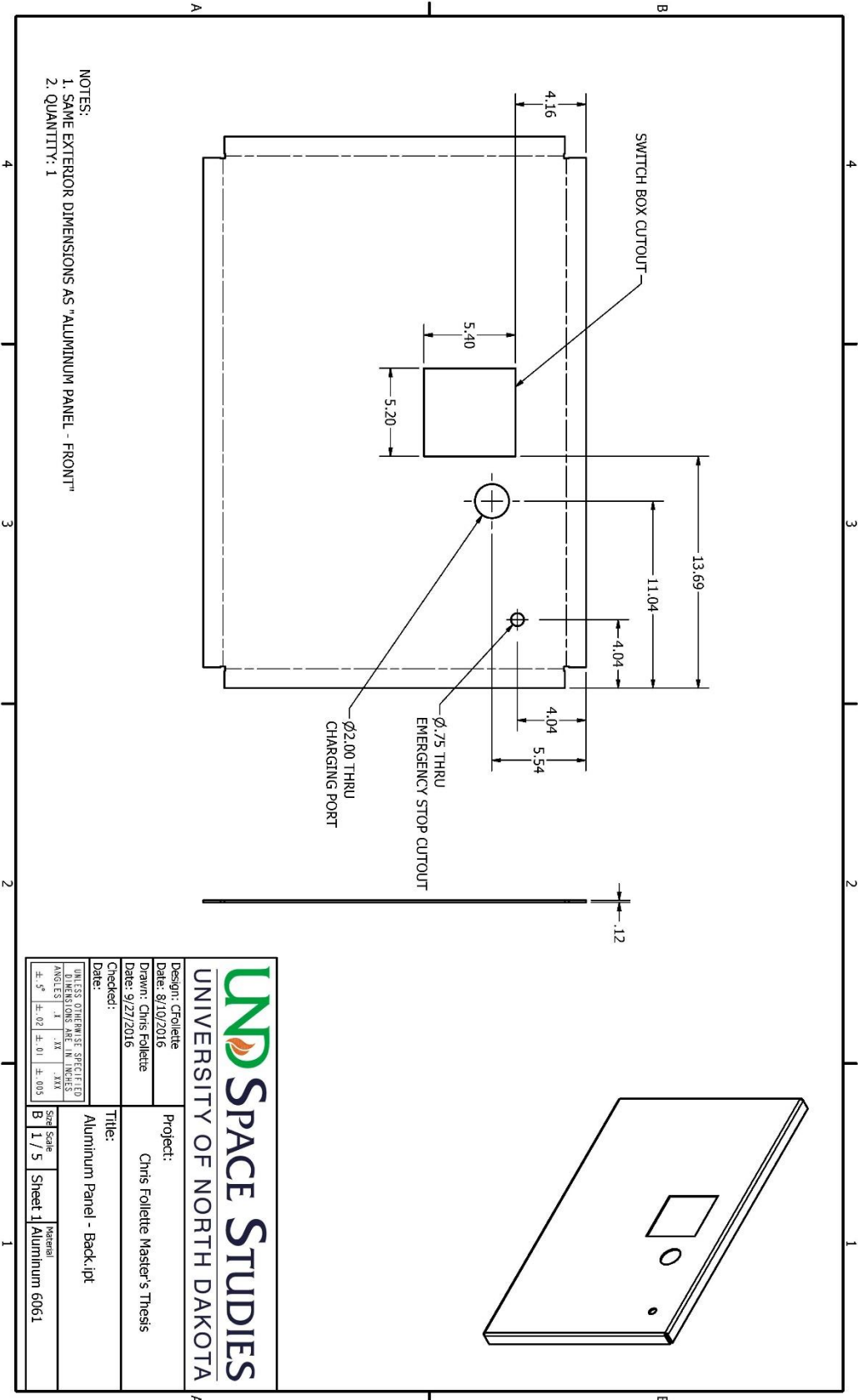
NOTES:
1. QUANTITY: 4

Design: Cfollette	Project:
Date: 11/9/2015	Chris Folllette Master's Thesis
Drawn: Chris Folllette	
Date: 9/22/2016	
Checked:	Title:
	Steel Tube - 3 inches ipt
<small>UNLESS OTHERWISE SPECIFIED DIMENSIONS ARE IN INCHES</small> <small>ANGLES</small>	<small>Size</small> <small>Scale</small> B
<small>±.5° ±.02 ±.01 ±.005</small>	<small>Sheet</small> 1
	<small>Material</small> Steel, Mild



NOTES:
1. QUANTITY: 8

		Title: Top Suspension Arm Tab.dpt	
Design: CFollette Date: 10/12/2015		Project: Chris Follette Master's Thesis	
Drawn: Chris Follette Date: 9/22/2016		Checked:	
<small>UNLESS OTHERWISE SPECIFIED DIMENSIONS ARE IN INCHES</small>		<small>Size Scale</small> B 1 : 1	
<small>ANGLES</small> $\pm .5^\circ$ $\pm .01$ $\pm .003$		<small>Material</small> 1 Steel, Mild	



NOTES:
 1. SAWE EXTERIOR DIMENSIONS AS "ALUMINUM PANEL - FRONT"
 2. QUANTITY: 1

UNIVERSITY OF NORTH DAKOTA
SPACE STUDIES

Design: Cfollette
 Date: 8/10/2016
 Drawn: Chris Follette
 Date: 9/27/2016
 Checked:

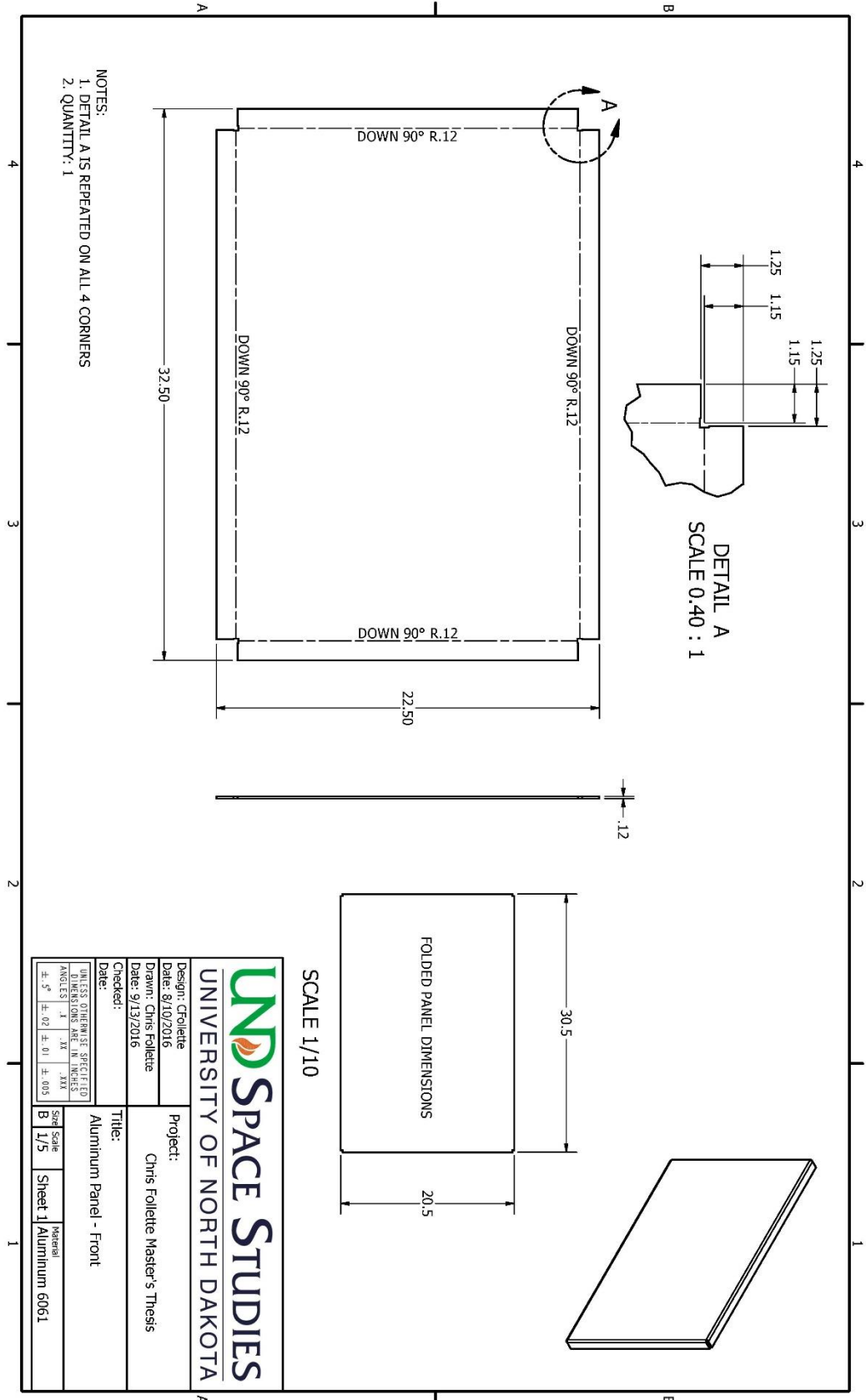
Project:
 Chris Follette Master's Thesis

Title:
 Aluminum Panel - Back:ipt

UNLESS OTHERWISE SPECIFIED
 DIMENSIONS ARE IN INCHES
 ANGLES IN DEGREES

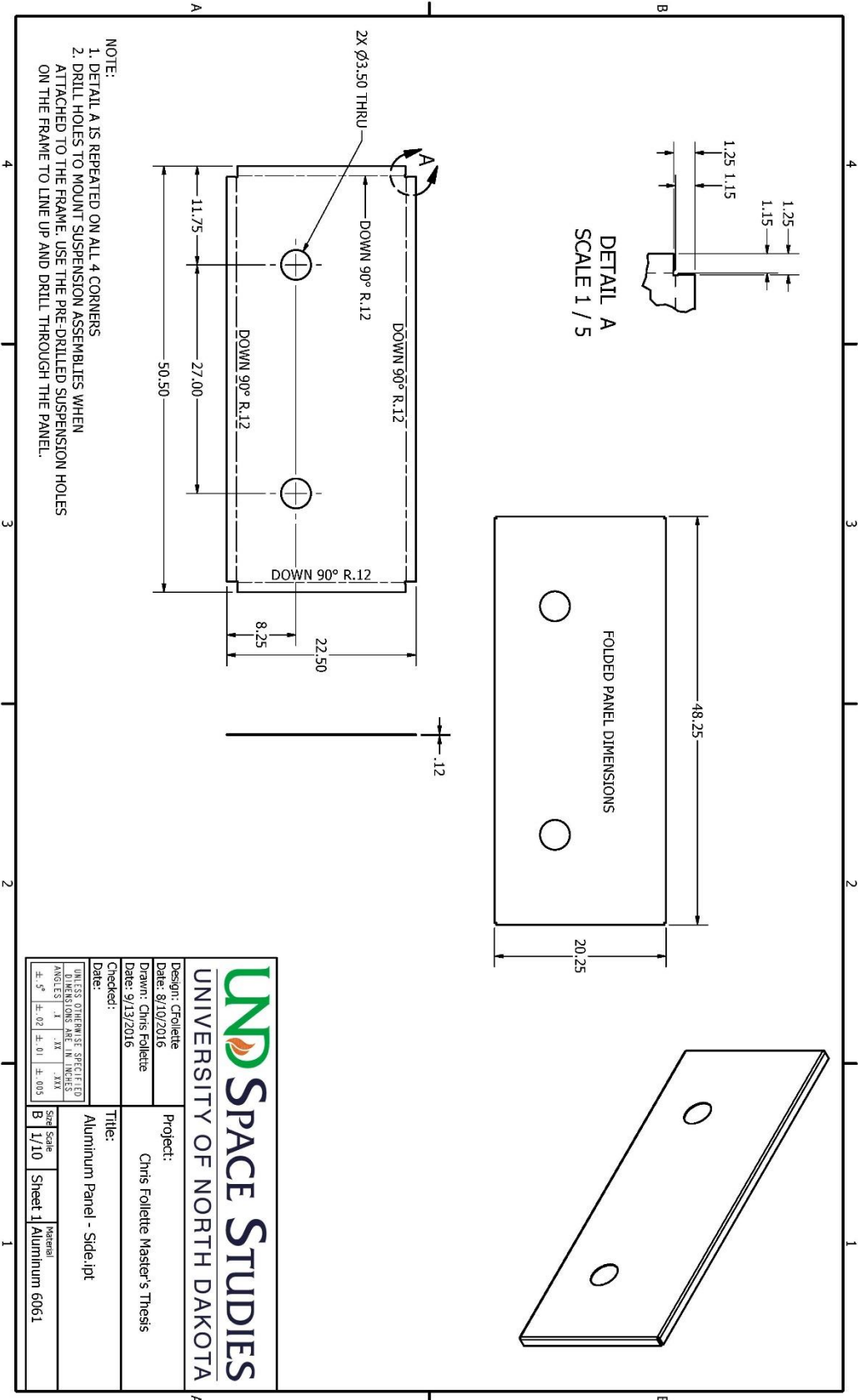
±.5"	±.02	±.01	±.003
------	------	------	-------

Size	B
Scale	1 / 5
Sheet	1
Material	Aluminum 6061



- NOTES:
 1. DETAIL A IS REPEATED ON ALL 4 CORNERS
 2. QUANTITY: 1

		UNIVERSITY OF NORTH DAKOTA	
Design: CFollotte Date: 8/10/2016 Drawn: Chris Follotte Date: 9/13/2016 Checked:		Project: Chris Follotte Master's Thesis	
Title: Aluminum Panel - Front		Size B	Scale 1/5
<small>UNLESS OTHERWISE SPECIFIED DIMENSIONS ARE IN INCHES ANGLES IN DEGREES</small>		Sheet 1	Material Aluminum 6061
±.5°	±.02	±.01	±.003

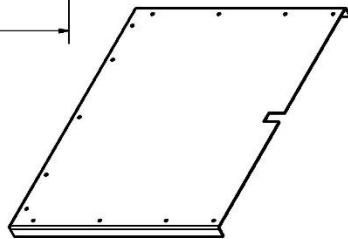
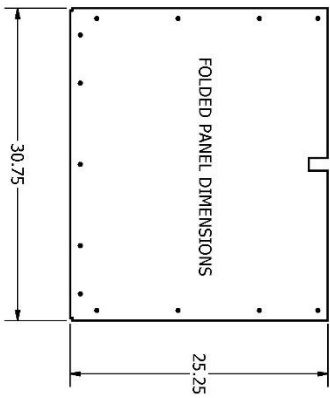
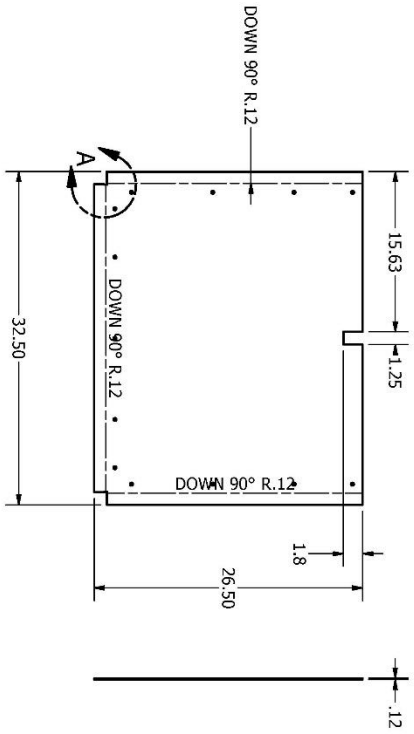
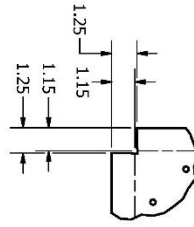


NOTE:
 1. DETAIL A IS REPEATED ON ALL 4 CORNERS
 2. DRILL HOLES TO MOUNT SUSPENSION ASSEMBLIES WHEN ATTACHED TO THE FRAME. USE THE PRE-DRILLED SUSPENSION HOLES ON THE FRAME TO LINE UP AND DRILL THROUGH THE PANEL.

UNIVERSITY OF NORTH DAKOTA
SPACE STUDIES

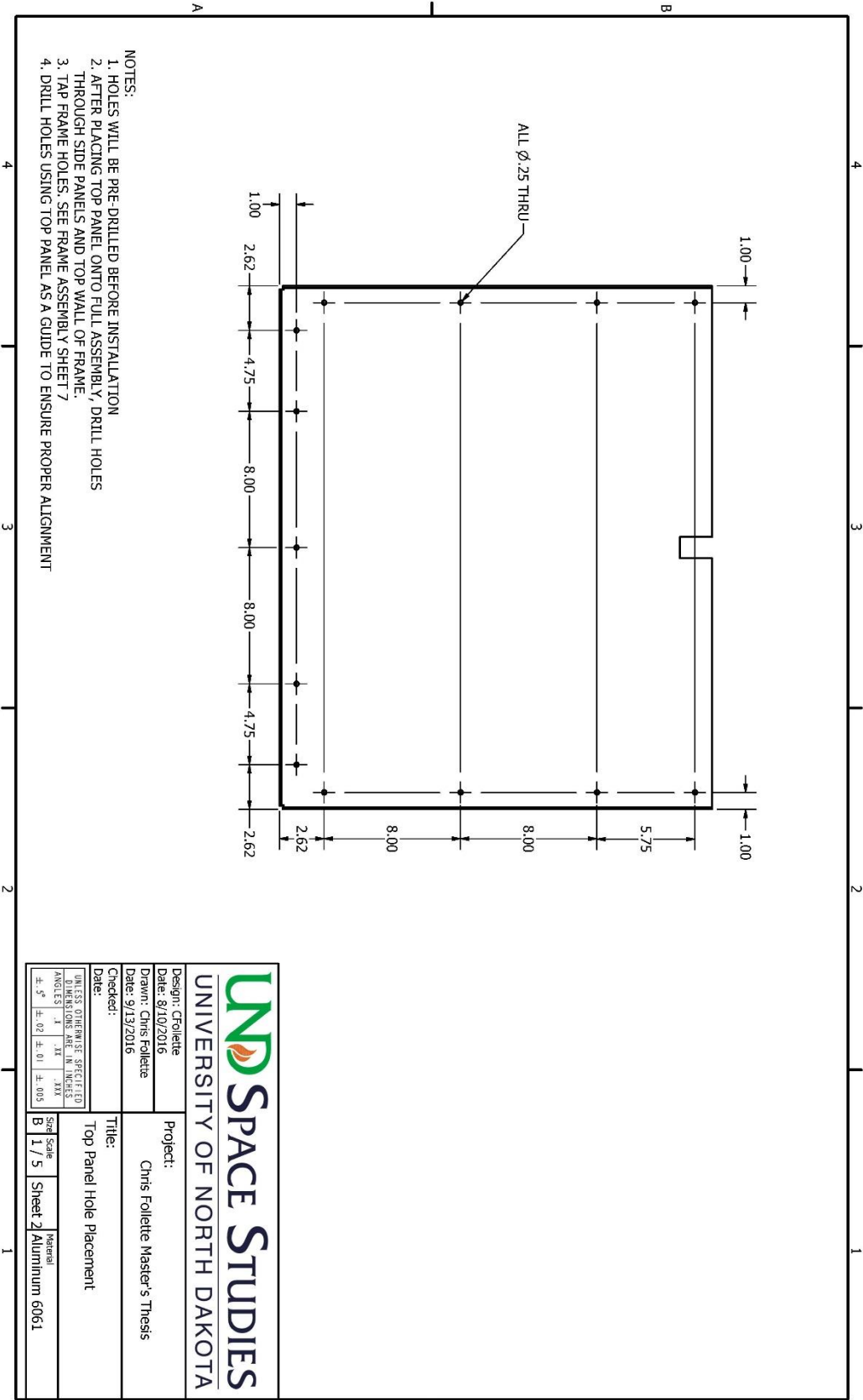
Design: Cfollette	Project:
Date: 8/10/2016	Chris Folllette Master's Thesis
Drawn: Chris Folllette	
Date: 9/13/2016	
Checked:	Title:
	Aluminum Panel - Side.rpt
UNLESS OTHERWISE SPECIFIED DIMENSIONS ARE IN INCHES ANGLES IN DEGREES	Size Scale
±.5° ±.02 ±.01 ±.005	B 1/10
	Sheet 1
	Material
	Aluminum 6061

DETAIL A
SCALE 1 / 5

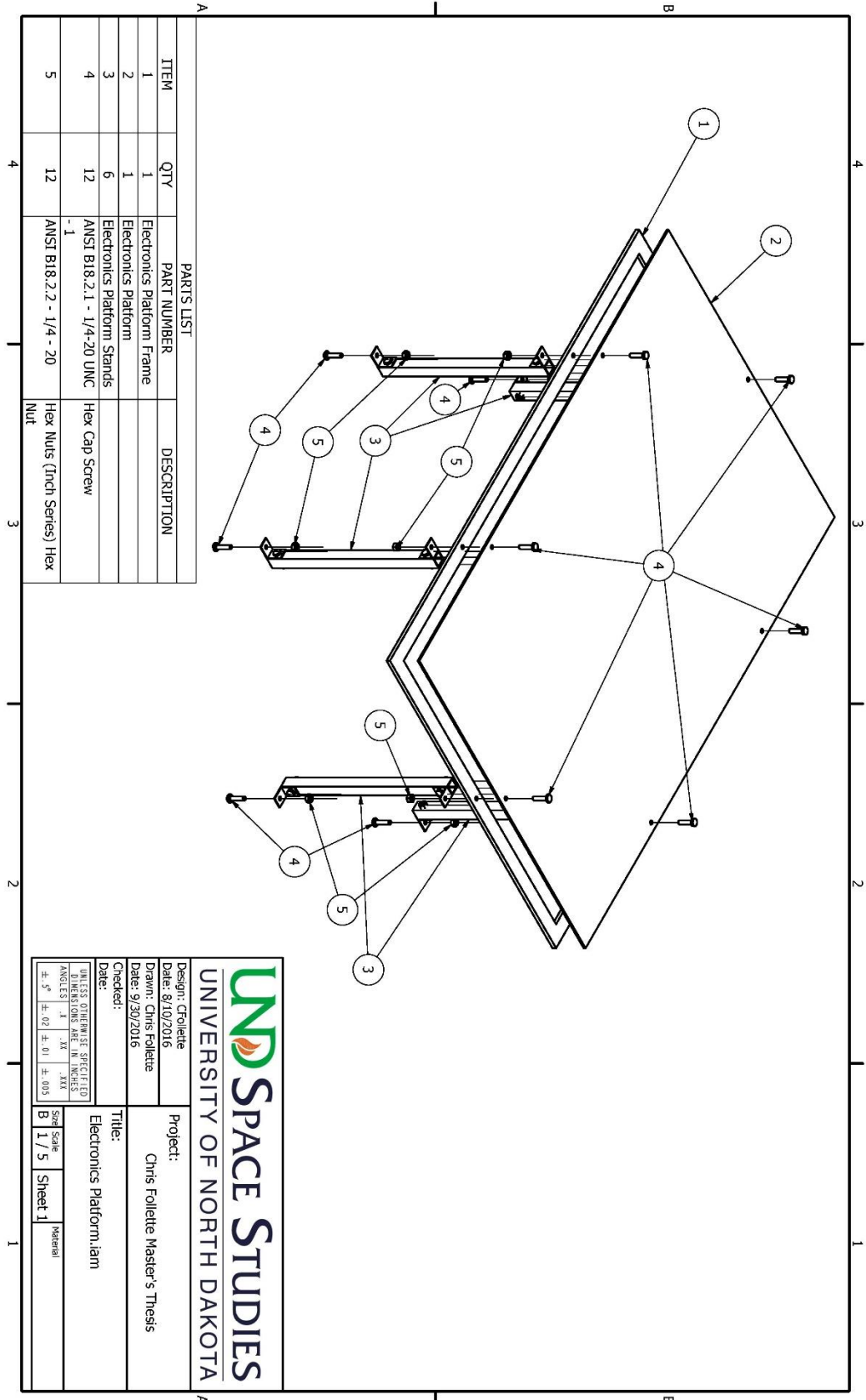


NOTE:
1. DETAIL A IS REPEATED ON BOTH BOTTOM CORNERS

		UNIVERSITY OF NORTH DAKOTA	
		Project: Chris Follotte Master's Thesis	
Design: CFollotte Date: 8/10/2016		Drawn: Chris Follotte Date: 9/13/2016	
Checked:		Title: Aluminum Panel - Top.ipt	
UNLESS OTHERWISE SPECIFIED DIMENSIONS ARE IN INCHES ANGLES IN DEGREES		Size Scale B 1/10	Material Aluminum 6061
±.5°	±.02	±.01	±.003



- NOTES:
1. HOLES WILL BE PRE-DRILLED BEFORE INSTALLATION
 2. AFTER PLACING TOP PANEL ONTO FULL ASSEMBLY, DRILL HOLES THROUGH SIDE PANELS AND TOP WALL OF FRAME.
 3. TAP FRAME HOLES. SEE FRAME ASSEMBLY SHEET 7
 4. DRILL HOLES USING TOP PANEL AS A GUIDE TO ENSURE PROPER ALIGNMENT



PARTS LIST

ITEM	QTY	PART NUMBER	DESCRIPTION
1	1		Electronics Platform Frame
2	1		Electronics Platform
3	6		Electronics Platform Stands
4	12		ANST B18.2.1 - 1/4-20 UNC Hex Cap Screw
5	12		ANST B18.2.2 - 1/4 - 20 Hex Nuts (Ftinch Series) Hex Nut

Design: Crouette
Date: 8/10/2016

Drawn: Chris Follotte
Date: 9/30/2016

Checked:

Project: Chris Follotte Master's Thesis

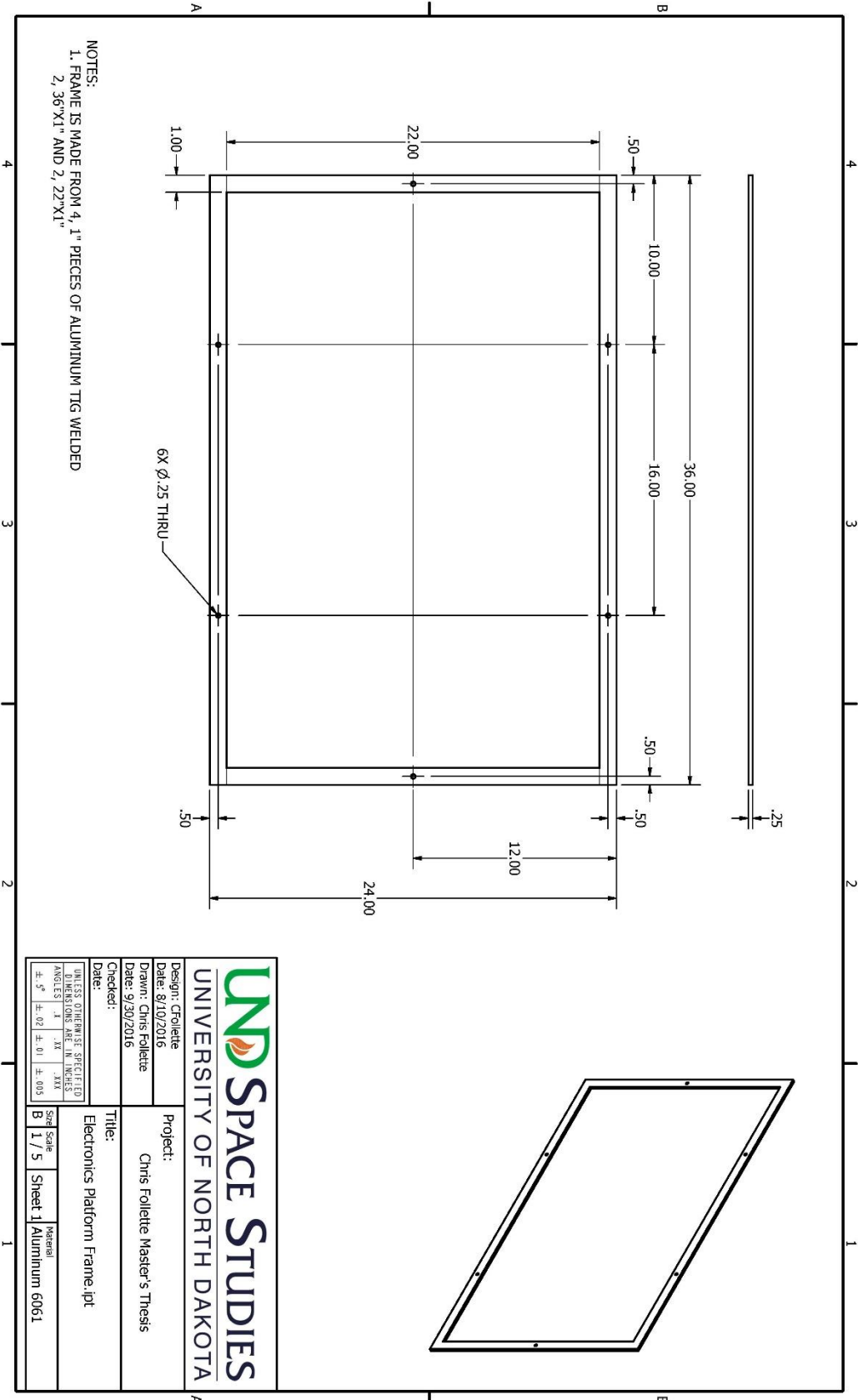
Title: Electronics Platform.iam

Size Scale: B 1 / 5

Sheet 1

UNLESS OTHERWISE SPECIFIED DIMENSIONS ARE IN INCHES

±.5°	±.02	±.01	±.003
------	------	------	-------



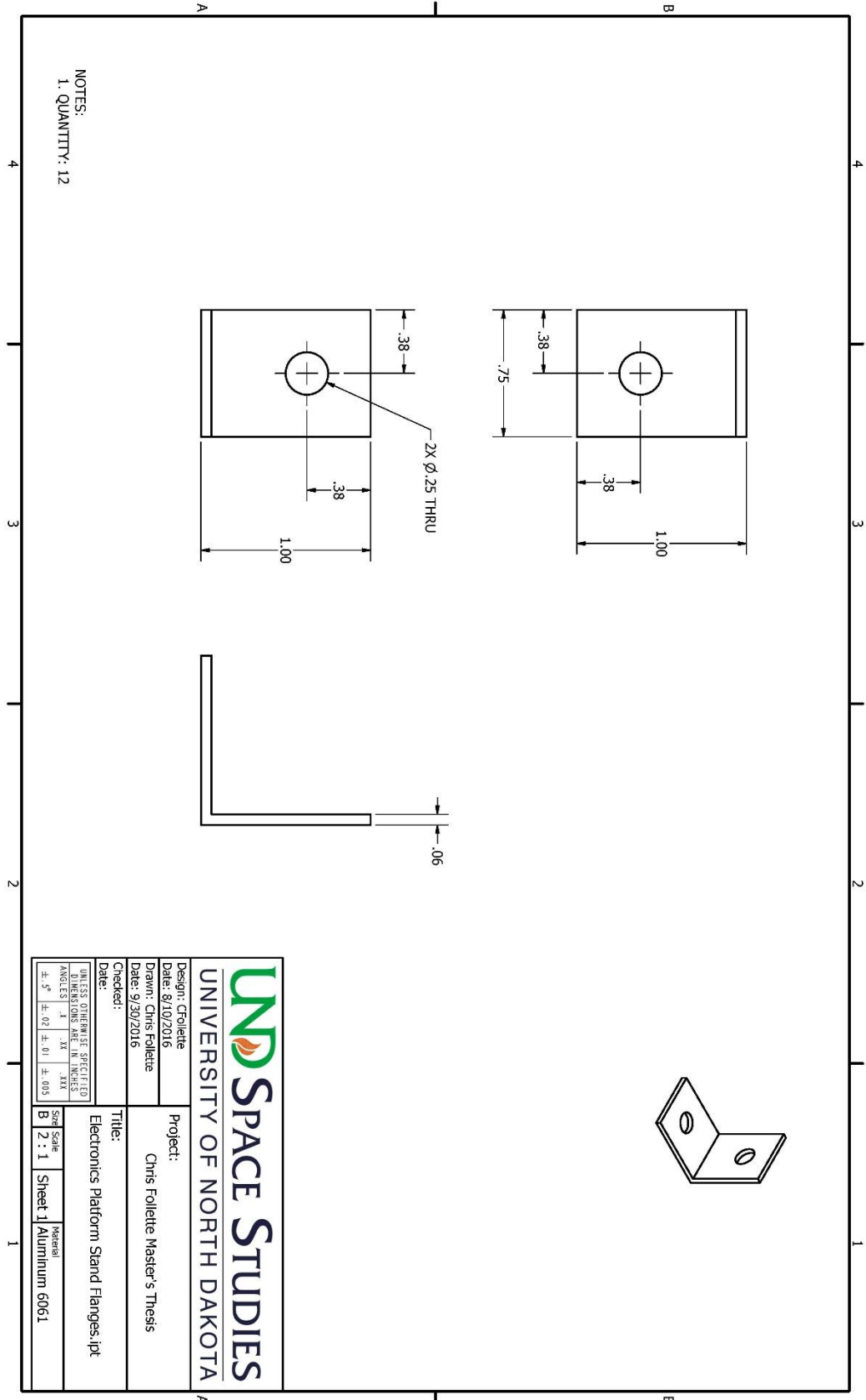
- NOTES:
 1. FRAME IS MADE FROM 4, 1" PIECES OF ALUMINUM TIG WELDED
 2. 36"X1" AND 2, 22"X1"

UNIVERSITY OF NORTH DAKOTA
SPACE STUDIES

Design: Cfollette
 Date: 8/10/2016
 Drawn: Chris Folllette
 Date: 9/30/2016
 Checked:

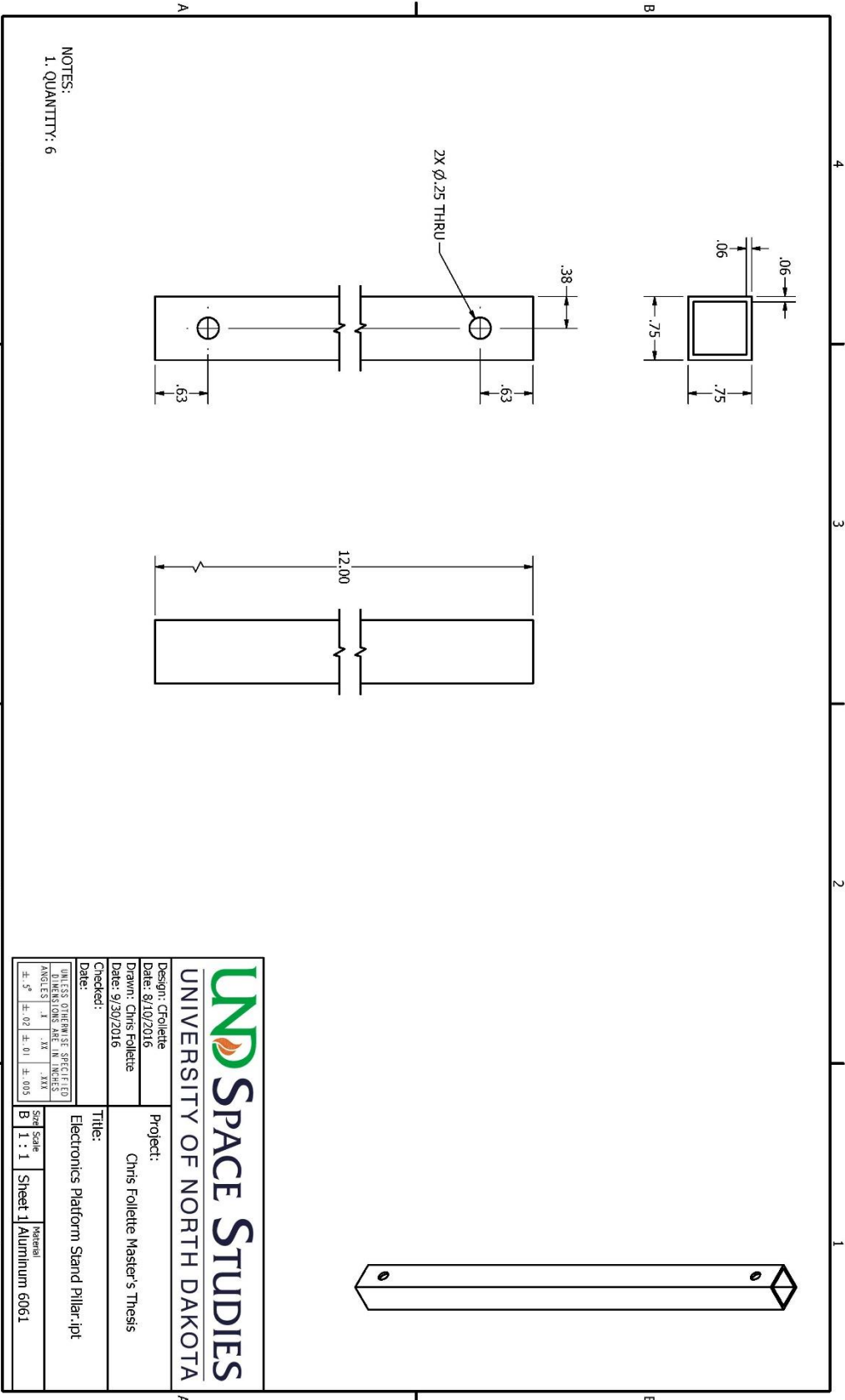
Project: Chris Folllette Master's Thesis
 Title: Electronics Platform Frame.ipt

UNLESS OTHERWISE SPECIFIED DIMENSIONS ARE IN INCHES	Size	Material
±.5° ±.02 ±.01 ±.003	B 1 / 5	Sheet 1 Aluminum 6061



NOTES:
1. QUANTITY: 12

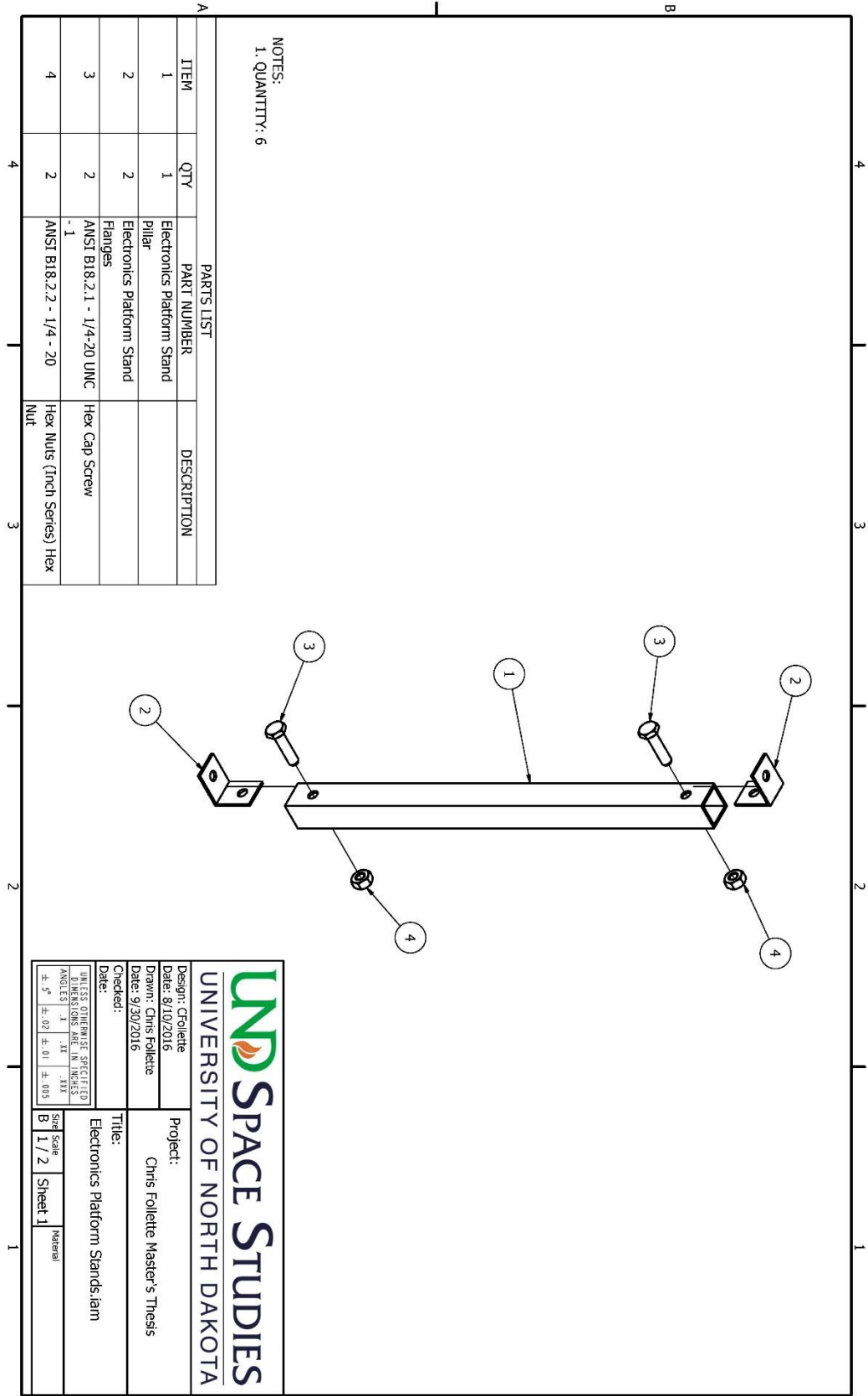
Design: CFollette	Project:
Date: 8/10/2016	Chris Follette Master's Thesis
Drawn: Chris Follette	
Date: 9/30/2016	
Checked:	Title:
	Electronics Platform Stand Flanges.ipt
<small>UNLESS OTHERWISE SPECIFIED DIMENSIONS ARE IN INCHES</small> <small>ANGLES</small>	<small>Size</small> B
<small>±.5° ±.02 ±.01 ±.003</small>	<small>Scale</small> 2 : 1
	<small>Sheet</small> 1
	<small>Material</small> Aluminum 6061



NOTES:
1. QUANTITY: 6


UND SPACE STUDIES
UNIVERSITY OF NORTH DAKOTA

Design: Cfollette Date: 8/10/2016	Project: Chris Folllette Master's Thesis		
Drawn: Chris Folllette Date: 9/30/2016	Title: Electronics Platform Stand Pillar.ipt		
Checked:			
UNLESS OTHERWISE SPECIFIED DIMENSIONS ARE IN INCHES			
±.5°	±.02	±.01	±.005
Size Scale B	1 : 1	Sheet 1	Material Aluminum 6061



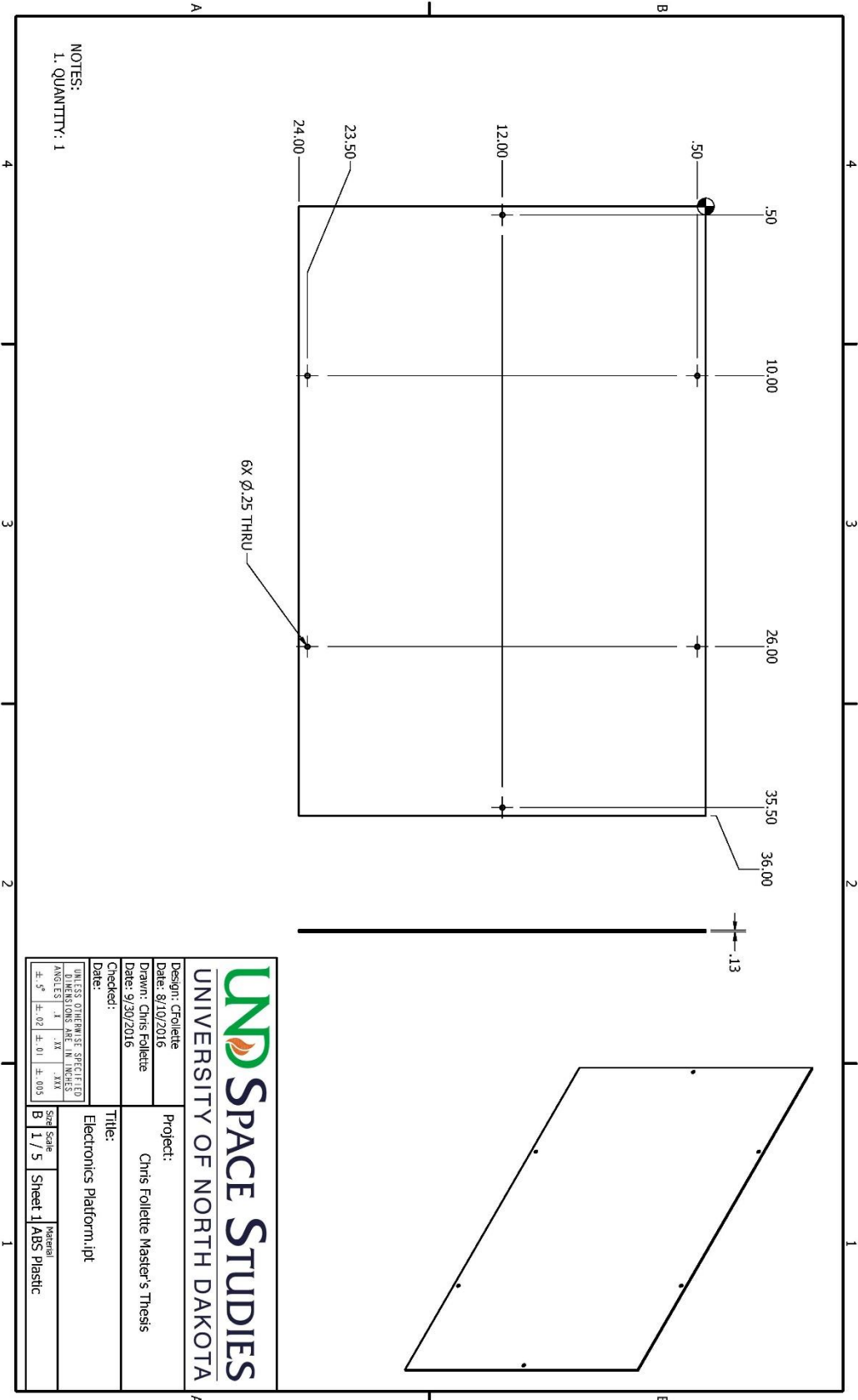
NOTES:
1. QUANTITY: 6

ITEM	QTY	PART NUMBER	DESCRIPTION
1	1	Electronics Platform Stand Pillar	
2	2	Electronics Platform Stand Flanges	
3	2	ANST B18.2.1 - 1/4-20 UNC - 1	Hex Cap Screw
4	2	ANST B18.2.2 - 1/4 - 20	Hex Nuts (Finch Series) Hex Nut



UNIVERSITY OF NORTH DAKOTA

Design: Crouette Date: 8/10/2016 Drawn: Chris Follotte Date: 9/30/2016 Checked:	Project: Chris Follotte Master's Thesis Title: Electronics Platform Stands.lam
UNLESS OTHERWISE SPECIFIED DIMENSIONS ARE IN INCHES ANGLES ° ' " .XXX ±.5° ±.01 ±.003	
Size Scale B 1 / 2	Sheet 1 Material



NOTES:
1. QUANTITY: 1

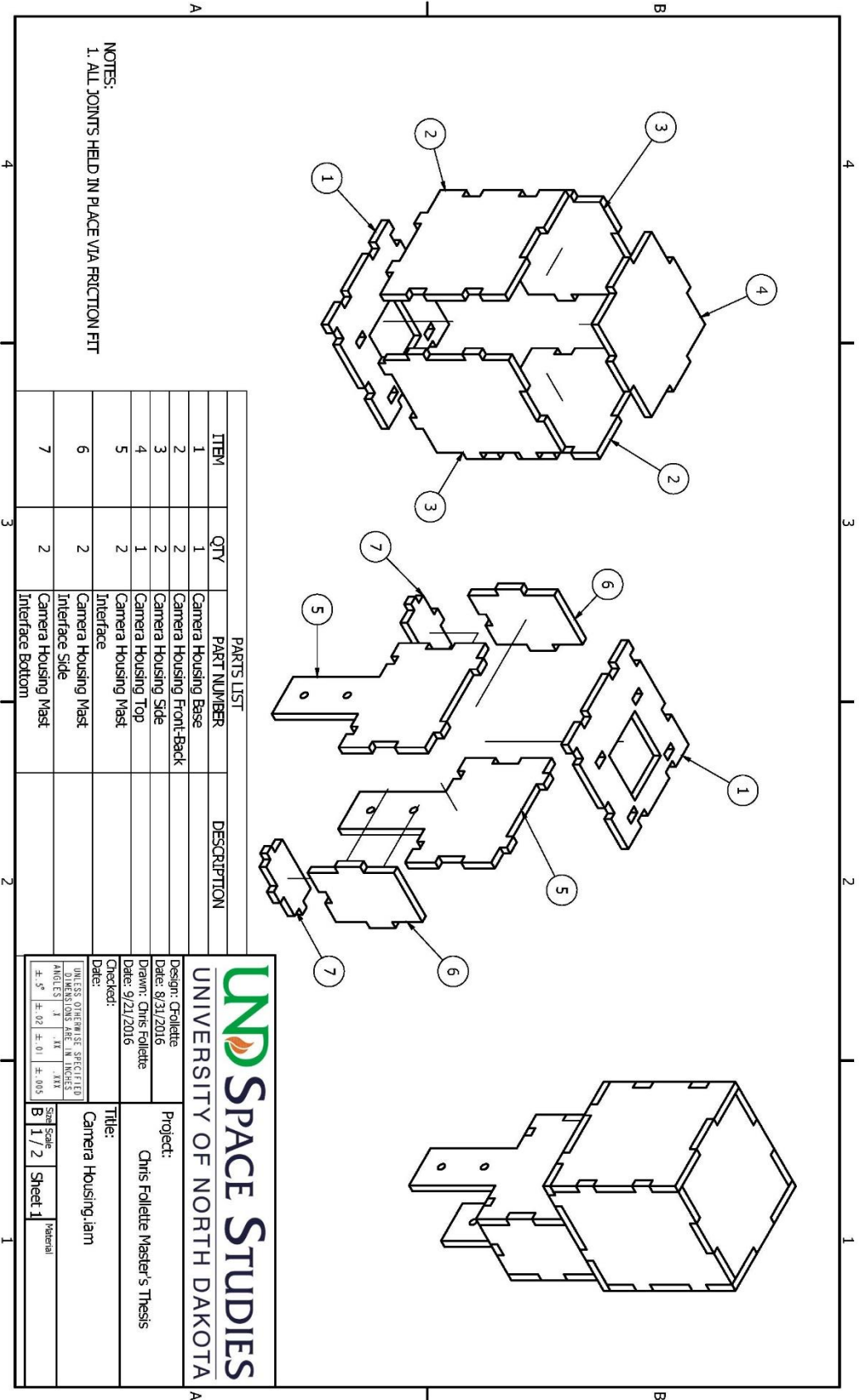
UNIVERSITY OF NORTH DAKOTA
SPACE STUDIES

Design: Cfollette
Date: 8/10/2016
Drawn: Chris Follette
Date: 9/30/2016
Checked:

Project:
Chris Follette Master's Thesis

Title:
Electronics Platform.ipt

UNLESS OTHERWISE SPECIFIED DIMENSIONS ARE IN INCHES ANGLES IN DEGREES	Size	Material
±.5° ±.02 ±.01 ±.003	Scale B 1 / 5	Sheet 1 ABS Plastic



NOTES:
 1. ALL JOINTS HELD IN PLACE VIA FRICTION FIT

ITEM	QTY	PART NUMBER	DESCRIPTION
1	1		Camera Housing Base
2	2		Camera Housing Front-Back
3	2		Camera Housing Side
4	1		Camera Housing Top
5	2		Camera Housing Mast Interface
6	2		Camera Housing Mast Interface Side
7	2		Camera Housing Mast Interface Bottom

UNDSpace STUDIES
 UNIVERSITY OF NORTH DAKOTA

Project: Chris Follie Master's Thesis

Design: Grollette
 Date: 8/31/2016

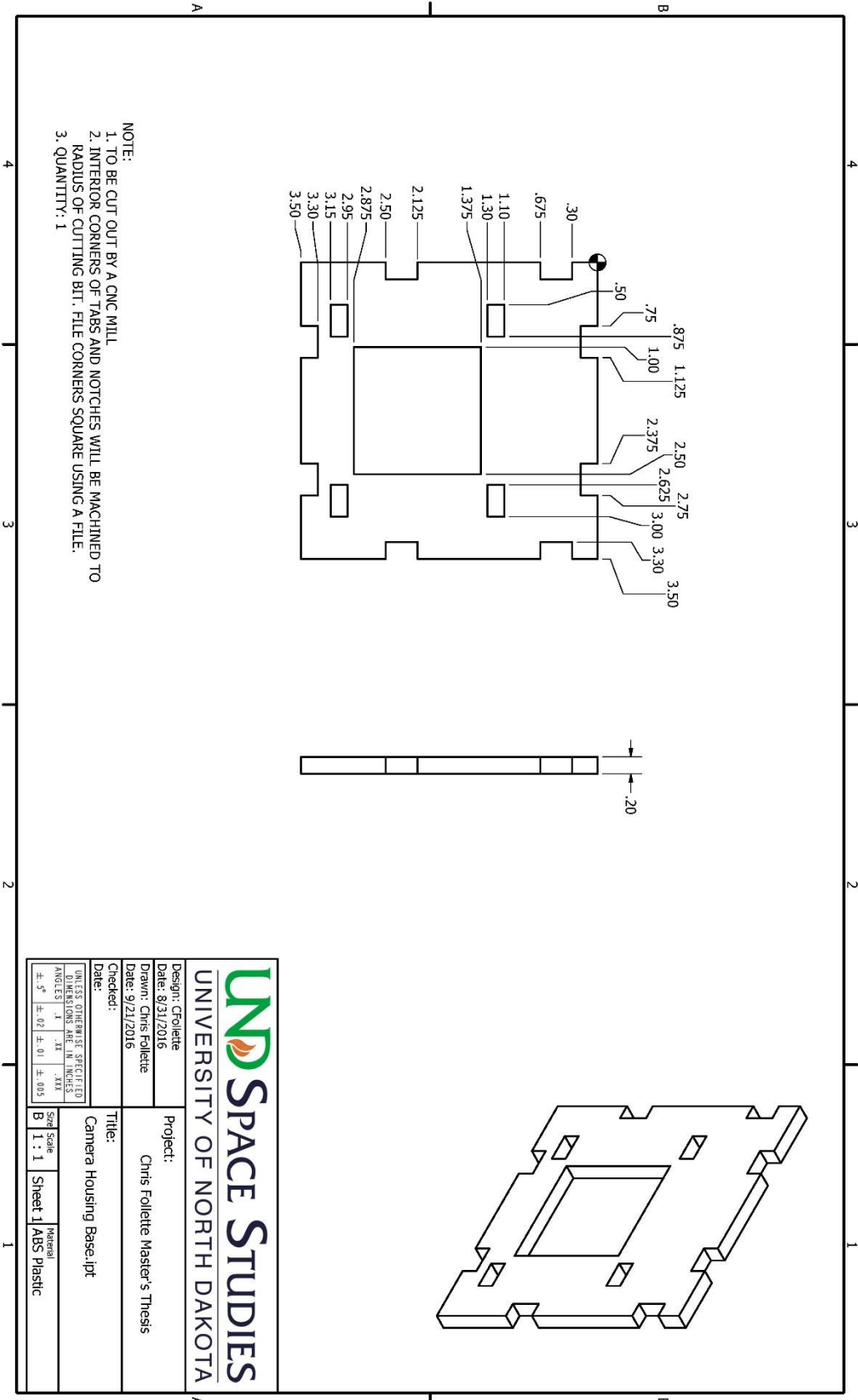
Drawn: Chris Follie
 Date: 9/21/2016

Checked:
 Date:

Title: Camera Housing.lam

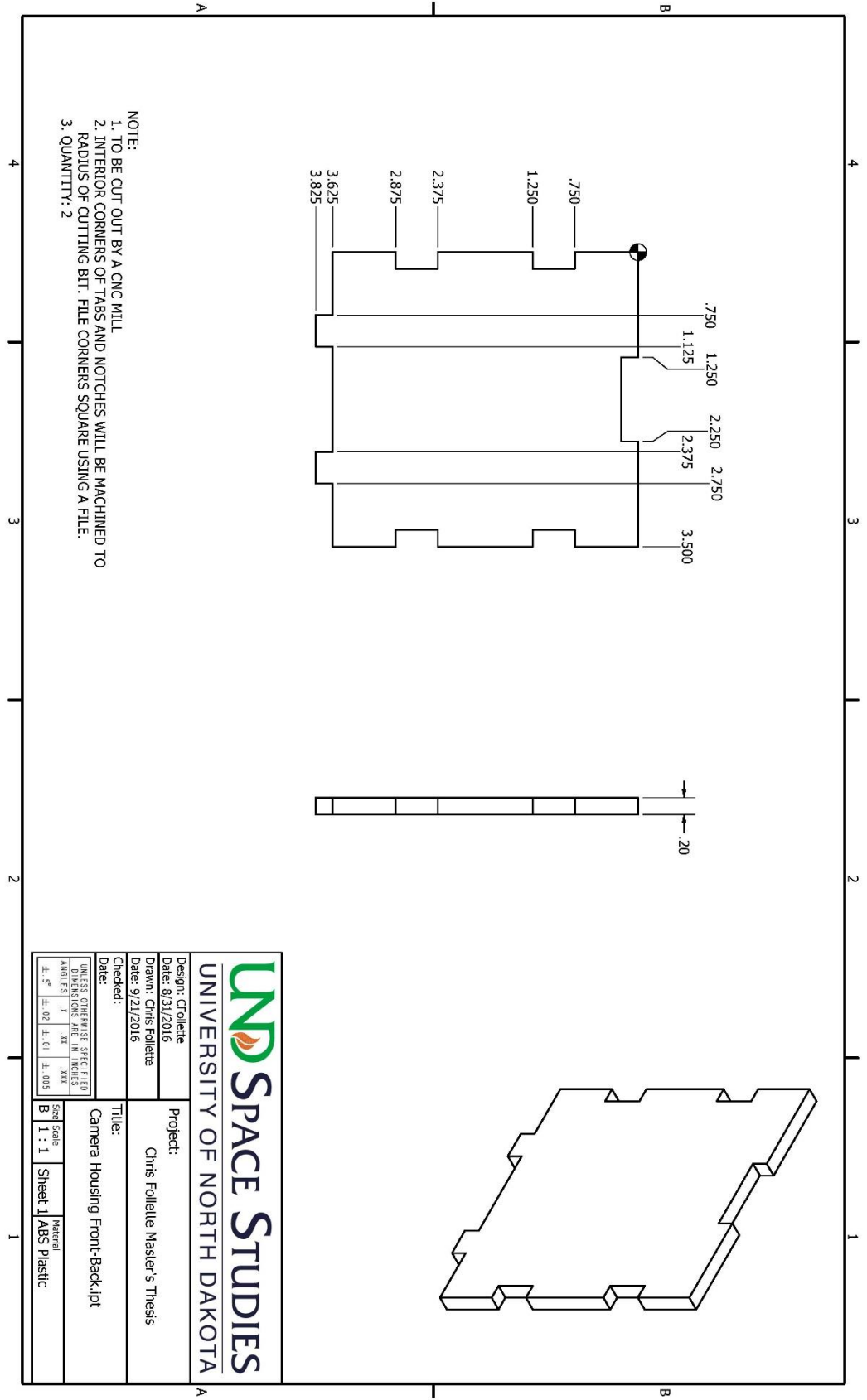
UNDS OF THE ENVIRONMENT SPECIFIED TOLERANCES ARE IN INCHES
 ±.5" ±.02 ±.01 ±.005

Sheet Scale: **B** 1 / 2
 Material: **Sheet 1**



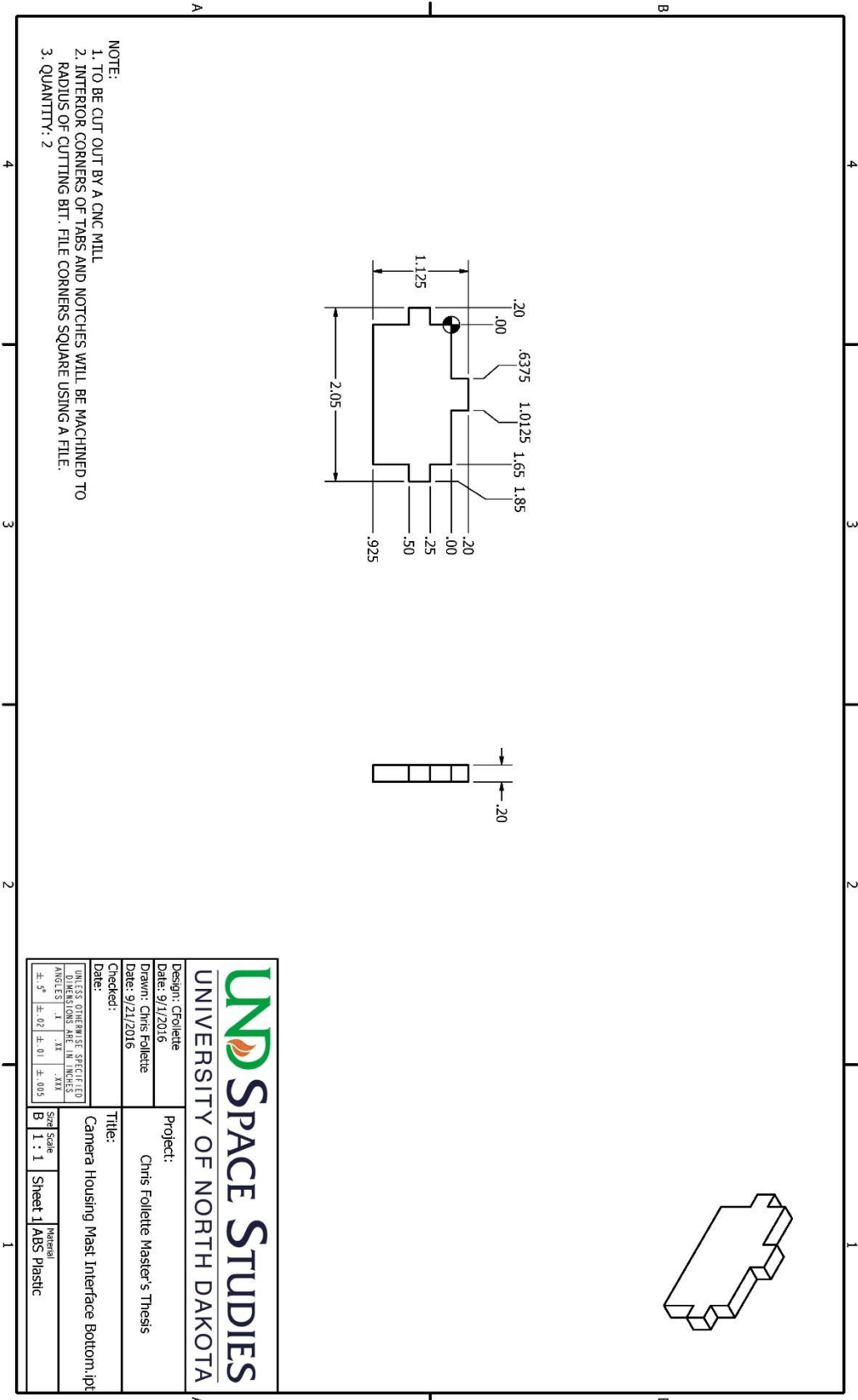
- NOTE:
1. TO BE CUT OUT BY A CNC MILL
 2. INTERIOR CORNERS OF TABS AND NOTCHES WILL BE MACHINED TO RADIUS OF CUTTING BIT. FILE CORNERS SQUARE USING A FILE.
 3. QUANTITY: 1

UNIVERSITY OF NORTH DAKOTA	
Design: Chris Folliette	Project: Chris Folliette Master's Thesis
Date: 9/31/2016	
Drawn: Chris Folliette	
Date: 9/21/2016	
Checked:	Title: Camera Housing Base.ipt
UNLESS OTHERWISE SPECIFIED DIMENSIONS ARE IN INCHES.	
ANGLES	±.5° ±.02 ±.01 ±.003
Size Scale	Material
B 1 : 1	Sheet 1 ABS Plastic



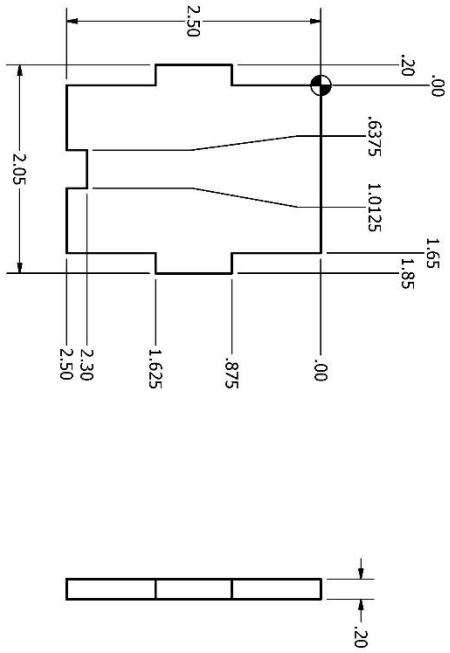
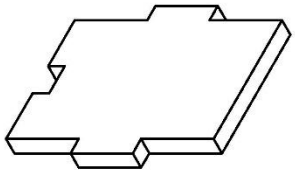
- NOTE:
1. TO BE CUT OUT BY A CNC MILL
 2. INTERIOR CORNERS OF TABS AND NOTCHES WILL BE MACHINED TO RADIUS OF CUTTING BIT. FILE CORNERS SQUARE USING A FILE.
 3. QUANTITY: 2

		Design: CFollette	Project:
		Date: 8/31/2016	
Drawn: Chris Follette		Date: 9/21/2016	Title:
Date:		Checked:	
<small>UNLESS OTHERWISE SPECIFIED DIMENSIONS ARE IN INCHES.</small> <small>TOLERANCES:</small> X ±.01 Y ±.01 Z ±.005		Size Scale	Material
B		1 : 1	Sheet 1 ABS Plastic



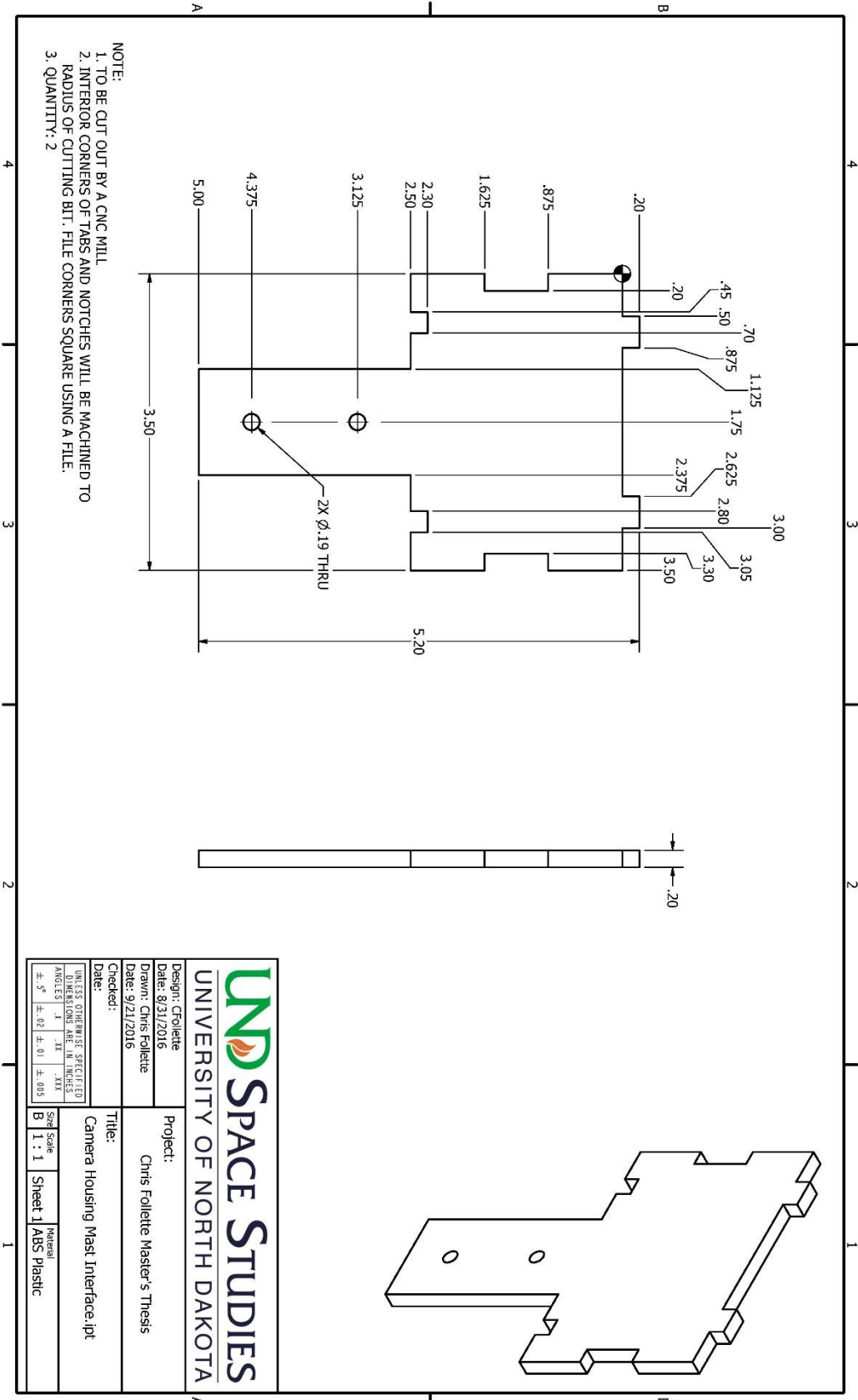
- NOTE:
1. TO BE CUT OUT BY A CNC MILL
 2. INTERIOR CORNERS OF TABS AND NOTCHES WILL BE MACHINED TO RADIUS OF CUTTING BIT. FILE CORNERS SQUARE USING A FILE.
 3. QUANTITY: 2

Design: CFollette Date: 9/1/2016 Drawn: Chris Follette Date: 9/21/2016 Checked:	Project: Chris Follette Master's Thesis
Title: Camera Housing Mast Interface Bottom.ipt	
UNLESS OTHERWISE SPECIFIED DIMENSIONS ARE IN INCHES ANGLES IN DEGREES ±.5° ±.02 ±.01 ±.003	Size Scale B 1 : 1 Sheet 1 Material ABS Plastic



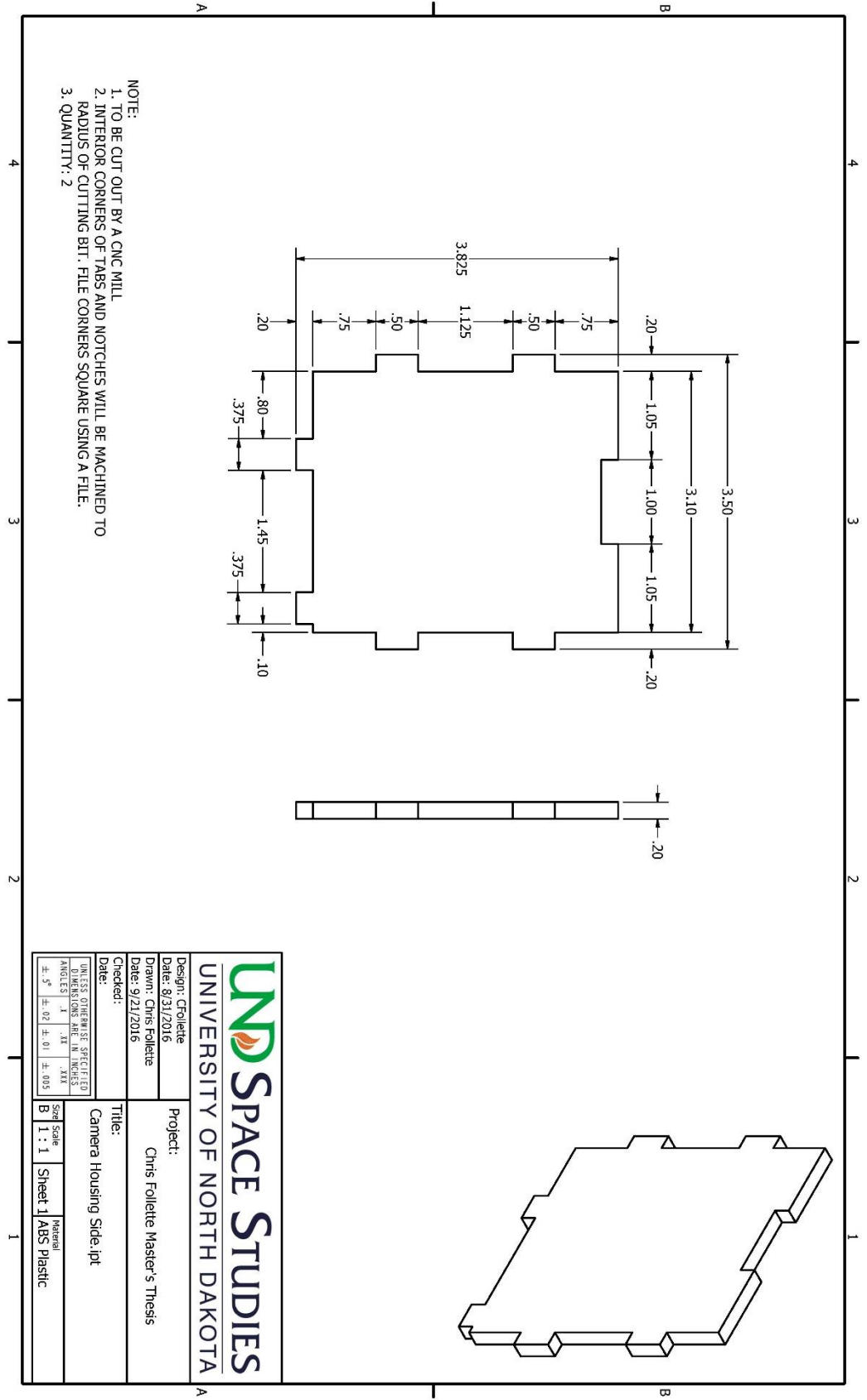
- NOTE:
1. TO BE CUT OUT BY A CNC MILL
 2. INTERIOR CORNERS OF TABS AND NOTCHES WILL BE MACHINED TO RADIUS OF CUTTING BIT. FILE CORNERS SQUARE USING A FILE.
 3. QUANTITY: 2

		Project:	
		Chris Folllette Master's Thesis	
Title:		Camera Housing Mast Interface Side.ipt	
Checked:		Size Scale	Material
Date: 9/21/2016		B 1 : 1	Sheet 1 ABS Plastic
DESIGNER: Chris Folllette DATE: 9/21/2016 DRAWN: Chris Folllette CHECKED: Chris Folllette TITLE: Camera Housing Mast Interface Side.ipt MATERIAL: ABS Plastic QUANTITY: 2		UNLESS OTHERWISE SPECIFIED DIMENSIONS ARE IN INCHES ANGLES IN DEGREES FINISHES: X .10 .40 .40 TOLERANCES: ±.02 ±.01 ±.003	



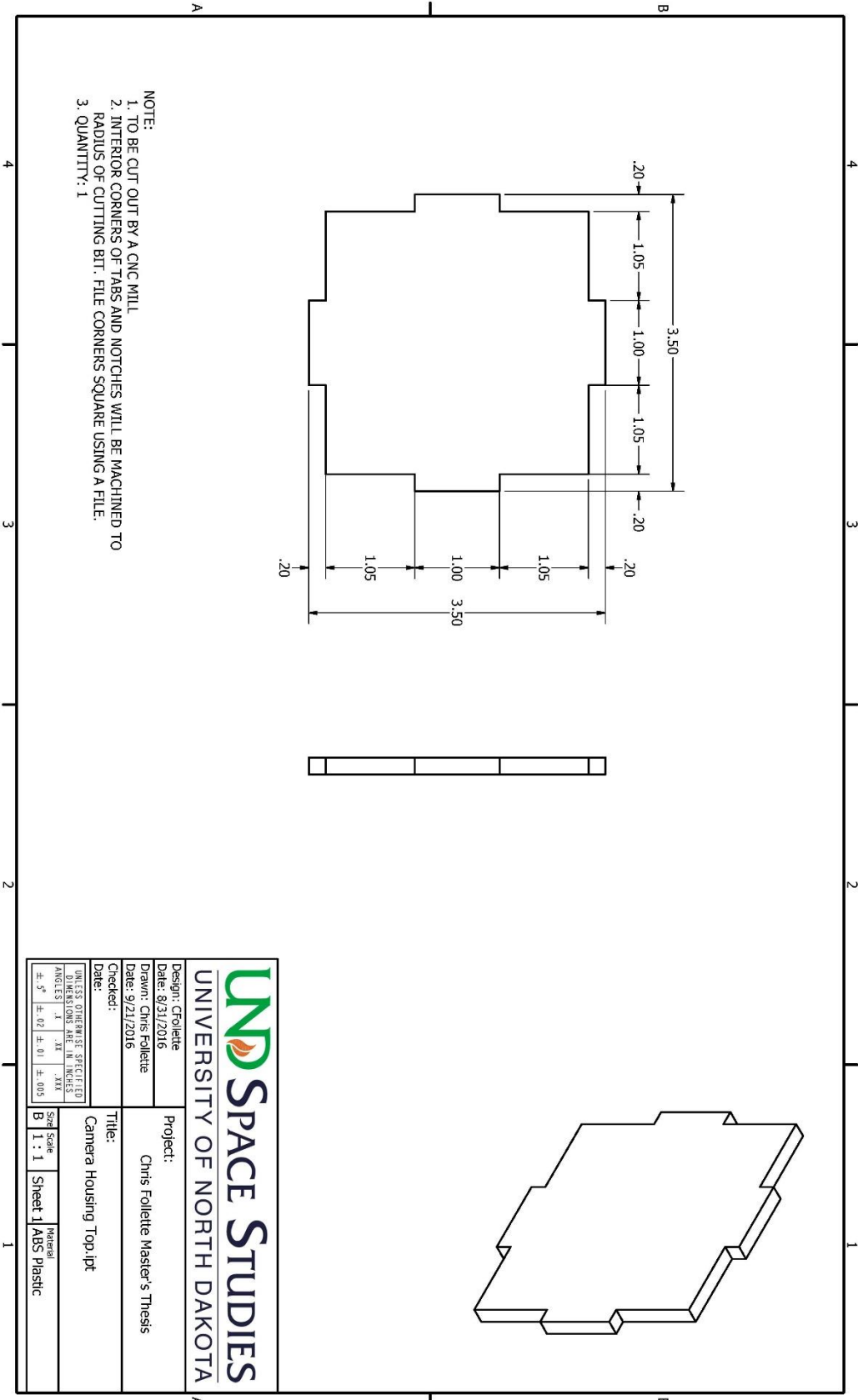
NOTE:
 1. TO BE CUT OUT BY A CNC MILL
 2. INTERIOR CORNERS OF TABS AND NOTCHES WILL BE MACHINED TO RADIUS OF CUTTING BIT. FILE CORNERS SQUARE USING A FILE.
 3. QUANTITY: 2

		Design: Cfollette	Project:
		Date: 8/31/2016	
Drawn: Chris Folllette		Date: 9/21/2016	Title:
Checked:			
<small>UNLESS OTHERWISE SPECIFIED DIMENSIONS ARE IN INCHES</small> <small>ANGLES ° ' " ±.01 ±.01 ±.003</small>		Size Scale	Material
		B 1 : 1	Sheet 1 ABS Plastic



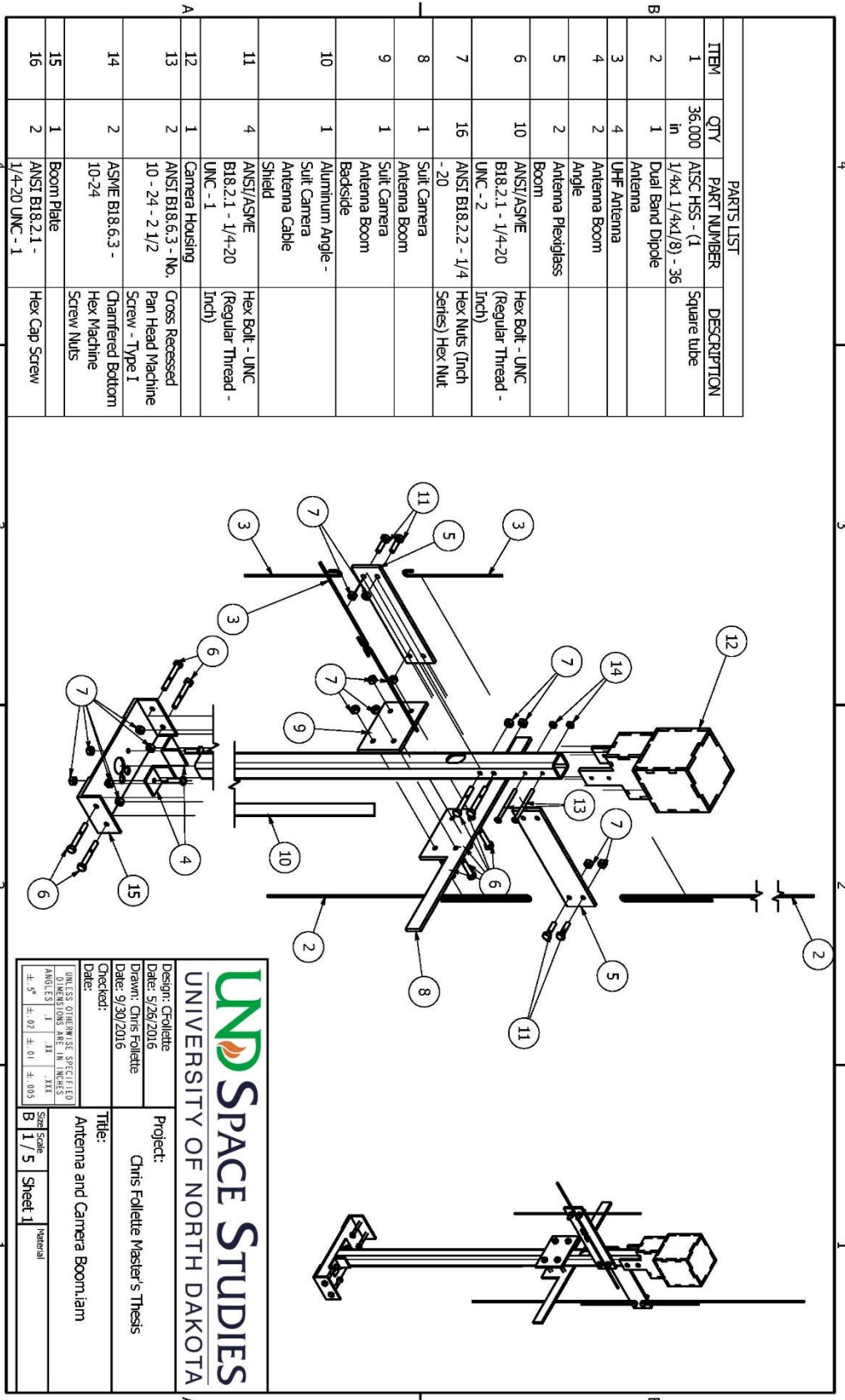
- NOTE:
1. TO BE CUT OUT BY A CNC MILL
 2. INTERIOR CORNERS OF TABS AND NOTCHES WILL BE MACHINED TO RADIUS OF CUTTING BIT. FILE CORNERS SQUARE USING A FILE.
 3. QUANTITY: 2

		Design: Cfollette	Project:				
		Date: 8/31/2016		Chris Folllette Master's Thesis			
Drawn: Chris Folllette		Date: 9/21/2016	Title:				
Checked:				Camera Housing Side, ipt			
<small>UNLESS OTHERWISE SPECIFIED DIMENSIONS ARE IN INCHES</small> <small>TOLERANCES</small>		<small>Size</small> <small>Scale</small>	<small>Material</small>				
±.5	±.02	±.01	±.003	B	1 : 1	Sheet 1	ABS Plastic



NOTE:
 1. TO BE CUT OUT BY A CNC MILL
 2. INTERIOR CORNERS OF TABS AND NOTCHES WILL BE MACHINED TO RADIUS OF CUTTING BIT. FILE CORNERS SQUARE USING A FILE.
 3. QUANTITY: 1

Design: Cfollette	Project:
Date: 8/31/2016	Chris Folllette Master's Thesis
Drawn: Chris Folllette	
Date: 9/21/2016	
Checked:	Title:
	Camera Housing Top.ipt
UNLESS OTHERWISE SPECIFIED DIMENSIONS ARE IN INCHES	Size Scale
ANGLES: $\pm .1$ $\pm .15$ $\pm .315$	B 1 : 1
$\pm .5$ $\pm .02$ $\pm .01$ $\pm .003$	Sheet 1 ABS Plastic
	Material

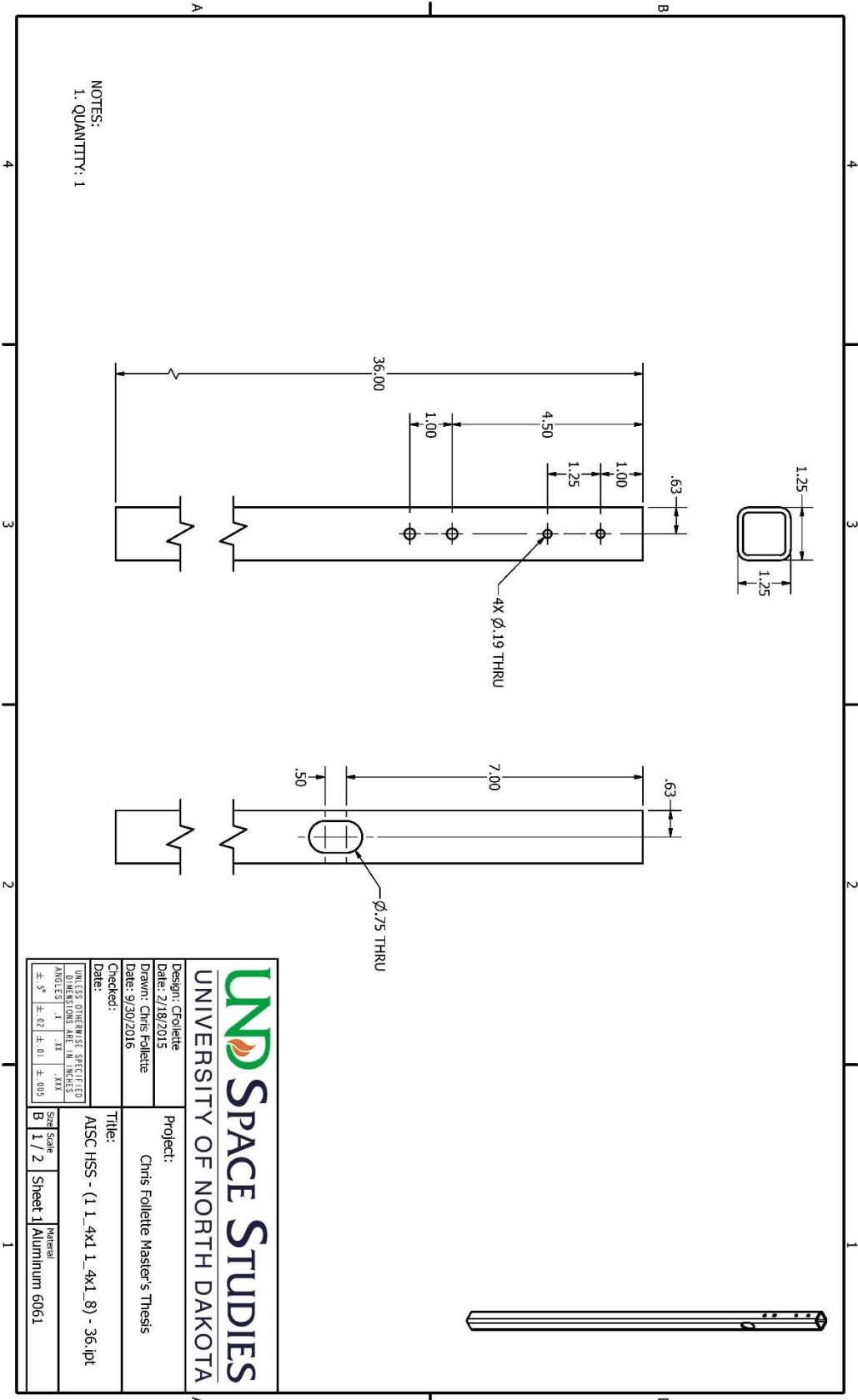


PARTS LIST			
ITEM	QTY	PART NUMBER	DESCRIPTION
1	36,000	ATSC HSS - (1 in 1/4x1 1/4x1/8) - 36	Square tube
2	1	Dual Band Dipole Antenna	
3	4	UHF Antenna	
4	2	Antenna Boom Angle	
5	2	Antenna Plexiglass Boom	
6	10	ANSI/ASME B18.2.1 - 1/4-20 UNC - 2	Hex Bolt - UNC (Regular Thread - Inch)
7	16	ANSI B18.2.2 - 1/4 - 20	Hex Nuts (Inch Series) Hex Nut
8	1	Suit Camera Antenna Boom	
9	1	Suit Camera Antenna Boom Backside	
10	1	Aluminum Angle - Suit Camera Antenna Cable Shield	
11	4	ANSI/ASME B18.2.1 - 1/4-20 UNC - 1	Hex Bolt - UNC (Regular Thread - Inch)
12	1	Camera Housing	
13	2	ANSI B18.6.3 - No. 10 - 24 - 2 1/2	Cross Recessed Pan Head Machine Screw - Type I
14	2	ASME B18.6.3 - 10-24	Charfered Bottom Hex Machine Screw Nuts
15	1	Boom Plate	
16	2	ANSI B18.2.1 - 1/4-20 UNC - 1	Hex Cap Screw

UNIVERSITY OF NORTH DAKOTA

UNSPACE STUDIES

Design: Ffollette	Project: Chris Folllette Master's Thesis
Date: 5/26/2016	
Drawn: Chris Folllette	
Date: 9/30/2016	
Checked:	Title: Antenna and Camera Boom/Iam
Date:	
UNLESS OTHERWISE SPECIFIED, DIMENSIONS ARE IN INCHES	
ANGLES: 1° 3X 3X	Size Scale: B 1/5
±.05 ±.02 ±.01 ±.005	Sheet 1
	Material: Material



NOTES:
1. QUANTITY : 1

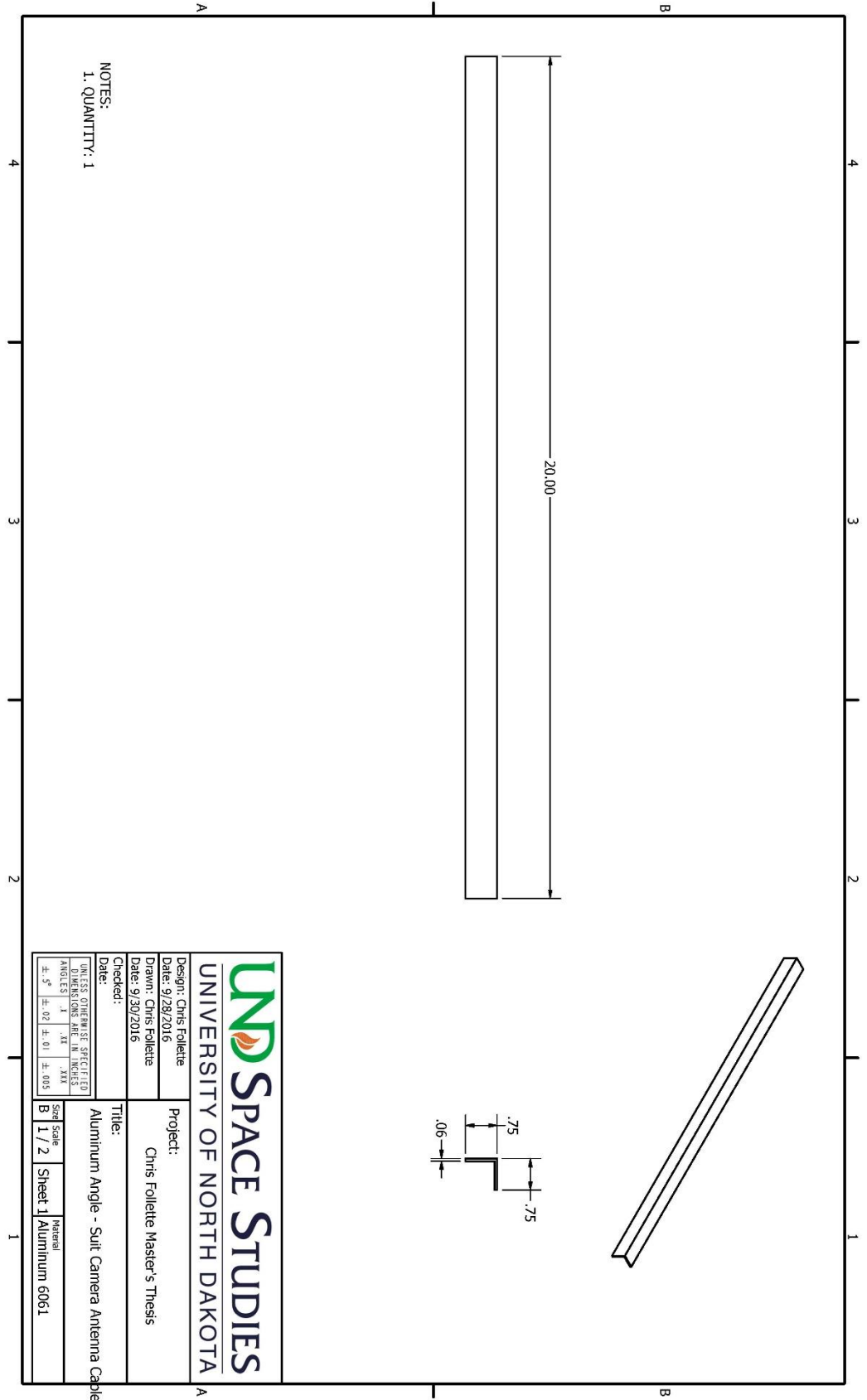
UNIVERSITY OF NORTH DAKOTA
SPACE STUDIES

Design: Cfollette
Date: 2/18/2015
Drawn: Chris Folllette
Date: 9/30/2016
Checked:

Project:
Chris Folllette Master's Thesis

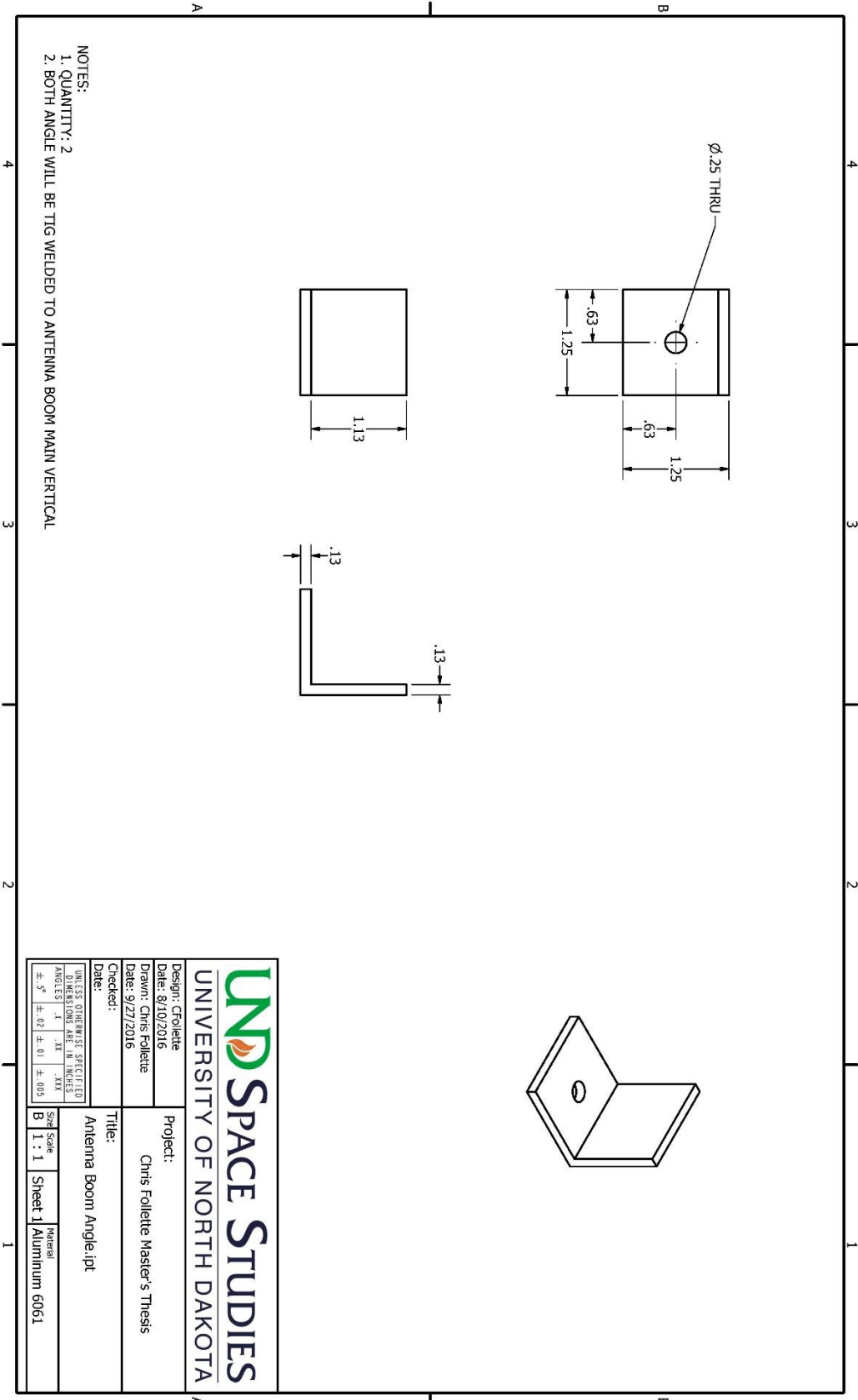
Title:
AISC HSS - (1 1_4x1 1_4x1 8) - 36.1pt

UNLESS OTHERWISE SPECIFIED	Size	Material
TOLERANCES ARE IN INCHES	1 / 2	Aluminum 6061
FRACTIONS	B	
±.5	±.02	±.01
±.005		



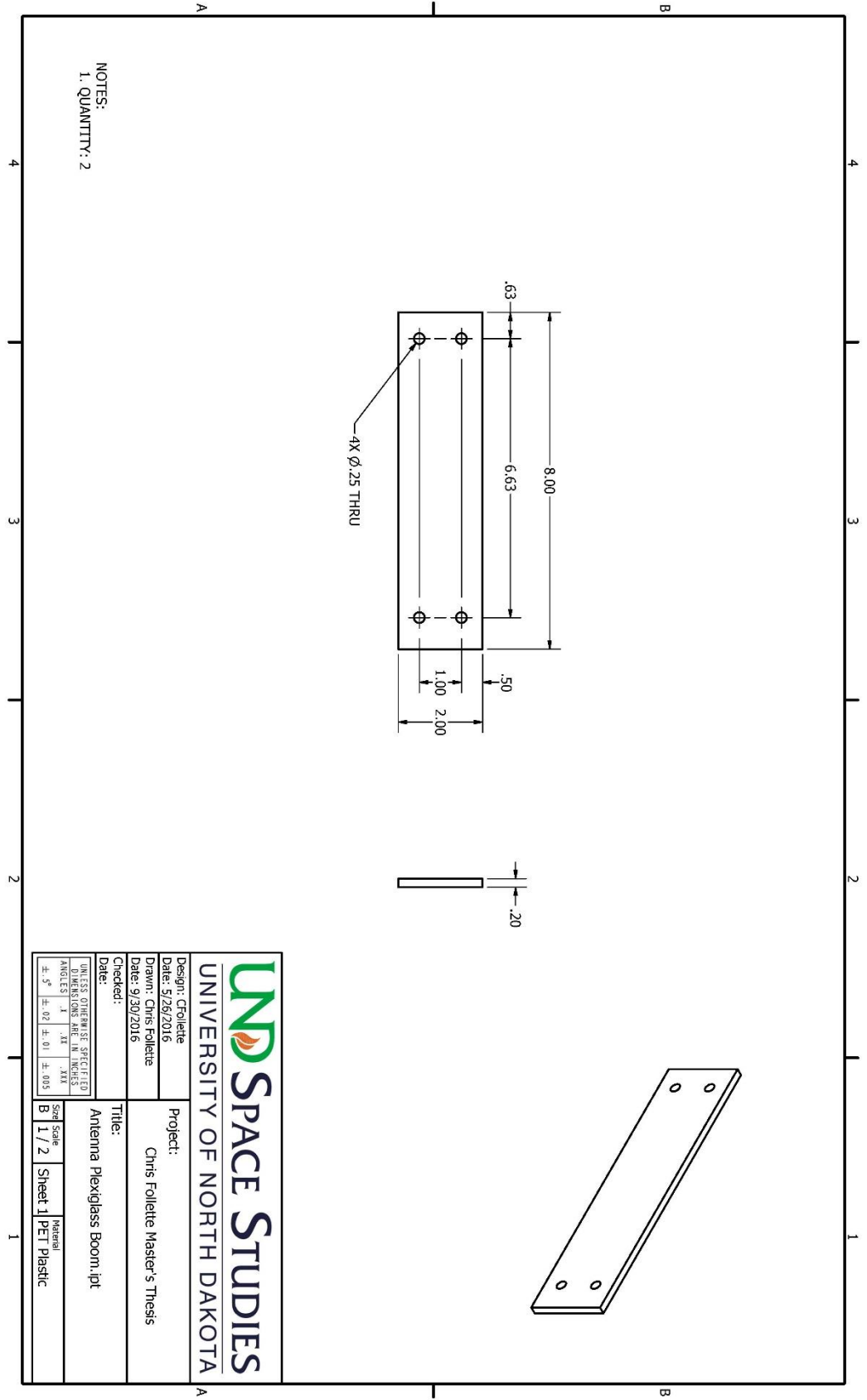
NOTES:
1. QUANTITY: 1

		Design: Chris Folllette	Project: Chris Folllette Master's Thesis
		Date: 9/28/2016	
Checked:		Date: 9/30/2016	Title: Aluminum Angle - Suit Camera Antenna Cable SI
UNLESS OTHERWISE SPECIFIED DIMENSIONS ARE IN INCHES		Size Scale	Material
ANGLES	±.01	B 1 / 2	Sheet 1 Aluminum 6061
±.5	±.02	±.01	±.003



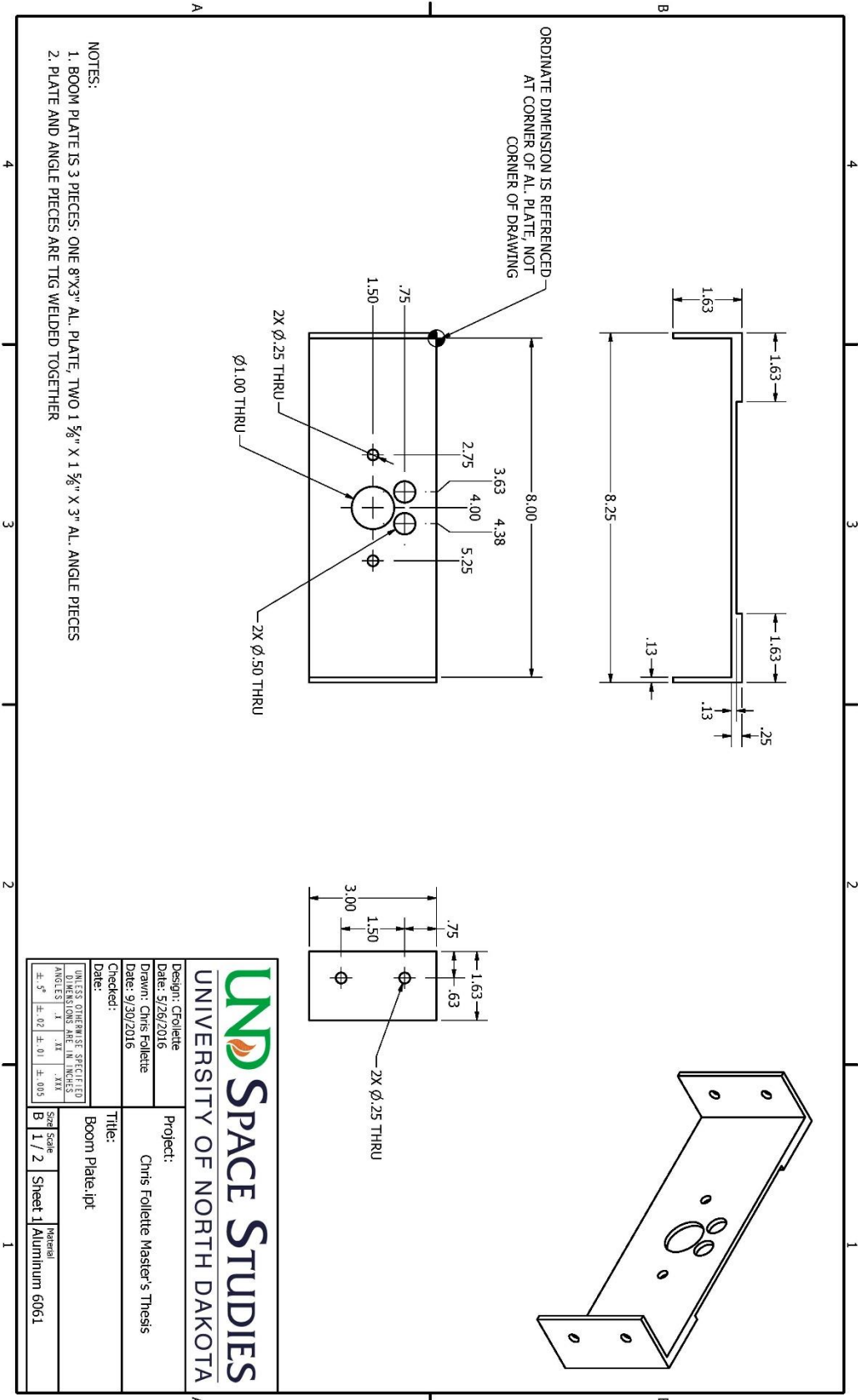
NOTES:
 1. QUANTITY: 2
 2. BOTH ANGLE WILL BE TIG WELDED TO ANTENNA BOOM MAIN VERTICAL

Design: CFollette	Project:
Date: 8/10/2016	Chris Follette Master's Thesis
Drawn: Chris Follette	
Date: 9/27/2016	
Checked:	Title:
	Antenna Boom Angle.ipt
UNLESS OTHERWISE SPECIFIED DIMENSIONS ARE IN INCHES ANGLES IN DEGREES	Size Scale
±.5° ±.02 ±.01 ±.003	B 1 : 1
	Sheet 1
	Material
	Aluminum 6061

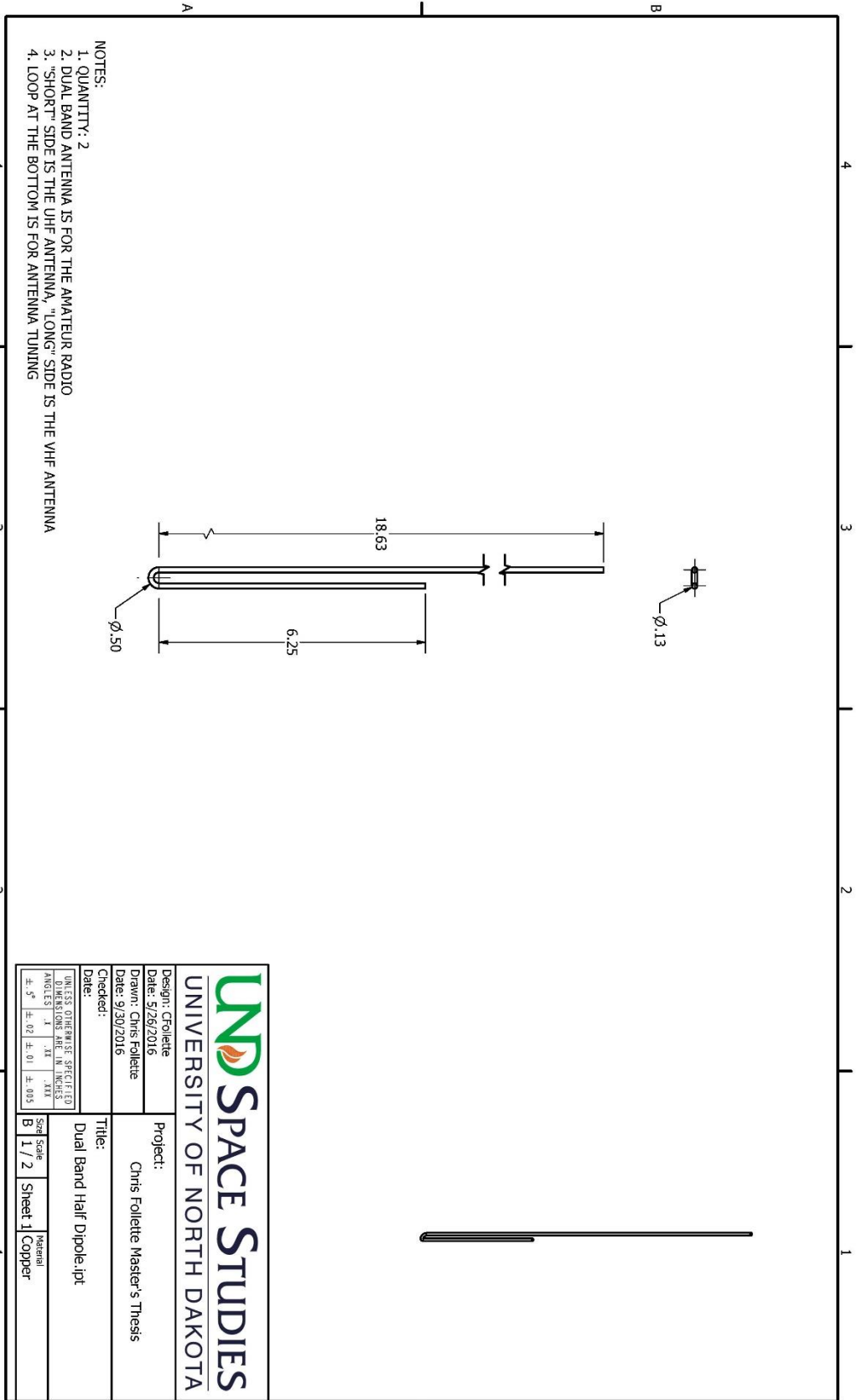


NOTES:
1. QUANTITY: 2

		Project:	
		Chris Folllette Master's Thesis	
Design: CFolllette		Title:	
Date: 5/26/2016		Antenna Plexiglass Boom.ipt	
Drawn: Chris Folllette		Material:	
Date: 9/30/2016		PET Plastic	
Checked:		Size Scale:	
UNLESS OTHERWISE SPECIFIED DIMENSIONS ARE IN INCHES		B 1 / 2	
±.5	±.02	±.01	±.003

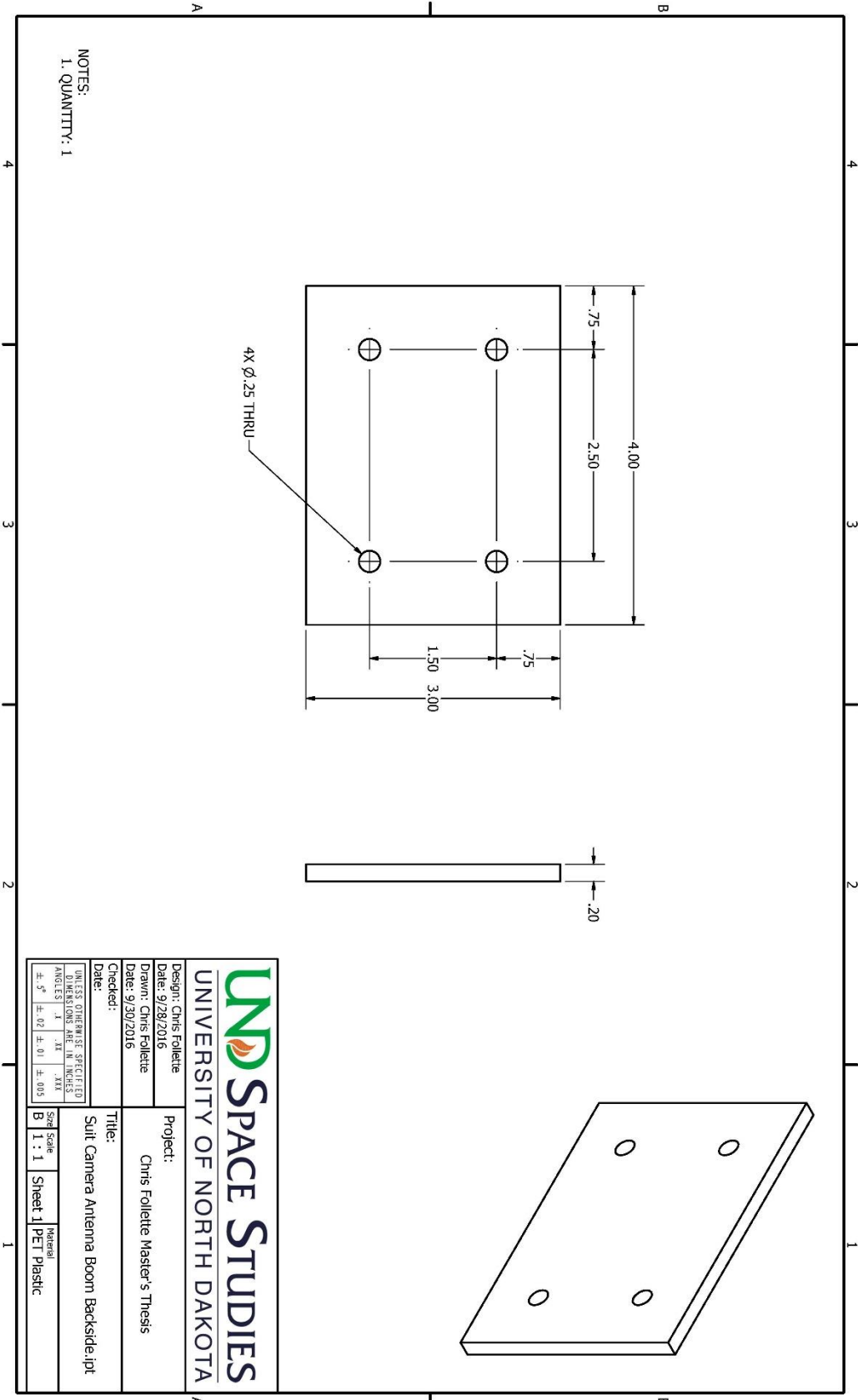


- NOTES:
1. BOOM PLATE IS 3 PIECES: ONE 8"X3" AL. PLATE, TWO 1 5/8" X 1 5/8" X 3" AL. ANGLE PIECES
 2. PLATE AND ANGLE PIECES ARE TIG WELDED TOGETHER



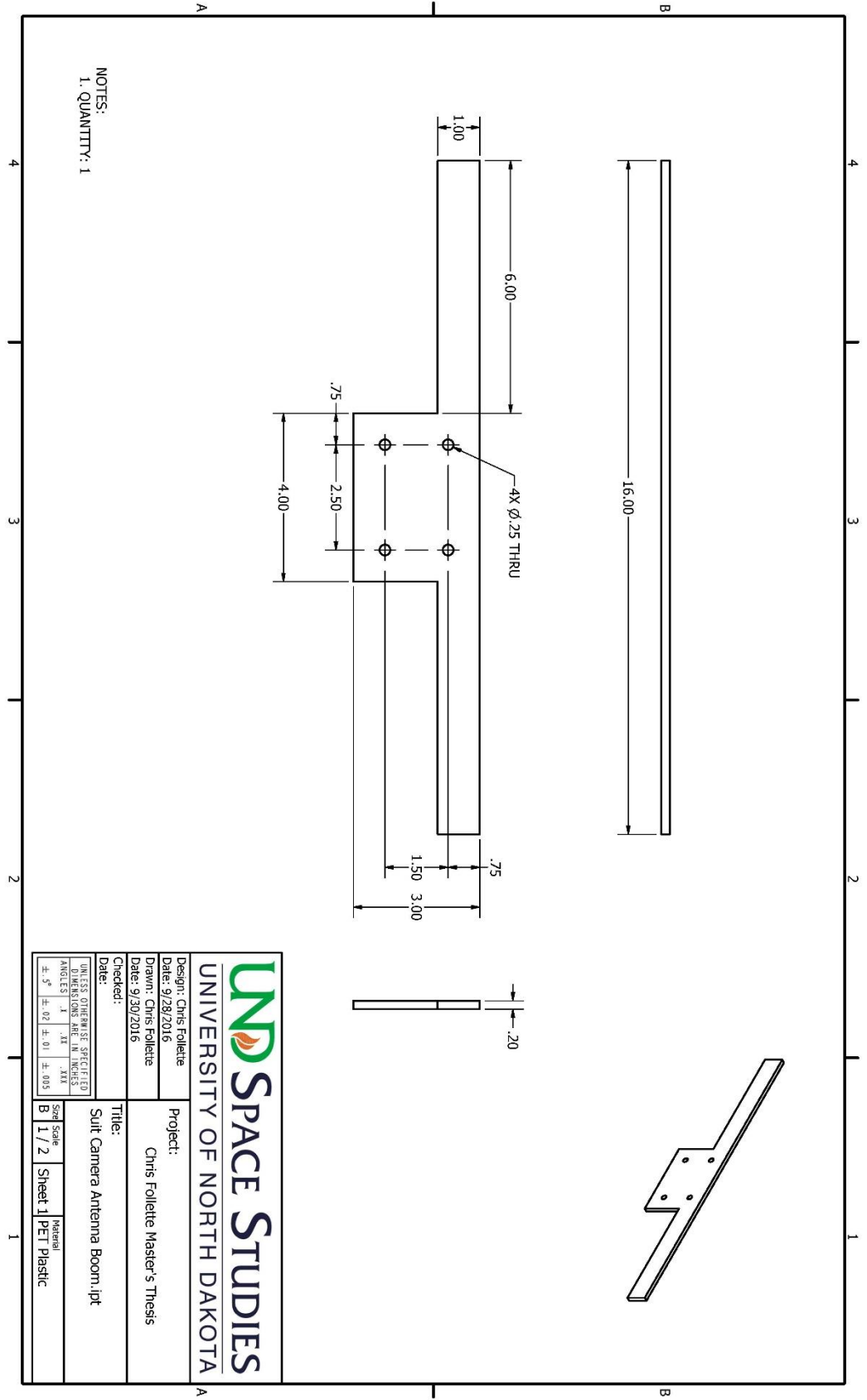
- NOTES:
1. QUANTITY: 2
 2. DUAL BAND ANTENNA IS FOR THE AMATEUR RADIO
 3. "SHORT" SIDE IS THE UHF ANTENNA, "LONG" SIDE IS THE VHF ANTENNA
 4. LOOP AT THE BOTTOM IS FOR ANTENNA TUNING

		Design: CFollette Date: 5/26/2016	
		Drawn: Chris Follette Date: 9/30/2016	
Checked:		Title: Dual Band Half Dipole.jpt	
<small>UNLESS OTHERWISE SPECIFIED DIMENSIONS ARE IN INCHES ANGLES IN DEGREES</small>		Size B	Material Copper
$\pm .5$	$\pm .02$	Scale 1 / 2	Sheet 1



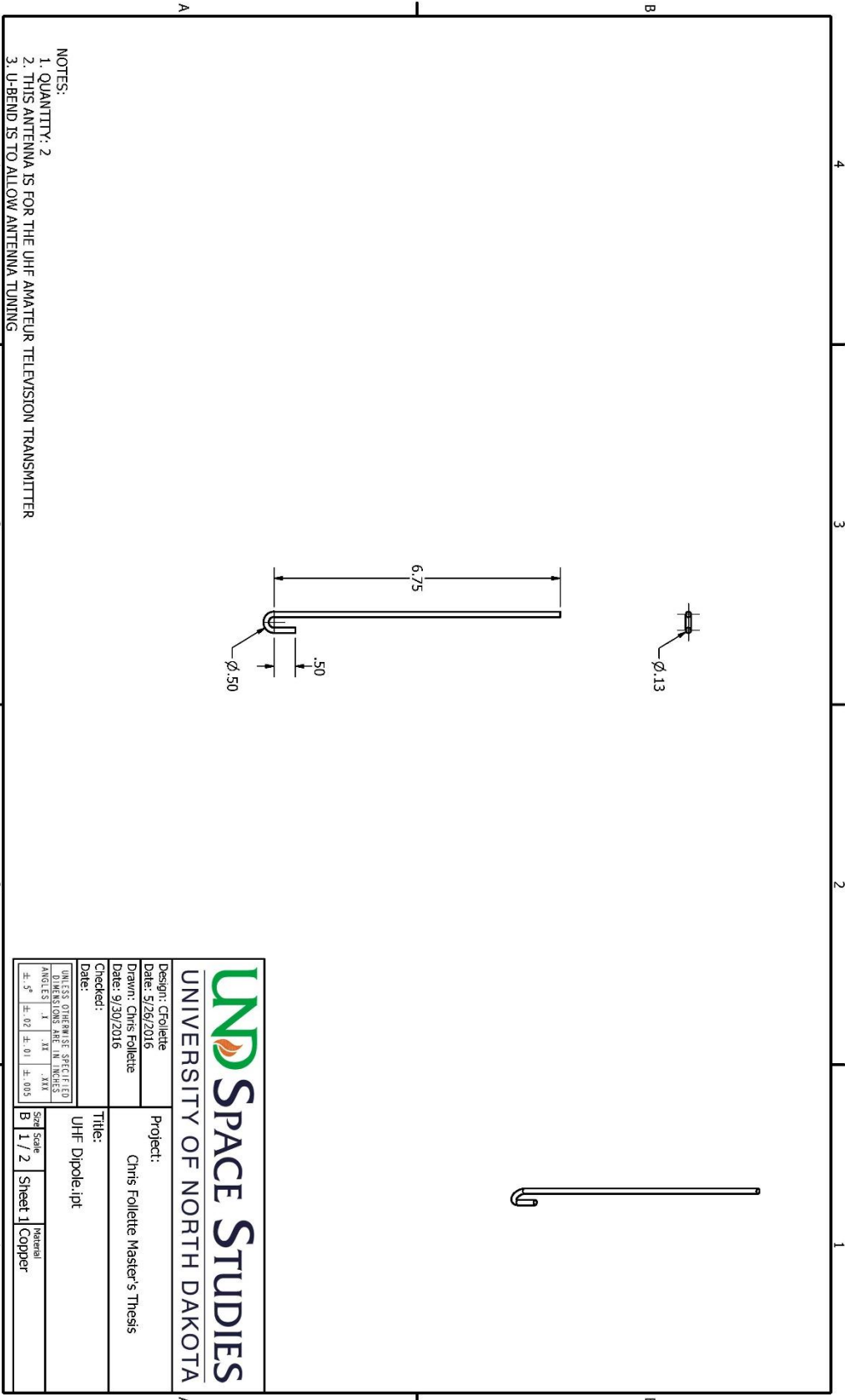
NOTES:
1. QUANTITY: 1

		Project:	
		Chris Folllette Master's Thesis	
Designer: Chris Folllette		Date: 9/28/2016	
Drawn: Chris Folllette		Date: 9/30/2016	
Checked:			
Title:		Suit: Camera Antenna Boom Backside.ipt	
UNLESS OTHERWISE SPECIFIED DIMENSIONS ARE IN INCHES		Size Scale	
ANGLES	±.1	±.1	±.01
±.5	±.02	±.01	±.003
B	1 : 1	Sheet 1	PET Plastic



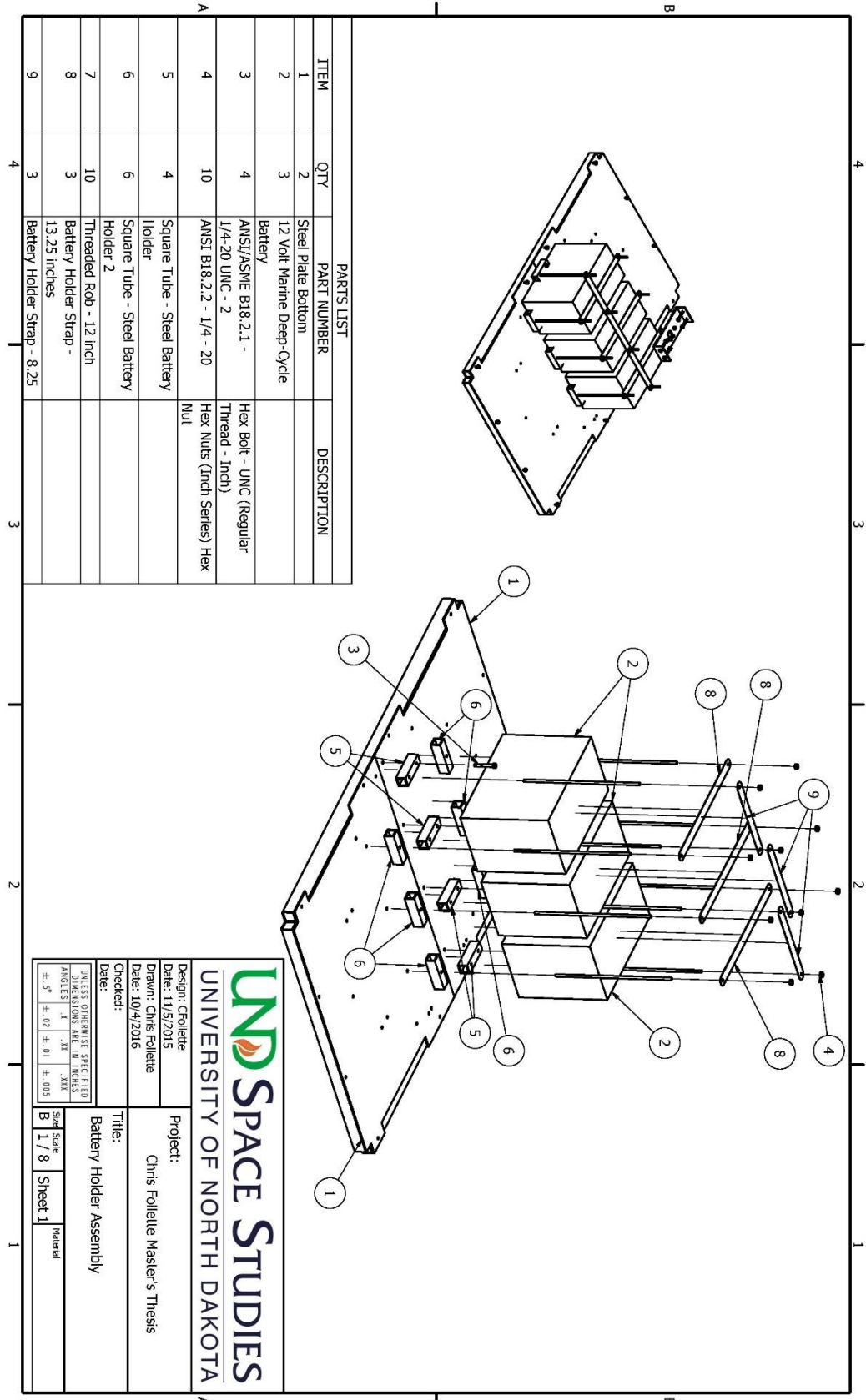
NOTES:
1. QUANTITY: 1

		Design: Chris Folllette Date: 9/28/2016	
		Drawn: Chris Folllette Date: 9/30/2016	
Checked:		Title: Suit Camera Antenna Boom.lpt	
<small>UNLESS OTHERWISE SPECIFIED DIMENSIONS ARE IN INCHES</small>		Size	Material
<small>TOLERANCES</small>	<small>FRACTIONS</small>	B	1 PET Plastic
<small>±.5</small>	<small>±.02</small>	1 / 2	Sheet 1



- NOTES:
1. QUANTITY: 2
 2. THIS ANTENNA IS FOR THE UHF AMATEUR TELEVISION TRANSMITTER
 3. U-BEND IS TO ALLOW ANTENNA TUNING

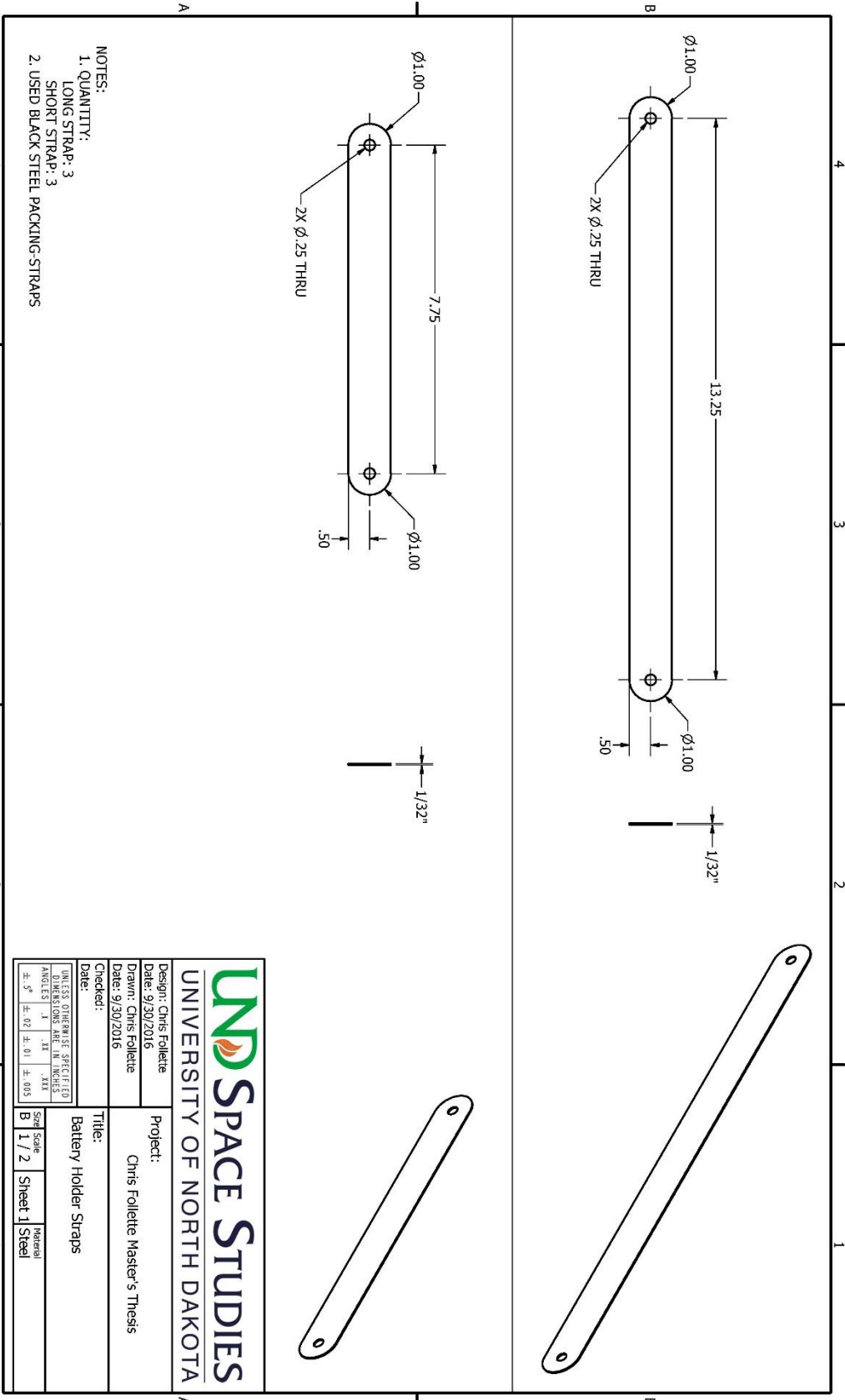
		Design: cFollette	Project:						
		Date: 5/26/2016		Chris Follette Master's Thesis					
Drawn: Chris Follette		Date: 9/30/2016	Title:						
Checked:		UHF Dipole.ipt							
<small>UNLESS OTHERWISE SPECIFIED DIMENSIONS ARE IN INCHES</small>		<table border="1"> <tr> <td>Size</td> <td>Scale</td> <td>Material</td> </tr> <tr> <td>B</td> <td>1 / 2</td> <td>Sheet 1 Copper</td> </tr> </table>	Size	Scale	Material	B	1 / 2	Sheet 1 Copper	
Size	Scale	Material							
B	1 / 2	Sheet 1 Copper							
<small>TOLERANCES UNLESS OTHERWISE SPECIFIED</small>									
ANGLES	± .1°	± .01	± .003						
± .5°	± .02	± .01	± .003						



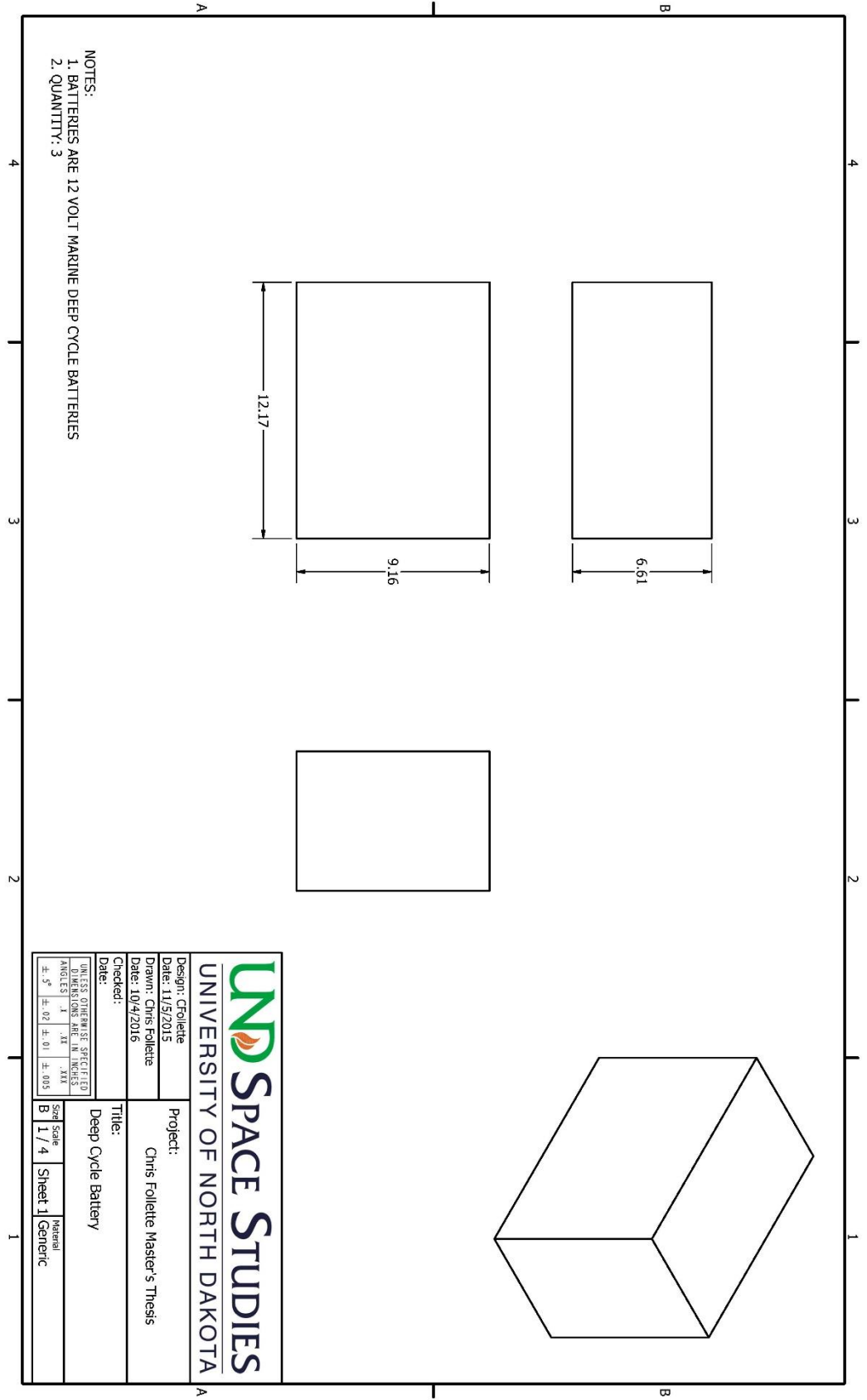
ITEM	QTY	PART NUMBER	DESCRIPTION
1	2	Steel Plate Bottom	
2	3	12 Volt Marine Deep-Cycle Battery	
3	4	ANSI/ASME B18.2.1 - 1/4-20 UNC - 2	Hex Bolt - UNC (Regular Thread - Inch)
4	10	ANSI B18.2.2 - 1/4 - 20	Hex Nuts (Inch Series) Hex Nut
5	4	Square Tube - Steel Battery Holder	
6	6	Square Tube - Steel Battery Holder 2	
7	10	Threaded Rob - 12 inch Battery Holder Strap -	
8	3	13.25 inches Battery Holder Strap -	
9	3	8.25 Battery Holder Strap -	

UNSPACE STUDIES
UNIVERSITY OF NORTH DAKOTA


<p>Design: Cfollette Date: 11/5/2015 Drawn: Chris Folllette Date: 10/4/2016 Checked:</p>	<p>Project: Chris Folllette Master's Thesis</p>
<p>Title: Battery Holder Assembly</p>	
<p>UNLESS OTHERWISE SPECIFIED DIMENSIONS ARE IN INCHES ANGLES ° ±.02 ±.01 ±.003</p>	<p>Size Scale B 1 / 8 Sheet 1 Material</p>

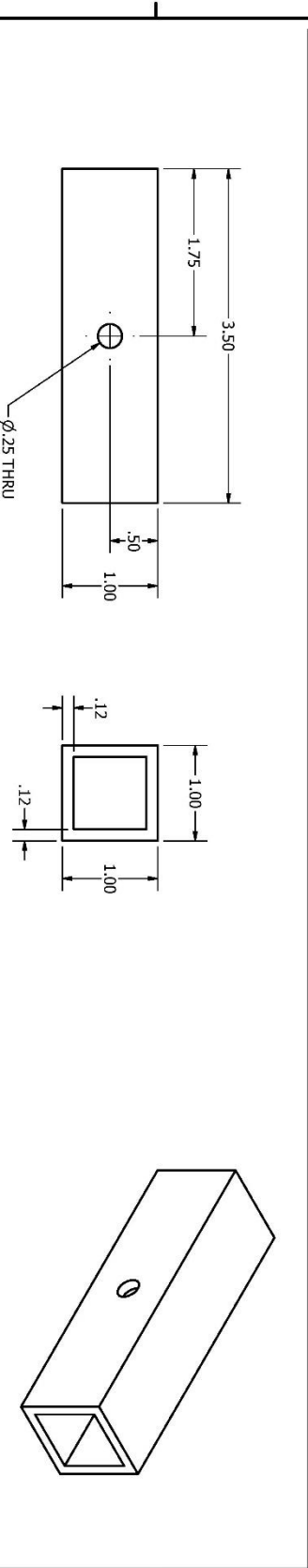
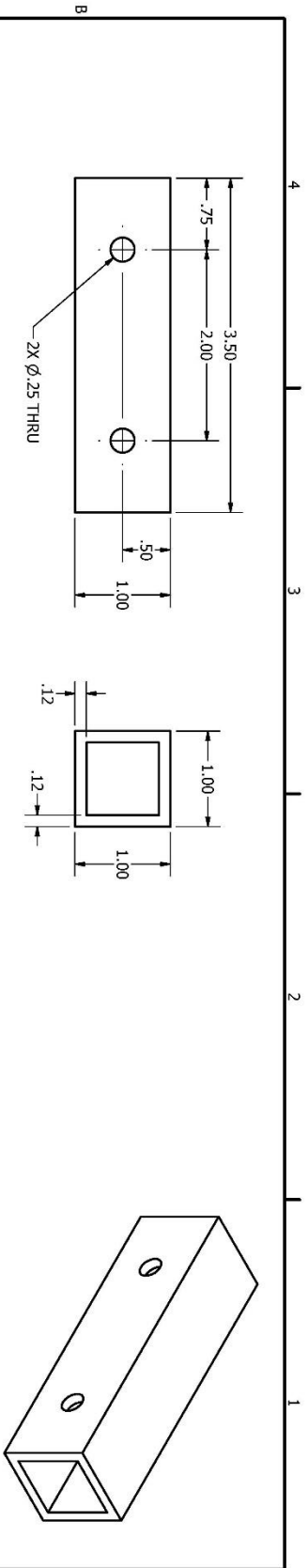


		Design: Chris Follette	Project: Chris Follette Master's Thesis
		Date: 9/30/2016	
Drawn: Chris Follette		Checked:	
Date: 9/30/2016		Title: Battery Holder Straps	
UNLESS OTHERWISE SPECIFIED DIMENSIONS ARE IN INCHES		Size Scale B 1 / 2	Material Sheet 1 Steel
±.5"	±.02	±.01	±.003



NOTES:
 1. BATTERIES ARE 12 VOLT MARINE DEEP CYCLE BATTERIES
 2. QUANTITY: 3

 SPACE STUDIES UNIVERSITY OF NORTH DAKOTA		Project: Chris Folllette Master's Thesis	
		Title: Deep Cycle Battery	
Design: Cfollette Date: 11/5/2015		Drawn: Chris Folllette Date: 10/4/2016	
Checked:		Date:	
UNLESS OTHERWISE SPECIFIED DIMENSIONS ARE IN INCHES		Size Scale B 1 / 4	Material Sheet 1 Generic
TOLERANCES	.125 ±.01 .125 ±.01 .125 ±.01	.125 ±.01 .125 ±.01 .125 ±.01	.125 ±.01 .125 ±.01 .125 ±.01



UNIVERSITY OF NORTH DAKOTA

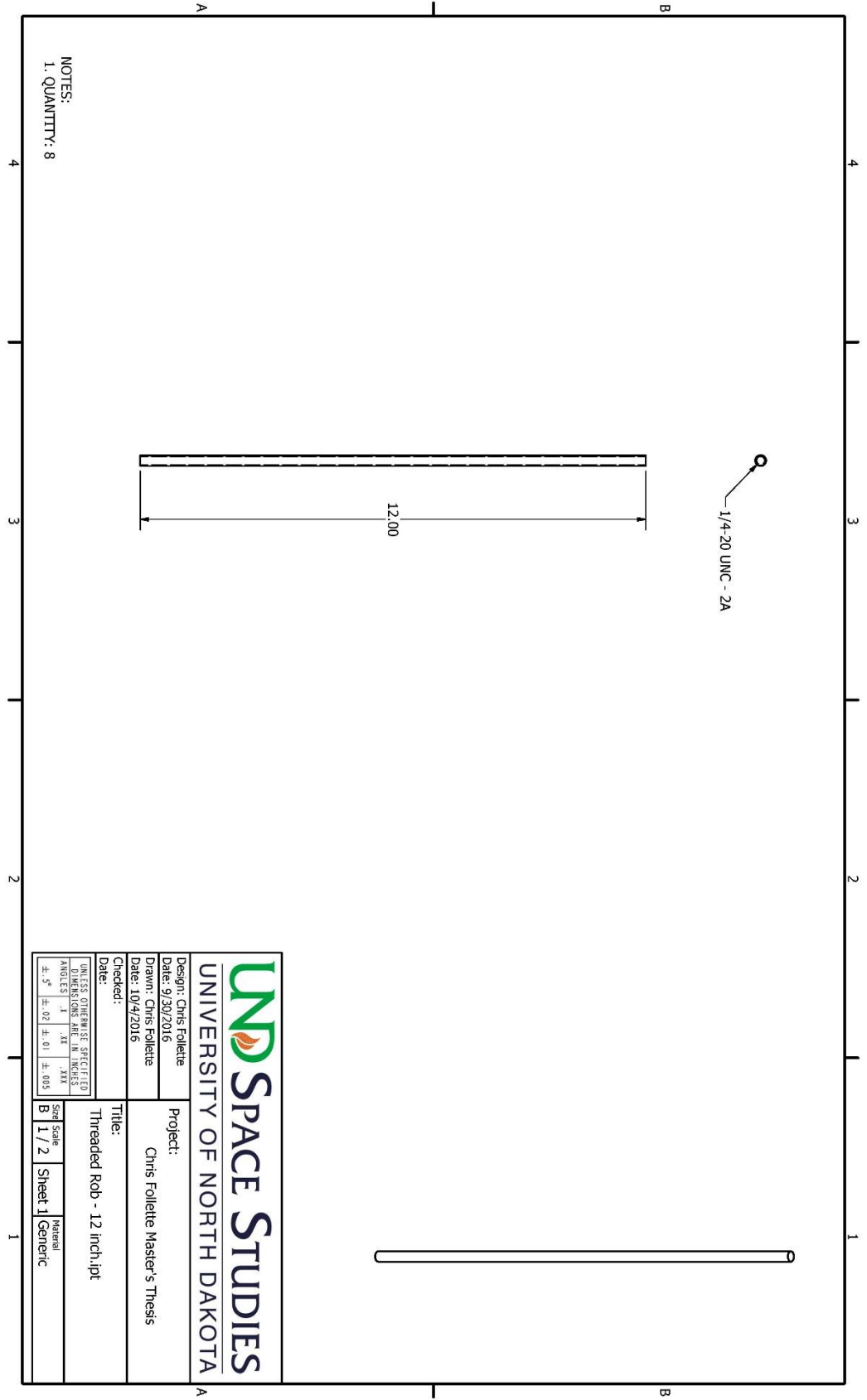
SPACE STUDIES

Project: Chris Folllette Master's Thesis

Title: Square Tube Battery Holders

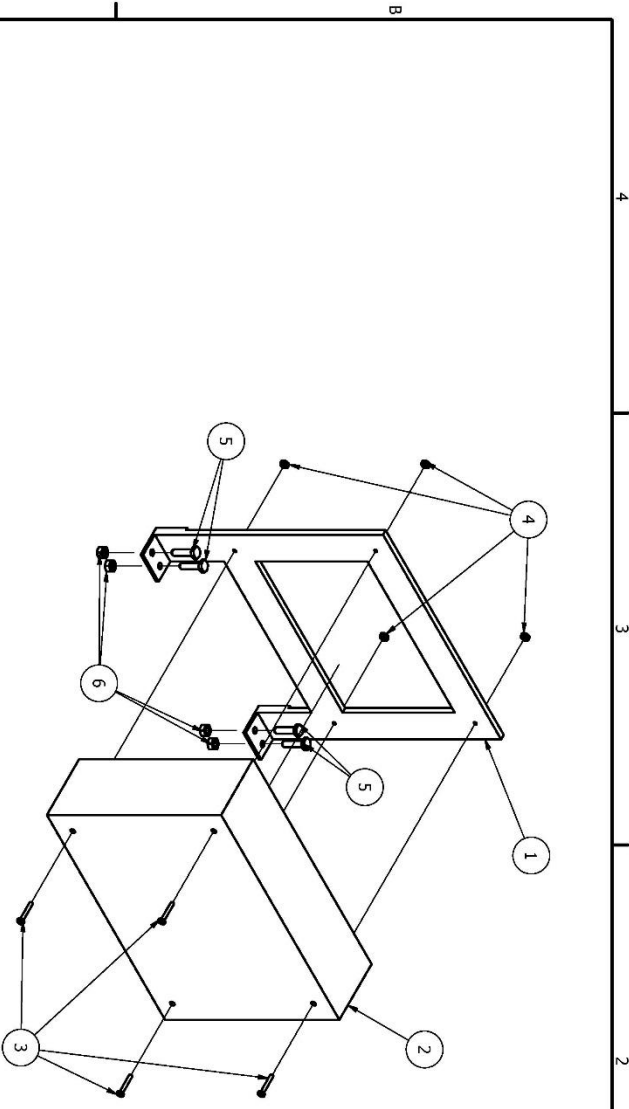
Designer: Chris Folllette Date: 9/30/2016 Drawn: Chris Folllette Date: 9/30/2016 Checked:	UNLESS OTHERWISE SPECIFIED DIMENSIONS ARE IN INCHES ANGLES IN DEGREES ±.5° ±.02 ±.01 ±.003
Size Scale B 1 : 1	Material Sheet 1 Steel, Carbon

NOTES:
 1. QUANTITY:
 2-HOLE: 4
 1-HOLE: 6



NOTES:
1. QUANTITY: 8

		Design: Chris Follette	
		Date: 9/30/2016	
		Drawn: Chris Follette	
		Date: 10/4/2016	
Checked:		Project: Chris Follette Master's Thesis	
Title: Threaded Rod - 12 inch.lpt		Material: Generic	
UNLESS OTHERWISE SPECIFIED DIMENSIONS ARE IN INCHES		Size Scale	Sheet 1
ANGLES	±.10	B 1 / 2	Generic
±.5	±.02	±.01	±.003



PARTS LIST		
ITEM	QTY	DESCRIPTION
1	1	Battery Charger Mount
2	1	NOCO Genius GEN3
3	4	Cross Recessed Binding Head Machine Screw - 1 Type
4	4	Chamfered Bottom Hex Machine Screw Nuts
5	4	Hex Cap Screw
6	4	Hex Nuts (1/4 Series) Hex Nut

UNSPACE STUDIES
UNIVERSITY OF NORTH DAKOTA

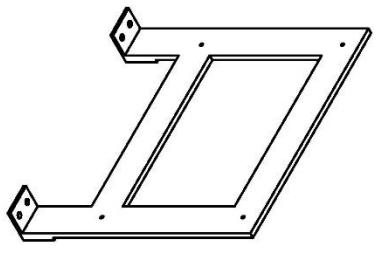
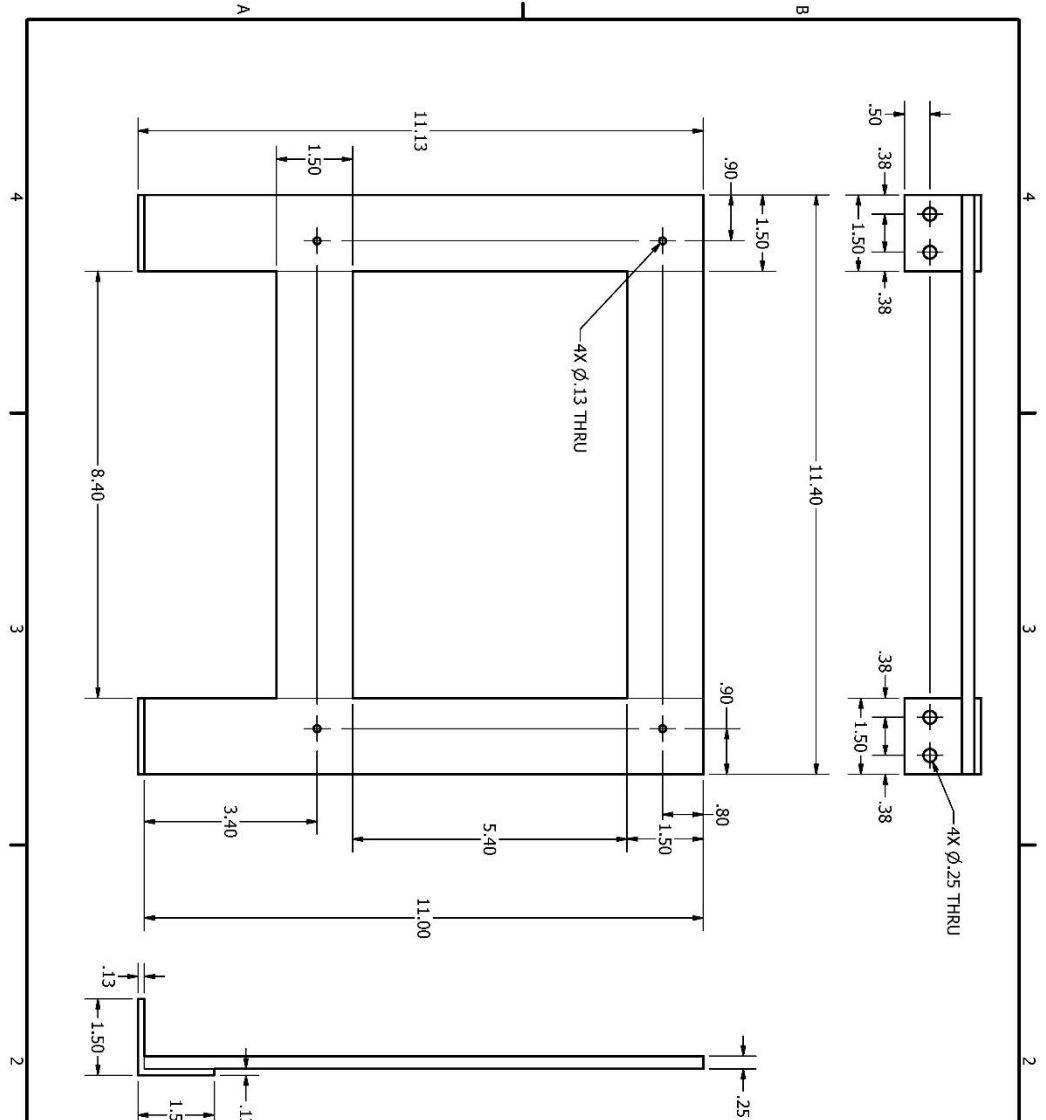
Project: Chris Folliette Master's Thesis

Designer: Chris Folliette
Date: 9/30/2016

Drawer: Chris Folliette
Date: 10/1/2016

Checked:

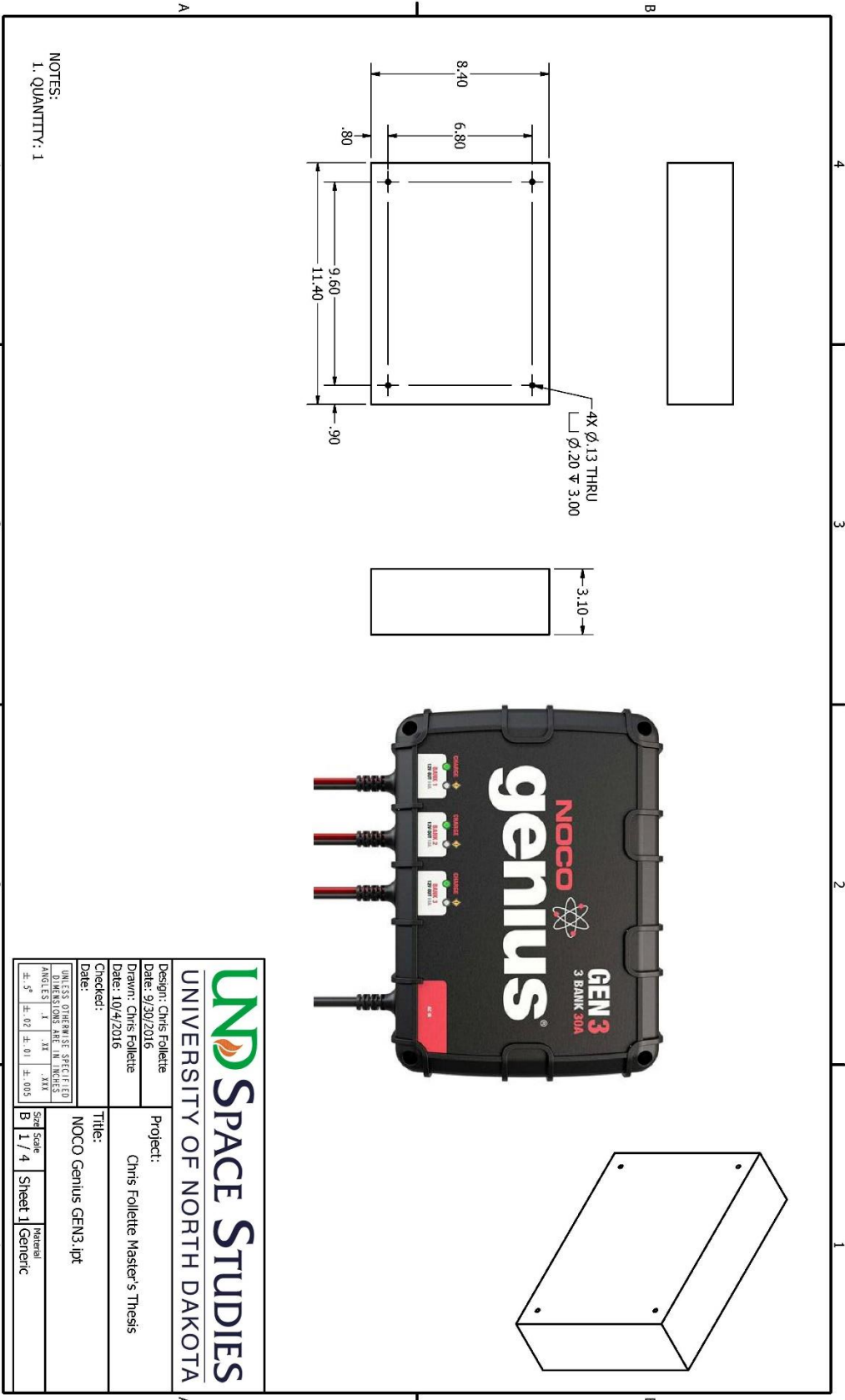
UNLESS OTHERWISE SPECIFIED	
ANGLES	±.5°
FRACTIONS	±.01
DECIMALS	±.005
SIZE	1/4
SHEET	1
TITLE	Battery Charger Assembly



- NOTES:
1. BATTERY CHARGER MOUNT IS MADE UP OF 4 PIECES OF 1.5" WIDTH AL. AND 2 PIECES OF AL. ANGLE.
 2. AL PIECES ARE: (2) 11" X 1.5" X 0.25"
(2) 8.4" X 1.5" X 0.25"
 3. ANGLE PIECES: (2) 1.5" X 1.5" X 0.125"
 4. ALL PIECES ARE TIG WELDED

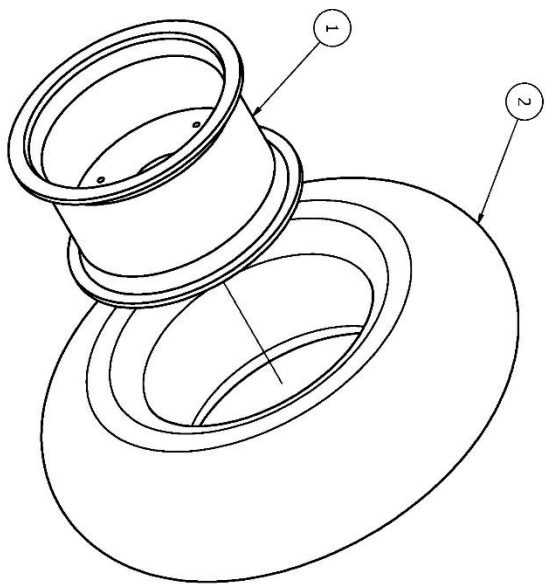
UNIVERSITY OF NORTH DAKOTA
SPACE STUDIES

Designer: Chris Follotte	Project:
Date: 9/30/2016	Chris Follotte Master's Thesis
Drawn: Chris Follotte	
Date: 10/1/2016	
Checked:	Title:
	Battery Charger Mount.ipt
UNIVERSITY OF NORTH DAKOTA SPECIFICATIONS AND TOLERANCES DIMENSIONS ARE IN INCHES ANGLES IN DEGREES	Size Scale
±.5° ±.02 ±.01 ±.003	B 1 / 2
	Sheet 1
	Material
	Aluminum 6061



NOTES:
 I. QUANTITY: 1

Designer: Chris Follette Date: 9/30/2016 Drawn: Chris Follette Date: 10/4/2016 Checked:	Project: Chris Follette Master's Thesis Title: NOCO Genius GEN3.ipt
UNLESS OTHERWISE SPECIFIED DIMENSIONS ARE IN INCHES ANGLES IN DEGREES FINISHES: .125 ±.01 ±.003	Size Scale: B 1/4 Sheet 1 of 1 Material: Generic



PARTS LIST			
ITEM	QTY	PART NUMBER	DESCRIPTION
1	1	Wheel Hub	4/156 Douglas .125 Wheel 10X6 2.0 + 4.0 KTM POLARIS YAMAHA
2	1	ATV Tire	Maxxis M957 Razr Cross ATV Tire 20X6X10

UND SPACE STUDIES
UNIVERSITY OF NORTH DAKOTA

Design: Cfollette
Date: 12/4/2015

Drawn: Chris Folllette
Date: 10/4/2016

Checked:

UNLESS OTHERWISE SPECIFIED
DIMENSIONS ARE IN INCHES
ANGLES IN DEGREES

±.5° ±.02 ±.01 ±.003

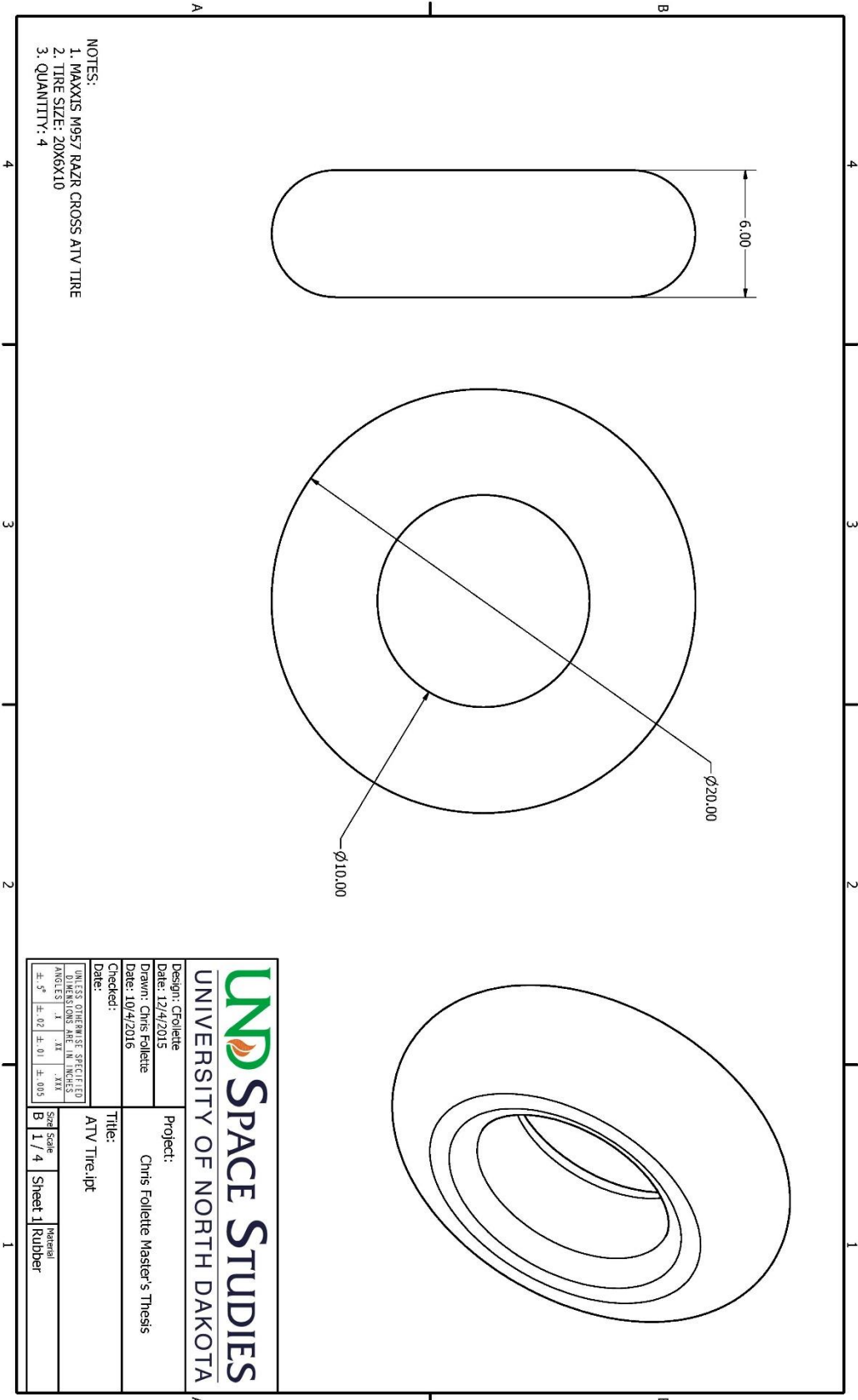
Project: Chris Folllette Master's Thesis

Title: Wheel-Hub Assembly.lam

Size Scale: B 1 / 4

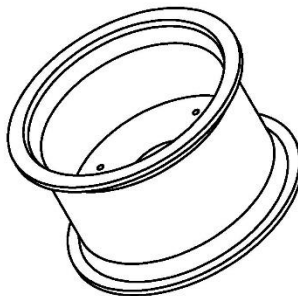
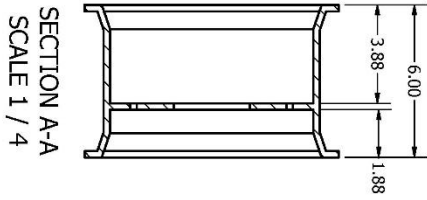
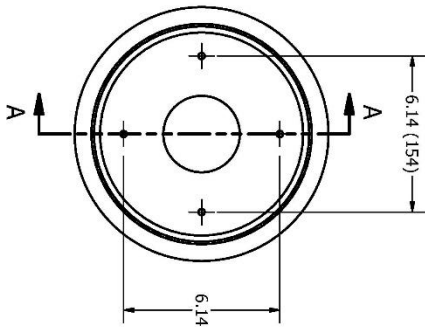
Sheet: 1

Material:



- NOTES:
1. MAXXIS M957 RAZR CROSS ATV TIRE
 2. TIRE SIZE: 20X6X10
 3. QUANTITY: 4

Design: Cfollette	Project:
Date: 12/4/2015	Chris Folllette Master's Thesis
Drawn: Chris Folllette	
Date: 10/4/2016	
Checked:	Title:
	ATV Tire.ipt
UNLESS OTHERWISE SPECIFIED DIMENSIONS ARE IN INCHES	Size Scale
ANGLES: 1/4° .1/8° .3/16°	B 1 / 4
±.5° ±.02 ±.01 ±.003	Sheet 1
	Material
	Rubber



- NOTES:
 1. 4/156 Douglar .125 Wheel 10X6 2.0 + 4.0 KTM POLARIS YAMAHA
 2. QUANTITY: 4

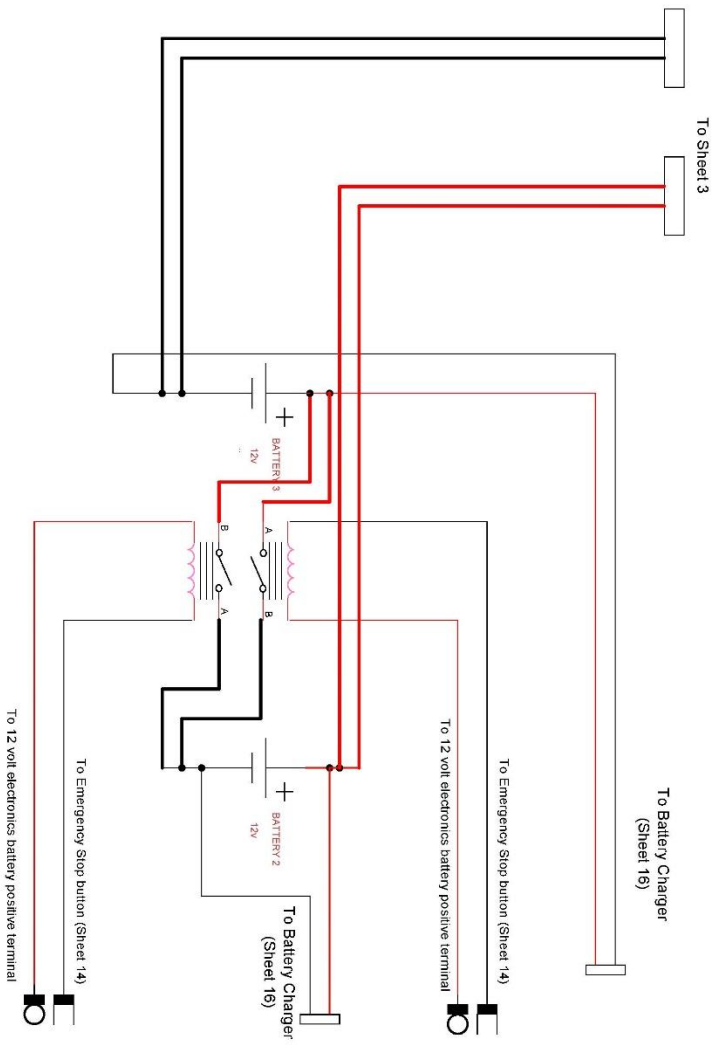
		Design: Cfollette	
		Date: 12/4/2015	
Project:		Drawn: Chris Folllette	
Date: 10/4/2016		Checked:	
Title:		Wheel Hub.ipt	
UNLESS OTHERWISE SPECIFIED DIMENSIONS ARE IN INCHES.		Size Scale	Material
±.5	±.02	B 1 / 4	Sheet 1 Aluminum 6061

Appendix C – Electrical Drawings

Rover Wiring Diagram

University of North Dakota
Department of Space Studies

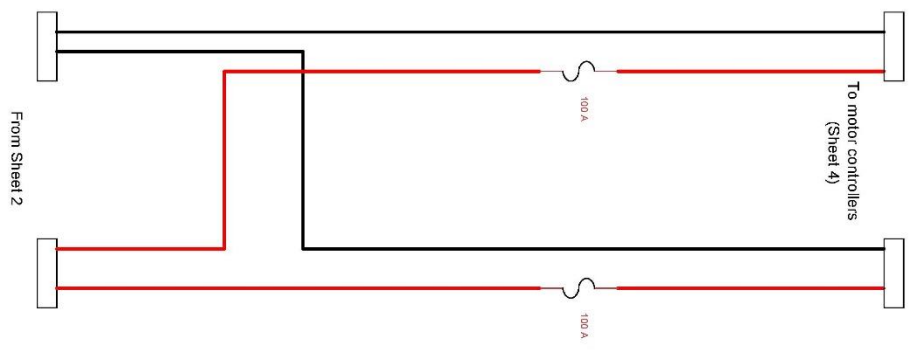
Title	Rover Wiring Diagram	Document
Author	Chris Foletto	Sheets
File	University of North Dakota ce Studies\Tm\Cad\Rover Wiring Diagram - Final	1 of 1
Revision	Date	
1.0	04/05/2017	



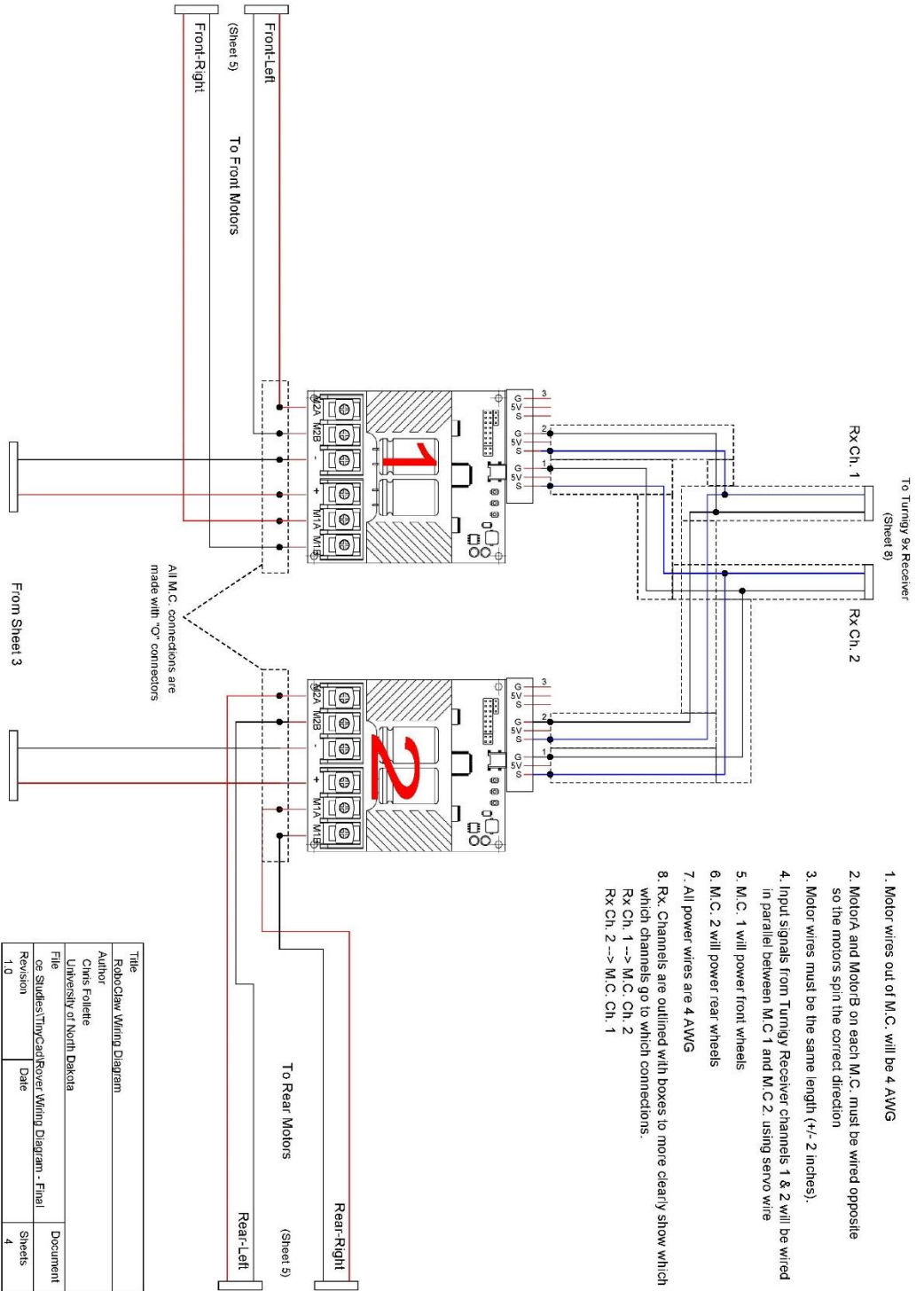
1. Connect the batteries in series. This will yield 24 volts, 105 Ah of power for the driving system
2. Power cable will be made of 2, 4 AWG wires.

Title	
Battery Wiring Harness	
Author	
Chris Foliote	
University or North Dakota	
File	
ce-Stuffest\TinyCad\Revnet Wiring Diagram - Final	
Revision	Date
1.0	
Document	
Sheets	
2	

1. The fuses are Waytek Model ANN-100

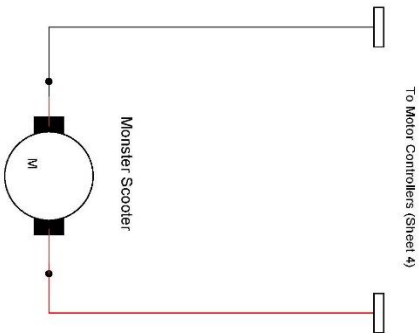


Title		Fuses	
Author		Chris Follette	
University of North Dakota			
File		ce Studies\TinyCard\Rever Wiring Diagram - Final	
Revision	Date	Sheets	
1.0		3	



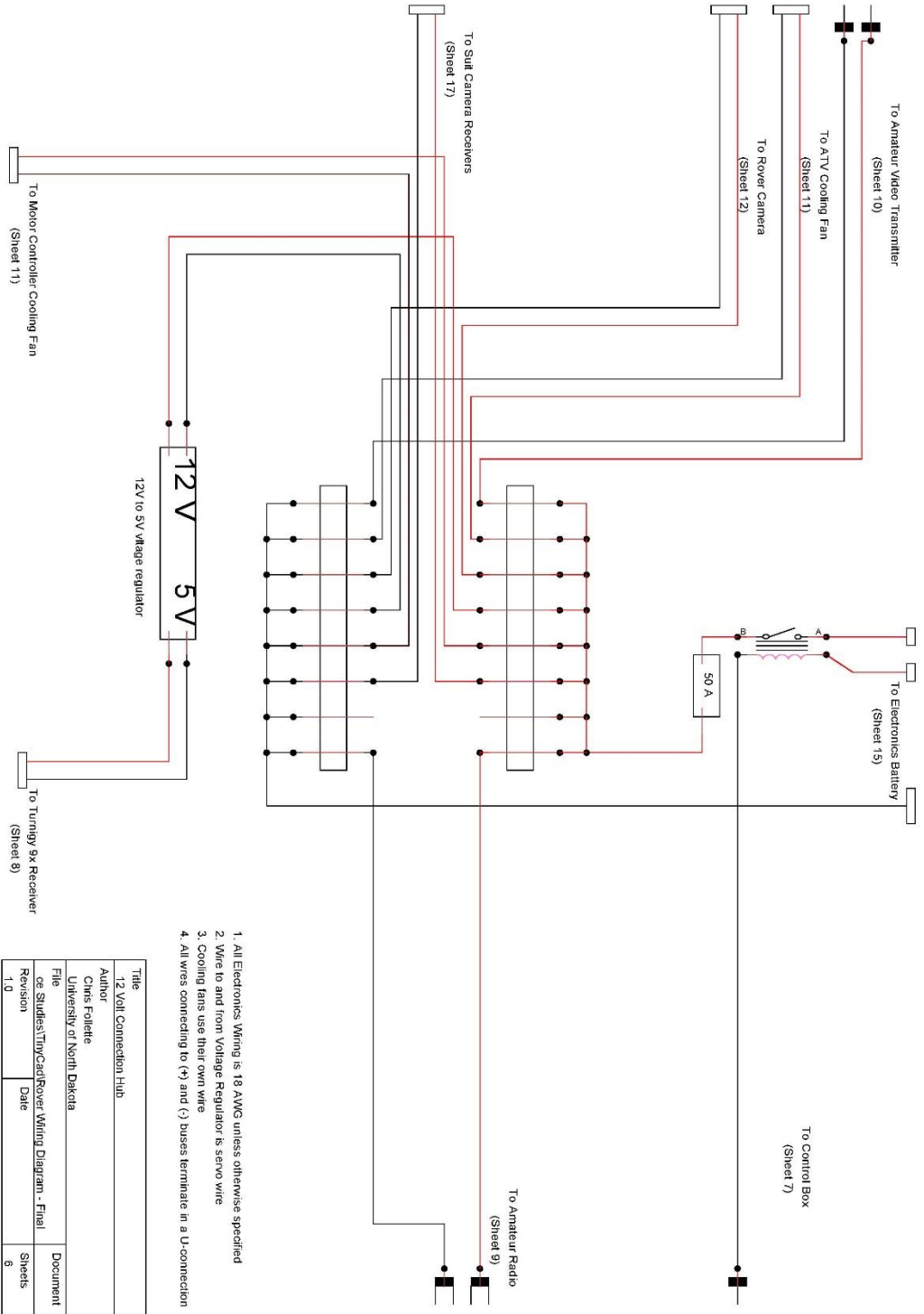
1. Motor wires out of M.C. will be 4 AWG
2. Motor A and Motor B on each M.C. must be wired opposite so the motors spin the correct direction
3. Motor wires must be the same length (+/- 2 inches).
4. Input signals from Turnigy Receiver channels 1 & 2 will be wired in parallel between M.C. 1 and M.C. 2, using servo wire
5. M.C. 1 will power front wheels
6. M.C. 2 will power rear wheels
7. All power wires are 4 AWG
8. Rx: Channels are outlined with boxes to more clearly show which channels go to which connections.
 Rx Ch. 1 --> M.C. Ch. 2
 Rx Ch. 2 --> M.C. Ch. 1

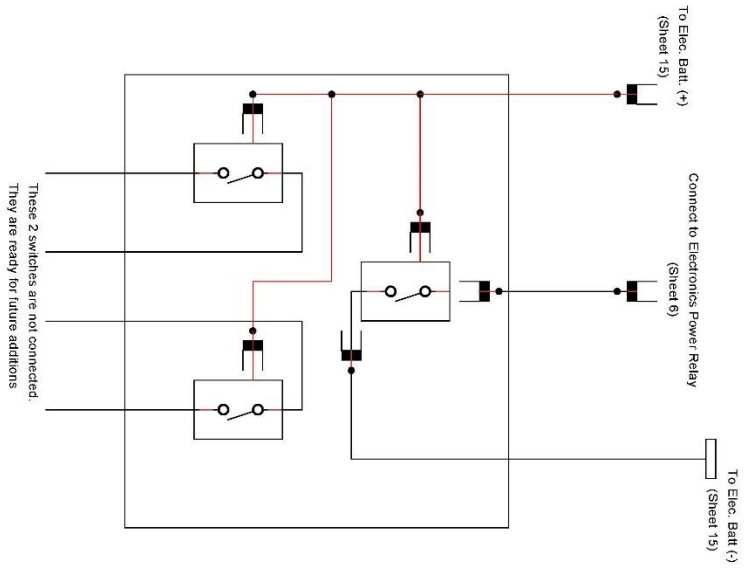
Title	RobotClaw Wiring Diagram
Author	Chris Follette
University or North Dakota	
File	Doc: Sulfest/TinyCard/RobotClaw Wiring Diagram - Final
Revision	Date
1.0	4



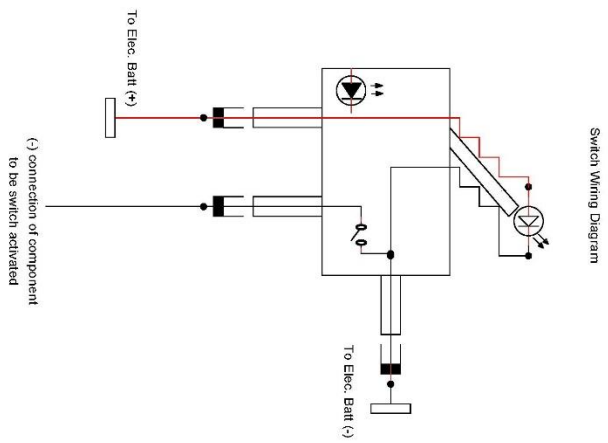
1. All motor wires need to be the same length.
2. Wire all 4 motors the same.

Title		Motor Wiring Diagram
Author		Chris Follette
University or North Dakota		
File		ce_Sulfas\TinyCard\Rever Wiring Diagram - Final
Revision	Date	
1.0		5

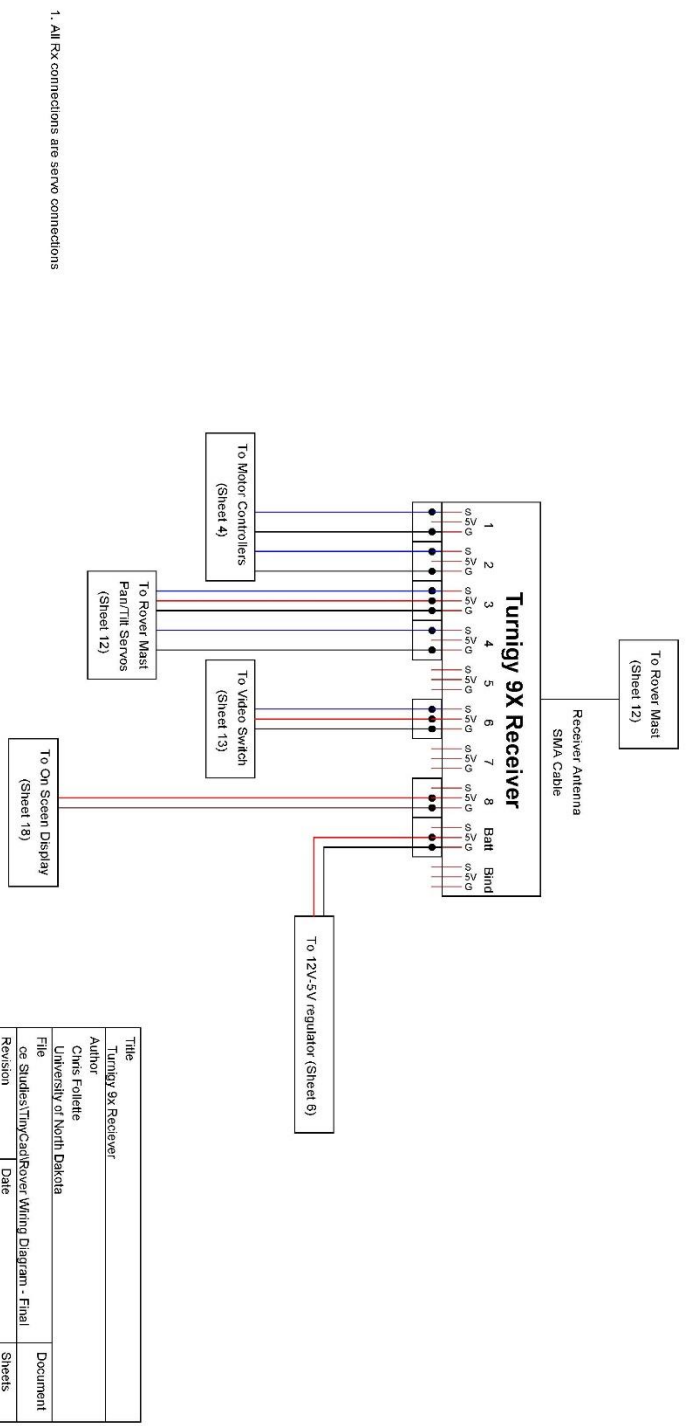




1. The switches are located inside the weatherproof box on the rear of rover
2. All switch LEDs are connected to the same wire. If rover is not in use for an extended period of time, disconnect the LED wire to prevent draining of battery. The LED is powered even when the switch is "OFF"

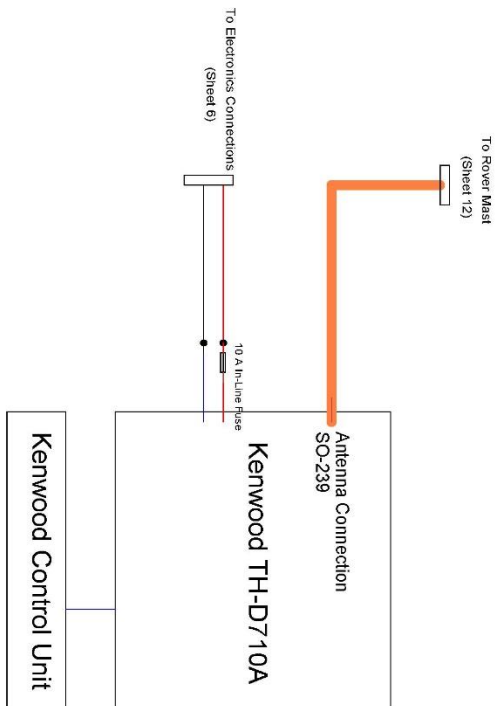


Title		Control Box
Author		Chris Foliente
University or North Dakota		
File		File: Steve\TinyCard\Rover Wiring Diagram - Final
Revision	Date	Sheets
1.0		7



1. All Rx connections are servo connections

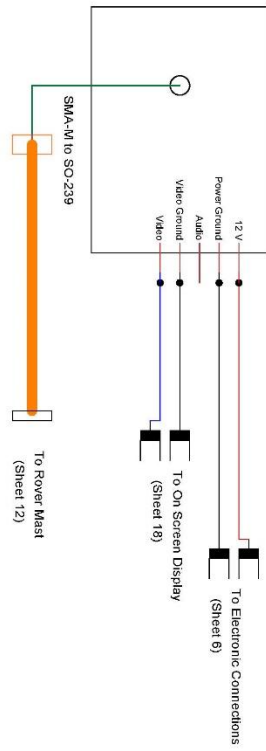
Title		Turnigy 9X Receiver
Author		Chris Follette
University or North Dakota		
File		0e_SlutfastTmyCrdtRover_Wiring_Diagram - Final
Revision	Date	Sheet 8
1.0		



- 1. Antenna cable is RG-8X
- 2. Antenna cable is terminated with PL-259

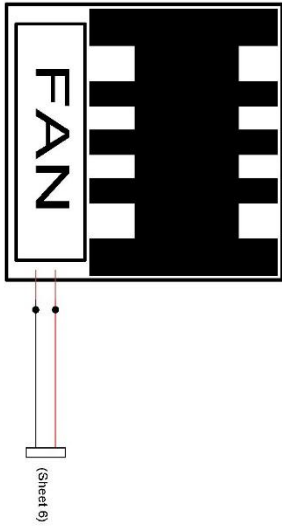
Title		Amateur Radio	
Author		Chris Follette	
University or North Dakota			
File		ce:Student\TmyCard\Rover Wiring Diagram - Final	
Revision	Date		
1.0		Document Sheets 9	

1. Antenna cable is terminated with PL-259



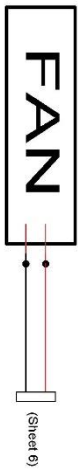
Title		Amateur Video Transmitter	
Author		Chris Foliote	
Institution		University of North Dakota	
File Name		SheetFastTinyCardRover Wiring Diagram - Final	
Revision	Date	Sheet	10
1.0		10	

Fan/Heat Sink for Amateur Video Transmitter

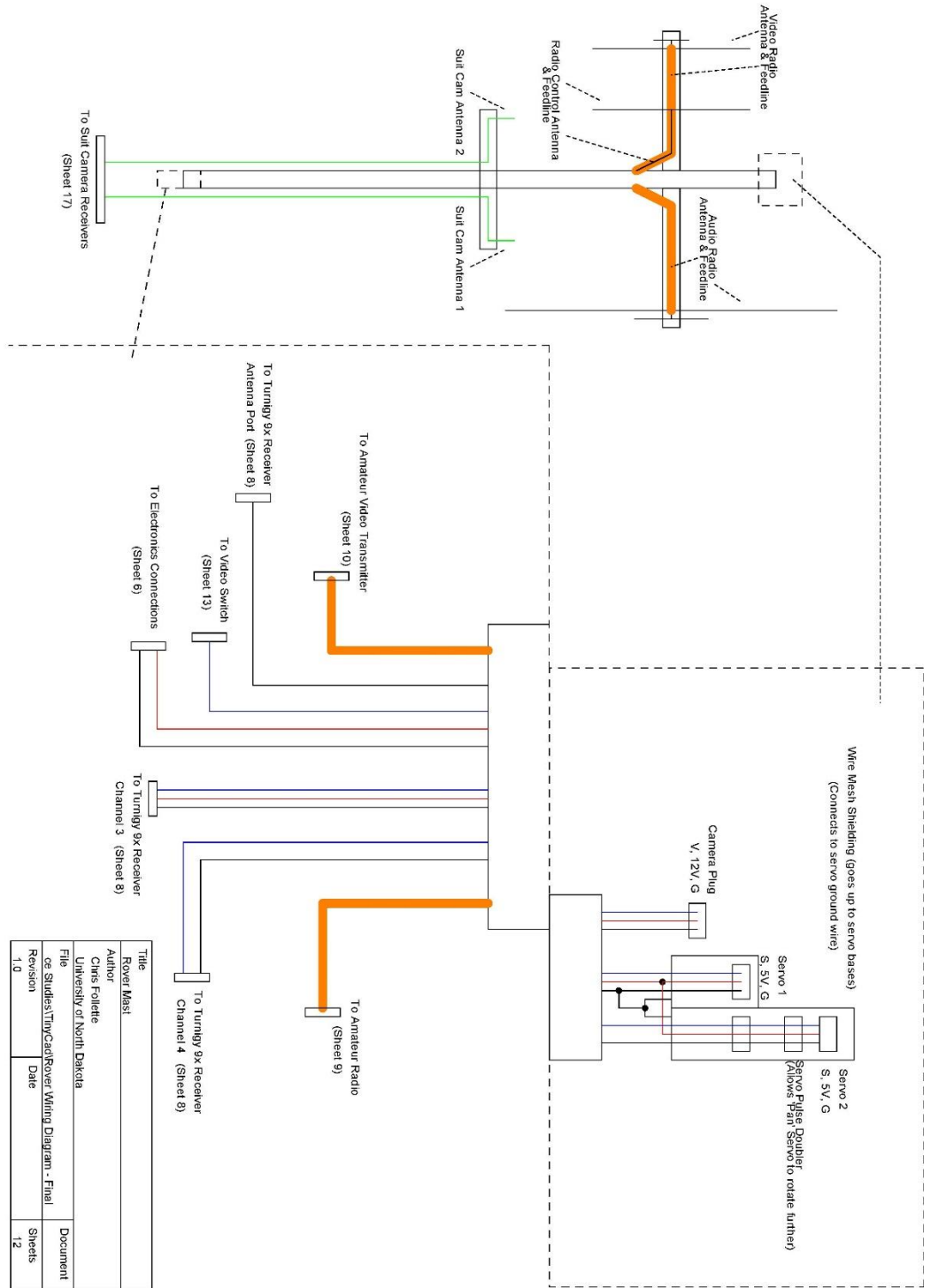


1. Both cooling fans are mounted on aluminum sheet metal supports.

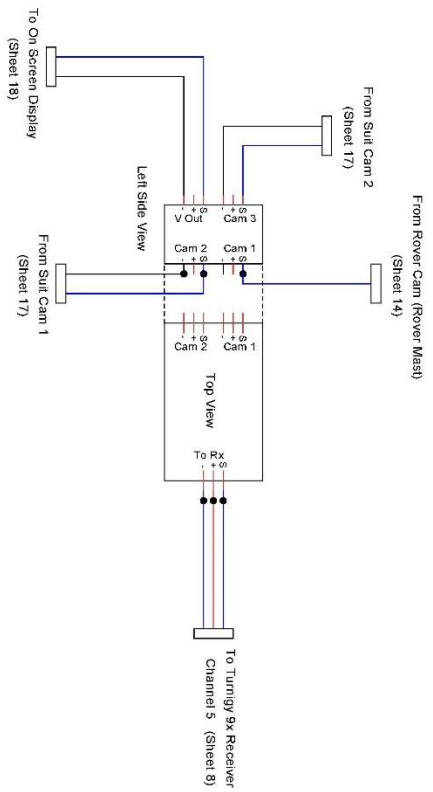
Motor Controller Cooling Fan



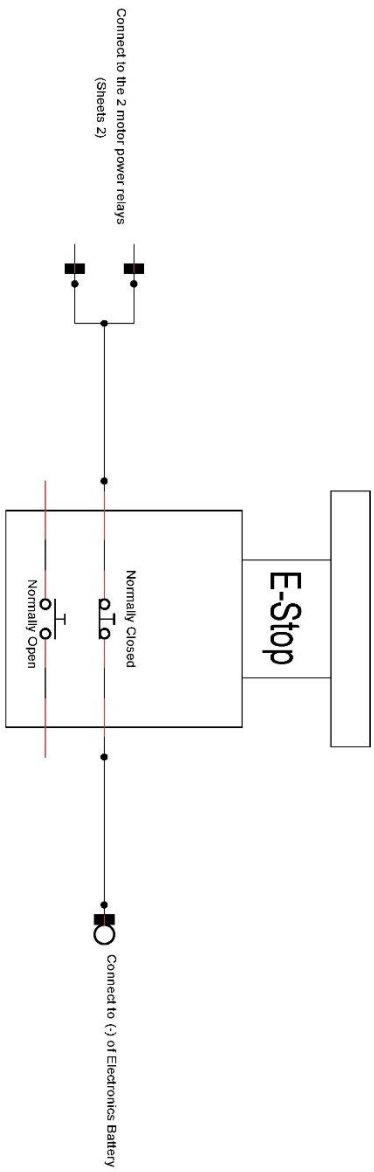
Title		Cooling Fans
Author		Chris Follette
University or North Dakota		
File		ce_Sulfas\TinyCard\Revex_Wiring_Diagram - Final
Revision	Date	
1.0		
Document		Sheets
		11



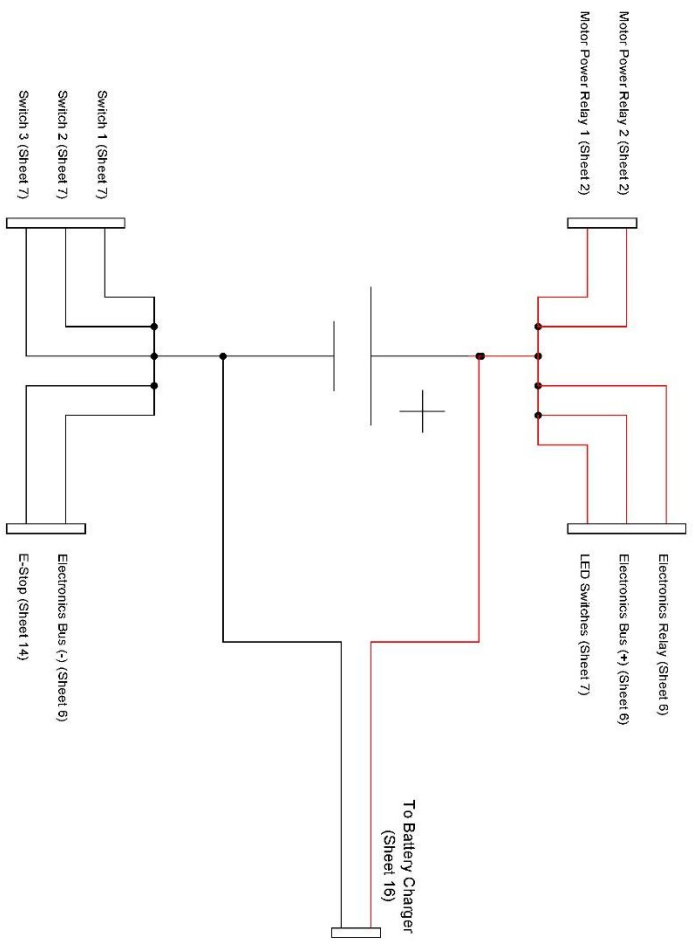
Title	
Rover Masi	
Author	
Chris Foliate	
University or North Dakota	
File	
ce_SurfastTinyCaviRover_Wiring_Diagram - Final	
Revision	Date
1.0	
Document	
Sheets	
12	



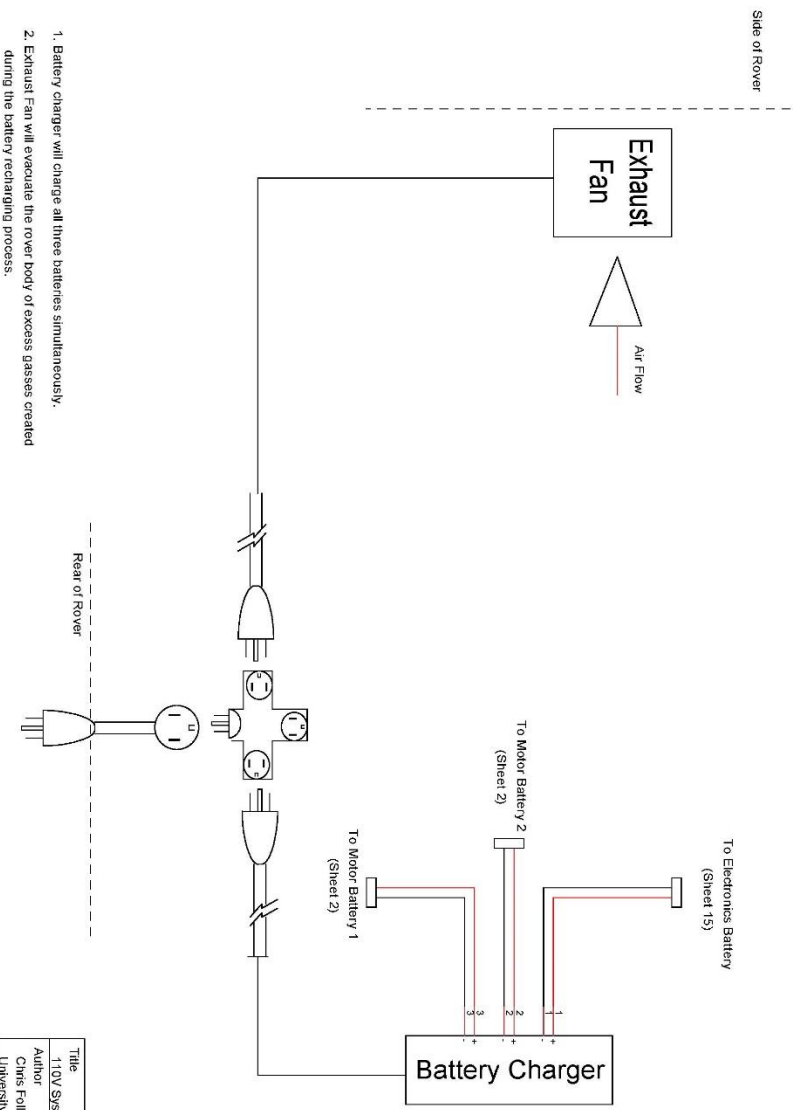
Title	Video Switch
Author	Chris Follette
	University of North Dakota
File	ce Studies\TinyCard\Rover Wiring Diagram - Final
Revision	Date
1.0	
	Document
	Sheets
	13



Title		Emergency Stop
Author		Chris Follette
University of North Dakota		
File	ce_Surfas\TinyCard\Rev1_Wiring Diagram - Final	
Revision	Date	
1.0		14



Title		Electronics Battery
Author		Chris Follete
File		University of North Dakota
Revision		1.0
Date		
Document		Wiring Diagram - Final
Revision		1.0
Date		
Sheets		15

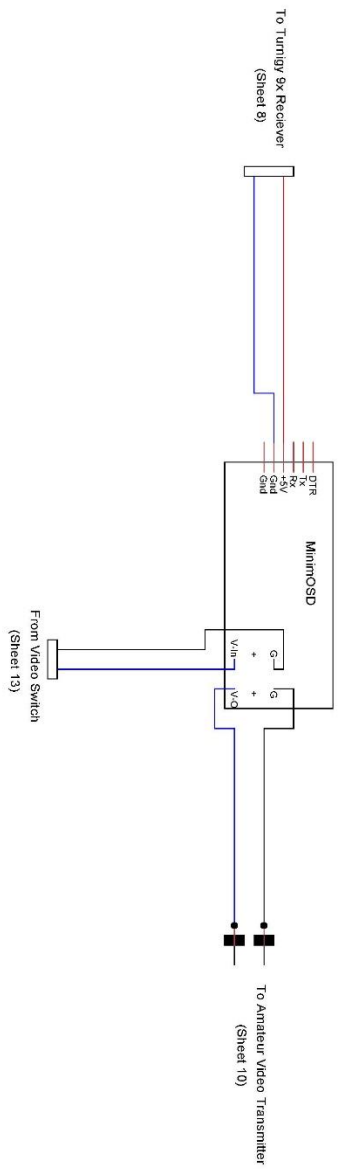


1. Battery charger will charge all three batteries simultaneously.
2. Exhaust Fan will evacuate the rover body of excess gasses created during the battery recharging process.

Title		110V System
Author		Chris Follette
University of North Dakota		
File		110V_Subsheet_TinyCar/Rover_Wiring_Diagram - Final
Revision	Date	
1.0		
Document		Sheets
		16



Title	Suit Camera Receivers
Author	Chris Follette
University or North Dakota	
File	ce_SuitcastTinyCardRover_Wiring_Diagram - Final
Revision	Date
1.0	
Document	17
Sheets	



Title	On Screen Display	
Author	Chris Foliote	
	University of North Dakota	
File	ce-Stuff-as-TinyCardRev1-Wiring-Diagram - Final	
Revision	Date	Document Sheets
1.0		18

References

- Alena, R., Gilbaugh, B., & Glass, B. (2001). *Communication System Architecture for Planetary Exploration*. Institute of Electrical and Electronics Engineers.
- Alena, R., Gilbaugh, B., Glass, B., & Braham, S. (2001). *Communication System Architecture for Planetary Exploration*. Institute of Electrical and Electronics Engineers.
- Anaheim Automation. (2016, Decemver 7). *GBPH-090x-CS Gearbox Page*. Retrieved from Anaheim Automation:
<http://www.anaheimautomation.com/products/gearbox/planetary-gearbox-item.php?sID=140&pt=i&tID=109&cID=30>
- ATV.com. (2017, January 13). *2004 Honda FourTrax Foreman® S*. Retrieved from ATV.com: <http://www.atv.com/specs/honda/utility/2004/fourtrax-foreman-reg/s.html>
- Browning, R. C., Baker, E. A., Herron, J. A., & Kram, R. (2006). Effects of obesity and sex on the energetic cost and preferred speed of walking. *Journal of Applied Physiology*, 390-398.
- Burridge, R. R., Graham, J., S&K Electronics, & Titan-Lincom. (2002). Providing Robotic Assistance during Extra-Vehicular Activity. *SPIE 4573, Mobile Robots XVI*.

- Burridge, R. R., Graham, J., Shillcutt, K., Hirsh, R., & Kortenkamp, D. (2003). Experiments with an EVA Assistant Robot. *7th International Symposium on Artificial Intelligence, Robotics and Automation in Space*. NARA, Japan.
- Cabrol, N. A. (2000). Astronaut-Rover Exploration Strategy (ARES) for the Human Exploration of Mars. *Lunar and Planetary Science XXXI*, (pp. 1164-1165). Houston.
- Cabrol, N. A., Kosmo, J. J., Trevino, R. C., Thomas, H., Eppler, D., Bualat, M. G., . . . Cockell, C. S. (1999). Results of the First Astronaut-Rover (ASRO) Field Experiment: Lessons and Directions for the Human Exploration of Mars. *Digital Avionics System Conference* (pp. 7.C.3-1 - 7.C.3-8 vol.2). St. Louis, MO: IEEE.
- Cisco. (2008, March 6). *RF Power Values*. Retrieved from Cisco.com: <https://www.cisco.com/c/en/us/support/docs/wireless-mobility/wireless-lan-wlan/23231-powervalues-23231.html>
- Clancey, W. J., Sierhuis, M., Alena, R. L., Graham, J. S., Tyree, K. S., Hirsh, R. L., . . . Rupert, S. M. (2007). *Automating CapCom Using Mobile Agents and Robotic Assistants*. Moffett Field: NASA.
- Engineering Toolbox. (2016, November 30). *Rolling Resistance*. Retrieved from The Engineering Toolbox: http://www.engineeringtoolbox.com/rolling-friction-resistance-d_1303.html
- Federal Communications Commission. (2017). 15.247 - Operation within the bands 902-928 MHz, 2400-2483.5 MHz, and 5725-5850 MHz. In *Code of Federal Regulations, Title 47, Chapter 1, Subchapter A, Part 15, Subpart C*.

Federal Communications Commission. (2017). 97.215 - Telecommand of model craft. In *Code of Federal Regulations, Title 47, Chapter 1, Subchapter D, Part 97, Subpart D*.

Harrington, B. D., & Voorhees, C. (2004). The Challenges of Designing the Rocker-Bogie Suspension for the Mars Exploration Rover. *37th Aerospace Mechanisms Symposium*. Houston.

Howard W. Sams & Co. (1986). *Handbook of Electronics Tables and Formulas*. Indianapolis: Macmillan, Inc.

Ion Motion Control. (2015). *RoboClaw Series Brushed DC Motor Controllers User Manual*.

Jet Propulsion Laboratory. (2016, December 17). *Wheels and Legs*. Retrieved from Mars Science Laboratory - Curiosity Rover:
<http://mars.nasa.gov/msl/mission/rover/wheelslegs/>

Kenwood Corporation. (n.d.). *TM-D710 Instruction Manual*.

KG0ZZ. (2011, March 30). *A Simple 2 m/70 cm Vertical Dipole Antenna*. Retrieved from Zed Zed's Workbench: http://www.amateurradio.bz/2m-70cm_vertical_dipole_antenna.html

Miller, D. P., & Lee, T.-L. (2002). High-Speed Traversal of Rough Terrain Using a Rocker-Bogie Mobility System. *Robotics 2002: The 5th International Conference and Exposition on Robotics for Challenging Situations and Environments*.

- Milliken, W. F., & Milliken, D. L. (1995). *Race Car Vehicle Dynamics*. Warrendale: Society of Automotive Engineers.
- Monster Scooter Parts. (2016, December 7). *24 Volt Motors*. Retrieved from Monster Scooter Parts:
<http://www.monsterscooterparts.com/catalogsearch/result/?q=24+volt+motor>
- NASA. (1997). *Human Exploration of Mars: The Reference Mission on the NASA Mars Exploration Study Team*. Houston, Texas: Lyndon B. Johnson Space Center.
- NASA. (1998). *Reference Mission 3.0: Addendum to the Human Exploration of Mars: The Reference Mission of the NASA Mars Exploration Study Team*. Hanover, MD: NASA.
- NASA. (2001). *The Mars Surface Reference Mission: A Description of Human and Robotic Surface Activities*. Hanover, MD: NASA.
- NASA. (2009). *K10 Robots: Scouts for Human Explorers*. Moffett Field: Ames Research Center.
- NASA JPL. (2016, November 1). *Live From Mars Photo Gallery*. Retrieved from Passport to Knowledge:
<http://passporttoknowledge.com/lfm/photos/images/marsokhod.gif>
- National Aeronautics and Space Administration. (2015). *NASA's Journey to Mars*. Washington, DC: National Aeronautics and Space Administration.

- Newman, D., & Barratt, M. (1997). Life Support and Performance Issues for Extravehicular Activity. In S. E. Churchill, *Fundamentals of Space Life Sciences* (p. 341). Malabar: Krieger Publishing Company.
- Polaris. (2016, December 20). *Half Shaft Spline Data*. Retrieved from https://www.polarissuppliers.com/sae_team/half_shaft_spline_data.pdf
- RCUniverse.com. (2017, 3 14). *2.4G 9 Channel remote TX & RX for Heli, Airplane, mode 2*. Retrieved from RCUniverse.com: http://www.rcuniverse.com/magazine/newproduct.cfm?product_id=4522
- Real World Interface. (n.d.). *ATRV-Jr Mobile Robot Tech Sheet*. Retrieved from http://www.cassinis.it/Siti%20ex%20Uni/ARL/projects/minerobots_archive/atrv_jr.pdf
- Ross, A., Kosmo, J., & Janoiko, B. (2010). *Historical synopses of desert RATS 1997-2010 and a preview of desert RATS 2011*. Houston: NASA Johnson Space Center.
- Seto, C. (2012). *DragonLink User Guide*.
- Seybold, J. S. (2005). *Introduction to RF Propagation*. Hoboken: John Wiley & Sons, Inc.
- Smart Battery. (2017, March 3). *24V 100AH Lithium Ion Battery*. Retrieved from Smart Battery - Lithium Ion Technology: <http://www.lithiumion-batteries.com/products/24-volt-lithium-batteries/24v-100ah-lithium-ion-battery.php>

Waytek. (2017, March 13). *ANN Fuses Very Fast Acting*. Retrieved from Waytek:

<https://www.waytekwire.com/datasheet/46167.pdf>